

HYDROLOGY OF THE TEXAS GULF COAST

AQUIFER SYSTEMS

By **Paul D. Ryder and Ann F. Ardis**

REGIONAL AQUIFER-SYSTEM ANALYSIS

U.S. GEOLOGICAL SURVEY
OPEN-FILE REPORT 91-64

Austin, Texas
1991

U.S. DEPARTMENT OF THE INTERIOR

MANUEL LUJAN, JR., *Secretary*

U.S. GEOLOGICAL SURVEY

Dallas L. Peck, *Director*

For sale by the Books and Open-File Reports Section, U.S. Geological Survey

Federal Center, Box 25425 Denver, Colorado 80225

CONTENTS

	Page
Abstract-----	1
Introduction-----	2
Gulf Coast aquifer systems regional study-----	2
Texas Gulf Coast subregional study-----	2
Purpose and scope-----	3
Method of investigation-----	3
Description of the area-----	3
Previous investigations-----	3
Hydrogeology-----	4
Hydrogeologic framework-----	4
Hydraulic properties-----	6
Horizontal hydraulic conductivity and transmissivity-----	6
Vertical hydraulic conductivity-----	7
Storage coefficient-----	7
Dissolved-solids concentration and density of water-----	8
Regional flow system-----	9
Predevelopment steady-state flow system-----	9
Conceptual model of system-----	9
Recharge and interaquifer leakage-----	9
Flow system, predevelopment to 1982-----	10
Ground-water development-----	10
Recharge, discharge, and distribution of flow, 1982-----	11
Subregional flow systems and hydrologic effects of development-----	13
Houston-Galveston area-----	13
Coastal rice-irrigation area-----	16
Evadale-Beaumont area-----	17
Kingsville area-----	18
Winter Garden area-----	19
Lufkin-Nacogdoches area-----	20
Other areas-----	21
Bryan-College Station area-----	21
Orange County-----	22
Potential for ground-water development-----	22
Summary-----	25
Selected references-----	28
Appendix-----	33
Digital model of predevelopment steady-state flow system-----	34
Digital model of transient flow system, predevelopment to 1982-----	34
Model grid and boundary conditions-----	35
Hydrologic input data-----	36
Calibration procedure and results-----	38
Sensitivity analysis-----	41

ILLUSTRATIONS

[Figures are at back of text]

Page

Figure 1-5.	Maps showing:	
	1. Relation of the Texas Gulf Coast study area to the onshore part of the Gulf Coast Regional Aquifer-System Analysis study area-----	46
	2. Relation of the Texas subregional modeled area to other subregional modeled areas and to the regional modeled area-----	47
	3. Location of the Texas Gulf Coast study area-----	48
	4. Mean annual precipitation in the Texas Gulf Coast study area-----	49
	5. Generalized outcrops of aquifers, permeable zones, and confining units-----	50
	6. Graph showing hydrogeologic section A-A'-----	51
	7. Map showing field and simulated hydraulic conductivity of coastal uplands aquifers and coastal lowlands permeable zones-----	52
8-16.	Maps showing simulated transmissivity of:	
	8. Permeable zone A-----	53
	9. Permeable zone B-----	54
	10. Permeable zone C-----	55
	11. Permeable zone D-----	56
	12. Permeable zone E-----	57
	13. The upper Claiborne aquifer-----	58
	14. The middle Claiborne aquifer-----	59
	15. The lower Claiborne-upper Wilcox aquifer-----	60
	16. The middle Wilcox aquifer-----	61
17-25.	Maps showing estimated dissolved-solids concentration in water from:	
	17. Permeable zone A-----	62
	18. Permeable zone B-----	63
	19. Permeable zone C-----	64
	20. Permeable zone D-----	65
	21. Permeable zone E-----	66
	22. The upper Claiborne aquifer-----	67
	23. The middle Claiborne aquifer-----	68
	24. The lower Claiborne-upper Wilcox aquifer-----	69
	25. The middle Wilcox aquifer-----	70
	26. Diagram showing conceptual model of aquifer systems and generalized representation in the digital model-----	71
27.	Map showing simulated predevelopment recharge and discharge in the outcrop areas of aquifers, permeable zones, and confining units-----	72
28.	Diagram showing simulated predevelopment vertical flow rates across hydrogeologic units in the study area-----	73
28a.	Graph showing simulated pumpage, recharge, and depletion of storage-----	74

ILLUSTRATIONS--Continued

Page

Figures 29-37.	Maps showing estimated pumpage in 1980, by 25-square-mile grid block, for:	
29.	Permeable zone A-----	75
30.	Permeable zone B-----	76
31.	Permeable zone C-----	77
32.	Permeable zone D-----	78
33.	Permeable zone E-----	79
34.	The upper Claiborne aquifer-----	80
35.	The middle Claiborne aquifer-----	81
36.	The lower Claiborne-upper Wilcox aquifer-----	82
37.	The middle Wilcox aquifer-----	83
38.	Map showing simulated recharge and discharge in the outcrop areas of aquifers, permeable zones, and confining units for 1982-----	84
39.	Map showing change in simulated recharge and discharge in the outcrop areas of aquifers, permeable zones, and confining units, predevelopment to 1982-----	85
40.	Diagram showing simulated 1982 vertical flow rates across hydrogeologic units in the study area-----	86
41-46.	Maps showing:	
41.	Locations of observation wells and precipitation stations in selected intensively pumped areas, and model subareas-----	87
42.	Ground-water pumpage in selected counties in the central part of the study area, 1960-85-----	88
43.	Location of subareas within the Houston-Galveston area (area 1) and average rates of pumping for 1979-----	89
44.	Decline of potentiometric surface of permeable zone A, predevelopment to 1982, and simulated 1982 horizontal flow vectors, Houston-Galveston area-----	90
45.	Decline of potentiometric surface of permeable zone B, predevelopment to 1982, and simulated 1982 horizontal flow vectors, Houston-Galveston area-----	91
46.	Decline of potentiometric surface of permeable zone C, predevelopment to 1982, and simulated 1982 horizontal flow vectors, Houston-Galveston area and Evadale-Beaumont area-----	92
47.	Graph showing ground-water levels in Harris County-----	93
48.	Map showing land-surface subsidence in the Houston-Galveston area, predevelopment to 1973-----	94
49.	Diagram showing simulated 1982 vertical flow rates across hydrogeologic units in model subarea II (fig. 41)-----	95
50.	Graph showing ground-water levels in Jackson County and precipitation data in Wharton County-----	96
51.	Diagram showing simulated 1982 vertical flow rates across hydrogeologic units in model subarea III (fig. 41)-----	97

ILLUSTRATIONS--Continued

	Page
52. Map showing ground-water pumpage in selected counties in the eastern part of the study area, 1960-85-----	98
53. Graph showing ground-water levels in Jasper and Hardin Counties-----	99
54. Diagram showing simulated 1982 vertical flow rates across hydrogeologic units in model subarea I (fig. 41)-----	100
55-56. Maps showing:	
55. Ground-water pumpage in selected counties in the western part of the study area, 1960-85-----	101
56. Change of potentiometric surface of permeable zone B, predevelopment to 1982, and simulated 1982 horizontal flow vectors, Kingsville area----	102
57. Graph showing ground-water levels in Kleberg County-----	103
58. Diagram showing simulated 1982 vertical flow rates across hydrogeologic units in model subarea IV (fig. 41)-----	104
59. Map showing change of potentiometric surface of the lower Claiborne-upper Wilcox aquifer, predevelopment to 1982, and simulated 1982 horizontal flow vectors, Winter Garden area-----	105
60-64. Graphs showing:	
60. Ground-water levels and precipitation data in Zavala County-----	106
61. Ground-water levels in Nacogdoches County-----	107
62. Projected fresh ground-water use for selected counties, 1985-2030-----	108
63. Measured and simulated water levels in the Houston-Galveston area, projected to 2030-----	109
64. Map showing projected land-surface subsidence in the Houston-Galveston area, 1973 to 2030-----	110
Figures 65-66. Graphs showing:	
65. Simulated water levels in southeastern Harris County, projected to 2030 with 1980 pumpage-----	111
66. Measured and simulated water levels in the Winter Garden area, projected to 2030-----	112
67. Diagram showing simulated 2030 vertical flow rates across hydrogeologic units in the study area-----	113
68-76. Maps showing potential areas for development of large ground-water supplies from	
68. Permeable zone A-----	114
69. Permeable zone B-----	115
70. Permeable zone C-----	116
71. Permeable zone D-----	117
72. Permeable zone E-----	118
73. The upper Claiborne aquifer-----	119
74. The middle Claiborne aquifer-----	120
75. The lower Claiborne-upper Wilcox aquifer-----	121
76. The middle Wilcox aquifer-----	122

ILLUSTRATIONS--Continued

	Page
77-81. Maps showing:	
77. Finite-difference grid superimposed on the modeled area and study area-----	123
78. Estimated altitude of the water table for the model constant-head boundary-----	124
79. Measured and simulated altitude of the potentiometric surface of permeable zone A in the Houston-Galveston area, 1982-----	125
80. Measured and simulated altitude of the potentiometric surface of permeable zone B in the Houston-Galveston area, 1982-----	126
81. Measured and simulated altitude of the potentiometric surface of permeable zone C in the Houston-Galveston and Evadale areas, 1982----	127
82-86. Graphs showing:	
82. Measured and simulated water levels in wells 1, 2, 9, and 11 in the Houston-Galveston area----	128
83. Measured and simulated water levels in wells 4, 7, 8, and 12 in the Houston-Galveston area----	129
84. Measured and simulated water levels in wells 3, 5, 6, and 10 in the Houston-Galveston area----	130
85. Measured and simulated water levels in wells 13, 14, and 15 in Jackson and Wharton Counties---	131
86. Measured and simulated water levels in wells 16 and 17 in the Evadale-Beaumont area-----	132
87. Map showing measured and simulated altitude of the potentiometric surface of permeable zone B in the Kingsville area, 1982-----	133
88. Graph showing measured and simulated water levels in wells 18, 19, 20, and 21 in the Kingsville area-----	134
89. Map showing measured and simulated altitude of the potentiometric surface of the lower Claiborne-upper Wilcox aquifer in the Winter Garden area, 1982-----	135
90-94. Graphs showing:	
90. Measured and simulated water levels in wells 22, 23, 24, and 26 in the Winter Garden area-----	136
91. Measured and simulated water levels in wells 27, 29, 30, and 31 in the Winter Garden area-----	137
92. Measured and simulated water levels in wells 25, 28, 32, and 34 in the Winter Garden area-----	138
93. Measured and simulated water levels in wells 33, 35, and 36 in the Winter Garden area-----	139
94. Measured and simulated water levels in wells 37, 38, and 39 in the Lufkin-Nacogdoches area----	140
95. Map showing measured and simulated land-surface subsidence in the Houston-Galveston area, predevelopment to 1973-----	141
96-101. Graphs showing:	
96. Sensitivity of simulated 1982 heads to change in horizontal hydraulic conductivity (Kh)-----	142

ILLUSTRATIONS--Continued

	Page
96-101. Graphs showing--Continued:	
97. Sensitivity of simulated 1982 heads to change in vertical hydraulic conductivity (Kv)-----	143
98. Sensitivity of simulated 1982 heads to changes in water density-----	144
99. Sensitivity of simulated 1982 heads to changes in aquifer storage coefficient (S)-----	145
100. Sensitivity of simulated water levels, 1910-82, to changes in storage coefficient (S)-----	146
101. Sensitivity of simulated water levels, 1910-82, to changes in storage coefficient (S)-----	147

TABLES

	Page
Table 1. Stratigraphic and hydrogeologic units for the coastal lowlands aquifer system-----	5a
2. Stratigraphic and hydrogeologic units for the coastal uplands aquifer system-----	5b
3. Horizontal hydraulic conductivity and transmissivity of aquifers and permeable zones based on calibrated model-----	6a
4. Vertical hydraulic conductivity of aquifers, permeable zones, and confining units based on calibrated model-----	7a
5. Calibrated storage coefficient for aquifers and permeable zones, and inelastic specific storage for compacting clays-----	7b
6. Estimated density of water in the hydrogeologic units-----	8a
7. Summary of changes in simulated heads and recharge rates resulting from a hypothetical increase in pumping rate, 1983 tp 2030-----	24a
8. Summary of simulated and measured predevelopment altitudes of potentiometric surfaces-----	34a
9. Summary of simulated and measured 1982 altitudes of potentiometric surfaces-----	38a
10. Summary of simulated and measured water levels in wells shown in figure 41-----	39a
11. Summary of calibration residual errors for 1982 heads and those resulting from changes in model variables-----	42a
12. Summary of calibration residual errors for land-surface subsidence and those resulting from changes in model variables-----	42b

CONVERSION FACTORS

<u>Multiply</u>	<u>By</u>	<u>To obtain</u>
inch (in.)	25.4	millimeter
inch per year (in/yr)	25.4	millimeter per year
foot (ft)	0.3048	meter
foot per day (ft/d)	0.3048	meter per day
foot per year (ft/yr)	0.3048	meter per year
mile (mi)	1.609	kilometer
square mile (mi ²)	2.590	square kilometer
million gallons per day (Mgal/d)	0.04381	cubic meter per second
gallon per minute (gal/min)	0.06309	liter per second
cubic foot per day (ft ³ /d)	0.02832	cubic meter per day
foot squared per day (ft ² /d)	0.0929	meter squared per day

Temperature can be converted from degrees Fahrenheit (°F) to degrees Celsius (°C) by the equation:

$$^{\circ}\text{C} = 5/9 (^{\circ}\text{F} - 32)$$

Sea level: In this report, "sea level" refers to the National Geodetic Vertical Datum of 1929--a geodetic datum derived from a general adjustment of the first-order level nets of the United States and Canada, formerly called Sea Level Datum of 1929.

HYDROLOGY OF THE TEXAS GULF COAST AQUIFER SYSTEMS

By

Paul D. Ryder and Ann F. Ardis

ABSTRACT

A complex, multilayered ground-water flow system exists in the Coastal Plain sediments of Texas. The Tertiary and Quaternary clastic deposits have an areal extent of 114,000 square miles onshore and in the Gulf of Mexico. Two distinct aquifer systems are recognized within the sediments, which range in thickness from a few feet to more than 12,000 feet. The older system--the Texas coastal uplands aquifer system--consists of four aquifers and two confining units in the Claiborne and Wilcox Groups. It is underlain by the practically impermeable Midway confining unit or by the top of the geopressed zone. It is overlain by the nearly impermeable Vicksburg-Jackson confining unit, which separates it from the younger coastal lowlands aquifer system. The coastal lowlands aquifer system consists of five permeable zones and two confining units that range in age from Oligocene to Holocene. The hydrogeologic units of both systems are exposed in bands that parallel the coastline. The units dip and thicken toward the Gulf. Quality of water in the aquifer systems is highly variable, with dissolved solids ranging from less than 500 to 150,000 milligrams per liter.

Substantial withdrawal from the aquifer systems began in the early 1900's and increased nearly continuously into the 1970's. The increase in withdrawal was relatively rapid from about 1940 to 1970. Adverse hydrologic effects, such as saltwater encroachment in coastal areas, land-surface subsidence in the Houston-Galveston area, and long-term dewatering in the Winter Garden area, were among some of the factors that caused pumping increases to slow or to cease in the 1970's and 1980's.

Ground-water withdrawals in the study area in 1980 were about 1.7 billion gallons per day. Nearly all of the withdrawal was from four units: Permeable zones A, B, and C of Miocene age and younger, and the lower Claiborne-upper Wilcox aquifer. Ground-water levels have declined hundreds of feet in the intensively pumped areas of Houston-Galveston, Kingsville, Winter Garden, and Lufkin-Nacogdoches. Water-level declines have caused inelastic compaction of clays which, in turn, has resulted in land-surface subsidence of more than one foot in an area of about 2,000 square miles. Maximum subsidence of nearly 10 feet occurs in the Pasadena area east of Houston.

A three-dimensional, variable-density digital model was developed to simulate predevelopment and transient flow in the aquifer systems. The modeled area is larger than the study area, and includes adjacent parts of Louisiana and Mexico. The transient model calibration period was from 1910 (predevelopment) to 1982. Model-generated head distributions, water-level hydrographs, and land-surface subsidence were matched to measured data in selected, intensively pumped areas.

For the study area, mean horizontal hydraulic conductivity in the calibrated model ranges from 10 feet per day for the middle Wilcox aquifer to 25 feet per day for permeable zone A. Mean transmissivity ranges from about 4,600 feet squared per day for the middle Claiborne aquifer to about 10,400 feet squared per day for permeable zone D. Mean vertical hydraulic conductivity ranges from 1.1×10^{-5} feet per day for the Vicksburg-Jackson confining unit, to 3.8×10^{-3} feet per day for permeable zone A. Mean values of calibrated storage coefficient range from 5.2×10^{-4} for the middle Claiborne aquifer to 1.7×10^{-3} for the middle Wilcox aquifer and permeable zone C. Calibrated inelastic specific storage values for clay beds in permeable zones A, B, and C in the Houston-Galveston area are 8.5×10^{-5} , 8.0×10^{-5} , and 8.0×10^{-6} feet⁻¹, respectively. These values are 85, 80, and 8 times greater than the estimated elastic specific storage value for the clays in permeable zones A, B, and C, respectively.

Recharge rates were mapped for predevelopment conditions as determined from a steady-state model calibration. A maximum rate of 3 inches per year was simulated in small areas, and the average rate for the study area was 0.34 inch per year. Total simulated recharge was 85 million cubic feet per day in the outcrop area. Recharge was equal to discharge in outcrop areas (79 million cubic feet per day) plus net lateral flow out of the study area (6 million cubic feet per day).

Rates of inflow and outflow to the ground-water system have nearly tripled from predevelopment to 1982 (85 to 276 million cubic feet per day) based on model simulation. Withdrawal of 231 million cubic feet per day was supplied principally by an increase in outcrop recharge and, to a lesser extent, from a decrease in natural discharge and release of water from storage in aquifers and compacting clay beds. The average simulated 1982 recharge rate for the study area was 0.52 inch per year, with a maximum simulated rate of 6 inches per year in Jackson and Wharton Counties.

Because withdrawal has caused problems such as saltwater intrusion, land-surface subsidence, and aquifer dewatering, the Texas Department of Water Resources has projected that ground-water use will decline substantially in most of the study area by the year 2030. Some areas remain favorable for development of additional ground-water supplies. Pumping from older units that are farther inland and in areas where potential recharge is greater will minimize adverse hydrologic effects.

INTRODUCTION

Gulf Coast Aquifer Systems Regional Study

The Gulf Coast Regional Aquifer-System Analysis (GC RASA) study was begun in 1980 as part of a federally funded program of the U.S. Geological Survey to provide a regional understanding and assessment of major aquifer systems in the United States. The GC RASA study is focused on the Gulf Coastal Plain sediments of Tertiary and Quaternary age. The study area consists of about 230,000 mi² onshore and about 60,000 mi² offshore (about 290,000 mi² total) in parts of Alabama, Arkansas, Florida, Illinois, Kentucky, Mississippi, Missouri, Tennessee, Texas, and all of Louisiana (fig. 1). A complete discussion and description of the GC RASA study is given in Grubb (1984).

Many reports and abstracts resulting from the study have been published or are in press. These reports generally cover all or parts of the aquifer systems in the GC RASA study. They describe one or a combination of various aspects of the Gulf Coast aquifer systems such as geology and stratigraphy, geochemistry, ground-water hydraulics and flow, ground-water development and use, and digital model development.

Final reports, regional and subregional in scope, that describe the hydrogeologic framework, hydrology, or geochemistry will be in a Professional Paper 1416 series that will consist of several chapters. This report is Chapter E in the series.

Texas Gulf Coast Subregional Study

The Texas Gulf Coast study is a part of the GC RASA study (fig. 1). Parts of the Texas Gulf Coast aquifer systems have sustained intensive ground-water development that has resulted in problems associated with large decreases of ground-water levels, land subsidence, and saltwater encroachment. Ground-water withdrawals were more than 600 Mgal/d in the Houston-Galveston area in 1980. Water levels in some wells declined from at or above land surface in the early 1900's to about 350 ft below land surface in the 1980's. The decreased artesian pressure head has caused land subsidence of almost 10 ft in the Pasadena area east of Houston during 1906-78 (Gabrysch, 1984b, p. 21). Extensive withdrawal has caused land subsidence in other areas, although less severe than in the Houston area.

Potential for saltwater encroachment is particularly great in the southwestern part of the study area. The city of Alice in Jim Wells County and the city of Brownsville in Cameron County have supplemented ground-water supplies with surface water because of saltwater encroachment (Texas Department of Water

Resources, 1984a, p. III-22-1). Because of saltwater encroachment, the cities of Agua Dulce, Banquette, Driscoll, and Bishop in Nueces County, and Kingsville in Kleberg County plan to supplement ground-water supplies with water from the Nueces River (Texas Department of Water Resources, 1984a, p. III-22-1).

Other areas within the Texas part of the GC RASA study area have potential for significant additional ground-water development, but the effects of large increases in development are not known. Management of the regional ground-water resource will require quantitative evaluation of the geologic, hydrologic, and chemical-quality characteristics of the system in addition to definition of the hydrogeologic boundaries that affect development potential.

Purpose and Scope

The objectives of the Texas Gulf Coast study are to: (1) Define the hydrogeologic framework and hydraulic characteristics of the aquifer systems; (2) delineate the extent of fresh to slightly saline water in the various hydrogeologic units; (3) describe and quantify the ground-water flow system; (4) analyze the hydrologic effects of man's development on the flow system; and (5) assess the potential of the aquifer systems for further development. A preliminary, or interim report (Ryder, 1988) describes in detail the hydrogeologic framework and the steady-state predevelopment flow system. Thus, a brief summary of these topics will be given in this report, and the emphasis of this report is on the effects of development and the potential for development.

Method of Investigation

The basic approach to meet the study objectives is to collect and analyze hundreds of borehole geophysical logs, to review previously published interpretive reports, and to use data files from the Geological Survey and other Federal and State agencies and commercially available files from the petroleum industry. From these analyses a regionally consistent hydrogeologic framework is defined. Additionally, the analyses provide: (1) The hydrologic boundaries of the aquifer systems; (2) a definition of selected water-quality properties; (3) initial estimates of aquifer and confining-unit hydraulic characteristics; (4) estimates of withdrawal in each of the various aquifers; and (5) where sufficient data exist, potentiometric-surface maps for determining any long-term decline in water levels from predevelopment to modern-day conditions. All of these resulting data are incorporated into a multilayered, digital ground-water flow model. Calibration of the model provides an improved estimate of aquifer and confining-unit hydraulic characteristics, a quantitative analysis of flow within and between each of the various aquifers, a better understanding of the total flow system, and a useful tool for assessing the potential of the aquifer systems for further development.

The Texas Gulf Coast study is one of five subregions of the GC RASA study for which digital models have been developed. The five subregional models are nested within the GC RASA regional model. The relation of the regional modeled area, with a grid having 102 rows, 58 columns and 10-mi grid-block spacing, to the five subregional modeled areas, each with 5-mi grid-block spacing, is shown in figure 2. The model grid is explained in more detail in the Appendix.

Description of the Area

The study area is located within the coastal plain of Texas, and extends from Mexico in the west to Louisiana in the east. It consists of about 90,000 mi² onshore and an additional 24,000 mi² in the Gulf for a total surface area of about 114,000 mi² (fig. 3). The northern boundary is the updip limit of the Texas Gulf Coast aquifer systems--the practically impermeable, predominantly marine clays of the Midway Group. The southern boundary extends to the edge of the continental shelf in the Gulf of Mexico.

The study area encompasses all or parts of 109 counties. The principal physiographic province is the Gulf Coastal Plain, and the major structural features are the Rio Grande embayment, San Marcos arch, East Texas embayment, Sabine uplift, and the Gulf of Mexico geosyncline (fig. 1). Land surface is characterized by a smooth, low-lying coastal plain that gradually rises toward the north and northwest where the more dissected

and rolling terrain reaches altitudes of as much as 600 ft in the eastern and central areas, and to as much as 900 ft in the west. The coastal uplands end at the contact with Cretaceous clay and limestone where the land surface generally rises steeply. Twelve major streams drain the area, flowing generally south-southeastward toward the Gulf. These are, from west to east, the Rio Grande, Nueces, Frio, San Antonio, Guadalupe, Colorado, Brazos, Navasota, Trinity, Neches, Angelina, and Sabine Rivers (fig. 4). Many large reservoirs that have been constructed on these and other streams supply substantial quantities of water for irrigation and municipal supply.

Average annual precipitation during 1951-80 varied greatly, ranging from about 21 in. in most of the Rio Grande valley in the southwest, to about 56 in. at the Texas-Louisiana boundary in the east (fig. 4). Average annual runoff for 1951-80 ranged from about 0.2 in. at the Rio Grande to more than 18 in. from the Houston area eastward into Louisiana (Gebert and others, 1987).

Previous Investigations

Numerous reports concerning the geology and hydrogeology of all or part of the study area have been written by personnel of the Geological Survey and other Federal and State agencies, consulting firms, and others. Several reports are regional in nature, including a report by the Texas Department of Water Resources (1984a) that describes the hydrology of the area and presents a comprehensive plan for future water development; a report by Baker and Wall (1976) that includes most of the study area and emphasizes the desirability of conjunctive use of ground water and surface water in any plans for future development; a report by Carr and others (1985) that includes much of the study area and applies digital modeling techniques to simulate flow in Miocene and younger deposits; a report by Baker (1979) that includes an area from Mexico to Louisiana and emphasizes the hydrogeologic framework of Miocene and younger units; a report by Baker (1986) that applies digital modeling to simulate predevelopment flow in Miocene deposits in a 25,000 mi² area in the eastern part, and a report by Jones and others (1976) that describes the hydrogeology of the Wilcox Group. Some of the many reports dealing with more local ground-water problems are referenced throughout this report where the published data or conclusions are helpful for describing and analyzing the regional ground-water flow system.

Several recent reports have been generated by the GC RASA study. Grubb (1984, 1987) presented an overview of the GC RASA. Hosman and Weiss (1988) described in detail the hydrogeologic framework for the Texas coastal uplands aquifer system. Weiss (1987) described methods for estimating dissolved-solids concentrations in water. Pettijohn and others (1988) presented maps of dissolved-solids concentrations. Ryder (1988) described the hydrogeology and predevelopment flow in the Texas Gulf Coast aquifer systems.

HYDROGEOLOGY

A detailed description of the hydrogeologic framework is given in Ryder (1988). A brief summary follows. Some model-derived values of transmissivity and horizontal and vertical hydraulic conductivity presented here are significantly different from those previously reported for the predevelopment model calibration. These properties are described in detail, as well as storage coefficient, which was estimated for the transient model calibration. Estimates of dissolved-solids concentrations and density of water are more accurate than reported previously.

Hydrogeologic Framework

Tertiary and Quaternary deposits of clay, silt, sand, and gravel as much as 12,000 ft thick underlie the Gulf Coastal Plain in Texas. The clastic sediments dip toward the Gulf of Mexico and thicken in that direction. The thick sequence of alternating fine- and coarse-grained sediments is subdivided into hydrogeologic units that can be represented as layers in a digital ground-water flow model. The number of model layers (hydrogeologic units) chosen is based on practical considerations for the scale of the system, objectives of the model study, and computer-cost limitations. Weiss and Williamson (1985) discussed the rationale and methodology for subdividing the Coastal Plain sediments into discrete hydrogeologic units for the GC RASA study.

Pre-Miocene sediments are distributed as relatively uniform sequences of predominantly fine- or coarse-grained material. Borehole geophysical data can be used to identify the intervals and to designate aquifers and confining units.

Miocene and younger deposits differ from pre-Miocene deposits. They exhibit more heterogeneity--the interfingering of many thin beds of differing texture and limited areal extent. Where the system is heterogeneous, Weiss and Williamson (1985) stated that the subdivision into layers should include an evaluation of depths of producing zones and the resultant vertical distribution of hydraulic head. In addition, borehole geophysical data are used to suggest relative permeabilities and delineate model layers that are more likely to have uniform hydraulic properties. Thus, Miocene and younger deposits at large pumping centers in Houston, Texas, and Baton Rouge, Louisiana, were subdivided into discrete units (Weiss and Williamson, 1985). These units are called "permeable zones" and confining units. The permeable zones typically contain discontinuous clay beds, in contrast to the pre-Miocene aquifers that are typically massive sand beds separated by regionally extensive clay beds.

The hydrogeologic units of the GC RASA study comprise three major aquifer systems (fig. 1). The Texas coastal uplands aquifer system occurs only in Texas; the coastal lowlands aquifer system occurs in Texas and several nearby states; the Mississippi embayment aquifer occurs in several states outside Texas. The two systems in Texas are separated by the poorly permeable Vicksburg-Jackson confining unit and are underlain by the practically impermeable Midway confining unit (tables 1 and 2). The Texas coastal uplands (hereafter simply the coastal uplands) and coastal lowlands aquifer systems consist of four aquifers, five permeable zones, and six confining units (including the Midway and Vicksburg-Jackson confining units). The definitions of the hydrogeologic units and the names assigned to them may not conform to conventional definitions and names as found in the published literature. The hydrogeologic units in the coastal uplands aquifer system are named for the group designation of the sediments that comprise the units (Hosman and Weiss, 1988). Grubb (1987) applied the designations "zone A" through "zone E" for the five permeable zones of the coastal lowlands aquifer system. Correlation of stratigraphic and hydrogeologic units is shown in table 1 for the coastal lowlands aquifer system and in table 2 for the coastal uplands aquifer system.

A note of explanation concerning the "Frio" Formation (table 1) and the Frio Clay (table 2) is due here. The "Frio" Formation is from Texas oilfield nomenclature. It refers to a thick section of sand that begins to appear about 3,000 ft below land surface. The "Frio" Formation has no correlation with the Frio Clay which is the updip nonmarine, time-equivalent of the subsurface Vicksburg Group (Baker, 1979, p. 36).

The hydrogeologic units are, from youngest to oldest: Permeable zone A (Holocene-upper Pleistocene deposits); permeable zone B (lower Pleistocene-upper Pliocene deposits); permeable zone C (lower Pliocene-upper Miocene deposits); zone D confining unit (middle Miocene deposits); permeable zone D (middle Miocene deposits); zone E confining unit (lower Miocene deposits); permeable zone E (lower Miocene-upper Oligocene deposits); Vicksburg-Jackson confining unit; upper Claiborne aquifer; middle Claiborne confining unit; middle Claiborne aquifer; lower Claiborne confining unit; lower Claiborne-upper Wilcox aquifer; middle Wilcox aquifer; Midway confining unit.

All but two of the units (zone D and zone E confining units exist only in the subsurface) crop out in bands that are essentially parallel to the coastline (fig. 5). Generally, the units dip south-southeastward toward the Gulf of Mexico and thicken in that direction. An exception is in the Sabine uplift in the northeast, where older units are again exposed at the surface and dip in all directions away from the uplift center.

The arrangement and subsurface extent of the hydrogeologic units that comprise the aquifer systems are shown by the hydrogeologic section in figure 6. The hydrogeologic section is useful in that it presents a simple, two-dimensional view of the interrelationship of aquifers, confining units, and hydrologic boundaries. The section was drawn through about the center of the study area and along a row of a finite-difference grid (fig. 2) that was used for digital modeling (to be discussed in the Appendix). It was constructed by using mean layer thickness values for the 25-mi² grid blocks. The line of section is nearly parallel to the dips of the units. The vertical scale is greatly exaggerated (more than 25 times); an absence of vertical exaggeration would show the attitude of the units as being more nearly horizontal.

Table 1.--Stratigraphic and hydrogeologic units for the coastal lowlands aquifer system.

SYSTEM	SERIES	TEXAS COASTAL LOWLANDS			HYDROGEOLOGIC UNIT NUMBERS IN THIS REPORT
		Modified from Baker (1979)		Grubb, 1987	
		STRATIGRAPHIC UNITS	HYDROGEOLOGIC UNITS	HYDROGEOLOGIC UNITS IN THIS REPORT	
QUATERNARY	HOLOCENE	Alluvium	CHICOT AQUIFER	Permeable zone A	1
	PLEISTOCENE	Beaumont Clay Montgomery Formation Bentley Formation Willis Sand		Permeable zone B	2
TERTIARY	PLIOCENE	Goliad Sand	EVANGELINE AQUIFER	Permeable zone C	3
	MIOCENE	Fleming Formation	BURKEVILLE CONFINING SYSTEM	zone D confining unit ^{1/}	4
		Oakville Sandstone		Permeable zone D	5
		Catahoula Sandstone or Tuff ^{2/}	CATAHOULA CONFINING SYSTEM (RESTRICTED) Jasper aquifer	zone E confining unit ^{1/}	6
		Anahuac Formation ^{1/}		Permeable zone E	7
	OLIGOCENE ^{2/}	"Frio" Formation ^{1/}			

^{1/} Present only in the subsurface

^{2/} Catahoula Tuff west of Lavaca County

Table 2.--Stratigraphic and hydrogeologic units for the coastal uplands aquifer system

		TEXAS COASTAL UPLANDS						
SYSTEM	SERIES	STRATIGRAPHIC UNITS Modified from Hosman and Weiss (1988)				STATE OF TEXAS MAJOR AND MINOR AQUIFERS (Muller and Price, 1979)	HYDROGEOLOGIC UNITS IN THIS REPORT (Hosman and Weiss, 1988)	HYDROGEOLOGIC UNIT NUMBERS IN THIS REPORT
		SOUTHERN		SOUTHEASTERN AND NORTHEASTERN				
TERTIARY	OLIGOCENE	Frio Clay	Vicks- burg Group ^{2/}	Frio Clay	Vicks- burg Group ^{2/}		Vicksburg-Jackson confining unit	8
	EOCENE	Jackson Group	Whitsett Formation	Whitsett Formation				
			Manning Clay	Manning Clay				
			Wellborn Sandstone	Wellborn Sandstone				
			Caddell Formation	Caddell Formation				
		Claiborne Group	Yegua Formation	Yegua Formaton			Upper Claiborne aquifer	9
			Laredo Formation	Cook Mountain Formation			Middle Claiborne confining unit	10
				Sparta Sand		Sparta ^{1/} (Minor aquifer)	Middle Claiborne aquifer	11
			El Pico Clay	Weches Formation			Lower Claiborne confining unit	12
	Queen City Sand			Queen City ^{1/} (Minor aquifer)				
	Bigford Formation		Reklaw Formation					
	Carrizo Sand	Carrizo Sand			Lower Claiborne- upper Wilcox aquifer	13		
	Wilcox Group	Undifferentiated	Undifferentiated	Carrizo- Wilcox (Major aquifer)	Middle Wilcox aquifer	14		
	PALEOCENE	Midway Group	Wills Point Formation	Wills Point Formation		Midway confining unit		
Kincaid Formation			Kincaid Formation					

- ^{1/} Not recognized west of Frio County
^{2/} Present only in the subsurface

The base of the combined systems is defined here as either the top of the Midway confining unit or the top of the geopressured zone. The geopressured zone occurs above the top of the Midway confining unit in downdip areas, where there is a transition from a predominantly sand facies to a predominantly clay facies. Very high pressures occur in this zone, which is evidence that hydraulic conductivities are very small with little or no upward migration of water. The top of the zone of geopressure is mapped by Wallace and others (1981). The irregular nature of the top of the geopressured zone is evident in the section. Also evident is the irregular nature of the units themselves. In some areas, they may be exposed but pinch out downdip, or they may not be exposed but exist only in the subsurface.

Hydraulic Properties

Initial estimates of aquifer properties were obtained from the literature or from analyses of field data. These estimates were tested in a digital ground-water flow model, and calibration of the model leads to refined estimates in some areas and for most hydrogeologic units. The hydraulic properties described below were obtained from the calibrated model.

Horizontal Hydraulic Conductivity and Transmissivity

Hydraulic conductivity for aquifers and permeable zones in the Gulf Coast aquifer systems was estimated by analyzing and averaging hundreds of aquifer tests and specific-capacity tests (Prudic, 1991). Statistical analyses of hydraulic conductivity showed that four subareas could be distinguished within the study area that contain significantly distinct geometric mean values (fig. 7). The mean values for the coastal uplands aquifers in subarea 1 are higher than for those in subarea 2, whereas the values for the coastal lowlands permeable zones in subarea 4 are higher than for those in subarea 3 and are the highest in the entire study area.

The initial estimates of hydraulic conductivity were refined during calibration of steady-state and transient ground-water flow models. A comparison of field determinations of hydraulic conductivity with those derived from model calibration is shown in figure 7 for the four subareas. Simulated values range from not greatly different from field values to about 1.5 times greater than field values in subarea 2.

Mean, minimum, and maximum grid-block values of hydraulic conductivity for each aquifer and permeable zone in the study area as derived from model calibration are shown in table 3. The values are designated as uniform in four of the units. This designation is made because the units are relatively undeveloped and field-test data are lacking, and further refinement of hydraulic conductivity with resulting areal variation among the grid blocks was not warranted. The hydraulic conductivity values range from 1 ft/d in the lower Claiborne-upper Wilcox aquifer (downdip in the Winter Garden area) to 102 ft/d in permeable zone A (in eastern Texas). Means range from 10 ft/d in the middle Wilcox aquifer to 25 ft/d in permeable zone A.

Tests to analyze sensitivity of the model to changes in selected model variables (discussed fully in the Appendix) show that the model is most sensitive to a decrease in horizontal hydraulic conductivity.

The thickness of each aquifer and permeable zone was described in detail by Ryder (1988). The transmissivity of each aquifer and permeable zone as derived through the calibration of the digital flow model is shown in figures 8-16. In general, the transmissivity is smallest in the extreme updip and downdip grid blocks, where thicknesses generally approach zero. Transmissivity within the study area reaches a maximum of more than 40,000 ft²/d in three units: Permeable zone A (fig. 8), permeable zone D (fig. 11), and permeable zone E (fig. 12). In permeable zone A, the largest transmissivity is at the Texas-Louisiana boundary where the hydraulic conductivity of the zone is high. The largest transmissivity in permeable zones D and E is in downdip areas where the units have a large thickness.

Mean, minimum, and maximum grid-block values of transmissivity for each aquifer and permeable zone in the study area are shown in table 3. Values range from less than 500 ft²/d in each layer to about 50,000 ft²/d in permeable zone A. Means range from about 4,600 ft²/d in the middle Claiborne aquifer to about 10,400 ft²/d in permeable zone D.

Table 3.--*Horizontal hydraulic conductivity and transmissivity of aquifers and permeable zones based on model calibration*

[<, less than]

Aquifer or permeable zone	Horizontal hydraulic conductivity (feet per day)			Transmissivity (feet squared per day)		
	Mean	Minimum	Maximum	Mean	Minimum	Maximum
Permeable zone A	25	12	102	6,956	<500	50,065
Permeable zone B	23	2	25	10,262	<500	27,534
Permeable zone C	15	7	31	9,298	<500	26,813
Permeable zone D	16	8	21	10,383	<500	49,258
Permeable zone E	15	(uniform)		7,766	<500	47,020
Upper Claiborne aquifer	15	(uniform)		5,998	<500	23,101
Middle Claiborne aquifer	15	(uniform)		4,602	<500	22,915
Lower Claiborne- upper Wilcox	23	1	72	4,659	<500	30,922
Middle Wilcox aquifer	10	(uniform)		10,071	<500	34,688

Vertical Hydraulic Conductivity

The vertical hydraulic conductivity values in table 4 were derived through the calibration of a digital ground-water flow model, wherein flow across a confining unit is the product of the vertical hydraulic-head gradient, the area of the grid block, and the effective leakance. The vertical hydraulic conductivity of a unit divided by the unit's thickness is defined as leakance. Effective leakance is the harmonic mean of the leakances of the confining unit, the underlying aquifer, and the overlying aquifer.

The grid-block means of the vertical hydraulic conductivity of the aquifers and permeable zones in table 4 are generally a few orders of magnitude smaller than the horizontal hydraulic conductivity of the aquifers and permeable zones (table 3). Means of the vertical hydraulic conductivity of confining units are smaller than those of the aquifers and permeable zones, and the vertical conductivity of confining units below the Vicksburg-Jackson is smaller than for the confining units above. Vertical hydraulic conductivity ranges from 1.0×10^{-6} to 1.0×10^{-1} ft/d. Means range from 1.1×10^{-5} ft/d for the Vicksburg-Jackson confining unit to 3.8×10^{-3} ft/d for permeable zone A.

Tests to analyze sensitivity of the model to changes in selected model variables (discussed in the Appendix) show that the model is moderately sensitive to change in vertical hydraulic conductivity.

Storage Coefficient

The storage coefficient for the confined aquifers and permeable zones was estimated by applying a specific storage value of 1.0×10^{-6} ft⁻¹ times the layer thickness. This specific storage value is an approximate value for most confined aquifers (Lohman, 1972, p. 8).

The storage coefficient of unconfined aquifers is virtually equal to the specific yield, which means that nearly all of the water is released from storage by gravity drainage (Lohman, 1972, p. 8). The lower Claiborne-upper Wilcox aquifer has an exceptionally high percentage of sand relative to other aquifers and permeable zones in the study area (Ryder, 1988, table 3; Hosman and Weiss, 1988, fig. 33). The sand has been significantly de-watered in parts of the outcrop because of intense withdrawal in the agricultural Winter Garden area. An initial specific yield of 0.2 was assumed for this unit in its outcrop area; this is the average value between the general limits of 0.1 and 0.3 for unconfined aquifers (Lohman, 1972, p. 54). The value was reduced during model calibration to a maximum of 0.15.

Some of the shallow sands in the outcrop of units other than the lower Claiborne-upper Wilcox aquifer undoubtedly have storage coefficient values appropriate for unconfined aquifers. However, for modeling purposes, it is assumed that there is no significant change in the shallow water table because (1) the sands are recharged sufficiently by precipitation and return flow from applied irrigation water, or (2) there is no significant ground-water withdrawal in the proximity of the sands. Thus, in the digital model a confined storage coefficient is assigned to these units.

Values of storage coefficient in table 5 are as large as 0.15, which is the estimated specific yield in the unconfined part of the lower Claiborne-upper Wilcox aquifer. Means range from 5.2×10^{-4} for the middle Claiborne aquifer to 1.7×10^{-3} for the middle Wilcox aquifer and permeable zone C.

Storage in confining units is considered negligible. However, significant amounts of water may be released from storage in younger clay beds in permeable zones A, B, and C when sufficient declines in head cause the beds to compact inelastically. The release of water by inelastic compaction of fine-grained deposits in these permeable zones causes land-surface subsidence. A digital model code incorporated from Leake and Prudic (1989) provides for the release of water by inelastic compaction of fine-grained deposits by converting from an elastic to an inelastic specific storage. This is done for the clay portion of a permeable zone when the head in a grid block declines below the critical head. The critical head is defined as the head that coincides with the maximum effective stress to which the deposits had previously been subjected.

Table 4.--*Vertical hydraulic conductivity of aquifers, permeable zones, and confining units based on calibrated model*

Aquifer, permeable zone, or confining unit	Vertical hydraulic conductivity (feet per day)		
	Mean	Minimum	Maximum
Permeable zone A	3.8×10^{-3}	2.4×10^{-6}	1.0×10^{-1}
Permeable zone B	1.3×10^{-3}	1.0×10^{-6}	5.0×10^{-2}
Permeable zone C	8.0×10^{-4}	5.3×10^{-6}	5.0×10^{-2}
Zone D confining unit	1.1×10^{-4}	1.0×10^{-4}	1.7×10^{-4}
Permeable zone D	1.3×10^{-4}	1.0×10^{-5}	8.3×10^{-4}
Zone E confining unit	1.1×10^{-4}	1.0×10^{-4}	1.3×10^{-4}
Permeable zone E	2.1×10^{-4}	1.0×10^{-4}	1.0×10^{-2}
Vicksburg-Jackson confining unit	1.1×10^{-5}	1.0×10^{-5}	1.5×10^{-5}
Upper Claiborne aquifer	2.3×10^{-3}	1.0×10^{-3}	5.0×10^{-2}
Middle Claiborne confining unit	4.1×10^{-5}	4.0×10^{-5}	5.4×10^{-5}
Middle Claiborne aquifer	4.6×10^{-4}	1.0×10^{-5}	1.0×10^{-2}
Lower Claiborne confining unit	2.1×10^{-5}	2.0×10^{-5}	3.4×10^{-5}
Lower Claiborne-upper Wilcox aquifer	2.0×10^{-3}	2.0×10^{-6}	1.0×10^{-2}
Middle Wilcox aquifer	1.0×10^{-4}	1.2×10^{-6}	1.2×10^{-3}

Table 5.--*Calibrated storage coefficient for aquifers and permeable zones, and inelastic specific storage for compacting clays*

Aquifer or permeable zone	Storage coefficient (dimensionless)		inelastic specific storage (ft ⁻¹)
	Mean	Maximum	
Permeable zone A	6.0 X 10 ⁻⁴	9.4 X 10 ⁻⁴	8.5 X 10 ⁻⁵
Permeable zone B	1.3 X 10 ⁻³	4.4 X 10 ⁻³	8.0 X 10 ⁻⁵
Permeable zone C	1.7 X 10 ⁻³	4.9 X 10 ⁻³	8.0 X 10 ⁻⁶
Permeable zone D	1.5 X 10 ⁻³	5.1 X 10 ⁻³	---
Permeable zone E	1.2 X 10 ⁻³	4.4 X 10 ⁻³	---
Upper Claiborne aquifer	7.8 X 10 ⁻⁴	2.5 X 10 ⁻³	---
Middle Claiborne aquifer	5.2 X 10 ⁻⁴	2.5 X 10 ⁻³	---
Lower Claiborne-upper Wilcox aquifer	5.7 X 10 ⁻⁴	0.15 ^{1/}	---
Middle Wilcox aquifer	1.7 X 10 ⁻³	5.2 X 10 ⁻³	---

^{1/} Specific yield assigned in outcrop area.

When the critical head decline is reached in model simulation, the initial specific storage value of $1.0 \times 10^{-6} \text{ ft}^{-1}$ is increased by factors of 85, 80, and 8 for the clay portions of permeable zones A, B, and C, respectively, in the Houston-Galveston area (table 5). These factors were determined during model calibration and resulted from matching land subsidence in model simulations to measured values. The details of observed and simulated land-surface subsidence will be discussed in the Appendix.

Dissolved-Solids Concentration and Density of Water

The concentration of dissolved solids in water is commonly used as an indication of the water's suitability for use. The terms used to describe water salinity in this report are as follows (Hem, 1985, p. 157):

Dissolved solids concentration (mg/L)

Fresh	0 - 1,000
Slightly saline	1,000 - 3,000
Moderately saline	3,000 - 10,000
Very saline	10,000 - 35,000
Briny	More than 35,000

Freshwater requires little or no treatment for most public and industrial use. Slightly saline water is marginal for many uses and often requires treatment or mixing with less mineralized water. The general term "saltwater" is used to describe water that is not fresh.

The areal distributions of dissolved-solids concentrations in water for the aquifers and permeable zones are shown in figures 17-25. The maps, modified from Pettijohn and others (1988), were generated from two types of data; (1) chemical analyses of water where dissolved-solids concentrations are less than 10,000 mg/L, and, (2) borehole geophysical log interpretations where concentrations are equal to or greater than 10,000 mg/L. Because concentrations of dissolved solids vary with depth within a given aquifer or permeable zone, a depth-integrated average dissolved-solids concentration was calculated for each 100-mi² grid block (regional grid, see fig. 2) in order to construct the maps (Pettijohn and others, 1988).

Dissolved-solids concentrations generally increase in a downdip, Gulfward direction. For most of the units, particularly the coastal lowlands permeable zones, dissolved-solids concentrations are higher in the west than in the east. Dissolved-solids concentrations range from less than 500 mg/L for nearly all of the units to 150,000 mg/L in a downdip area of permeable zone E (fig. 21). The areal extent of fresh to slightly saline water (dissolved-solids concentration less than 2,000 mg/L) is particularly small in permeable zone E (fig. 21) and in the upper Claiborne aquifer (fig. 22). This is apparently due, at least in part, to zone E confining unit and to the intervening, poorly permeable Vicksburg-Jackson confining unit, with a consequent restricted and sluggish flow system for these units.

When the dissolved-solids concentration of water approaches about 10,000 mg/L, the greater density of the water will begin to affect substantially its flow characteristics within the aquifer system. The technical aspects of variable density ground-water flow are explained by Kuiper (1985) whose model was used to simulate the flow system. Density of water in the aquifers and permeable zones was calculated by using a linear relation between density and dissolved-solids concentration (J.S. Weiss, U.S. Geological Survey, written commun., 1985). Density was corrected for the effects of mean water temperature and hydrostatic pressure at each grid block (A.K. Williamson, U.S. Geological Survey, written commun., 1987) before inclusion into the variable-density flow model. Grid-block values of density estimated for aquifers and permeable zones were assigned to subjacent confining units for modeling purposes. A statistical summary of water density (corrected for temperature and pressure) is given in table 6. Mean values range from 1.001 gram per cubic centimeter (g/cm^3) for the lower Claiborne-upper Wilcox aquifer to 1.027 g/cm^3 for zone D confining unit.

Table 6.--*Estimated density of water in the hydrogeologic units*

Aquifer, permeable zone, or confining unit	Water density at atmospheric pressure, 20 degrees Celsius (grams per cubic centimeter)		
	Mean	Minimum	Maximum
Permeable zone A	1.004	0.995	1.029
Permeable zone B	1.006	.995	1.048
Permeable zone C	1.019	.994	1.069
Zone D confining unit	1.027	.997	1.068
Permeable zone D	1.019	.994	1.087
Zone E confining unit	1.024	.995	1.087
Permeable zone E	1.020	.990	1.072
Vicksburg-Jackson confining unit	1.016	.990	1.072
Upper Claiborne aquifer	1.011	.988	1.047
Middle Claiborne confining unit	1.010	.988	1.047
Middle Claiborne aquifer	1.003	.990	1.046
Lower Claiborne confining unit	1.003	.994	1.046
Lower Claiborne-upper Wilcox aquifer	1.001	.988	1.020
Middle Wilcox aquifer	1.005	.989	1.047

REGIONAL FLOW SYSTEM

The predevelopment flow system was described in detail by Ryder (1988). He presented simulated predevelopment potentiometric-surface maps for each aquifer and permeable zone discussed herein. Further model calibration has resulted in considerably less flow in the predevelopment flow system than was previously reported but little change in potentiometric surfaces. The newer flow values are presented, including a map of recharge and discharge in the outcrop areas and a summary of vertical flow components for each layer. Changes in the flow system from predevelopment to 1982 are described, and a quantitative analysis of the simulated regional flow system for 1982 is presented.

Predevelopment Steady-State Flow System

The flow system prior to development is assumed to be a steady-state system in which inflow from the recharge areas is equal to outflow in the discharge areas. There is no net accretion to or release of water from storage in the aquifer systems. The assumption of steady state seems reasonable over long-term conditions. Climatic changes, sea-level changes, and tectonic movements that may have been occurring over the past hundreds or thousands of years have been neither rapid nor significant enough to preclude the establishment of steady-state conditions.

Conceptual Model of System

Water in the Texas Gulf Coast aquifer systems generally originates as precipitation that falls on the outcrops of the various hydrogeologic units. Most of the precipitation is returned to the atmosphere by evaporation and by plant transpiration. Much of the remaining precipitation runs into streams that drain into the Gulf of Mexico, while a small amount, on the order of a few inches per year, infiltrates to the water table in topographically high parts of the outcrops. After reaching the water table, most of the water moves downgradient for relatively short distances and is discharged in topographically low areas in the outcrop, in the form of evapotranspiration, seepage, and stream baseflow. A smaller, but significant part of the water enters a deeper confined part of the aquifer where vertical head gradients cause upward or downward leakage into adjacent units.

A variation of the above conceptual model occurs in the southwestern part of the study area. Westward from a line through Corpus Christi and San Antonio, average annual precipitation ranges from about 30 to about 21 in.. In this area of lesser precipitation, many of the streams are intermittent, and streamflow that does occur is often a source of recharge to the aquifers. Although springs and seeps generally are not visible, it is probable that a small, net ground-water discharge occurs in topographically low areas. Ground water is discharged principally by evapotranspiration in this part of the study area, with transpiration by phreatophytes, such as pecans, salt cedars, and mesquite, having a major role.

The conceptual model of the aquifer systems consists of four aquifers, five permeable zones, and six confining units as shown in figure 26. The water table in the uppermost 150 ft of the outcrop areas of the units is assumed to be at a constant altitude, thus providing recharge to and discharge from the deeper parts of the flow system. The relation between the conceptual model of the system and the digital model also is shown in figure 26. The construction of the digital model was discussed in detail by Ryder (1988) and is summarized in the Appendix.

Recharge and Interaquifer Leakage

Simulated values of recharge and discharge in the outcrop areas of the hydrogeologic units under predevelopment conditions are shown in figure 27. The pattern of recharge and discharge is a reflection of topography, with recharge occurring on topographically high areas, and discharge occurring in the stream valleys, low-lying coastal areas, and in the Gulf. The highest values of recharge, 1 to 3 in/yr, were simulated over relatively small areas. Generally, values of recharge and discharge are between 0 and 1 in/yr. The average recharge in the study area is 0.34 in/yr. Because the discharge area is larger, the average discharge rate is only 0.18 in/yr. For those wanting a more detailed discussion of the technical aspects of recharge and interaquifer leakage, see Ryder (1988, p. 102-103).

A summary of the upward, downward, and net vertical flow rates for the outcrop and downdip parts of each aquifer and permeable zone is given in figure 28. The rates are for the study area only. The net leakage is always upward into the overlying unit. Net leakage rates range from nearly 0 out of the lowermost unit to 24 million ft³/d into the uppermost unit.

Simulation indicates a total recharge in the outcrop areas of 85 million ft³/d. The middle Claiborne aquifer receives the largest share, 16 million ft³/d, closely followed by permeable zones B, A, and C with 15, 13, and 13 million ft³/d, respectively. Because steady-state conditions are assumed, the total recharge rate of 85 million ft³/d is offset by an equal rate consisting of discharge in the outcrop (79 million ft³/d) and net lateral flow out of the study area (6 million ft³/d). Of the discharge in the outcrop areas, permeable zone A was simulated as discharging the most—37 million ft³/d or nearly 50 percent of the total. Factors that account for the large rates of recharge and discharge in permeable zone A are its relatively large outcrop area, and its relatively large values of vertical and horizontal hydraulic conductivity.

Flow System, Predevelopment to 1982

A digital ground-water flow model was calibrated for transient conditions, predevelopment to 1982, and is discussed in detail in the Appendix. Some model input data and results are presented here to quantify changes in the flow system from predevelopment to 1982, and to provide a quantitative description of the regional flow system in 1982.

Ground-Water Development

The estimated average pumping rates for selected time intervals for 1910-82 are shown below (for modeling purposes, it is assumed that there was no significant regional development prior to 1911):

Pumping period	Time interval	<u>Average pumping rate</u>	
		(Million ft ³ /d)	(Million gal/d)
1	1910	0	0
2	1911-37	34	254
3	1938-47	62	464
4	1948-57	122	913
5	1958-62	156	1,167
6	1963-67	189	1,414
7	1968-72	221	1,653
8	1973-76	222	1,661
9	1977-81	231	1,728
10	1982	231	1,728

The pumping rates were relatively small and constant from 1911 to the late 1930's; rates nearly doubled during the 1940's, and doubled again during the 1950's. Increases in pumping rates were smaller after 1957, and a leveling-off of rates is apparent after 1968.

Cumulative volumes of withdrawal, net recharge, and release of water from storage in the Texas Gulf Coast aquifer systems are shown in figure 28a. These values are simulated by the model for the period 1910-82. By 1982, an estimated 3.2 trillion ft³ of water had been withdrawn from the aquifer systems. Of this, 2.4 trillion ft³ or 75 percent had been derived from recharge, and 0.8 trillion ft³ or 25 percent had been derived from storage in aquifers and compacting clay beds.

The withdrawal distribution for 1980 was used for the simulation periods 1977-81 and 1982. Details of the withdrawal estimates are in the Appendix (see section "Hydrologic Input Data"). In 1980, total withdrawal from the aquifer systems in the study area was 231 million ft³/d (1.73 billion gal/d). About 90 percent of the withdrawal was from 4 units: Permeable zones A, B, and C, and the lower Claiborne-upper Wilcox aquifer. The remaining two permeable zones and three aquifers were relatively undeveloped. The areal distribution of 1980 withdrawal for each aquifer and permeable zone is shown in figures 29-37. The withdrawal is shown by 25-mi² grid block, where withdrawal for a block equals or exceeds 0.5 Mgal/d.

Withdrawal for permeable zone A is shown in figure 29. The largest withdrawal is centered in Jackson and Wharton Counties. Moderate to large withdrawal extends southward to the coast and eastward into Harris County. In 1980, permeable zone A was the most intensively pumped unit in the study area.

Intense withdrawal from permeable zone B is centered in Harris County, with moderate withdrawal extending into Galveston County (fig. 30). There is moderate withdrawal in updip areas in Colorado, Lavaca, Jackson, and Victoria Counties. Permeable zone B was the second most intensively pumped unit in 1980.

Intense withdrawal from deep wells in permeable zone C also is centered in Harris County (fig. 31). Withdrawal from permeable zones D and E, and from the upper and middle Claiborne aquifers is relatively small (figs. 32-35).

Withdrawal from the lower Claiborne-upper Wilcox aquifer is moderate to large in the western counties of Zavala, Dimmit, Frio, La Salle, Atascosa, and Wilson (fig. 36). Withdrawal is relatively small and scattered in the central and eastern areas. This was the third most intensively pumped unit in 1980. Scattered and relatively small withdrawal from the middle Wilcox aquifer occurs in the central and eastern areas (fig. 37).

Recharge, Discharge, and Distribution of Flow, 1982

The concept of a shallow water table that is replenished by precipitation and kept at an essentially constant altitude on an average annual basis is valid for undeveloped areas, and probably for developed areas receiving a large amount of precipitation such as in the east. In some areas, however, such as in the west where withdrawal is large and precipitation is relatively small, dewatering has caused the water table to decline over the years.

The head for the water table is held constant through time, but the flow into or out of the boundary layer is the product of the vertical gradient between the constant head and the head in the aquifer, and the conductance to flow between the two layers. This conductance is the harmonic mean conductance of the bottom one-half of the constant-head grid block and the top one-half of the aquifer grid block. The amount of flow into or out of the constant-head layer can be reduced (to zero, if desired) by reducing the conductance in the desired grid blocks during model calibration.

For the permeable zones of the coastal lowlands system, the extremely large amount of vertical anisotropy, caused by the numerous interspersed clay layers, precludes the existence of water-table conditions except in the shallowest sands in the upper few feet or few tens of feet in the outcrop areas. It is assumed that these shallow sands are recharged sufficiently by precipitation and by return flow from applied irrigation water so that there is no increase or decrease in the shallow water table on a long-term basis.

There are suggestions by some investigators of a long-term rise in the shallow water table in agricultural areas because of return flow from applied irrigation water. Evidence to substantiate this is lacking. Long-term observation of the water level in a shallow well in an intensively pumped area of Jackson County shows a long-term decline (to be discussed in detail in the next section). It is not known whether the water-level change in this one well is representative of a regional water-level change in the shallow sands. In the absence of further evidence, it is assumed that there is no long-term change in the shallow water table that would significantly affect the rates of recharge, discharge, and storage changes as computed in the model simulations.

Simulated values of recharge and discharge in the outcrop areas of the hydrologic units for the final year of the model simulation, 1982, are shown in figure 38. Two features are apparent in figure 38 when compared to predevelopment recharge (fig. 27): The decrease in size of discharge areas compared to recharge areas, and the appearance of high rates of recharge in the central and western parts of the study area. Thus, ground-water development causes a decrease in natural discharge as well as an increase in recharge.

The average 1982 recharge in the study area is 0.52 in/yr, and the average discharge rate, excluding withdrawal, is 0.15 in/yr. As much as 6 in/yr of recharge occurs in Wharton and Jackson Counties. In this and adjacent areas, there is concentrated withdrawal for irrigation (mainly rice) from updip parts of permeable zones A and B. In these areas, the water withdrawn is supplied by local recharge. Where ground water is withdrawn for irrigation in outcrop areas, a considerable amount of applied irrigation water may reenter the aquifer by downward percolation. Jorgensen (1975, p. 55) estimated that as much as 30 percent of ground water pumped for irrigation in the Katy area returned to the Chicot aquifer (permeable zones A and B; table 1). The Katy area is an area west of Houston that includes parts of Harris, Waller, and Fort Bend Counties; recharge in this area is as much as 5 in/yr (fig. 38). Thus, the recharge rates in figure 38, and as discussed generally in this report, may also include a considerable amount of return flow from irrigation in certain areas.

Another location of relatively high recharge, up to 4 in/yr, is in and near the outcrop of the lower Claiborne-upper Wilcox aquifer in northern Zavala and northern Frio Counties. This is also an area of intensive withdrawal for irrigation, and return flow from irrigation water probably makes up a substantial part of the recharge as shown in figure 38. Mackey (1987) estimated that as much as 54 percent of irrigation withdrawal from the sand and gravel High Plains aquifer is returned to the aquifer in part of the panhandle area of northwest Texas. The similar nature of the aquifer materials and hydrologic conditions suggest that this higher value of return flow could be applicable to Zavala and Frio Counties.

Concentrated withdrawal for municipal and industrial use in the Houston-Galveston area is mainly from deep wells in highly confined permeable zones. Excess water is generally discharged to surface drainage systems, with little opportunity for return to the ground-water system. Recharge in the immediate vicinity is restricted by intervening clay beds. Deep cones of depression are developed until the cones intercept sufficient recharge, or derive additional water from storage mainly from inelastic compaction of clays to satisfy withdrawal. Recharge tends to be less in the Houston-Galveston area compared to the rice-irrigation areas in Wharton and Jackson Counties, as shown in figure 38.

The difference in simulated rates of recharge and discharge in the outcrop areas between predevelopment and 1982 is shown in figure 39. The area of greatest increase in recharge or decrease in discharge is in the updip areas of permeable zones A and B extending from the Guadalupe River in the south to the Trinity River in the east. Although the area south of Houston has changed from a discharging to a recharging area, the increased recharge is small when considering that there is large withdrawal in this area. Gabrysch (1977) reported that the presence of the Beaumont Clay overlying the permeable zones in this area restricts recharge.

A more moderate increase in recharge is in the coastal uplands units in western and northern Zavala County, and in the northern parts of Frio, Atascosa, and Wilson Counties. Another area of substantial increase in recharge, but of much less areal extent, is in the coastal uplands units along the Brazos River, near the junction of Milam, Robertson, Burleson, and Brazos Counties. Moderate to large withdrawal for irrigation and municipal supplies in this area is from several aquifers. Substantial but relatively smaller increases in recharge in other areas are scattered and of small areal extent.

A summary of outcrop recharge, outcrop discharge, vertical leakage, withdrawal, and change in storage in each hydrogeologic unit in the study area for 1982 is shown in figure 40. For the combined units, net recharge in the outcrop areas supplied 76 percent of the total discharge (withdrawal plus a small amount of lateral outflow), while 24 percent of the discharge was derived from depletion of storage in aquifers and inelastic compaction of clay beds. Highest net recharge rates were in the outcrops of the four most intensively pumped units: permeable zones A, B, and C, and the lower Claiborne-upper Wilcox aquifer. Nearly 47 percent, or 84 million ft³/d, of the net recharge was into the most intensively pumped unit--permeable zone A.

Net downdip leakage tended to be from a unit with lesser withdrawal into an overlying or underlying unit with greater withdrawal. The highest rate of net vertical leakage was 6 million ft³/d upward into permeable zone C from permeable zone D.

The change in the flow system between predevelopment and 1982 is dramatic. Flow through the system has more than tripled. Withdrawal in 1982 was almost three times the predevelopment recharge rate, as seen in the following summary:

RECHARGE AND STORAGE (million ft ³ /d)		DISCHARGE: (million ft ³ /d)	
<u>Predevelopment conditions</u>			
Total recharge	85	Outcrop discharge	79
		Lateral outflow	6
<u>1982 Conditions</u>			
Total recharge	219	Pumpage	231
Decrease in storage	57	Outcrop discharge	40
	<u>276</u>	Lateral outflow	<u>5</u>
			276

SUBREGIONAL FLOW SYSTEMS AND HYDROLOGIC EFFECTS OF DEVELOPMENT

For a more detailed analysis of the flow system, the study area was divided along model rows into four model subareas, labeled I through IV in figure 41. The lines separating the subareas were chosen to be nearly parallel to flow lines in the various hydrogeologic units, or to follow approximately the axes of ground-water divides located between cones of depression developed on the 1982 potentiometric surfaces of intensively pumped hydrologic units (model layers).

Six intensively pumped areas were selected for further description and model analysis; they are the circled areas in figure 41 and are labeled 1 through 6. The areas were selected on the basis of large withdrawal that has caused significant declines in heads over a substantial area, with present or potential adverse hydrologic effects. The six areas nearly coincide with six "critical areas" proposed for this part of the State by the Texas Water Commission (written commun., 1986). The Commission defined a critical area as an area that is experiencing or that is expected to experience critical ground-water problems. The six circled areas in figure 41 are referred to in this report as the:

1. Houston-Galveston area.
2. Coastal rice-irrigation area.
3. Evadale-Beaumont area.
4. Kingsville area.
5. Winter Garden area.
6. Lufkin-Nacogdoches area.

Houston-Galveston Area

The Houston-Galveston area, area 1 in figure 41, comprises all or parts of eight counties: Chambers, Galveston, Brazoria, Fort Bend, Waller, Harris, Montgomery, and Liberty. Ground-water withdrawal data for 1960-85 for counties with the most intense withdrawal within area 1 are shown in figure 42. Withdrawal in

Waller and Fort Bend Counties in the west is predominantly for irrigation use, and withdrawal in Brazoria County in the south is about evenly divided between irrigation use and nonirrigation use. Withdrawal in Harris and Galveston Counties in the east is predominantly for municipal and industrial use. Withdrawal in Harris County is larger than the combined withdrawal from the other counties in area 1, with a total pumping rate of 380 Mgal/d in 1985. The most apparent trends in withdrawal are the declines in pumping rates in Harris and Galveston Counties since 1970 (fig. 42).

In reports that describe this area, several local areas have been defined as shown in figure 43. These are: Katy, Houston, Pasadena, Baytown-Laporte, Johnson Space Center, Alta Loma, and Texas City. Average rates of withdrawal in each local area for 1979 are also shown in figure 43. In the Katy area, recent municipal withdrawal has been added to the agricultural withdrawals that were used primarily for rice irrigation. The Houston area includes the city of Houston and the surrounding metropolitan area. Ground-water withdrawals are primarily for municipal use. Flowing wells (with depths ranging from about 700 to 1,300 ft) were common in the area in the 1890's; heads were 15 to 30 ft above land surface. Historically, withdrawals in the Houston area have steadily increased. In 1930, average private and public withdrawal in the Houston area was 52 Mgal/d. By 1932, water levels had lowered to 80 ft below land surface in downtown Houston (White and others, p. 10-11, 1932). Vertical gradients are now downward from the water table in most of the Houston area, which means there is a potential for deeper units to receive recharge from the water table. This is consistent with model simulation results.

The Pasadena area is east of Houston and includes a heavily industrialized zone along the Houston Ship Channel. In 1937, a Pasadena paper mill added 19 Mgal/d of ground-water withdrawals to the area which accelerated water-level declines (White, 1938). This area has experienced large ground-water withdrawals since 1937, with peak usage in 1968. Surface water has also been used throughout the history of development, but in 1977 surface water became the primary source of water for the area. The adjoining areas of Baytown-Laporte and the Johnson Space Center also experienced drastic reductions in industrial ground-water withdrawal when surface-water use was increased in the mid-1970's.

In the Alta Loma area, ground-water withdrawals are used for public supply for the town of Alta Loma and the city of Galveston. At the "old" Alta Loma well field in Galveston County, heads in wells ranging from 726 to 868 ft deep were 28 feet above land surface in 1893; by 1939 water levels were 45 to 50 feet below land surface (Petitt and Winslow, 1955, p.24). Ground-water withdrawals gradually increased in the County, mostly as a result of industrial expansion in the Texas City area. Since the early 1970's, ground-water use in the Alta Loma and Texas City areas has decreased substantially because of increased reliance on surface water.

Withdrawal in the Houston-Galveston area is from permeable zones A, B, and C. The 1980 withdrawal distribution by layer and by model grid block is shown in figures 29-31. Withdrawal has created large cones of depression in the potentiometric surfaces of the three layers, with the centers located in the general area of the city of Houston. Head declines for permeable zones A, B, and C are shown in figures 44, 45, and 46, respectively. The maps were constructed by subtracting 1982 measured heads (mean heads in 25-mi² grid blocks) from measured predevelopment heads for each permeable zone. Maximum head declines range from nearly 200 ft for permeable zone A to more than 400 ft for permeable zone C.

Hydrographs of wells 9, 7, and 3 in figure 47 were selected for analysis because of their long-term record and close proximity of the wells to the centers of the cones of depression developed in permeable zones A, B, and C, respectively. The hydrograph for well 9, located in southeastern Harris County in the Baytown-Laporte area (fig. 43), shows a continuous water-level decline until about 1976, when a substantial recovery of water levels began and continued into the 1980's. The hydrographs for wells 7 and 3 located in the Houston area (fig. 43) show a more or less continuous decline in water levels from the early 1940's to the middle 1980's.

Well 9 is in an area of southeastern Harris County that has experienced severe land-surface subsidence. The large ground-water withdrawals have reduced the artesian pressure sufficiently to cause water from included and adjacent clay beds to flow into the sands. Water flows out of the compressible clays due to inelastic compaction which is largely irreversible. The loss of water from the clays results in a permanent loss of pore space. Land subsidence is approximately equivalent in volume to the reduction of pore space in the

compacted clays. As shown on figure 48, an area of about 2,000 mi² around the cities of Galveston and Houston has undergone subsidence of more than 1 foot. From the beginning of man's development up to 1973, maximum land subsidence of nearly 9 ft has been recorded (fig. 48). Gabrysch (1984b) noted that from 1906-78 the Pasadena area east of Houston may have experienced as much as 10 ft of land subsidence.

Subsidence in low-lying areas of Harris and Galveston Counties, combined with proximity to the Gulf of Mexico, has increased the risk of flood damage to residential and commercial properties. Subsidence has also caused activation of faults, and this has led to structural damage (Harris-Galveston Coastal Subsidence District, written commun., 1983). With the creation of the Houston-Galveston Coastal Subsidence District in 1975, there has been a growing emphasis on reduction of ground-water withdrawal coupled with an increased reliance on surface-water supplies. Pumping rates in the late 1970's and early and middle 1980's were substantially reduced in much of southeastern Harris County and in Galveston County; this has caused a recovery of water levels and a cessation or sharp decrease in the rate of land-surface subsidence in that area.

In addition to the head declines in permeable zones A, B, and C, figures 44-46 show horizontal flow for these zones as simulated by the model for 1982. The ground-water flow directions and relative magnitudes are computed at the intersection of four adjacent grid blocks. A flow vector, as represented by an arrow on figures 44-46, is the vector addition of the average of the two adjacent X-direction flows and the average of the two adjacent Y-direction flows. The size of the arrowhead indicates the order of magnitude (integer component of the logarithm, base 10 (\log_{10})) of the flow, and the length of the arrow is proportional to the mantissa of the \log_{10} flow (Williamson and others, 1990, p. 76). The flow patterns are similar for the three zones, with the flow generally converging on areas that have the greatest amount of drawdown. The large withdrawals of ground water in the Houston-Galveston area have reversed the coastward hydraulic gradients causing saltwater to move toward the centers of pumping.

An interesting circulating pattern of ground-water flow is shown in offshore areas of permeable zone C (fig. 46). The circulation cells occur because of density forces resulting from heat and solute gradients as the denser, heavier water overturns to get under the fresher, lighter water (Williamson and others, 1990, p. 76).

The simulated average interstitial velocity of saltwater moving toward the pumping centers in 1982, assuming an effective porosity of 0.2 for the sands, is 22 ft/yr for permeable zone A, 41 ft/yr for permeable zone B, and 111 ft/yr for permeable zone C. These are average simulated velocities for water moving through the sands in each permeable zone (zones A, B, and C); water in individual sand beds may actually have greater or smaller velocity, depending upon permeability.

Lateral migration of saltwater was evident in 1954, when observation wells near the freshwater-saltwater interface in Harris County had an increase in chloride concentration of 122 mg/L since 1951 (Winslow and others, 1957). Saltwater contamination was also occurring in the shallower Chicot wells near the Houston Ship Channel (Baker and Wall, 1976). Changes in chloride concentrations with depth have been analyzed along the Ship Channel. The interpretations of the chemical data, along with head differences, indicate that saltwater is moving both vertically and laterally toward the Chicot aquifer (Jorgensen, 1977). The city of Galveston had to replace the Alta Loma well field northward because the "old" well field was contaminated by movement of saltwater from below and from downdip (Petit and Winslow, 1955).

A summary of 1982 withdrawal, change in storage, and vertical flow rates (recharge and leakage) for each unit in model subarea II is shown in figure 49. The area encompasses the major cones of depression developed in permeable zones A, B, and C in the Houston-Galveston area. About 90 percent of the total withdrawal in subarea II is from permeable zones A, B, and C. Small amounts of net lateral flow between model subareas are quantified by the "L" term in the diagram (fig. 49). On the basis of simulation, net recharge in the outcrop areas accounted for 68 percent of the total pumping rate of 102 million ft³/d (763 Mgal/d) for all units in subarea II. Net recharge includes a decrease of natural discharge and an increase in induced recharge. Part of the induced recharge may include a return flow from applied irrigation water, as discussed earlier. Twenty-eight percent of the pumping rate was derived from depletion of ground water in storage, and the remaining 4 percent was net lateral inflow from adjacent model subareas (I and III). Nearly 61 percent of the net recharge was in the outcrop of permeable zone A. The highest rate of net vertical leakage was 9 million ft³/d downward into permeable zone B from permeable zone A.

In the Houston-Galveston area, model results indicate that about 21.9 million ft³/d or 76 percent of the 29 million ft³/d of water released from storage from all model layers (fig. 49) during the 1982 simulation period was from inelastic compaction of clays in permeable zones A, B, and C. The following table summarizes the simulated rates of water released from storage from these permeable zones for 1982:

Hydrogeologic unit	Pumping rate in 1982 (million ft ³ /d)	Total rate of release of water from storage		Rate of release of water resulting from inelastic compaction of clays	
		Amount (million ft ³ /d)	Percent of pumpage	Amount (million ft ³ /d)	Percent of pumpage
Permeable zone A	35	0.9	2.6	0.8	2.3
Permeable zone B	35	12.3	35	11.9	34
Permeable zone C	22	10.8	49	9.2	42

For the combined zones A, B, and C, about 26 percent of the pumping rate of 92 million ft³/d is supplied from storage releases; about 24 percent of the pumping rate is supplied from the component of storage that results from inelastic compaction of clays.

Coastal Rice-Irrigation Area

The coastal rice-irrigation area is shown as area 2 in figure 41. It consists of most of Jackson and Wharton Counties and parts of Colorado, Lavaca, Victoria, and Matagorda Counties. Withdrawal is mainly for irrigation, as shown in figure 42 for Wharton, Jackson, and Matagorda Counties. Rice is the major crop in the area, and the two-crop rice season requires large amounts of water for irrigation.

Withdrawal in area 2 is mostly from permeable zone A. A substantial amount of water is withdrawn from permeable zone B, mainly in the outcrop area, but other hydrologic units are essentially undeveloped. The 1980 withdrawal distribution by grid blocks is shown in figures 29 and 30 for permeable zone A and permeable zone B, respectively. As mentioned previously, model results indicate that the water withdrawn in this area is supplied by local recharge. Water derived from artesian storage in the units has been relatively small, and steep cones of depression, such as those in the Houston area, have not developed.

Ground-water withdrawal began in the early 1900's. Originally, artesian pressures were large enough to produce flowing wells from the Chicot and Evangeline aquifers (table 1). As pumping increased, most wells ceased to flow by the mid-1940's (Loskot and others, 1982, p. 33). In the early 1950's, there was a sharp increase in withdrawal because of a period of below-normal precipitation combined with the introduction of the two-crop rice season. The largest water-level declines from 1944 to 1964 were in the western section of Wharton County and in the southeastern section of Jackson County. In western Matagorda County from 1944 to 1967, withdrawal for irrigation resulted in water-level declines of as much as 52 ft (Hammond, 1969, p. 32).

Hydrographs of wells 14a and 15 in Jackson County are shown in figure 50, as is a graph of mean annual precipitation in southwestern Wharton County. Well 14a is located in northwestern Jackson County near intense withdrawal in permeable zone A. However, the well is only 76 ft deep, and is open to the

Holocene alluvium above the intensively pumped zone. The water table in well 14a has declined at a rate of about 0.6 ft/yr since the late 1930's, with periods of partial recovery in 1958-61 and 1969-74 when precipitation was at or above normal (fig. 50). Baker and Follett (1973, p.18) used this well and other data to conclude that shallow sands in the area have been dewatered on a long-term basis (nearly 40 years), and that recharge from rainfall has been unable to stabilize the water table. They further concluded that the reduction in the gradient of the water table toward the Lavaca River has probably reduced stream baseflow. However, it is not known whether the water-level change in this one well is representative of a regional water-level change in the shallow sands. In the absence of further evidence, it is assumed that there is no long-term change in the shallow water table that would significantly affect the rates of recharge, discharge, and storage changes as computed in the model simulations. Well 15 is open to permeable zone A and is in the vicinity of moderate to large withdrawal from that zone. The water level in well 15 has been declining at an average rate of about 1.4 ft/yr since the middle 1950's (the beginning of record).

The large withdrawal in the coastal rice-irrigation area has resulted in compaction of clays present within the permeable zones. From 1900 to 1975, the land surface subsided less than a foot over most of the area, but Carr and others (1985, fig. 37) show as much as 1.5 ft of subsidence in eastern Jackson and western Matagorda Counties. Because the subsidence is fairly evenly distributed over large, mostly rural areas, the undesirable effects sometimes associated with subsidence are minimized.

Saltwater encroachment is a potential threat in this area, either by lateral migration updip or by vertical migration where freshwater sands are overlain by saltwater-bearing deposits. Saltwater encroachment is not currently a serious threat to the quality of ground water used in the coastal rice-irrigation area.

Simulated horizontal flow vectors for permeable zone A show a general zone of convergence near the intersection of Jackson, Wharton, and Matagorda Counties (fig. 44) resulting from intense withdrawal. A summary of 1982 flow components for units within model subarea III is shown in figure 51. The simulated net recharge in the outcrop areas was 98 percent of the total pumping rate of 58 million ft³/d for all units. Nearly 67 percent of the net recharge was in the outcrop of permeable zone A. About 4 million ft³/d of water was released from storage in the simulations. A net lateral flow out of the model subarea amounted to about 3 million ft³/d. The highest rate of net vertical leakage was 5 million ft³/d upward into permeable zone A from permeable zone B.

Evadale-Beaumont Area

The Evadale-Beaumont area is area 3 in figure 42. Included in this area are large ground-water withdrawals at the city of Evadale in southwest Jasper County, and moderate withdrawals at the city of Beaumont's well field in southeast Hardin County (fig. 52). Withdrawal in Jasper County has been fairly constant since 1970, but withdrawal in Hardin County, mainly for nonirrigation use, has risen since 1975.

Withdrawal at Evadale is about evenly divided between permeable zone B and permeable zone C. Withdrawal in the Beaumont well field is from permeable zone B. The 1980 withdrawal distribution by grid blocks is shown in figures 30 and 31 for permeable zone B and permeable zone C, respectively. Prior to 1955, ground-water resources in the Evadale area were relatively undeveloped. Predevelopment water levels in the lowest sands of permeable zone C that contained freshwater (locally called the Evangeline aquifer; table 1), were 20 to 30 ft above land surface (Wesselman, 1967). In 1955, a paper mill began withdrawals of nearly 18 Mgal/d. Production increased to about 42 Mgal/d by 1970 and remained at approximately that rate through 1980. In Jefferson County, fresh ground-water supplies are limited. Prior to 1958, the city of Beaumont relied entirely on surface water. By 1965, Beaumont was pumping 6 Mgal/d from the well field in Hardin County. It was the approximate rate through 1980.

Sufficient data were available to map the head declines for permeable zone C at Evadale (fig. 46). The map was constructed by subtracting 1982 measured heads from measured predevelopment heads. The map shows between 150 and 200 ft of drawdown centered at Evadale, with the cone extending to surrounding counties.

Hydrographs of well 16 in Jasper County and well 17 in Hardin County are shown in figure 53. Well 16 is located near the center of the drawdown cone at Evadale and is open to permeable zone C. Between 1955 and 1967, the water level in well 16 declined about 190 ft. From 1968 to 1985, the water level declined only about 20 ft.

Well 17 is located near the city of Beaumont's well field and is open to permeable zone B. From about 1960 to 1968, the water level in well 17 declined 50 ft (about 5.5 ft/yr). During the next 6 years, the water level declined about 15 ft, and from 1974-82 was essentially stable (fig. 53).

In 1954, a network of bench marks was installed in and around the paper mill at Evadale to measure land-surface subsidence. The maximum differential subsidence from 1955 to 1963 was 0.228 ft (Wesselman, 1967, p. 58). This was at a point where the water-level difference, between the original reference point and the point of maximum subsidence, was about 25 ft. Recent measurements of subsidence are not available. However, if the ratio 0.228/25 is valid, the estimated maximum land-surface subsidence is nearly 2 ft at the center of the cone where the maximum drawdown is 210 ft.

Simulated horizontal flow vectors in figure 45 show an area of convergence in permeable zone B at the Beaumont well field, and another zone of convergence at Evadale. A similar flow pattern at Evadale is seen for permeable zone C (fig. 46). A summary of 1982 flow components for model subarea I is shown in figure 54. Model simulations show a net recharge in the outcrop areas that was 84 percent of the total discharge rate (pumping plus a small lateral outflow) for all units in subarea I. Sixteen percent of the discharge was derived from ground-water storage. The withdrawal was fairly evenly distributed among permeable zones A and B, the lower Claiborne-upper Wilcox aquifer, and the middle Wilcox aquifer (fig. 54).

Kingsville Area

The Kingsville area is designated as area 4 in figure 41. It consists of parts of Kleberg, Nueces, and Jim Wells Counties. Ground-water withdrawals are largest in Kleberg County (fig. 55), and withdrawal is concentrated in the city of Kingsville's well field located near the Kleberg-Nueces County line. Withdrawal in area 4 is mainly from permeable zone B (see fig. 30 for the 1980 grid-block distribution). Flowing wells existed in the area in the early 1900's, one of which was at the railroad station in Kingsville. This well, open at a depth of about 600 to 700 ft, was reported to have had an artesian head of 20 ft above land surface (Livingston and Bridges, 1936). From 1901 to 1935, ground-water withdrawal in the Kingsville area was about 2 Mgal/d, which included supplies to small municipalities and small-scale irrigation (Groschen, 1985, p. 15). Since then, a steady increase of municipal and industrial withdrawal has lowered water levels. The aggregate withdrawal for Kleberg, Nueces, and Jim Wells Counties has been relatively constant since 1970 at about 16 Mgal/d (fig. 55). Concentrated withdrawal in and near the city of Kingsville, about 6.5 Mgal/d in 1980, has created a steep cone of depression in the potentiometric surface of permeable zone B, with the center of the cone near Kingsville.

A map of the head decline in permeable zone B is shown in figure 56. It represents the difference between measured predevelopment heads and measured 1982 heads. The 1982 head measurements are taken from Groschen (1985, fig. 9), who related the heads to the confined portion of the Evangeline aquifer (table 1). The heads also are applicable to the pumped interval of permeable zone B in this area, the upper part of the Goliad Sand (table 1). Drawdowns exceed 200 ft at the Kingsville well field, and the cone of depression extends to surrounding counties (fig. 56).

A hydrograph of well 19 in Kleberg County is shown in figure 57. Well 19 is open to permeable zone B and is located a short distance west of the center of the drawdown cone. From 1933 to 1972, the water level in well 19 declined 155 ft or at an average rate of about 4 ft/yr. From 1972-85, the water level was essentially stable.

The large water-level declines and proximity to saltwater in overlying and underlying deposits and downdip have created the potential for movement of saltwater into the freshwater. In the Kingsville area, Groschen (1985, p. 17) considered the upper limit of dissolved-solids concentration of freshwater to be 2,000

mg/L. The major source of potential contamination is saltwater in the overlying deposits, as opposed to saltwater encroachment from the Gulf of Mexico (Groschen, 1985, p. 59). Originally, the hydrostatic pressure in the producing zone B was higher than in the overlying deposits which contain saltwater. As well discharges increased and exceeded recharge, the hydraulic gradient was reversed, creating the potential for saltwater to flow into the pumped zone. The natural quality of water in the producing zone is marginal for drinking, and any deterioration due to saltwater encroachment is of serious concern (Groschen, 1985, p. 5).

Some municipalities reportedly have experienced water-quality problems and have taken, or plan to take, corrective measures. The city of Alice in Jim Wells County has supplemented its ground-water supplies with surface water because of saltwater encroachment. Also because of saltwater encroachment, the cities of Agua Dulce, Banquette, Driscoll, and Bishop in Nueces County, and Kingsville in Kleberg County plan to supplement ground-water supplies with water from the Nueces River (Texas Department of Water Resources, 1984a, p. III-22-1). Groschen (1985, p. 58) concluded that the pumping from zone B in the Kingsville area has most likely not created water-quality degradation on a regional scale.

Although there have been large water-level declines in deposits that are similar in age to those in the Houston area, subsidence in the Kingsville area for 1917 through 1976 has been estimated at less than 0.3 ft (Muller and Price, 1979, p. 42).

Simulated horizontal flow vectors in figure 56 are shown converging on the center of the drawdown cone near Kingsville. The large flows to the southwest in Jim Hogg, Brooks, Starr, and Hildago Counties are not the result of ground-water withdrawal. Land-surface gradients, and thus the estimated water-table gradients, are steeper here than elsewhere in the study area, and ground water is flowing naturally in greater volume downdip toward the Gulf.

A summary of 1982 flow components for model subarea IV is shown in figure 58. Most of the withdrawal in model subarea IV is from the lower Claiborne-upper Wilcox aquifer in the Winter Garden area.

Winter Garden Area

The Winter Garden area is intensively pumped area 5 in figure 41. It is defined as all or major parts of Zavala, Dimmit, Frio, La Salle, and Atascosa Counties, and minor parts of Bexar, Wilson, and McMullen Counties. The combination of infrequent killing frosts and fertile soils make the Winter Garden area ideal for garden vegetables and other food crops. Relatively little precipitation (about 21 to 29 in/yr from west to east) and a general lack of surface-water resources necessitate the withdrawal of large amounts of ground water for irrigation. Withdrawal is almost entirely from the lower Claiborne-upper Wilcox aquifer.

During the early development of irrigation, flowing wells were common in the Winter Garden area. The artesian head southeast of Carrizo Springs was estimated to be 18 to 40 ft above land surface (Turner and others, 1948). A few springs flowed into Carrizo Creek in Dimmit County, but by 1929, with continued withdrawal, springs on the creek no longer flowed. In Atascosa County, the first flowing well was drilled in 1904 in the city of Poteet. In 1929-30, intensive withdrawal for irrigation was predominantly within 5 mi of Poteet. A drastic increase in withdrawal in the Winter Garden area beginning about 1950 was caused by widespread drought. Increases in population, industry, and irrigated acreage have caused higher rates of ground-water withdrawal.

Largest withdrawals for most years are in Zavala, Frio, Atascosa, Dimmit, and La Salle Counties, in that order (fig. 55). Withdrawals for the three most intensively pumped counties in 1980--Zavala, Frio, and Atascosa--were spread fairly evenly (see figures 55 and 36). The intense withdrawal, which has exceeded recharge in this relatively dry area, has been mostly from the deep, confined parts of the lower Claiborne-upper Wilcox aquifer, and has caused a very large cone of depression. The drawdown map shown in figure 59 represents the difference between measured predevelopment heads and measured 1982 heads in the lower Claiborne-upper Wilcox aquifer. The largest drawdowns, in excess of 250 ft, are in south-central Zavala County and at the boundary of southeastern Zavala and northeastern Dimmit Counties. Drawdowns exceed 100 ft in at least six counties (fig. 59).

Simulated horizontal flow vectors in figure 59 are shown converging in the vicinity of Zavala, Dimmit, Frio, and LaSalle Counties. Water is flowing toward the pumping center from a very large area, with the largest flows coming from the outcrop area.

Hydrographs of wells 23 and 24 and precipitation data in Zavala County are shown in figure 60. Well 23 is more than 1,000 ft deep in the confined part of the aquifer; it is located near the center of the cone of depression in south-central Zavala County. From 1947-56, the water level in well 23 declined 270 ft or about 27 ft/yr. The rapid decline resulted in large part from widespread drought conditions in the early and middle 1950's, when pumping demands were great and recharge rates minimal. Water levels recovered significantly in the late 1950's when precipitation returned to normal or above normal, but the trend continued downward in the 1960's until a decline of 355 ft below the 1947 level occurred in 1967 (fig. 60). A significant recovery occurred again beginning about 1968, and water levels appear to be relatively stable in the 1970's and 1980's.

Well 24 (fig. 60) is located in the outcrop of the lower Claiborne-upper Wilcox aquifer in the northeast corner of Zavala County. The well is relatively shallow (260 ft deep) and is in the proximity of moderate to large withdrawal in the downdip, confined parts of the aquifer. The water table in well 24 declined about 70 ft from 1953-67, or more than 4 ft/yr. From 1968-85, the water table declined about 25 ft, or about 1.5 ft/yr. Total decline for 1953-85 is about 95 ft, which means that a minimum of 95 ft of the aquifer has been dewatered in this area where the aquifer is unconfined.

Water-level declines in the Winter Garden area have produced undesirable effects, one of which is greater pumping lifts. In some cases, pump intakes have been lowered, wells deepened, or larger pumps installed. All of these factors result in increased pumping costs. In addition, saltwater is reported to be leaking downward from overlying deposits through old well bores and contaminating the aquifer. Muller and Price (1979, p. 18) noted that this problem is especially evident in Dimmit County, where saltwater from the overlying Bigford Formation is leaking downward through old well bores. The hydraulic gradient between the lower Claiborne confining unit and the lower Claiborne-upper Wilcox aquifer has been reversed as a result of the intense withdrawal. The old wells may have been poorly constructed initially or have been improperly plugged, and saltwater moves downward to mix with freshwater in the aquifer. Klemm and others (1976, p. 23) caution that continued increase in development of the aquifer could result in widespread contamination as a result of interformational leakage.

In model subarea IV (fig. 58), about 33 million ft³/d were pumped from the lower Claiborne-upper Wilcox aquifer during 1982 (nearly all in the Winter Garden area). Model results suggest that about 48.5 percent of the withdrawal was derived from aquifer storage (including dewatering of the aquifer), and about 39.4 percent was from net recharge in the outcrop area. The remaining 12 percent was from net upward leakage from the middle Wilcox aquifer (6 percent) and net downward leakage from the middle Claiborne aquifer (6 percent).

Lufkin-Nacogdoches Area

The Lufkin-Nacogdoches area, area 6 in figure 41, consists of most of Nacogdoches and Angelina Counties. There is concentrated withdrawal from industrial well fields located between the cities of Lufkin and Nacogdoches and straddling the Nacogdoches-Angelina County line (fig. 52). The two cities also maintain well fields for municipal supplies, and the combined withdrawal has created a steep cone of depression on the potentiometric surface of the lower Claiborne-upper Wilcox aquifer. Drawdowns of water levels near the pumping centers ranged to nearly 500 ft from the late 1930's to the late 1960's (William F. Guyton and Associates, 1970, p. 23). The major withdrawal is in Angelina County, and withdrawal from both counties has remained nearly constant during the 1970's and 1980's (fig. 52).

In 1907, hydraulic head in wells open to the Carrizo Sand (upper part of the lower Claiborne-upper Wilcox aquifer; table 2) in the city of Nacogdoches was as much as 40 ft above land surface (Deussen, 1914). The city of Nacogdoches began pumping from the Carrizo Sand in the early 1900's. After 30 yrs of pumping, water levels had declined about 39 ft. A large paper mill and the city of Lufkin began pumping from the

Carrizo Sand in the late 1930's. Since then, water levels in the Carrizo have declined as much as 500 ft near the center of pumping. The water-level declines become less severe as distance increases northward away from the paper mill and towards the outcrop of the Carrizo Sand.

According to William F. Guyton and Associates (1970), the cone of depression is causing some brackish water to move toward the Lufkin and paper mill well fields. The movement is slow, and periodic observations may allow sufficient time to relocate wells when necessary.

Head data are insufficient to construct an accurate map of the potentiometric surface for development conditions, but a few observation wells with long-term record exist near the pumping centers. One such well is well 37 located in Nacogdoches County a short distance east of the major pumping center at the large paper mill. A hydrograph of well 37 is shown in figure 61. The well is 900 ft deep and opens to the lower Claiborne-upper Wilcox aquifer. The water level in well 37 has declined almost continuously since the beginning of record in 1947, with a total decline of 300 ft. The rate of decline mainly reflects pumping rates; it was rapid in the earlier years and becomes more gradual until the 1980's, when there appears to be no further decline (fig. 61).

The pumping rate from the lower Claiborne-upper Wilcox aquifer in model subarea I was estimated at 8 million ft³/d for 1982 (fig. 54). More than one-half of this withdrawal is in the Lufkin-Nacogdoches area. Of the 8 million ft³/d of withdrawal, model results indicate that 25 percent is derived from decrease in aquifer storage, and the remainder is derived equally from recharge in outcrop areas and net downward leakage from the middle Claiborne aquifer.

Other Areas

Intense ground-water development has occurred in some areas without causing large, extensive cones of depression and without the threat of adverse effects, such as significant land-surface subsidence or aquifer dewatering. Two such areas are the Bryan-College Station area and most of Orange County.

Bryan-College Station Area

The Bryan-College Station area is located along the Brazos River, and includes parts of Brazos, Burleson, and Robertson Counties. Considerable amounts of ground water are pumped in this area for irrigation and municipal supplies (fig. 42). The water is being withdrawn from several aquifers, which has minimized drawdowns in any single unit. The Yegua Formation (upper Claiborne aquifer; table 2) crops out in a belt that runs through the Bryan-College Station area, and the Sparta Sand (table 2) crops out just north of the Brazos County line. Texas Agricultural and Mechanical University (Texas A&M) at College Station has pumped water from the Yegua Formation since the institution's establishment in 1886. By the 1970's, Texas A&M, College Station, and Bryan were all using water from wells in the Sparta Sand and Wilcox Group (table 2). In 1970, the city of Bryan was the largest user of ground water for public supply in Brazos and Burleson Counties (Follett, 1974).

In 1948, irrigation with water from the Brazos River alluvium began in Robertson County (Hughes and Magee, 1962, p.1). Little water was pumped from the alluvium prior to this date. But the drought of the early 1950's led to the search for additional quantities of water for irrigation on the flood plain (Cronin and Wilson, 1967 p. 1). From 1950-64, the number of irrigation wells pumping from the alluvium increased at a rapid rate. Withdrawal for irrigation decreased from 1964 to 1969, as Brazos County increased its surface-water use (Follett, 1974, p. 26). Approximately 98 percent of the ground water used for irrigation is pumped from the flood-plain alluvium, but no ground water is pumped from the alluvium for municipal uses.

By 1961, the water levels in the flood-plain alluvium had probably recovered from the intense pumping during 1950 to 1957 (Follett, 1974). Then, from 1961 to 1971, the water levels again declined in the flood-plain alluvium northwest of Bryan. According to Cronin and Wilson (1967, p. 32), the decline may have been the result of withdrawals from the underlying Sparta Sand (table 2), which is in direct hydraulic connection with the alluvium. Withdrawal from the Sparta Sand reduced the artesian pressure, which may have caused water from the alluvium to move downward in response to the change in head.

Orange County

The development of ground water in Orange County, located in southeast Texas, began relatively slowly. From 1910 to 1940, ground water was pumped for public supply, saw mills, railroads, and oil and gas production. By 1941, total ground-water withdrawal was only 2.6 Mgal/d (Wesselman, 1965, p.27). The principal source of water in this area is from the lower part of the Chicot aquifer (permeable zone B). In the early 1900's, prior to large-scale withdrawal, the deep wells had large artesian flows. In the city of Orange, the heads in the lower part of the Chicot aquifer were estimated to be about 25 to 30 feet above sea level (Wesselman, 1965, p. 28). The artesian pressure decreased as more wells were drilled and withdrawals increased. The demand for water increased during World War II, and by 1950 the declining heads caused all the deep wells to stop flowing (Wesselman, 1965, p.28). Because of increased withdrawal and below-normal rainfall, the potentiometric surface in 1962 was below sea level throughout most of the County. The largest declines have been in the southeastern part of the County, an area of moderate to large industrial withdrawal. Water levels rose throughout most of the County between 1980 and 1985 because of a decrease in withdrawals. Ground-water levels in the the city of Orange recovered as much as 14 ft (Bonnett and Williams, 1987, p. 24).

In the coastal area of Orange County, there is the potential for vertical (upconing) and lateral encroachment of saltwater. Upconing is likely to occur when sand beds containing saltwater are not separated by clay beds from the freshwater sands. In some areas of Orange County, thin layers of clay separate the freshwater sands from sands containing saltwater. Increased withdrawal from 1963 to 1980 led to an increase in chloride concentrations in wells in an industrial area near the city of Orange. The upconing is directly related to pumping, and is evident when wells with high chloride concentrations are surrounded by wells with lower chloride concentrations (Bonnet and Williams, 1987, p. 16-22). Movement of saltwater updip, toward the center of pumping, has also been observed in the lower part of the Chicot aquifer (table 1) in southeastern Orange County (Gabrysch and McAdoo, 1972, p. 10). From 1980 to 1984, the decreases in withdrawals have caused chloride concentrations to stabilize throughout the county.

Land-surface subsidence, resulting from decreased artesian pressures, has been measured in the area. Some parts of eastern and western Orange County have experienced more than 0.5 ft of land-surface subsidence in the years 1900 to 1975 (Carr and others, 1985, fig. 25). This subsidence is much less than the amount measured in the Houston-Galveston area.

POTENTIAL FOR GROUND-WATER DEVELOPMENT

In the previous section, the history of development was described for the more intensively pumped areas along with some of the problems associated with that development. There has been little development in a large part of the study area, and large quantities of ground water are available for various uses.

The availability of ground-water supplies will depend on the amount of withdrawal that can be sustained without exceeding acceptable limits of: (1) Water-level declines; (2) land-surface subsidence; (3) saltwater encroachment at the coast; (4) contamination from saltwater in adjacent beds or from downdip; and (5) reduced streamflow.

Reports that include a regional description of ground-water use and availability, projected ground-water requirements, and potential problems associated with future development include those by the Texas Department of Water Resources (1984a, 1984b, 1985), and Baker and Wall (1976). A common characteristic of problem areas is that large ground-water withdrawal is concentrated in small areas. Some general ways to reduce withdrawal and the potential or existing adverse effects of withdrawal are: (1) Water- conservation practices; (2) construction of reservoirs and more dependence on surface-water supplies; (3) relocation of well fields and spreading the withdrawal over a larger area; (4) importation of water from nonproblem areas; (5) artificial recharge; and (6) desalination of salty ground water.

Pumping from older units that are farther inland can minimize land-surface subsidence and saltwater encroachment. If the withdrawal is in areas with more abundant precipitation, the potential for recharge is greater and aquifer dewatering is less likely to be a problem.

Fresh ground-water use for 1985 and projected use for 2000 and 2030 are shown for selected counties in the study area (fig. 62). The projections, made by the Texas Water Development Board, are tentative and undergo constant revision and updating depending on the many changing technical and socio-economic factors. Ground-water use in eight out of the nine most intensively pumped counties in 1985 is projected to decrease by 2030 (fig. 62). Total decrease for the eight counties is expected to be from 872 Mgal/d in 1985 to 392 Mgal/d in 2030, an average decrease of about 55 percent.

The largest decrease, 143 Mgal/d, is projected for Harris County, closely followed by a projected decrease of 131 Mgal/d for Wharton County. Harris, Wharton, Jackson, Jasper, and Colorado Counties are part of a region designated by the State as the Southeast Texas and Upper Gulf Coast Region (Texas Department of Water Resources, 1984a, fig. 1). Although total water use is projected to increase in this region by about 20 percent from 1980 to 2030, ground-water use is projected to decrease by about 29 percent. According to the Texas Department of Water Resources (1984a, p. 53), an increasing dependence on surface-water supplies will be necessary to prevent further land subsidence and saltwater encroachment.

Zavala, Frio, and Atascosa Counties are within the Winter Garden area. In an area designated as the South Central Texas Region, the Texas Department of Water Resources (1984a, p. 51) projects shortages of water for irrigation, primarily in the Winter Garden area, to be about 151 Mgal/d by 2030.

It is apparent that the future development of ground water in the study area is a complex matter, with projected large decreases in withdrawal for some areas and projected increases for other areas. Such withdrawal projections could be simulated in the ground-water flow model, but such complex simulations are beyond the scope of this study. However, the model was used to simulate two simplified projected withdrawal scenarios. In the first, the calibration period from predevelopment to 1982 was extended to the year 2030 with the 1980 pumping rate remaining in effect for 1983-2030. In the second simulation, the calibration period from predevelopment to 1982 was again extended to the year 2030, but with an additional pumping rate of 0.5 Mgal/d assigned to each grid block (25 mi² area) in all aquifers and permeable zones where the block contained mean dissolved solids concentrations of 2,000 mg/L or less and had a thickness greater than 25 ft. An analysis of the two simulations provides a qualitative evaluation of the response of aquifer systems to additional large development.

Representative water-level hydrographs for the 1910-2030 simulations are shown for permeable zones A, B, and C in Harris County (fig. 63). The well locations are shown in figure 41. In this section, simulated water levels will be discussed along with measured water levels in specific wells. Note that a simulated water level is the average water level for a large volume of aquifer sediments having the areal dimension of a model grid block (25 mi²) and an average aquifer thickness for that block.

Well 9 in figure 63 is open to permeable zone A in an area of southeastern Harris County where withdrawal from most zones has been substantially reduced starting in 1976 and continuing into the 1980's. Simulation of continual pumping at the 1980 rate resulted in little additional drawdown in well 9 after 1982.

Wells 7 and 3 in figure 63 are open to permeable zones B and C, respectively, in an area of southwest Harris County where pumping rates have generally continued to increase in the 1970's and through 1980. Wells 7 and 3 had an additional simulated drawdown of 100 and 130 ft, respectively, between 1982 and 2030. Both drawdown curves are approaching horizontal near the end of the simulation period, signifying little further change in storage.

For the second simulation, involving increased withdrawal, about 50 ft of additional drawdown was simulated in well 9 after 1982. Simulated drawdowns in wells 7 and 3 after 1982 were 160 and 220 ft, respectively. The rates of decline of the water levels for wells 9, 7, and 3 from 1983-2030 averaged 1.0, 3.3, and 4.6 ft/yr, respectively, compared to rates of 0.1, 2.1, and 2.7 ft/yr for the first simulation with 1980 withdrawal.

Overall declines in heads in the Houston-Galveston area during the simulations caused additional land-surface subsidence as shown in figure 64. (As part of the model calibration, land-surface subsidence in the Houston-Galveston area from predevelopment to 1973 was simulated by the model. A comparison of measured

and simulated land subsidence is shown in figure 95 and is discussed in detail in the Appendix.) For the model simulation with 1980 withdrawal during 1983-2030, land subsidence in eastern Harris County and Galveston County increased by about 1 to 3 ft from 1973 to 2030 (fig. 64). For the same period, the land surface subsided by more than 4 ft in southwest Harris and northeast Fort Bend Counties.

Additional land-surface subsidence in southeastern Harris County beyond the 1980's may seem contradictory. Model results (fig. 63) indicate that a maximum water-level drawdown in the block containing well no. 9 occurred in 1976. The drawdown is from a block in permeable zone A. Projected drawdowns in this block to the year 2030 were never as large as in 1976. Thus, if water levels in the block containing well no. 9 are representative of ground-water levels in southeastern Harris County, additional land subsidence to the year 2030 would not be expected. Because the model is projecting additional subsidence in southeastern Harris County, and specifically in the grid block containing well no. 9, the model output was further analyzed. Drawdowns for permeable zone B in this grid block (fig. 65) follow a pattern similar to that for permeable zone A (fig. 63). However, water levels in permeable zone C (fig. 65) show a continuous decline from 1910-2030, thus accounting for additional land-surface subsidence in the model simulations.

The additional land-surface subsidence in southeastern Harris County and adjacent areas, as projected from 1983 to 2030, results from 1980 pumping rates (the most recent withdrawal data available for the model simulations). Pumping rates in the southeastern Harris County area continued to decline substantially through 1986. Land-surface subsidence data provided by the Houston-Galveston Coastal Subsidence District (written commun., 1987) show a continuing marked decrease or total cessation in the rate of subsidence at monitored sites in southeastern Harris County and in Galveston County through 1986.

For the simulation with increased withdrawal superimposed on the 1980 pumping rate, land-surface subsidence from 1973 to 2030 is more than 5 ft in eastern Harris County, and more than 7 ft in northeastern Fort Bend County (fig. 64).

Well 23 in figure 66 is located downdip in the lower Claiborne-upper Wilcox aquifer in southern Zavala County. With the 1980 pumping rate continuing for 1983-2030, simulated drawdown for this period was 45 ft. Well 24 in figure 66 is located in the outcrop of the lower Claiborne-upper Wilcox aquifer in northeastern Zavala County. The depth of the well is reported as 260 ft. With the 1980 pumping rate continuing, simulated drawdown between 1982 and 2030 was 60 ft. Because the aquifer is under water-table conditions, an additional 60 ft of the aquifer was dewatered at this location. By 2030, about 73 percent of the aquifer would be dewatered at this location.

For the simulation with additional withdrawal, drawdowns for 1983-2030 at wells 23 and 24 were 205 and 130 ft, respectively (fig. 66). Average rates of decline of the water levels in wells 23 and 24 for 1983-2030 were 4.3 and 2.7 ft/yr, respectively, compared to rates of 0.9 and 1.2 ft/yr for the first simulation. The aquifer at well 24 would be almost totally dewatered by the year 2030.

Major components of the ground-water budget are presented for the simulation with increased withdrawal superimposed on the 1980 pumping rate. A summary of withdrawal, change in storage, and vertical flow rates in the exposed and downdip parts of each hydrogeologic unit in the modeled area for the year 2030 is shown in figure 67. Net recharge in the outcrop areas of all units accounted for about 82 percent of the total pumping rate of 548 million ft³/d, with about 16 percent of the pumping rate accounted for by water released from storage in aquifers and compacting clay beds, and about 2 percent contributed by net lateral flow into the study area. Highest recharge rates would occur in the outcrops of the most intensively pumped units, with 140 million ft³/d or 31 percent of total net recharge entering the uppermost and most intensively pumped unit--permeable zone A (fig. 67).

The highest net leakage rate was 26 million ft³/d downward into the lower Claiborne-upper Wilcox aquifer, followed by 23 million ft³/d downward into permeable zone B (fig. 67).

A summary of changes in pumping rates, heads, and recharge rates for each aquifer and permeable zone is given in table 7 for the simulation with increased withdrawal. Increases in pumping rates range from 10

Table 7.--Summary of changes in simulated heads and recharge rates resulting from hypothetical increase in pumping rate, 1983 to 2030

Aquifer or permeable zone	1980 pumping rate (million cubic feet per day)	1983-2030 pumping rate (million cubic feet per day)	Increase in pumping rate (million cubic feet per day)	Mean decrease in head from 1982 head (feet)	Mean increase in recharge rate in outcrop area from 1982 rate (inches per year)
Permeable zone A	86	121	35	13	0.2
Permeable zone B	51	84	33	28	.6
Permeable zone C	29	63	34	45	.5
Permeable zone D	4	34	30	98	.5
Permeable zone E	1	11	10	76	.4
Upper Claiborne aquifer	2	16	14	48	.5
Middle Claiborne aquifer	5	51	46	120	.8
Lower Claiborne- upper Wilcox aquifer	43	104	61	276	1.1
Middle Wilcox aquifer	10	64	54	160	.5

million ft³/d for permeable zone E to 61 million ft³/d for the lower Claiborne-upper Wilcox aquifer. Mean head decreases between 1982 and 2030 range from 13 ft for permeable zone A to 276 ft for the lower Claiborne-upper Wilcox aquifer. Head declines for the latter aquifer are especially large down dip in the Winter Garden area, where freshwater is found at unusually great depths but aquifer transmissivity is small. For the combined units, the mean increase in the recharge rate in the outcrops over the 1982 rate is 0.35 in/yr. The mean increases for the individual units range from 0.2 in/yr for permeable zone A to 1.1 in/yr for the lower Claiborne-upper Wilcox aquifer (table 7).

A final analysis of aquifer potential for development utilizes the difference between (1) 2030 water level simulated with additional withdrawal and (2) the 2030 water levels simulated with 1980 withdrawal continuing from 1982 to 2030. Because water levels in the simulations are the integrated result of all hydrologic properties and conditions, such as aquifer transmissivity, nearness to outcrop or recharge source, and vertical leakage, the head difference between the two simulations provides some measure of the capacity of the aquifer systems to accept additional large development. This water-level difference is shown for each aquifer and permeable zone in figures 68 through 76. Also shown on the maps are areas within each aquifer and permeable zone that are designated as having more or less potential for future ground-water development. In addition to the difference in head as just described, other subjective criteria for rating the areas include:

1. Aquifer thickness: An area having a mean grid-block thickness of less than 25 ft is designated as having only some or limited potential for additional development;
2. Dissolved-solids concentration of water: An area having a mean dissolved-solids concentration greater than 2,000 mg/L is designated as having limited potential for additional development;
3. Recharge potential: Precipitation, and thus recharge potential, is generally progressively smaller from east to west.

The rating of areas in each aquifer and permeable zone is subjective and is meant only to show areas within a given aquifer that have relatively more or less potential for additional large development. The ratings do not necessarily indicate that a particular aquifer has more potential for development than another. For the development potential, it is generally assumed that the potential for saltwater intrusion at the coast and elsewhere is minimal and within acceptable limits. It is also assumed that additional land-surface subsidence, as discussed previously, is within acceptable limits. Examination of figures 68 through 76 shows that the potential for future development in each aquifer and permeable zone is generally rated more favorably from west to east across the study area.

For the middle Wilcox aquifer, the simulation with the superimposed withdrawal is significantly affected in the extreme northeast corner of the study area by nearness to the no-flow boundary (fig. 76). Testing of the effects of the no-flow lateral boundaries on the simulations (discussed in the Appendix) shows that this is the only area and the only aquifer so affected.

SUMMARY

Gulf Coastal Plain sediments as much as several thousand feet thick were represented as discrete aquifers, permeable zones, and confining units in a multilayered digital model. The bases for selecting the number of hydrogeologic units (model layers) include practical considerations of size of the area, objectives of the model study, and computer cost limitations. Electrical-log interpretations of lithology, and vertical head differences at major pumping centers in Texas and Louisiana were used to delineate hydrogeologic units.

Two aquifer systems are recognized for the Texas Gulf Coast: the Texas coastal uplands aquifer system and the coastal lowlands aquifer system. The coastal uplands aquifer system consists of four aquifers and two confining units in the Wilcox and Claiborne Groups. The system is bounded from below by the practically impermeable clays of the Midway Group, or by the top of the geopressured zone. The overlying Vicksburg-Jackson confining unit separates the coastal uplands and the younger coastal lowlands aquifer systems. The coastal lowlands aquifer system consists of five permeable zones and two confining units that range in age from Holocene to Oligocene. Water quality in the aquifer systems varies from freshwater to brines, with dissolved solids concentrations ranging from a few hundred to as much as 150,000 mg/L.

In 1980, ground-water withdrawals in the study area, an area of about 114,000 mi², were 1.7 billion gal/d. Withdrawal has caused large cones of depression in the potentiometric surfaces, particularly in the Houston-Galveston and Winter Garden areas, where water levels have declined hundreds of feet over large areas since the beginning of development. Inelastic compaction of clays has resulted in land-surface subsidence of more than 1 ft in an area of about 2,000 mi². As much as 10 ft of subsidence has occurred in the Pasadena area east of Houston. Movement of saltwater toward pumping centers by vertical migration or from downdip has caused water-quality problems. The potential for contamination is greatest along the coastal margins. Saltwater contamination and land-surface subsidence have prompted an increasing reliance on surface water for municipal and industrial supplies.

A three-dimensional, variable-density digital flow model was developed for simulation of predevelopment and transient flow conditions. The area simulated extends beyond the study area to include parts of Louisiana and Mexico. No-flow boundaries were used at the updip and downdip extent of the hydrologic units and at the eastern and western limits. A constant-head water-table boundary provides recharge to the units in their outcrop areas.

The model calibration period was from 1910 (predevelopment) to 1982. Simulated 1982 heads, long-term hydrographs, and land-surface subsidence were matched to measured data in selected, intensively pumped areas.

Mean horizontal hydraulic conductivity of hydrologic units in the calibrated model ranges from 10 ft/d for the middle Wilcox aquifer to 25 ft/d for permeable zone A. Mean transmissivity ranges from about 4,600 ft²/d for the middle Claiborne aquifer to about 10,400 ft²/d for permeable zone D. Mean vertical hydraulic conductivity ranges from 1.1×10^{-5} ft/d for the Vicksburg-Jackson confining unit, to 3.8×10^{-3} ft/d for permeable zone A. Mean values of calibrated storage coefficient range from 5.2×10^{-4} for the middle Claiborne aquifer to 1.7×10^{-3} for the middle Wilcox aquifer and permeable zone C. Calibrated inelastic specific storage values for clay beds in permeable zones A, B, and C in the Houston-Galveston area are 8.5×10^{-5} , 8.0×10^{-5} , and 8.0×10^{-6} ft⁻¹, respectively.

Model results indicate that recharge was the source of about 76 percent of the discharge in the study area (withdrawal plus a small net lateral outflow) for 1982; release of water from aquifer storage and compacting clay beds provided the remaining 24 percent. The average 1982 recharge rate for the calibrated simulation was 0.52 in/yr; the average discharge, not including ground-water withdrawal, was 0.15 in/yr. As much as 6 in/yr of recharge was simulated in the coastal rice-irrigation area; perhaps as much as 30 percent of this rate is return flow of ground water that has been pumped for irrigation.

A combination of intense withdrawal and low precipitation has caused long-term dewatering of the lower Claiborne-upper Wilcox aquifer in the Winter Garden area. Long-term dewatering of shallow sands was observed in a well in Jackson County, a part of the coastal rice-irrigation area where precipitation is more abundant than in the Winter Garden area. A regional assessment of dewatering in the coastal rice-irrigation area is precluded because of a lack of data.

Ground-water use is projected to decline substantially in most of the study area by the year 2030, as problems such as saltwater intrusion, land-surface subsidence, and aquifer dewatering become worse. The digital flow model developed for this study was used to simulate the flow system to 2030 assuming two pumping scenarios: (1) The 1980 pumping rate was applied to 1983-2030; and (2) an additional pumping stress of 0.5 Mgal/d per 25 mi² was superimposed on the 1980 pumping rate in those areas where water contains less than 2,000 mg/L dissolved-solids concentration and the aquifer thickness is at least 25 ft; this rate was used for the period 1983-2030.

Additional water-level declines, several feet of additional land subsidence in the Houston-Galveston area, and increased recharge rates were projected for the year 2030 in both simulations. The difference between the 2030 heads generated by the two model simulations, along with other factors such as aquifer thickness, dissolved-solids concentration of water, and recharge potential provided the criteria for rating areas

within the aquifers and permeable zones as having relatively more or less potential for future development. The potential for future development in each aquifer and permeable zone becomes higher from west to east across the study area.

Permeable zone A has the highest potential for development of additional large ground-water supplies. Because it crops out over its entire landward extent, recharge is generally always nearby and water-level declines are not large. The potential for development is also high for large areas of permeable zones B and C. Areas for potential development are small for permeable zones D and E and for the upper Claiborne aquifer, largely because these units contain relatively little freshwater. The middle Claiborne, lower Claiborne-upper Wilcox and middle Wilcox aquifers have some potential for development, mostly in the eastern areas.

Some general ways to reduce ground-water withdrawal or the adverse effects of withdrawal are: (1) Water conservation practices; (2) construction of reservoirs and more dependence on surface-water supplies; (3) relocation of well fields and spreading the withdrawal over a larger area; (4) importation of water from nonproblem areas; (5) artificial recharge; and (6) use of desalinated ground water.

SELECTED REFERENCES

- Ackerman, D.J., 1989, Hydrology of the Mississippi River Valley alluvial aquifer, south-central United States--A preliminary assessment of the regional flow system: U.S. Geological Survey Water-Resources Investigations Report 88-4028, 74 p.
- Arthur, J.K., and Taylor, R.E., 1989, Definition of geohydrologic framework and preliminary simulation of ground-water flow in the Mississippi embayment aquifer system, south-central United States: U.S. Geological Survey Water-Resources Investigations Report 86-4364, 110 p.
- Baker, E.T., Jr., 1965, Ground-water resources of Jackson County, Texas: Texas Water Development Board Report 1, 229 p.
- 1979, Stratigraphic and hydrogeologic framework of part of the Coastal Plain of Texas: Texas Department of Water Resources Report 236, 43 p.
- 1985, Texas Ground-water resources, *in* National Water Summary 1984: U.S. Geological Survey Water-Supply Paper 2275, p. 397-402.
- 1986, Hydrology of the Jasper aquifer in the southeast Texas Coastal Plain: Texas Water Development Board Report 295, 64 p.
- Baker, E.T., Jr., and Follett, C.R., 1973, Effects of ground-water development on the proposed Palmetto Bend Dam and Reservoir in southeast Texas: U.S. Geological Survey Water-Resources Investigations Report 18-73, 70 p.
- Baker, E.T., Jr., and Wall, J.R., 1976, Summary appraisals of the Nation's ground-water resources, Texas-Gulf region: U.S. Geological Survey Professional Paper 813-F, 29 p.
- Baker, R.C., and Dale, O.C., 1961, Ground-water resources of the Lower Rio Grande Valley area, Texas: Texas Board of Water Engineers Bulletin 6014, vol. I, 81 p., vol. II, 336 p.
- Barnes, B.A., Follett, C.R., and Sundstrom, R.W., 1944, Ground-water supply of Bryan, Texas: Texas State Board of Water Engineers Report M025.
- Bonnett, C.W., and Williams, J.F., III, 1987, Development of ground-water resources in the Orange County area, Texas and Louisiana, 1980-spring 1985: U.S. Geological Survey Water-Resources Investigations Report 87-4158, 50 p.
- Brahana, J.V., and Mesko, T.O., 1988, Hydrogeology and preliminary assessment of regional flow in the upper Cretaceous and adjacent aquifers in the northern Mississippi embayment: U.S. Geological Survey Water-Resources Investigations Report 87-4000, 65 p.
- Carr, J.E., Meyer, W.R., Sandeen, W.M., and McLane, I.R., 1985, Digital models for simulation of ground-water hydrology of the Chicot and Evangeline aquifers along the Gulf Coast of Texas: Texas Department of Water Resources Report 289, 101 p.
- Cronin, J.G., and Wilson, C.A., 1967, Ground water in the flood-plain alluvium of the Brazos River, Whitney Dam to vicinity of Richmond, Texas: Texas Water Development Board Report 41, 223 p.
- Deussen, A., 1914, Geology and underground waters of the southeastern part of the Texas Coastal Plain: U.S. Geological Survey Water-Supply Paper 335, 365 p.
- Duffin, G.L., and Elder, G.R., 1979, Variations in specific yield in the outcrop of the Carrizo Sand in South Texas as estimated by seismic refraction: Texas Department of Water Resources Report 229, 57 p.
- Elder, G.R., Duffin, G.L., and Rodriguez, Eulogio, Jr., 1980, Records of wells, water levels, pumpage, and chemical analyses of water from the Carrizo aquifer in the Winter Garden area, Texas, 1970 through 1977: Texas Department of Water Resources Report 254, 125 p.
- Ellisor, A.C., 1944, Anahuac Formation: American Association of Petroleum Geologists Bulletin, v. 28, no. 9, p. 1355-1375.
- Follett, C.R., 1974, Ground-water resources of Brazos and Burleson Counties, Texas: Texas Water Development Board Report 185, 196 p.
- Freeze, R.A., and Cherry, J.A., 1979, Groundwater: New Jersey, Prentice-Hall, Inc., 604 p.
- Gabrysch, R.K., 1977, Approximate areas of recharge to the Chicot and Evangeline aquifer systems in the Houston-Galveston area, Texas: U.S. Geological Survey Open-File Report 77-754, 1 map.
- 1984a, Ground-water withdrawals and changes in water levels in the Houston District, Texas 1975-79: Texas Department of Water Resources Report 286, 42 p.

- 1984b, Ground-water withdrawals and land-surface subsidence in the Houston-Galveston region, Texas, 1906-80: Texas Department of Water Resources Report 287, 64 p.
- Gabrysch, R.K., and Bonnett, C.W., 1975, Land-surface subsidence in the Houston-Galveston region, Texas: Texas Water Development Board Report 188, 19 p.
- Gabrysch, R.K., and McAdoo, G.D., 1972, Development of ground-water resources in the Orange County area, Texas and Louisiana, 1963-71: Texas Water Development Board Report 156, 47 p.
- Garza, Sergio, 1977, Artificial recharge for subsidence abatement at the NASA-Johnson Space Center, phase 1: U.S. Geological Survey Open-File Report 77-219, 82 p.
- Garza, Sergio, Jones, B.D., and Baker, E.T., Jr., 1987, Approximate potentiometric surfaces for the aquifers of the Texas coastal uplands aquifer system, 1980: U.S. Geological Survey Hydrologic Investigations Atlas 704, scale 1:1,500,000.
- Gebert, W.A., Graczyk, D.J., and Krug, W.R., 1987, Average annual runoff in the United States, 1951-80: U.S. Geological Survey Hydrologic Investigations Atlas HA-710, 1 sheet, scale 1:7,500,000.
- Groschen, G.E., 1985, Simulated effects of projected pumping on the availability of freshwater in the Evangeline aquifer in an area southwest of Corpus Christi, Texas: U.S. Geological Survey Water-Resources Investigations Report 85-4182, 103 p.
- Grubb, H.F., 1984, Planning report for the Gulf Coast Regional Aquifer-System Analysis in the Gulf of Mexico Coastal Plain, United States: U.S. Geological Survey Water-Resources Investigations Report 84-4219, 30 p.
- 1986, Gulf Coastal Plain regional aquifer-system study, *in* Sun, Ren Jen, ed., Regional Aquifer-System Analysis Program of the U.S. Geological Survey - Summary of Projects, 1978-84: U.S. Geological Survey Circular 1002, p. 152-161.
- 1987, Overview of the Gulf Coast Regional Aquifer-System Analysis, south-central United States: *in*, Vecchioli, John, and Johnson, A.I., eds., Aquifers of the Atlantic and Gulf Coastal Plain: American Water Resources Association, Monograph No. 9, p. 101-118.
- Hammond, W.W., Jr., 1969, Ground-water resources of Matagorda County, Texas: Texas Water Development Board Report 91, 180 p.
- Helm, D.C., 1975, One-dimensional simulation of aquifer system compaction near Pixley, California; 1, Constant parameters: Water Resources Research, v. 11, no. 3, p. 465-478.
- 1976, One-dimensional simulation of aquifer system compaction near Pixley, California; 2, Stress-dependent parameters: Water Resources Research, v. 12, no. 3, p. 375-391.
- Hem, J.D., 1985, Study and interpretation of the chemical characteristics of natural water: U.S. Geological Survey Water-Supply Paper 2254, 3rd Edition, 264 p.
- Hosman, R.L., and Weiss, J.S., in press, Geohydrologic units of the Mississippi embayment and Texas coastal uplands aquifer systems, south-central United States: U.S. Geological Survey Professional Paper 1416-B.
- 1988, Geohydrologic units of the Mississippi embayment and Texas coastal uplands aquifer systems, south-central United States: U.S. Geological Survey Open-File Report 88-316, 21 p.
- Hubbert, M.K., 1940, The theory of ground-water motion: Journal of Geology, v. XLVIII, no. 8, p. 785-944.
- Hughes, W.F., and Magee, A.C., 1962, An economic analysis of irrigated cotton production, Middle Brazos River Valley, 1955-58: Texas A&M University, MP-580, 12 p.
- Jones, P.H., Stevens, P.R., Wesselman, J.B., and Wallace, R.H., Jr., 1976, Regional appraisal of the Wilcox Group in Texas for subsurface storage of fluid wastes: U.S. Geological Survey Open-File Report 76-394, 107 p.
- Jorgensen, D.G., 1975, Analog-model studies of ground-water hydrology in the Houston district, Texas: Texas Water Development Board report 190, 84 p.
- 1977, Salt-water encroachment in aquifers near the Houston Ship Channel, Texas: U.S. Geological Survey Open-File Report, 76-781, 45 p.
- Jorgensen, D.G., and Gabrysch, R.K., 1974, Simulated water-level changes resulting from proposed changes in ground-water pumping in the Houston, Texas, area: U.S. Geological Survey Open-File Report, 3 sheets.
- Klemt, W.B., Duffin, G.L., and Elder, G.R., 1976, Ground-water resources of the Carrizo aquifer in the Winter Garden area of Texas: Texas Water Development Board Report 210, v. 1, 30 p.
- Kuiper, L.K., 1981, A comparison of the incomplete Cholesky-conjugate gradient method with the strongly implicit method as applied to the solution of two-dimensional groundwater flow equations: Water Resources Research, v. 17(4), p. 1082-1086.

- 1983, A numerical procedure for the solution of the steady state variable density groundwater flow equation: *Water Resources Research*, v. 19(1), p. 234-240.
- 1985, Documentation of a numerical code for the simulation of variable density ground-water flow in three dimensions: U.S. Geological Survey Water-Resources Investigations Report 84-4302, 90 p.
- 1986, A comparison of several methods for the solution of the inverse problem in two-dimensional steady state groundwater flow modeling: *Water Resources Research*, v. 22(5), p. 705-714.
- Leake, S.A., and Prudic, D.E., 1989, Documentation of a computer program to simulate aquifer-system compaction using the modular finite-difference ground-water flow model: U.S. Geological Survey Open-File Report 88-482, 80 p.
- Livingston, Penn, and Bridges, T.W., 1936, Ground-water resources of Kleberg County, Texas: U.S. Geological Survey Water-Supply Paper 773-D, p. 197-232.
- Lohman, S.W., 1972, Ground-water hydraulics: U.S. Geological Survey Professional Paper 708, 70 p.
- Lohman, S.W., Bennett, R.R., Brown, R.H., Cooper, H.H., Jr., Drescher, W.J., Ferris, J.G., Johnson, A.I., McGuinness, C.L., Piper, A.M., Rorabaugh, M.I., Stallman, R.W., and Theis, C.V., 1972, Definitions of selected ground-water terms--revisions and conceptual refinements: U.S. Geological Survey Water-Supply Paper 1988, 21 p.
- Loskot, C.L., Sandeen, W.M., and Follett, C.R., 1982, Ground-water resources of Colorado, Lavaca, and Wharton Counties, Texas: Texas Department of Water Resources Report 270, 245 p.
- Luszczynski, N.J., 1961, Head and flow of ground water of variable density: *Journal of Geophysical Research*, v. 66, no. 12, p. 4247-4256.
- Mackey, G.W., 1987, Comparison of irrigation pumpage and change in water storage of the High Plains aquifer in Castro and Parmer Counties, Texas, 1975-83: U.S. Geological Survey Water-Resources Investigations Report 87-4032, 48 p.
- Martin, Angel, Jr., and Whiteman, C.D., Jr., 1989, Regional ground-water flow in the coastal lowlands aquifer system in parts of Alabama, Florida, Louisiana, and Mississippi--A preliminary analysis: U.S. Geological Survey Water-Resources Investigations Report 88-4100, 88 p.
- Mesko, T.O., Ackerman, D.J., and Williamson, A.K., 1990, Ground-water pumpage from the Gulf Coast aquifer systems, 1960-85, south-central United States: U.S. Geological Survey Water-Resources Investigations Report 89-4180, 177 p.
- Meyer, W.R., and Carr, J.E., 1979, A digital model for simulation of ground-water hydrology in the Houston area, Texas: Texas Department of Water Resources Report LP-103, 27 p., 3 app.
- Muller, D.A., and Price, R.D., 1979, Ground-water availability in Texas, estimates and projections through 2030: Texas Department of Water Resources Report 238, 77 p.
- Payne, J.N., 1968, Hydrologic significance of the lithofacies of the Sparta Sand in Arkansas, Mississippi, and Texas: U.S. Geological Survey Professional Paper 569-A, 17 p.
- 1970, Geohydrologic significance of lithofacies of the Cockfield Formation of Louisiana and Mississippi and of the Yegua Formation of Texas: U.S. Geological Survey Professional Paper 569-B, 14 p.
- 1972, Hydrologic significance of lithofacies of the Cane River Formation or equivalents of Arkansas, Louisiana, Mississippi, and Texas: U.S. Geological Survey Professional Paper 569-C, 17 p.
- 1975, Geohydrologic significance of lithofacies of the Carrizo Sand of Arkansas, Louisiana, and Texas and the Meridian Sand of Mississippi: U.S. Geological Survey Professional Paper 569-D, 11 p.
- Pettitt, B.M., and Winslow, A.G., 1955, Geology and ground-water resources of Galveston County, Texas: Texas Board of Water Engineers Bulletin 5502, 219 p.
- Pettijohn, R.A., 1986, Processing water-chemistry data, Gulf Coast aquifer systems, south-central United States, with summary of dissolved-solids concentrations and water types: U.S. Geological Survey Water-Resources Investigations Report 86-4186, 42 p.
- Pettijohn, R.A., Weiss, J.S., and Williamson, A.K., 1988, Dissolved-solids concentrations and water temperatures for aquifers in the Gulf Coast aquifer systems, south-central United States: U.S. Geological Survey Water-Resources Investigations Report 88-4082, map, scale 1:3,500,000, 5 sheets.
- Preston, R.D., 1983, Occurrence and quality of ground water in the vicinity of Brownsville, Texas: Texas Department of Water Resources Report 279, 98 p.
- Prudic, D.E., 1991, Estimates of hydraulic conductivity from aquifer-test analyses and specific-capacity data, gulf coast regional aquifer systems, south-central United States: U.S. Geological Survey Water Resources Investigations Report 90-4121, 38 p.

- Prudic, D.E., and Williamson, A.K., 1984, Evaluation of a technique for simulating a compacting aquifer system in the Central Valley of California, U.S.A: International Association of Hydrological Sciences Publication no. 151, p. 53-63.
- Ratzlaff, K.W., 1982, Land-surface subsidence in the Texas coastal region: Texas Department of Water Resources Report 272, 26 p.
- Ryder, P.D., 1988, Hydrogeology and predevelopment flow in the Texas Gulf Coast aquifer systems: U.S. Geological Survey Water-Resources Investigations Report 87-4248, 109 p.
- Shafer, G.H., and Baker, E.T., Jr., 1973, Ground-water resources of Kleberg, Kenedy, and southern Jim Wells Counties, Texas: Texas Water Development Board Report 173, 162 p.
- Solley, W.B., Merk, C.F., and Pierce, R.R., 1988, Estimated use of water in the United States in 1985: U.S. Geological Survey Circular 1004, 82 p.
- Texas Department of Water Resources, 1984a, Water for Texas--A comprehensive plan for the future: Texas Department of Water Resources GP-4-1, v. 1, 72 p.
- 1984b, Water for Texas--Technical appendix: Texas Department of Water Resources GP-4-1, v. 2.
- 1985, Water use, projected water requirements, and related data and information for the metropolitan statistical areas in Texas: Texas Department of Water Resources Report LP-201, 226 p.
- Texas Water Development Board, 1986, Surveys of irrigation in Texas--1958, 1964, 1969, 1974, 1979, and 1984: Texas Water Development Board Report 294, 242 p.
- Turner, S.F., 1938, Ground water in the vicinity of Bryan and College Station, Texas: Texas State Board of Water Engineers Miscellaneous Report, 44 p.
- Turner, S.F., Robinson, T.W., and White, W.N., 1948, Geology and ground-water resources of the Winter Garden district, Texas, 1948: U.S. Geological Survey Water-Supply Paper 1481, 248 p.
- U.S. Geological Survey, 1985, National water summary 1984--Hydrologic events, selected water-quality trends, and ground-water resources: U.S. Geological Survey Water-Supply Paper 2275, 467 p.
- Wallace, R.H., Jr., Wesselman, J.B., and Kramer, T.F., 1981, Map of the occurrence of geopressure in the northern Gulf of Mexico basin, in Bebout, D.G., and Backman, A.L., eds., Proceedings of the 5th geopressured-geothermal energy conference: Louisiana Geological Survey-Louisiana State University-U.S. Department of Energy, Baton Rouge, Louisiana, October 13-15, 1981, map, scale 1:1,000,000, 1 sheet.
- Weiss, J.S., 1987, Determining dissolved-solids concentrations in mineralized ground water of the Gulf Coast aquifer systems using electric logs, in Vecchioli, John, and Johnson, A.I., eds., Aquifers of the Atlantic and Gulf Coastal Plain: American Water Resources Association, Monograph No. 9, p. 130-150.
- Weiss, J.S., and Williamson, A.K., 1985, Subdivision of thick sedimentary units into layers for simulation of ground-water flow: Ground Water, v. 23, no. 6, p. 767-774.
- Wesselman, J.B., 1965, Geology and ground-water resources of Orange County, Texas: Texas Water Commission Bulletin 6516, 112 p.
- 1967, Ground-water Resources of Jasper and Newton Counties, Texas: Texas Water Development Board Report 59, 186 p.
- 1971, Ground-water resources of Chambers and Jefferson Counties, Texas: Texas Water Development Board Report 133, 183 p.
- White, W.N., 1938, Progress report on the ground-water resources of the Houston district, Texas: Texas State Board of Water Engineers Miscellaneous Report, 7 p.
- White, W.N., Livingston, Penn, and Turner, S.F., 1932, Ground-water resources of the Houston-Galveston area, Texas, in Ground-water resources of the Houston-Galveston area and adjacent region, Texas, 1939: Texas Board of Water Engineers Miscellaneous Report, p. 1-16.
- William F. Guyton and Associates, 1970, Ground-water conditions in Angelina and Nacogdoches Counties, Texas: Texas Water Development Board Report 110, 125 p.
- Williams, T.A., and Williamson, A.K., 1989, Estimating water-table altitudes for regional ground-water flow simulation, gulf coast aquifer systems, south-central United States: Ground Water v. 27, no. 3, p. 333-340.
- Williamson, A.K., 1987, Preliminary simulation of ground-water flow in the gulf coast aquifer systems, south-central United States, in Vecchioli, John, and Johnson, A.I., eds., Aquifers of the Atlantic and Gulf Coastal Plain: American Water Resources Association, Monograph No. 9, p. 119 -137.
- Williamson, A.K., Grubb, H.F., and Weiss, J.S., 1990, Ground-water flow in the Gulf Coast aquifer systems, south-central United States--A preliminary analysis: U.S. Geological Survey Water-Resources Investigations Report 89-4071, 124 p.

- Wilson, T.A., and Hosman, R.L., 1988, Geophysical well-log database for the Gulf Coast aquifer systems, south-central United States: U.S. Geological Survey Open-File Report 87-677, 213 p.
- Winslow, A.G., Doyel, W.W., and Wood, L.A., 1957, Salt water and its relation to fresh ground water in Harris County, Texas: U.S. Geological Survey Water-Supply Paper 1360-F, p. 375-407.
- Winslow, A.G., and Wood, L.A., 1959, Relation of land subsidence to ground-water withdrawals in the upper Gulf Coast region, Texas: Mining Eng., p. 1030-1034.
- Wood, L.A., 1956, Availability of ground water in the Gulf Coast region of Texas: U.S. Geological Survey Open-File Report, 55 p.
- Wood, L.A., Gabrysch, R.K., and Marvin, Richard, 1963, Reconnaissance investigations of the ground-water resources of the Gulf Coast region, Texas: Texas Water Commission Bulletin 6305, 114 p.

APPENDIX

The calibration of the digital model that was used to describe and quantify the regional and subregional flow systems in previous sections is detailed in this section. Because the details of the predevelopment digital flow model were presented in a previous report (Ryder, 1988), only a brief summary of the updated predevelopment model calibration will be presented. The transient model calibration includes additional data, such as pumping rates, development heads, and storage coefficients; thus a detailed discussion will follow.

A numerical model developed by Kuiper (1985) was used to simulate the ground-water flow system. The model simulates variable-density ground-water flow in three dimensions. The ground-water density is variable in space, but is assumed to be constant in time. Horizontal and vertical flow is computed for aquifers and permeable zones, and vertical flow is computed for confining units. The model utilizes an integrated finite-difference grid, wherein the six-sided grid blocks are rectangular when viewed from the vertical direction. The sides of the blocks are vertical planes, but their top and bottom surfaces follow the curvature of the hydrogeologic units (Kuiper, 1985). The strongly implicit procedure (SIP) was selected for solving the approximating flow equations. Kuiper (1985) presents a complete documentation of the model, including detailed instructions for the use of the computer program.

A numerical technique used to simulate land-surface subsidence and release of water from storage resulting from compacting fine-grained sediments was obtained from Leake and Prudic (1989). The technique for the simulation of compaction and land subsidence was incorporated into the model by L.K. Kuiper (U.S. Geological Survey, written commun., 1987).

Digital Model of Predevelopment Steady-State Flow System

As stated previously, further model calibration resulted in substantial differences in simulated aquifer and confining-unit properties, and consequently in simulated flow compared to the preliminary model results reported in Ryder (1988). However, statistical analyses of the residual errors (simulated aquifer heads minus measured aquifer heads) as shown in table 8 are similar to those previously reported in Ryder (1988, table 6). This similarity in simulated heads and difference in simulated flow rates results because the steady-state calibration does not provide a unique solution. When the distribution and amount of both recharge and discharge and the distribution of vertical and horizontal hydraulic conductivities are unknown, the calibration of a steady-state model to a set of water levels provides a solution, which may or may not be correct. Proportionately changing all values of hydraulic conductivities will result in the same set of simulated heads, but the flow through the system will be different because it is proportional to the assigned hydraulic conductivity values.

Residuals in table 8 range from a minimum value of -187 ft for permeable zone D to a maximum value of 184 ft for the lower Claiborne-upper Wilcox aquifer. Residuals are largest for the lower Claiborne-upper Wilcox aquifer, with a standard deviation of 47 ft and an absolute mean of 53 ft. Permeable zone A has the smallest residuals, with a standard deviation of 12 ft and an absolute mean of 9 ft. For the combined aquifers and permeable zones, the standard deviation is 40 ft and the absolute mean is 30 ft.

The statistical analyses show that when the changed vertical and horizontal hydraulic conductivities, necessitated by the transient model calibration, are incorporated into the predevelopment, steady-state model, the predevelopment model calibration is statistically about the same as the original calibration.

Digital Model of Transient Flow System, Predevelopment to 1982

Transient model simulations allow for ground-water levels and flow to change with time in response to changes in the amount of recharge and discharge caused by man-induced stresses such as pumpage. Transient ground-water flow was simulated for the period 1910-82 to determine the effects caused by pumpage on water levels and flow in the aquifer systems. Initial water levels for 1910 were assumed equal to the predevelopment heads generated from the calibrated steady-state model. Ground-water pumpage was added as a discharge and averaged over periods ranging from 1 to 27 years. Estimates of storage coefficients were added to the model and were adjusted during model calibration along with the values of vertical and horizontal hydraulic

Table 8.--Summary of simulated and measured predevelopment altitudes of potentiometric surfaces

Aquifer or permeable zone	Total grid blocks with measured heads	Mean of residuals (feet)	Minimum residual (feet)	Maximum residual (feet)	Standard deviation (feet)	Absolute mean of residuals (feet)
All	4,588	12	-187	184	40	30
Permeable zone A	621	2	-59	37	12	9
Permeable zone B	906	9	-69	54	20	17
Permeable zone C	495	6	-148	115	34	25
Permeable zone D	259	-29	-187	103	46	43
Permeable zone E	68	-18	-104	77	31	27
Upper Claiborne aquifer	136	29	-33	149	39	34
Middle Claiborne aquifer	544	13	-59	129	41	34
Lower Claiborne-upper Wilcox aquifer	596	47	-84	184	47	53
Middle Wilcox aquifer	963	16	-97	172	44	37

conductivity. Calibration was achieved when model-computed water levels reasonably matched selected hydrographs of wells and areally distributed water levels as measured in 1982. In areas of known land subsidence, the inelastic specific storage values of clays were adjusted until the amount and distribution of simulated land subsidence reasonably matched measured land subsidence.

Model Grid and Boundary Conditions

The model finite-difference grid superimposed on the modeled area and study area is shown in figure 77. The grid consists of 106 rows and 77 columns uniformly spaced 5 mi apart. The modeled area extends beyond the study area to include parts of Louisiana and Mexico, and has an areal extent of 149,000 mi².

The general direction of ground-water flow prior to development was nearly parallel to the eastern and western boundaries of the study area; the flow paths followed the dips of the aquifers toward the Gulf. Little flow could be expected to enter or leave the study area under predevelopment conditions or where there has been little development, and the lateral boundaries of the model are designated as no-flow boundaries.

However, intense development in the Lake Charles area of southwestern Louisiana has caused a substantial amount of flow across the Texas-Louisiana border in the uppermost coastal lowlands permeable zones. Primarily for this reason, the eastern no-flow boundary was allowed to follow row 1 of the grid into southeastern Louisiana so that it increases to a maximum distance of about 195 mi from the Texas-Louisiana border (fig. 77).

The validity of retaining the lateral no-flow boundaries for the transient model calibration was tested by placing constant heads in the grid blocks just inside the no-flow boundaries. The constant heads were placed along the lateral edges in all layers, and the altitudes assigned to the constant heads were the starting heads (predevelopment) for the transient calibration. The transient predevelopment to 1982 simulation was run with the new boundaries, and the resulting simulated 1982 heads were compared to the 1982 heads simulated by the transient calibration. For all layers, the head changes at the boundaries of the study area were small in comparison to the residual errors (differences between simulated and measured heads) present in the model calibration. It is concluded that designation of the lateral boundaries as no-flow boundaries had no significant effect on the transient model calibration.

Another test of the no-flow lateral boundaries was made for the simulation involving the superposition of additional, hypothetical pumpage on 1980 pumping rates, and continuing the simulation to the year 2030. For this simulation, the constant-head lateral boundaries as described above were in effect for the entire simulation period--predevelopment to 2030. Differences in head caused by the changed boundary conditions were analyzed for all model layers. The heads in the middle Wilcox aquifer were significantly affected in the extreme northeastern corner of the study area (fig. 76). Head changes elsewhere for all other layers were small and of little consequence.

The base of the flow system is a no-flow boundary, which represents the top of the Midway confining unit, a thick deposit of nearly impermeable marine clays, or the top of the geopressured zone where it occurs above the top of the Midway confining unit. It is assumed that abnormally high pressures in the geopressured zone are the result of greatly reduced permeability, which, in turn, precludes the possibility of significant flow out of this zone.

The updip limit of the flow system, where the aquifer system pinches out, is a no-flow boundary. The downdip limit of the flow system is defined as the edge of the Continental Shelf. It is at a great distance from the coastline and is treated as a no-flow boundary.

The top of the simulated flow system is bounded by a layer of constant-head grid blocks that represent the water table in the uppermost 150 ft of the exposed portions of the units. The water table is shown in figure 78. Details of its construction are given in Ryder (1988) and in Williams and Williamson (1989). Altitude of the water table ranges from essentially sea level at the coast and in the Gulf to more than 800 ft above sea level in the west.

The concept of a shallow water table that is replenished by precipitation and kept at an essentially constant altitude on an average annual basis is valid for undeveloped areas, and probably for developed areas receiving a large amount of precipitation such as in the east. In some areas, however, such as the west where withdrawal is large and precipitation is relatively small, dewatering has caused the water table to decline over the years. The model grid blocks representing the outcrop of the lower Claiborne-upper Wilcox aquifer were assigned a specific yield rather than an artesian storage coefficient, as follows:

Row	Column	Specific yield	Row	Column	Specific yield	Row	Column	Specific yield
2	22	0.15	23	11	0.15	78	21	0.15
2	31-35	0.15	25	12	0.15	79	19-21	0.15
3	20	0.15	31	16	0.15	80	19	0.15
3	38	0.15	33	18	0.15	80	20	0.15
4	20	0.15	34	18	0.15	81	18-19	0.15
6	38	0.15	35	18	0.15	82	18	0.15
7	38	0.15	39	19	0.15	83	17	0.15
8	38	0.15	40	19	0.15	84	16	0.15
9	38	0.15	47	20	0.15	85	15-16	0.15
11	10	0.15	48	20	0.15	86	14-15	0.15
12	20	0.15	52	21	0.15	87	13-14	0.15
13	20	0.15	55	22	0.15	88	13	0.15
14	8	0.15	58	23	0.15	89	12-13	0.15
14	20	0.15	61	24	0.15	90	12	0.15
15	8	0.15	62	24	0.15	91	12	0.15
15	20	0.15	64	25	0.15	92	11	0.15
16	20	0.15	65	25	0.15	93	11	0.10
16	21	0.15	68	24	0.15	94	11	0.10
17	20-21	0.15	69	24	0.15	94	17-18	0.10
17	26-28	0.15	70	24	0.15	95	13-18	0.10
18	9	0.15	71	24	0.15	96	16-18	0.10
18	20-23	0.15	72	24	0.15	97	17-18	0.10
18	25-27	0.15	73	23	0.15	98	17-19	0.10
19	10	0.15	74	23	0.15	99	18-20	0.10
19	20	0.15	75	23	0.15	100	19-20	0.10
19	25	0.15	76	22	0.15	101	20	0.10
21	11	0.15	77	21-22	0.15			

The head for the water table is held constant through time, but the flow into or out of the boundary layer is the product of the vertical gradient between the constant head and the head in the aquifer, and the conductance to flow between the two layers. This conductance is the harmonic mean conductance of the bottom one-half of the constant-head grid block and the top one-half of the aquifer grid block. The amount of flow into or out of the constant-head layer can be reduced (to zero, if desired) by reducing the conductance in the desired grid blocks during the model calibration.

Hydrologic Input Data

Starting heads for the transient model are the calibrated predevelopment heads. Initial estimates of hydraulic conductivity were determined from the steady-state model. Water density was estimated as discussed earlier; it was not adjusted during model calibration. Thicknesses of the units were discussed in detail in Ryder (1988).

In general, pumping periods for the model were chosen on 5-yr intervals to coincide with irrigation pumpage surveys done by the State approximately every 5 yrs beginning in 1958 (Texas Water Development Board, 1986). Public and industrial pumpage data are more accurate than irrigation pumpage data and are generally available on an annual or more frequent basis from State and local files and from published reports. Average public and industrial pumping rates were calculated for the appropriate pumping periods.

Pumping rates prior to 1958 were estimated from historical pumpage data found in various published reports. These data were less comprehensive and sometimes less accurate than post-1958 rates, particularly in regard to irrigation pumpage. Longer pumping periods were selected for the pre-1958 simulations. For the Houston-Galveston area, detailed records of public and industrial pumpage showed a significant shift in pumpage distributions after 1976. Thus a 4-yr pumping period was selected for 1973-76. A single-year pumping period was chosen for 1982 to quantify the flow system for that year. The locations and depths of the pumping wells were used to assign pumpages to 5-mi grid blocks for the appropriate model layers. As an example, the 1980 grid-block distributions of pumping rates that are applicable for the period 1977-82 are shown in figures 29-37. The pumping periods for the model and average pumping rates for the study area are summarized as follows:

Pumping period	Time interval	<u>Average Pumping Rate</u>	
		(Million ft ³ /d)	(Million gal/d)
1	1910	0	0
2	1911-37	34	254
3	1938-47	62	464
4	1948-57	122	913
5	1958-62	156	1,167
6	1963-67	189	1,414
7	1968-72	221	1,653
8	1973-76	222	1,661
9	1977-81	231	1,728
10	1982	231	1,728

A complete description and listing of pumpage data by State, county, model layer, and 5-mi grid block are given in Mesko and others (1990) for the GC RASA study.

During the calibration process, simulated heads are matched to measured heads. Two forms of measured head data were compiled for calibration purposes: (1) Potentiometric-surface maps in four intensively pumped areas (areas 1, 3, 4, and 5 in fig. 41) for 1982, the final year of the calibration period, and (2) hydrographs from 39 wells in six intensively pumped areas (fig. 41) that show water-level changes with time. Water-level data were obtained from the files of the Texas Water Development Board and Texas Water Commission (formerly the Texas Department of Water Resources) and the U.S. Geological Survey, and from published reports and maps.

The water levels that were selected to construct the 1982 potentiometric-surface maps generally are averages of the measurements in the wells for the time period beginning in June 1981 and ending in June 1983. Only single measurements that were made in the spring of 1982 were used for many wells; these wells provided supplementary data in areas where more detailed measurements were sparse. The water-level data were plotted, and potentiometric contours were drawn only through areas where a sufficient number of measurements existed. From the potentiometric contour maps, average head values for each 25-mi² grid block were determined for statistical comparison with simulated heads.

The wells for which hydrographs were constructed were selected on the following basis: (1) Even coverage of the major producing zones in the intensively pumped areas, (2) even distribution within the cones of depression, and (3) long-term record.

Initial estimates of storage coefficient values for aquifers and permeable zones were discussed in the earlier section "Storage Coefficient". The release of water by inelastic compaction of fine-grained deposits in permeable zones A, B, and C comprises a large percentage of total water released from storage during the transient simulations. This release of water also causes land-surface subsidence which was briefly discussed earlier. A digital model code incorporated from Leake and Prudic (1989) provides for the release of water by inelastic compaction of fine-grained deposits by converting from an elastic to an inelastic specific storage. This is done for the clay portion of a permeable zone when the head in a grid block declines below the critical head. The critical head is defined as the head that coincides with the maximum effective stress to which the deposits had previously been subjected.

If the computed head in a grid block recovers, the storage coefficient again becomes the elastic value, and the previous minimum head becomes the new critical head. If the head should decline below the new critical head, the storage coefficient again becomes the inelastic value, and so on. Simulated land-surface subsidence is the product of head decline below the critical head in each time step multiplied by the inelastic storage coefficient. See Leake and Prudic (1989) for a complete discussion and documentation of the land-subsidence simulation code, with qualifying assumptions and limitations.

Carr and others (1985, p. 45) concluded from a model calibration in the Houston area that a preconsolidation stress of 70 ft approximates the maximum effective stress to which deposits have been subjected prior to ground-water development. This means that 70 ft of head decline (from predevelopment starting heads) must occur at a model grid block before the first model conversion to an inelastic storage coefficient occurs. A critical head of 70 ft was adopted for the Texas GC RASA model.

Carr and others (1985, p. 35) related subsidence of the land surface, clay thickness, and decrease in artesian pressure for 1943-73 to derive inelastic storage coefficient values of the clay beds in the Houston area. In their computations, specific unit-compaction values are derived. These are an approximation of specific storage if the resulting compaction approximates the ultimate compaction from an applied stress. Mean specific unit-compaction values were $1.0 \times 10^{-4} \text{ ft}^{-1}$ for the Chicot aquifer and $1.8 \times 10^{-5} \text{ ft}^{-1}$ for the Evangeline aquifer. In an earlier study in the Houston area, Meyer and Carr (1979, p. 13) calculated a mean specific unit-compaction value of $8.7 \times 10^{-5} \text{ ft}^{-1}$ for the Chicot aquifer and $1.5 \times 10^{-5} \text{ ft}^{-1}$ for the Evangeline aquifer. These values were used as guidelines for initial estimates of inelastic storage coefficient for the clay intervals of permeable zones A, B, and C. (See table 1 for the relationship between the Chicot and Evangeline aquifers and permeable zones A, B, and C.)

Calibration Procedure and Results

The transient model was calibrated by adjusting horizontal and vertical hydraulic conductivity and elastic and inelastic storage coefficients until: (1) measured potentiometric surfaces and hydrographs in intensively pumped areas were reasonably matched by simulated heads; and (2) the cumulative measured land-surface subsidence in the Houston-Galveston area from predevelopment to 1973 was reasonably matched by simulated land subsidence. Calibration was aided by applying the results of a parameter-estimation model (L.K. Kuiper, U.S. Geological Survey, written commun., 1987), which automatically adjusts values of model variables so that the residual errors are minimized.

The Houston-Galveston area is shown as area 1 in figure 41. Simulated and measured 1982 potentiometric surfaces of permeable zones A, B, and C in the Houston-Galveston area are shown in figures 79, 80, and 81, respectively. The best fit of the simulated to the measured surfaces is for permeable zone B. The simulated potentiometric surface of permeable zone A is generally higher than the measured surface, while the simulated surface of permeable zone C is lower than the measured surface in the center of the cone of depression. Statistically, the absolute means of the residuals are 34 ft for permeable zone A, 25 ft for permeable zone B (includes residuals in Kingsville area), and 35 ft for permeable zone C (includes residuals in the Evadale area) (table 9).

Table 9.--Summary of simulated and measured 1982 altitudes of potentiometric surfaces

Aquifer or permeable zone	Total grid blocks with measured heads	Mean of residuals (feet)	Minimum residual (feet)	Maximum residual (feet)	Standard deviation (feet)	Absolute mean of residuals (feet)
Permeable zone A	121	27	-26	108	35	34
Permeable zone B	192	9	-96	72	29	25
Permeable zone C	89	1	-117	91	42	35
Lower Claiborne-upper Wilcox aquifer	216	17	-75	82	30	30

Hydrographs of water levels in wells 1, 2, 9, and 11 (see fig. 41) open to permeable zone A in the Houston-Galveston area are shown in figure 82. Wells 1 and 2 are on the northwestern rim of the 1982 cone of depression, well 11 is on the southern rim, and well 9 is near the center of the cone. Residual errors for the water levels are computed as the difference between simulated and measured where both exist at the end of a pumping period. The absolute means of the water-level residuals for wells 1, 2, 9, and 11 are 7, 9, 36, and 40 ft, respectively (table 10).

Hydrographs of water levels in wells 4, 7, 8, 12, and 10 (see fig. 41) open to permeable zone B in the Houston-Galveston area are shown in figures 83 and 84. Wells 4, 7, and 8 are near the center of the 1982 cone of depression, well 10 is on the eastern rim, and well 12 is on the southeastern rim. The absolute means of the water-level residuals for wells 4, 7, 8, 12, and 10 are 22, 23, 55, 52, and 73 ft, respectively (table 10).

Hydrographs of water levels in wells 3, 5, and 6 (see fig. 41) open to permeable zone C in the Houston-Galveston area are shown in figure 84. The wells are in the steep part of the 1982 cone of depression and are fairly well distributed about its center. The absolute means of the water-level residuals for wells 3, 5, and 6 are 49, 36, and 63 ft, respectively (table 10).

Hydrographs of water levels in wells 13, 14, and 15 open to permeable zone A in Jackson and Wharton Counties are shown in figure 85. All three wells are in the proximity of intense pumpage from permeable zone A for mainly rice irrigation; however, drawdowns are small in comparison to the Houston area. The absolute means of the water-level residuals for wells 13, 14, and 15 are 6, 9, and 6 ft, respectively (table 10).

The Evadale-Beaumont area is shown as area 3 in figure 41. Pumpage in the city of Evadale's well field (at the Jasper-Hardin County line) is from zones B and C. The simulated and measured 1982 potentiometric surfaces of permeable zone C in the well field area are shown in figure 81. The two surfaces are reasonably well matched. A water-level hydrograph of well 16 (see fig. 41) open to permeable zone C and located near the center of the 1982 cone of depression is shown in figure 86. The absolute mean of the water-level residuals for well 16 is 34 ft (table 10).

A water-level hydrograph of well 17 (see fig. 41), which is open to permeable zone B and located just north of the city of Beaumont's well field at the Jefferson-Hardin County line, is shown in figure 86. Pumpage in the well field is from permeable zone B. The absolute mean of the water-level residuals for well 17 is 13 ft (table 10).

The Kingsville area is shown as area 4 in figure 41. Pumpage in the city of Kingsville's well field in Kleberg County is from permeable zone B. A distinctive feature of the simulated and measured 1982 potentiometric surfaces shown in figure 87 is the shift of the simulated cone of depression toward the east. This was the result of having to shift pumpage, which was located between grid blocks, to the bordering eastern grid block. Water-level hydrographs of wells 18, 19, 20, and 21 open to permeable zone B are shown in figure 88. Wells 18 and 19 are on the western rim of the 1982 cone of depression and nearer to the center than wells 20 and 21, which are on the eastern rim. The absolute means of the water-level residuals for wells 18, 19, 20, and 21 are 55, 42, 17, and 22 ft, respectively (table 10).

The Winter Garden area is shown as area 5 in figure 41. Pumpage is mostly from the lower Claiborne-upper Wilcox aquifer. The 1982 simulated and measured potentiometric surfaces of the lower Claiborne-upper Wilcox aquifer are shown in figure 89. The absolute mean of the water-level residuals for the aquifer in the Winter Garden area is 30 ft (table 9).

Water-level hydrographs of 15 wells open to the lower Claiborne-upper Wilcox aquifer in the Winter Garden area are shown in figures 90-93. Wells 23 and 26 (fig. 90), well 29 (fig. 91), and wells 25 and 32 (fig. 92) are nearest the center of the huge cone of depression. The remaining wells are located on the flanks of the cone in all directions from the center. Absolute means of the water-level residuals for the wells range from 8 ft for well 24 to 83 ft for well 34 (table 10).

Table 10.--Summary of simulated and measured water levels in wells shown in figure 41

Well number	Aquifer or permeable zone	Absolute mean of residuals (feet)	Well number	Aquifer or permeable zone	Absolute mean of residuals (feet)
1	Permeable zone A	7	21	Permeable zone B	22
2	Permeable zone A	9	22	Lower Claiborne-upper Wilcox aquifer	57
3	Permeable zone C	49	23	Lower Claiborne-upper Wilcox aquifer	53
4	Permeable zone B	22	24	Lower Claiborne-upper Wilcox aquifer	8
5	Permeable zone C	36	25	Lower Claiborne-upper Wilcox aquifer	61
6	Permeable zone C	63	26	Lower Claiborne-upper Wilcox aquifer	54
7	Permeable zone B	23	27	Lower Claiborne-upper Wilcox aquifer	10
8	Permeable zone B	55	28	Lower Claiborne-upper Wilcox aquifer	26
9	Permeable zone A	36	29	Lower Claiborne-upper Wilcox aquifer	65
10	Permeable zone B	73	30	Lower Claiborne-upper Wilcox aquifer	30
11	Permeable zone A	40	31	Lower Claiborne-upper Wilcox aquifer	9
12	Permeable zone B	52	32	Lower Claiborne-upper Wilcox aquifer	79
13	Permeable zone A	6	33	Lower Claiborne-upper Wilcox aquifer	36
14	Permeable zone A	9	34	Lower Claiborne-upper Wilcox aquifer	83
15	Permeable zone A	6	35	Lower Claiborne-upper Wilcox aquifer	37
16	Permeable zone C	34	36	Lower Claiborne-upper Wilcox aquifer	37
17	Permeable zone B	13	37	Lower Claiborne-upper Wilcox aquifer	53
18	Permeable zone B	55	38	Lower Claiborne-upper Wilcox aquifer	91
19	Permeable zone B	42	39	Lower Claiborne-upper Wilcox aquifer	87
20	Permeable zone B	17			

The Lufkin-Nacogdoches area is shown as area 6 in figure 41. A steep cone of depression has developed on the potentiometric surface of the lower Claiborne-upper Wilcox aquifer as a result of intense pumpage centered between Angelina and Nacogdoches Counties. Data do not exist to construct an accurate post-development potentiometric surface. Hydrographs of water-levels in wells 37, 38, and 39 open to the lower Claiborne-upper Wilcox aquifer in the Lufkin-Nacogdoches area are shown in figure 94. Wells 37 and 38 are located east of and nearest the pumping center; well 39 is located southeast of the concentrated pumpage. The absolute means of the water-level residuals for wells 37, 38, and 39 are 53, 91, and 87 ft, respectively (table 10). Simulated heads are much higher than measured heads in the three wells near the center of withdrawal.

Simulated and measured cumulative land-surface subsidence in the Houston-Galveston area from predevelopment to 1973 is shown in figure 95. The simulated subsidence tends to be somewhat less than measured values in the center of greatest subsidence, and somewhat greater in far western Harris and northeastern Fort Bend Counties. The absolute mean of the subsidence residuals for the 196 grid blocks is 0.6 ft.

Calibrated values of horizontal and vertical hydraulic conductivity and transmissivity are presented in figures 7 through 16 and in tables 3 and 4. A summary of calibrated elastic storage coefficient values is presented in table 5. Calibrated inelastic specific storage values for fine-grained deposits in permeable zones A, B, and C in the Houston-Galveston area are $8.5 \times 10^{-5} \text{ ft}^{-1}$, $8.0 \times 10^{-5} \text{ ft}^{-1}$, and $8.0 \times 10^{-6} \text{ ft}^{-1}$, respectively.

The model calibration is sufficiently accurate for its intended purpose--to provide estimates of aquifer properties and to identify in a general way the sources and quantities of flow in the aquifer systems. Practical considerations of objectives of the model study, scale of the system, and computer-cost limitations have determined important factors such as the number of model layers and grid-block size. Some of the differences between simulated and measured heads that were just described may seem large, on the order of a few tens of feet. A listing of some important sources of error in model calibration and resulting simulated heads and flow rates is as follows:

1. There is inherent difficulty in estimating values for a set of model variables that minimize residual errors in head and land subsidence in a complex, interrelated system of numerous aquifers, permeable zones, and confining units.
2. The physical system is overgeneralized by the restricted number of model layers, particularly for the coastal lowlands aquifer system where there is a large amount of heterogeneity. Additional layers would improve model accuracy in areas such as Houston, where the vertical distributions of numerous pumpage and head data are reasonably well known. A related source of error is that the model simulations assume that pumping and observation wells are open to the full length of the aquifer or model layer--generally, this is not true. Thus, simulated heads can only be approximations of measured heads.
3. In general, the accuracy of simulation models decreases with increasing grid-block size. The large grid-block size, 25 mi^2 , may lead to overgeneralization of the input data and poor resolution of model results in some areas. For example, in the Houston area pumpage and head data are of sufficient density to warrant smaller grid spacing. Another example is Kingsville, where significant error was introduced because the city's well field lies almost exactly between the centers of the large grid blocks.
4. The accuracy of simulated development heads and drawdowns is dependent upon correct predevelopment starting heads. Simulated starting heads are subject to considerable error in some areas.
5. The model must simulate average conditions over long time periods (generally of 5-yr duration after 1958). This is necessitated by long periods of unknown or poorly understood irrigation pumpage data, as well as variations in recharge.
6. A considerable portion of modeled recharge rates in some areas may consist of return flow from irrigation pumpage to the ground-water system. Such rates of return flow generally are unknown or poorly understood.
7. It is uncertain whether or not there is a long-term net dewatering of shallow sands in the eastern part of the study area, where precipitation is more abundant. Such knowledge may be important in evaluating modeled estimates of the amount of ground-water pumpage derived from recharge and from releases from storage.

8. Simulation of land-surface subsidence is subject to the following additional sources of error (Prudic and Williamson, 1984): (a) The critical head in the clay portion of a permeable zone is assumed to be equal to the head in the sand deposits. However, time is needed for a head change to propagate through the clay deposits. Ignoring the time lag affects the distribution and amount of the simulated subsidence. (b) Water is assumed to be released from the inelastic compaction of clays instantaneously with a head decline below the critical head. There may be a lag time of several years between observed subsidence and a head change in coarse-grained deposits as the head change gradually propagates through the fine-grained deposits. (c) The inelastic specific storage is assumed to be constant. However, lab tests indicate that the amount of water released from inelastic compaction is a function of applied stress. In addition, the vertical hydraulic conductivity of the compacting deposits, treated as a constant in the model, should theoretically decrease with time. Most of the errors associated with item 8 tend to be minimized because of the large time periods for averaging pumpages in the model simulations.

Insight into the relative amount of error in simulated heads and land-surface subsidence resulting from incorrect estimates of aquifer and confining-unit properties can be gained by analyzing the sensitivity of the model calibration to changes in selected model variables.

Sensitivity Analysis

Ten transient model simulations were made in order to test the sensitivity of the model to changes in the calibrated values of horizontal and vertical hydraulic conductivity, water density, storage coefficient, and initial critical head (for land-surface subsidence). The changes for the 10 model simulations are summarized in the following table:

Model simulation	Property change
1	Horizontal hydraulic conductivity (K_h) of all aquifers and permeable zones = calibrated $K_h \times 1.5$
2	Horizontal hydraulic conductivity (K_h) of all aquifers and permeable zones = calibrated $K_h \times 0.5$
3	Vertical hydraulic conductivity (K_v) of all model layers = calibrated $K_v \times 1.5$
4	Vertical hydraulic conductivity (K_v) of all model layers = calibrated $K_v \times 0.5$
5	Water density (DEN) = 1.000 g/cm^3 in all model layers
6	DEN = calibrated DEN + 0.010 g/cm^3 for grid blocks in all model layers where DEN is greater than 1.002 g/cm^3
7	Storage coefficient (S) of all aquifers and permeable zones = calibrated $S \times 1.5$
8	Storage coefficient (S) of all aquifers and permeable zones = calibrated $S \times 0.5$
9	Initial critical head (D) for conversion to inelastic storage coefficient = calibrated $D \times 1.5$
10	Initial critical head (D) for conversion to inelastic storage coefficient = calibrated $D \times 0.5$

Each change was uniform over the modeled area with the exceptions noted above. When the value of each property was changed for a model simulation, the values of all other properties remained unchanged from their calibrated values. Because recharge and discharge are simulated by a head-dependent flux boundary, these values are allowed to change with any change in head in the sensitivity simulations.

The sensitivity simulations are evaluated by: (1) Showing graphically the change from 1982 calibrated heads in permeable zones A, B, and C along row 43 of the model grid (fig. 77), and in the lower Claiborne-upper Wilcox aquifer along row 91; (2) statistically comparing the new residual errors for 1982 simulated and measured potentiometric surfaces with calibration residuals; (3) statistically comparing the new residual errors for simulated and measured predevelopment to 1973 land-surface subsidence with calibration residuals; and (4) comparing graphically and statistically simulated and measured hydrographs for selected wells in the Houston and Winter Garden areas.

Row 43 was selected because it goes approximately through the centers of the cones of depression in permeable zones A, B, and C in the Houston-Galveston area. Row 91 goes approximately through the center of the cone of depression in the lower Claiborne-upper Wilcox aquifer in the Winter Garden area.

The horizontal hydraulic conductivity of the aquifers and permeable zones was increased by 50 percent for the first sensitivity simulation. The changes in 1982 heads in intensively pumped units along the two model rows are shown in figure 96. Heads are greater than calibrated heads within the cones of depression developed in permeable zones A, B, and C in the Houston-Galveston area, and in the lower Claiborne-upper Wilcox aquifer in the Winter Garden area. For each unit, the peak departure from calibrated heads occurs where the cone of depression is steepest. Peak departures range from 20 ft for permeable zone A to 150 ft for permeable zone C. For permeable zones A, B, and C, the departure of heads from calibrated heads is almost negligible beyond the coastline (beyond about column 50).

Statistical analyses of the residual errors for 1982 simulated and measured potentiometric surfaces resulting from the increased horizontal hydraulic conductivity are shown in table 11. Absolute means of the residuals increased from 34 ft (calibrated value) to 41 ft for permeable zone A, from 25 to 42 ft for permeable zone B, from 35 to 54 ft for permeable zone C, and from 30 to 56 ft for the lower Claiborne-upper Wilcox aquifer.

The effect of increased conductivity on land-surface subsidence in the Houston-Galveston area is shown statistically in table 12. The absolute mean of the residual errors for simulated and measured predevelopment to 1973 land-surface subsidence increased from a calibrated value of 0.6 ft to 0.8 ft.

A 50-percent decrease in horizontal hydraulic conductivity results in head departures that are nearly mirror images of those shown for the 50-percent increase (fig. 96). However, the departures are larger, with peak departures ranging from -37 ft for permeable zone A to -350 ft for permeable zone C. Absolute means of the 1982 head residuals are 28 ft for permeable zone A, 54 ft for permeable zone B, 87 ft for permeable zone C, and 74 ft for the lower Claiborne-upper Wilcox aquifer (table 11). The residuals for permeable zone A are an improvement over the calibration residuals. The reduced horizontal hydraulic conductivity causes additional drawdown that is generally needed in the Houston-Galveston area for an improved calibration. However, statistical data for the other units shown in table 11 indicate that the reduced hydraulic conductivity resulted in much poorer matches of simulated and measured heads. The absolute mean of the land-surface subsidence residuals is 0.9 ft (table 12).

For the third model sensitivity simulation, the vertical hydraulic conductivity of all model layers was increased by 50 percent. Generally, the increase had the same effect as the increase in horizontal hydraulic conductivity--to raise the heads above the calibrated heads (fig. 97). Peak departures from calibrated heads are much smaller, ranging from 11 ft for permeable zone A to 30 ft for the lower Claiborne-upper Wilcox aquifer. Absolute means of the 1982 head residuals are 37 ft for permeable zone A, 25 ft for permeable zone B, 35 ft for permeable zone C, and 39 ft for the lower Claiborne-upper Wilcox aquifer (table 11). The absolute mean of the land-surface subsidence residuals is 0.7 ft (table 12).

A 50-percent decrease in vertical hydraulic conductivity results in head departures that are nearly mirror images of those shown for the 50-percent increase (fig. 97). As for the case with horizontal conductivity, the departures are larger, with peak departures ranging from -25 ft for permeable zone A to -50 ft for the lower Claiborne-upper Wilcox aquifer. For permeable zone C, there is a rise in heads of about 10 to 15 ft extending from column 43 to the downdip limit.

Table 11.--*Summary of calibration residual errors for 1982 heads and those resulting from changes in model variables*

Aquifer or permeable zone	Grid blocks with mea- sured heads	Change in model variable	Mean of residuals (feet)	Minimum residual (feet)	Maximum residual (feet)	Standard deviation (feet)	Absolute mean of residuals (feet)
Permeable zone A	121	CALIBRATION	27	-26	108	35	34
		1.5 X KH's ^{1/}	34	-32	102	39	41
		0.5 X KH's	7	-69	87	35	28
		1.5 X KV's ^{2/}	34	-25	104	35	37
		0.5 X KV's	5	-69	77	39	35
		densities = 1.0	24	-39	95	36	34
		densities >1.002					
		= +0.01	24	-38	95	35	34
Permeable zone B	192	1.5 X S ^{3/}	29	-35	101	37	37
		0.5 X S	14	-46	84	34	31
		CALIBRATION	9	-96	72	29	25
		1.5 X KH's	36	-63	105	33	42
		0.5 X KH's	-48	-405	38	64	54
		1.5 X KV's	12	-94	78	29	25
		0.5 X KV's	-4	-125	62	38	30
		densities = 1.0	6	-94	73	32	26
Permeable zone C	89	densities >1.002					
		= +0.01	5	-96	72	31	25
		1.5 X S	24	-82	82	32	34
		0.5 X S	-24	-147	69	39	36
		CALIBRATION	1	-117	91	42	35
		1.5 X KH's	40	-68	137	54	54
		0.5 X KH's	-84	-454	28	108	87
		1.5 X KV's	7	-109	90	41	35
Lower Claiborne- upper Wilcox aquifer	216	0.5 X KV's	-14	-125	96	46	39
		densities = 1.0	-4	-124	116	44	35
		densities >1.002					
		= +0.01	-1	-115	77	41	34
		1.5 X S	20	-68	117	45	38
		0.5 X S	-36	-190	44	51	45
		CALIBRATION	17	-75	82	30	30
		1.5 X KH's	52	-89	114	38	56
		0.5 X KH's	-66	-235	90	61	74
		1.5 X KV's	36	-50	85	29	39
		0.5 X KV's	-14	-116	78	35	30
		densities = 1.0	14	-75	81	28	26
		densities >1.002					
		= +0.01	19	-74	83	31	30
		1.5 X S	38	-55	128	33	42
		0.5 X S	-20	-114	46	30	27

^{1/} KH = horizontal hydraulic conductivity.

^{2/} KV = vertical hydraulic conductivity.

^{3/} S = storage coefficient or specific yield.

Table 12.—*Summary of calibration residual errors for land-surface subsidence and those resulting from changes in model variables*

Change in model variable	Grid blocks with measured subsidence	Mean of residuals (feet)	Minimum residual (feet)	Maximum residual (feet)	Standard deviation (feet)	Absolute mean of residuals (feet)
CALIBRATION	196	-0.2	-2.5	2.1	0.7	0.6
1.5 X KH ^{1/}		-.6	-3.7	1.6	.8	.8
0.5 X KH		.4	-1.2	7.4	1.3	.9
1.5 X KV ^{2/}		-.4	-2.8	2.0	.7	.7
0.5 X KV		.2	-2.0	3.2	.9	.7
density = 1.0		-.2	-2.5	2.4	.8	.6
density >1.002 = density + 0.01		-.2	-2.5	2.4	.8	.6
1.5 X S ^{3/}		-.02	-1.9	4.5	1.0	.7
0.5 X S		-.5	-3.9	1.3	.8	.7
.5 X D ^{4/} = 105 feet		-.5	-3.2	1.8	.7	.7
.5 X D = 35 feet		.3	-1.9	3.1	.9	.7

^{1/} KH = horizontal hydraulic conductivity.

^{2/} KV = vertical hydraulic conductivity.

^{3/} S = storage coefficient.

^{4/} D = head decline that must occur before model converts to inelastic storage value.

Absolute means of the potentiometric-surface residuals are 35 ft for permeable zone A, 30 ft for permeable zone B, 39 ft for permeable zone C, and 30 ft for the lower Claiborne-upper Wilcox aquifer (table 11). The absolute mean of the land-surface subsidence residuals is 0.7 ft (table 12).

For the fifth model sensitivity simulation, the density of the water in all model layers was given a uniform value equal to 1.000 g/cm^3 . For permeable zones A, B, and C, the changed density produced essentially no change from the calibrated heads where the units originally contained fresh to slightly saline water (dissolved-solids concentration less than about $3,000 \text{ mg/L}$) (fig. 98). Farther downdip in the three zones, the heads departed from the calibrated heads in an upward direction, with peak departures ranging from 15 ft for permeable zone A to 240 ft for permeable zone C. For the lower Claiborne-upper Wilcox aquifer along row 91, heads departed from calibrated heads in a downward direction, with a peak departure of -43 ft (fig. 98).

Absolute means of the 1982 potentiometric-surface residuals were nearly identical to the calibrated values for permeable zones A and B, and C (table 11). The absolute mean for the lower Claiborne-upper Wilcox residuals is 26 ft, an improvement over the calibrated value of 30 ft because of the additional drawdown downdip in the Winter Garden area. The statistical data for the land-surface subsidence residuals are nearly the same as for the calibrated values (table 12).

For the next model simulation, the water density in all model layers was increased by 0.010 g/cm^3 for those grid blocks where the density was greater than 1.002 g/cm^3 . The changed density produced essentially no change from the calibrated heads where the units originally contained fresh to slightly saline water (fig. 98). For downdip blocks in zones A, B, and C, the heads were a few feet lower than calibrated heads. For the extreme downdip blocks in the lower Claiborne-upper Wilcox aquifer, the heads were a few feet higher. Statistical data for the potentiometric-surface and land-surface subsidence residuals were nearly identical to the calibrated values (tables 11 and 12).

The seventh model sensitivity simulation consisted of increasing the storage coefficient of all aquifers and permeable zones by 50 percent. The increase tended to raise the heads above the 1982 calibrated heads for the inland parts of rows 43 and 91 (fig. 99). Peak departures from calibrated heads range from 7 ft for permeable zone A to 42 ft for permeable zone C.

Absolute means of the 1982 potentiometric-surface residuals are 37, 34, 38, and 42 ft for permeable zones A, B, C, and the lower Claiborne-upper Wilcox aquifer, respectively (table 11). The absolute mean of the land-surface subsidence residuals is 0.7 ft (table 12).

A 50-percent decrease in the storage coefficient had the opposite effect of the 50-percent increase. The heads are lower than the 1982 calibrated heads (fig. 99), with peak departures ranging from -17 ft for permeable zone A to -75 ft for permeable zone C. The departures are larger for the decrease in storage coefficient compared to the increase.

The effect of the decreased storage coefficient on 1982 potentiometric-surface residuals produced mixed results. For permeable zone A and the lower Claiborne-upper Wilcox aquifer, the statistical values of simulated to measured heads are slightly better than the calibration values, while the residuals for zones B and C are considerably worse than calibrated values (table 11). The absolute mean of the land-surface subsidence residuals is 0.7 ft (table 12).

An additional test of the sensitivity of the model to the change in storage coefficient consists of comparing the new drawdown distributions over time to calibrated values and to measured values. This was done at five observation wells located near the centers of large cones of depressions. Three wells in the Houston area are open to permeable zones A, B, and C (fig. 100). Two wells in the Winter Garden area are open to the lower Claiborne-upper Wilcox aquifer (fig. 101).

Simulated water levels for the three model simulations (calibration, 50-percent increase and 50-percent decrease in storage coefficient) are compared to measured water levels in the five wells at the end of each time step (where measured water levels exist). The results, in terms of absolute means of the residuals, are as follows:

Well no. (see figs. 41, 100, and 101)	Aquifer or permeable zone	Period compar- ison	<u>Absolute mean of residuals (feet)</u>		
			Calibra- tion	50-percent increase in storage	50-percent decrease in storage
9	Permeable zone A	1957-82	36	52	19
7	Permeable zone B	1947-82	23	45	28
3	Permeable zone C	1947-82	49	73	23
23	Lower Claiborne- upper Wilcox	1947-82	53	60	40
29	Lower Claiborne- upper Wilcox	1957-82	65	84	33

For the five wells, the increase in storage coefficient produces residuals that are substantially larger than the calibration residuals. However, the decrease in storage coefficient produces residuals that are substantially better for four of the five wells. Only for well no. 7, open to permeable zone B in the Houston area, are the calibration residuals smaller. Although a smaller storage coefficient may seem indicated, at least for some areas in some layers, the following factors may suggest otherwise: (1) The specific storage estimate of 1.0×10^{-6} ft⁻¹ is approaching a minimum value for confined clastic sediments; (2) the number of hydrographs (five) is a small sample considering the large areal extent of the major cones of depression in the study area; (3) the head as measured in a well may be an average over a smaller vertical thickness of aquifer than the thickness assigned to the model block. Thus, to obtain a match of simulated and measured water levels, the storage coefficient may have to be adjusted downward to account for the lesser thickness open to the well; and (4) other factors that may contain considerable errors, such as estimates of starting heads and pumpage, exert a large influence on the configuration of the simulated hydrographs.

Final model sensitivity simulations were made to test the effect of raising and lowering the initial critical head on land-surface subsidence residuals. A 50-percent increase in initial critical head, from 70 to 105 ft, produces a rise in the absolute mean of the residuals from a calibrated value of 0.6 to 0.7 ft (table 12). A 50-percent reduction of the initial critical head, from 70 to 35 ft, produces the same absolute mean of the residuals as did the increase—0.7 ft. Thus, the critical head does not seem sensitive to the simulation of land subsidence, but it may affect the simulation of drawdowns in the model.

To summarize the sensitivity analysis:

1. The sensitivity of the model calibration is tested by analyzing the impact of a changed model variable on 1982 potentiometric-surface residuals, hydrograph residuals, and land-surface subsidence residuals.
2. The model is most sensitive and has the highest residuals when horizontal hydraulic conductivity is decreased by 50 percent. An exception is for permeable zone A, where a 50-percent decrease causes smaller 1982 head residuals.
3. The model is moderately sensitive to 50-percent changes in vertical hydraulic conductivity and storage coefficient.
4. The model is least sensitive to changes in water density.

ILLUSTRATIONS

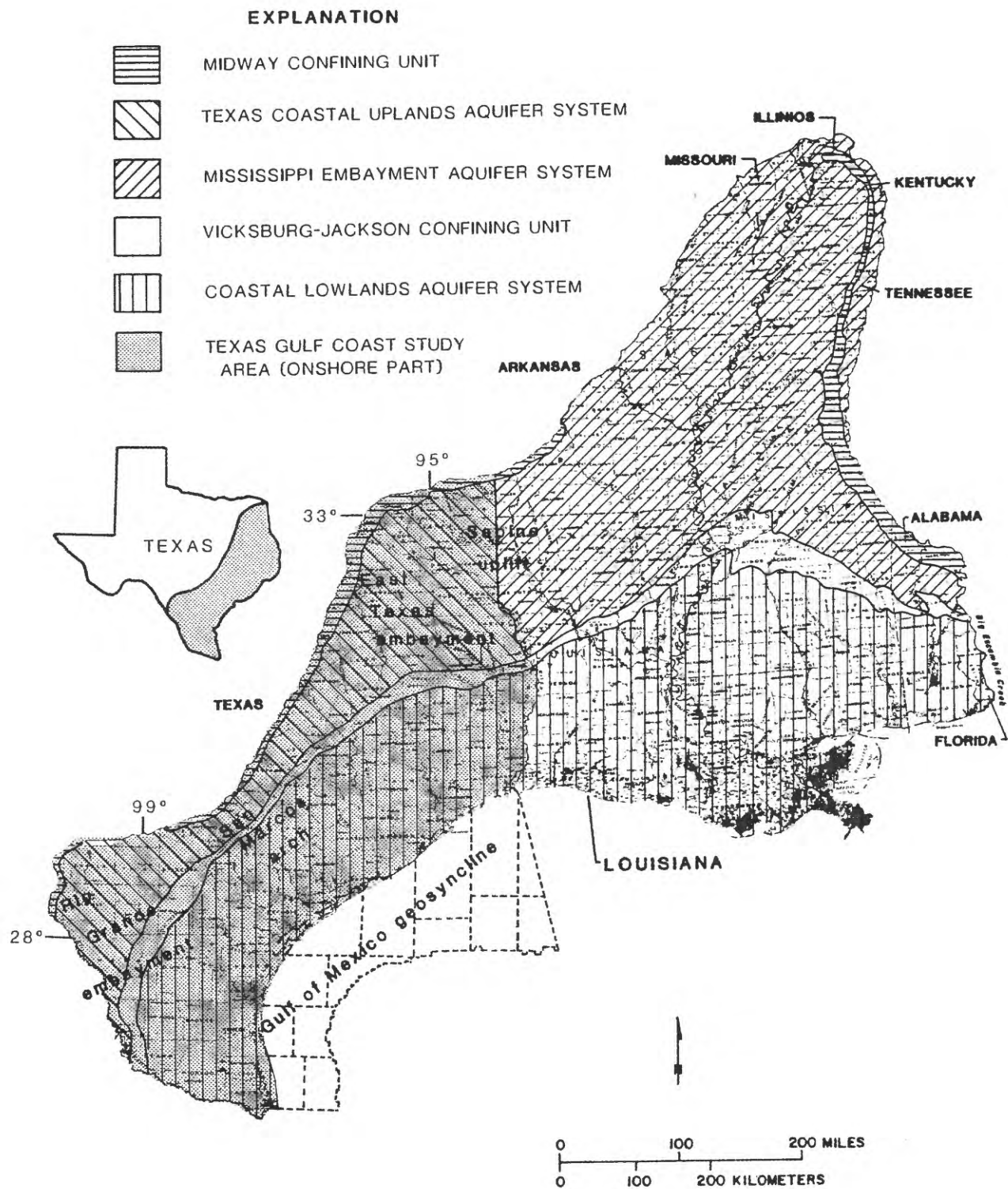


Figure 1.--Relation of Texas Gulf Coast study area to onshore part of the Gulf Coast Regional Aquifer-System Analysis study area. (Modified from Grubb, 1984)

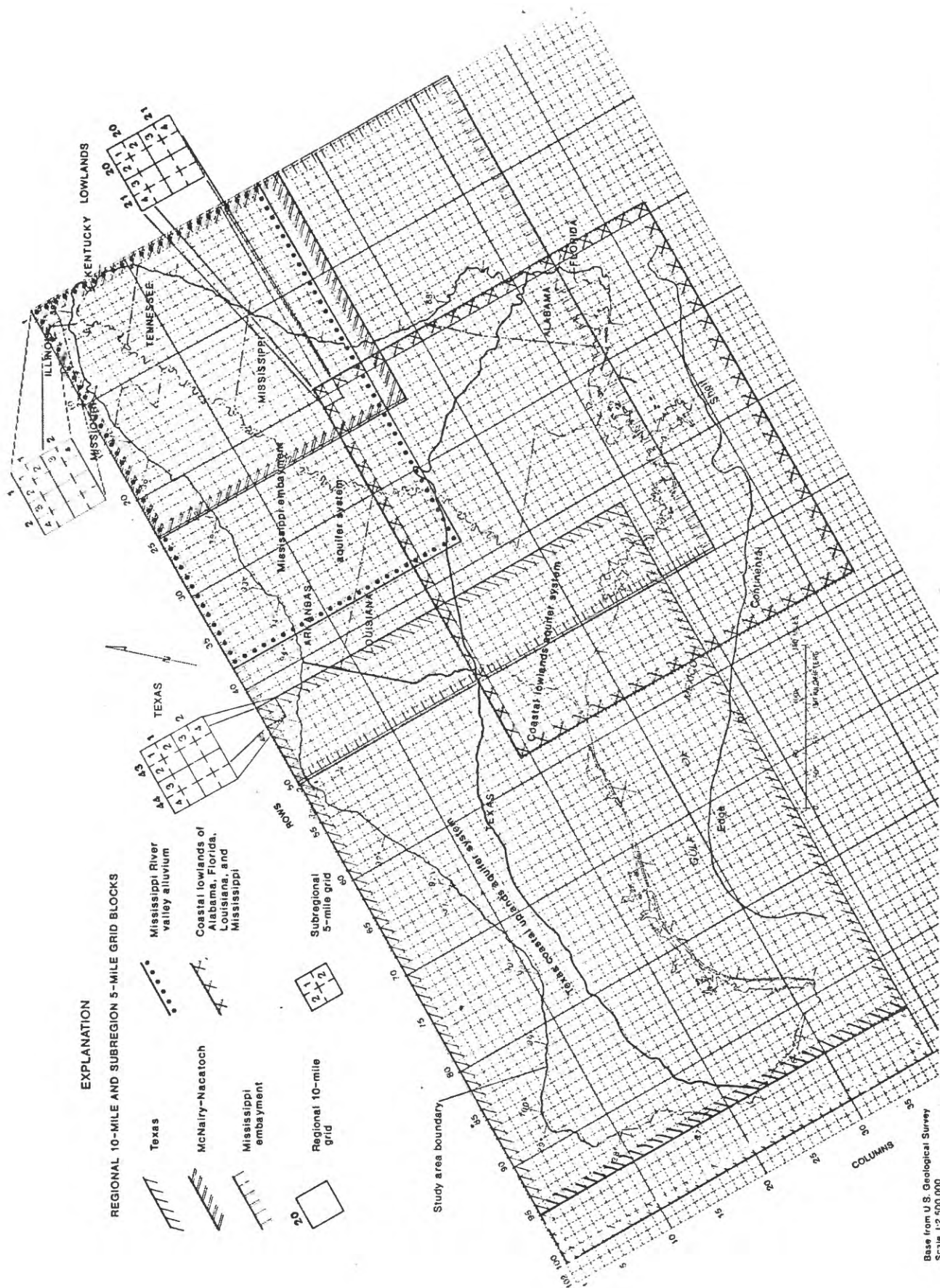
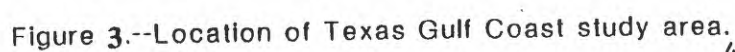


Figure 2--Relation of the Texas subregional modeled area to other subregional modeled areas and to the regional modeled area

-----OFFSHORE AREAS



EXPLANATION

—48— LINE OF EQUAL MEAN ANNUAL
PRECIPITATION—Interval 2 and 4 inches

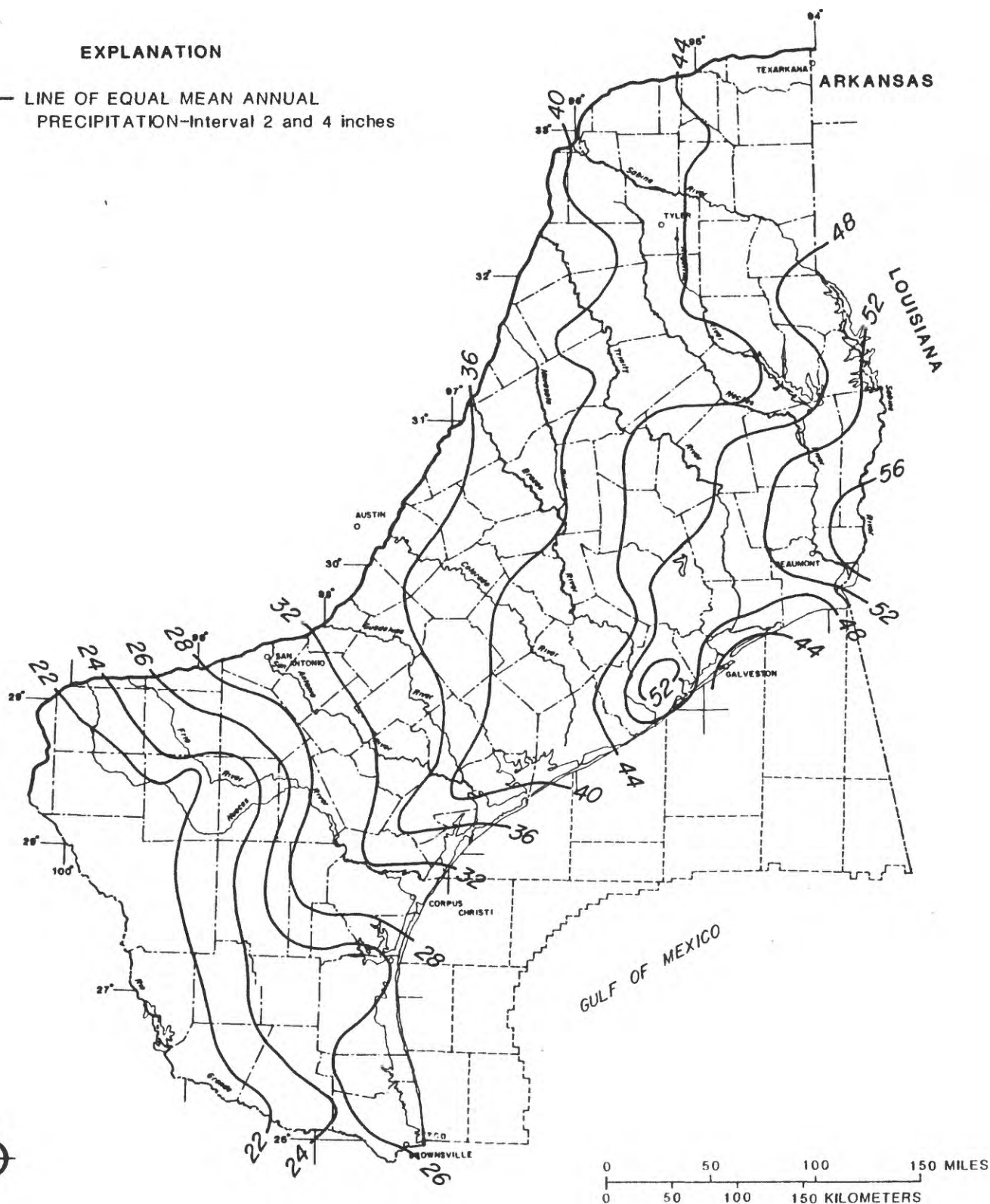


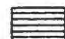



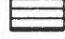
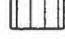
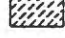



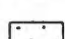


Figure 4.--Mean annual precipitation in the Texas Gulf Coast study area. Based on National Oceanic and Atmospheric Administration records for the period 1951-80. (Modified from Texas Department of Water Resources, 1984, fig. 5).

EXPLANATION

-  MIDWAY CONFINING UNIT
-  MIDDLE WILCOX AQUIFER
-  LOWER CLAIBORNE-UPPER WILCOX AQUIFER
-  LOWER CLAIBORNE CONFINING UNIT
-  MIDDLE CLAIBORNE AQUIFER
-  MIDDLE CLAIBORNE CONFINING UNIT
-  UPPER CLAIBORNE AQUIFER
-  VICKSBURG-JACKSON CONFINING UNIT
-  LOWER MIOCENE-UPPER OLIGOCENE PERMEABLE ZONE
-  MIDDLE MIOCENE PERMEABLE ZONE
-  LOWER PLIOCENE-UPPER MIOCENE PERMEABLE ZONE
-  LOWER PLEISTOCENE-UPPER PLIOCENE PERMEABLE ZONE
-  HOLOCENE-UPPER PLEISTOCENE PERMEABLE ZONE

A—A' LINE OF HYDROGEOLOGIC SECTION

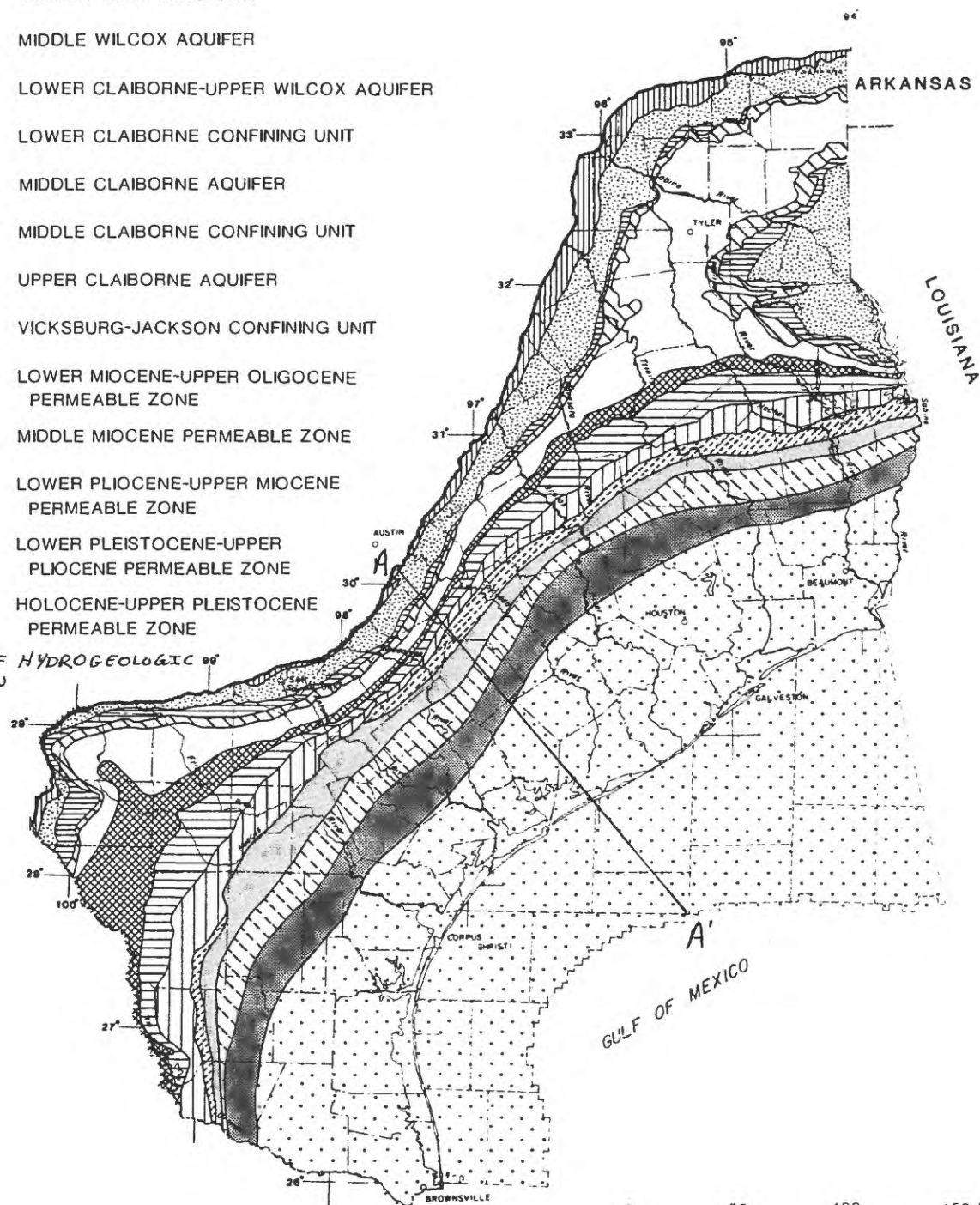


Figure 5.—Generalized outcrops of aquifers, permeable zones, and confining units.

EXPLANATION

HYDROGEOLOGIC UNITS

1	Permeable zone A
2	Permeable zone B
3	Permeable zone C
4	Zone D confining unit
5	Permeable zone D
6	Zone E confining unit
7	Permeable zone E
8	Vicksburg-Jackson confining unit
9	Upper Claiborne aquifer
10	Middle Claiborne confining unit
11	Middle Claiborne aquifer
12	Lower Claiborne confining unit
13	Lower Claiborne-upper Wilcox aquifer
14	Middle Wilcox aquifer
	Midway confining unit

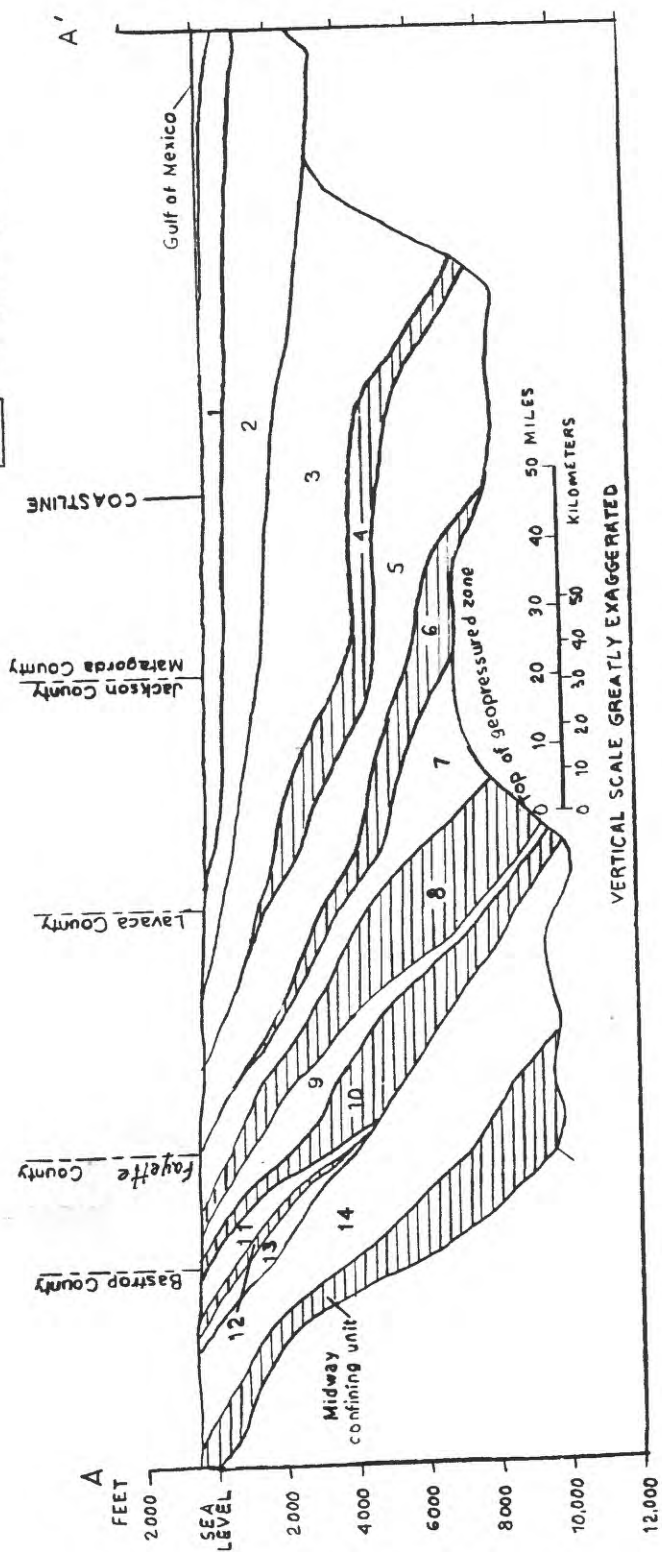
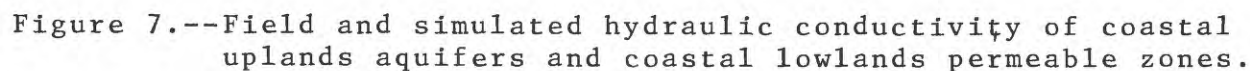


Figure 6 .--Hydrogeologic section A-A'. Line of section shown on figure 5.

BOUNDARY OF SUBAREAS

18 (23)	Estimated from aquifer-test analyses
13 (99)	Estimated from specific-capacity data

21 MEAN HYDRAULIC CONDUCTIVITY, IN FEET
PER DAY, IN CALIBRATED DIGITAL MODEL



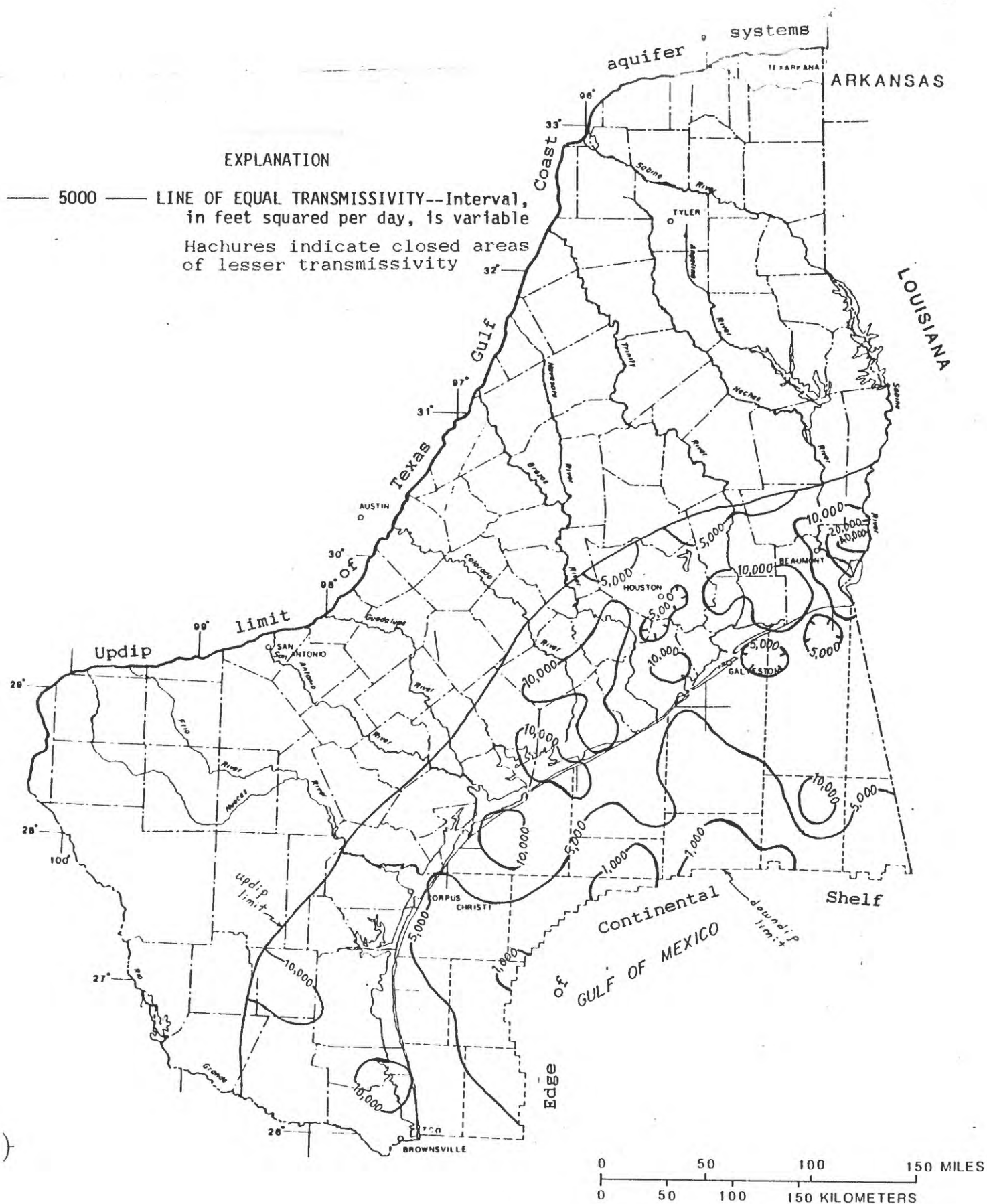


Figure 8.--Simulated transmissivity of permeable zone A.

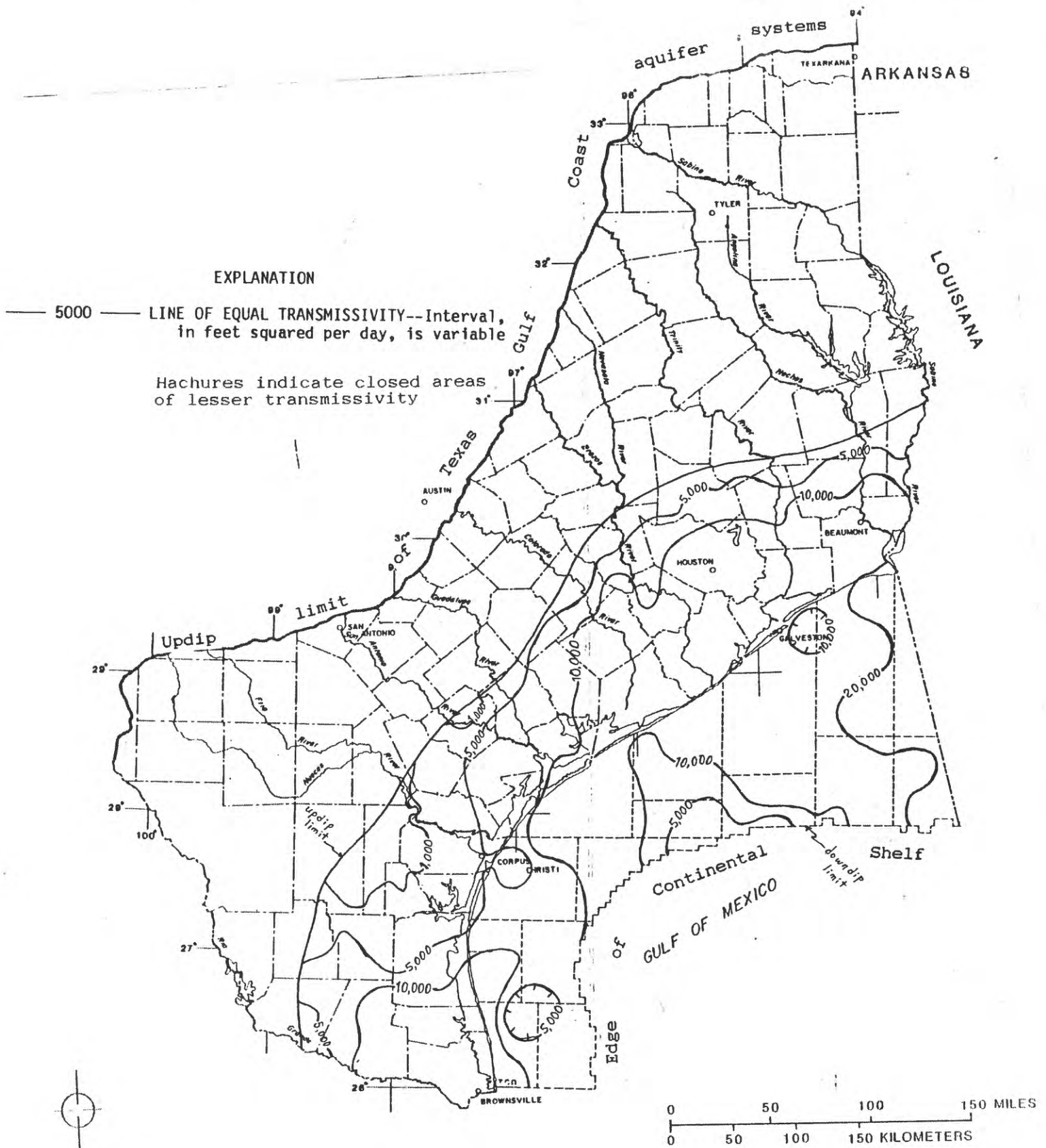


Figure 9.--Simulated transmissivity of permeable zone B.

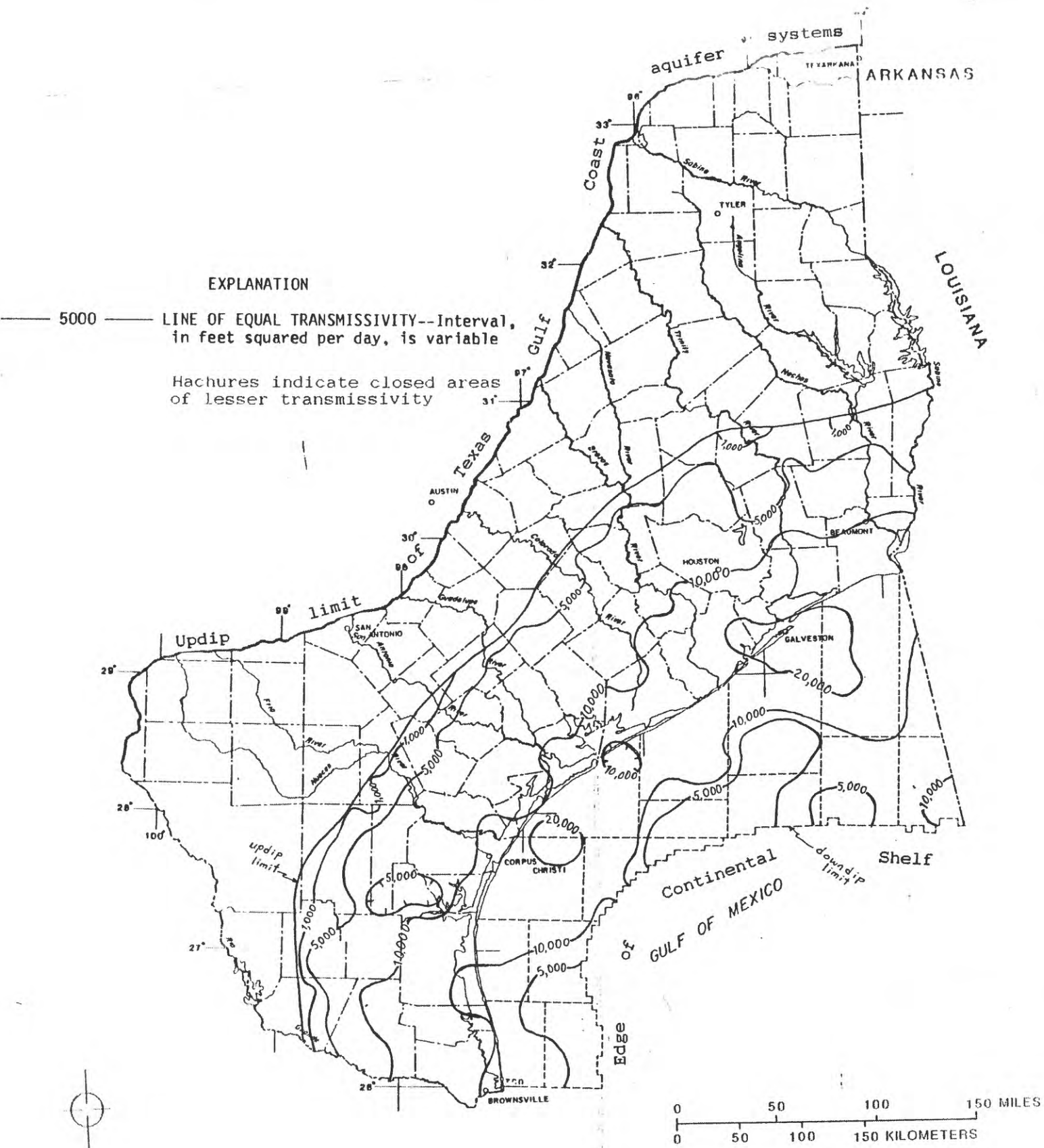


Figure 10.--Simulated transmissivity of permeable zone C.

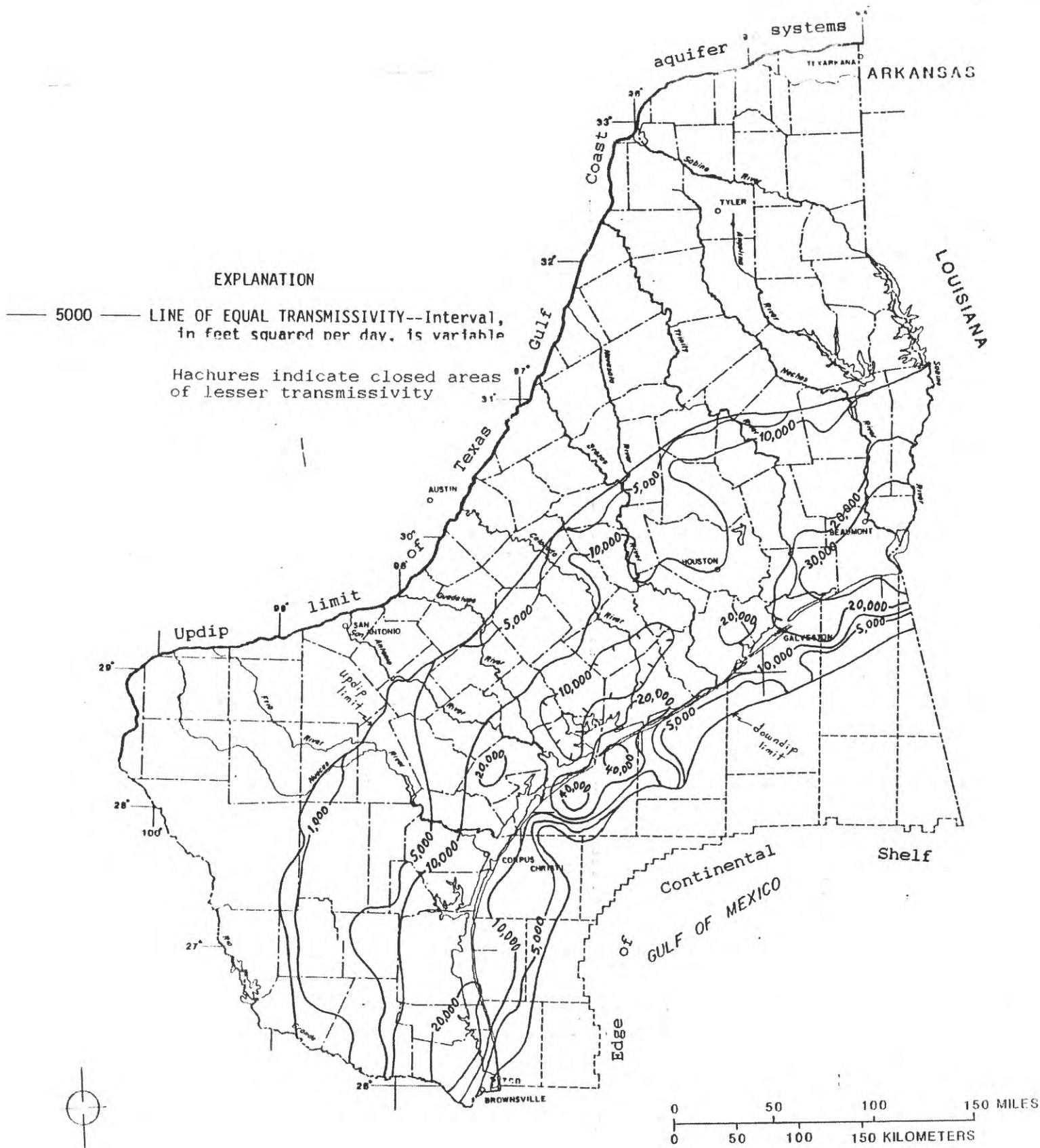


Figure 11.--Simulated transmissivity of permeable zone D.

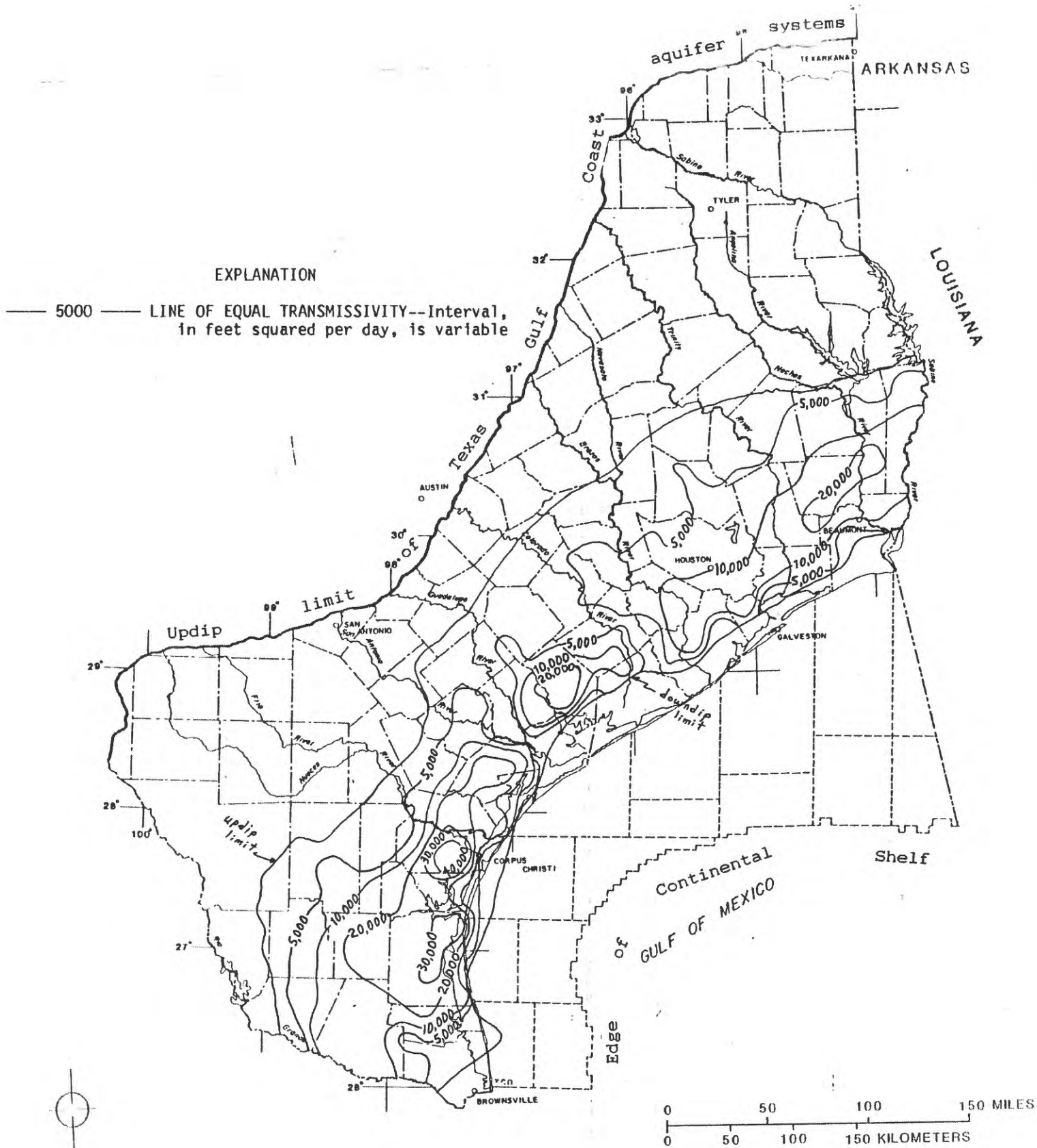


Figure 12 ---Simulated transmissivity of permeable zone E.

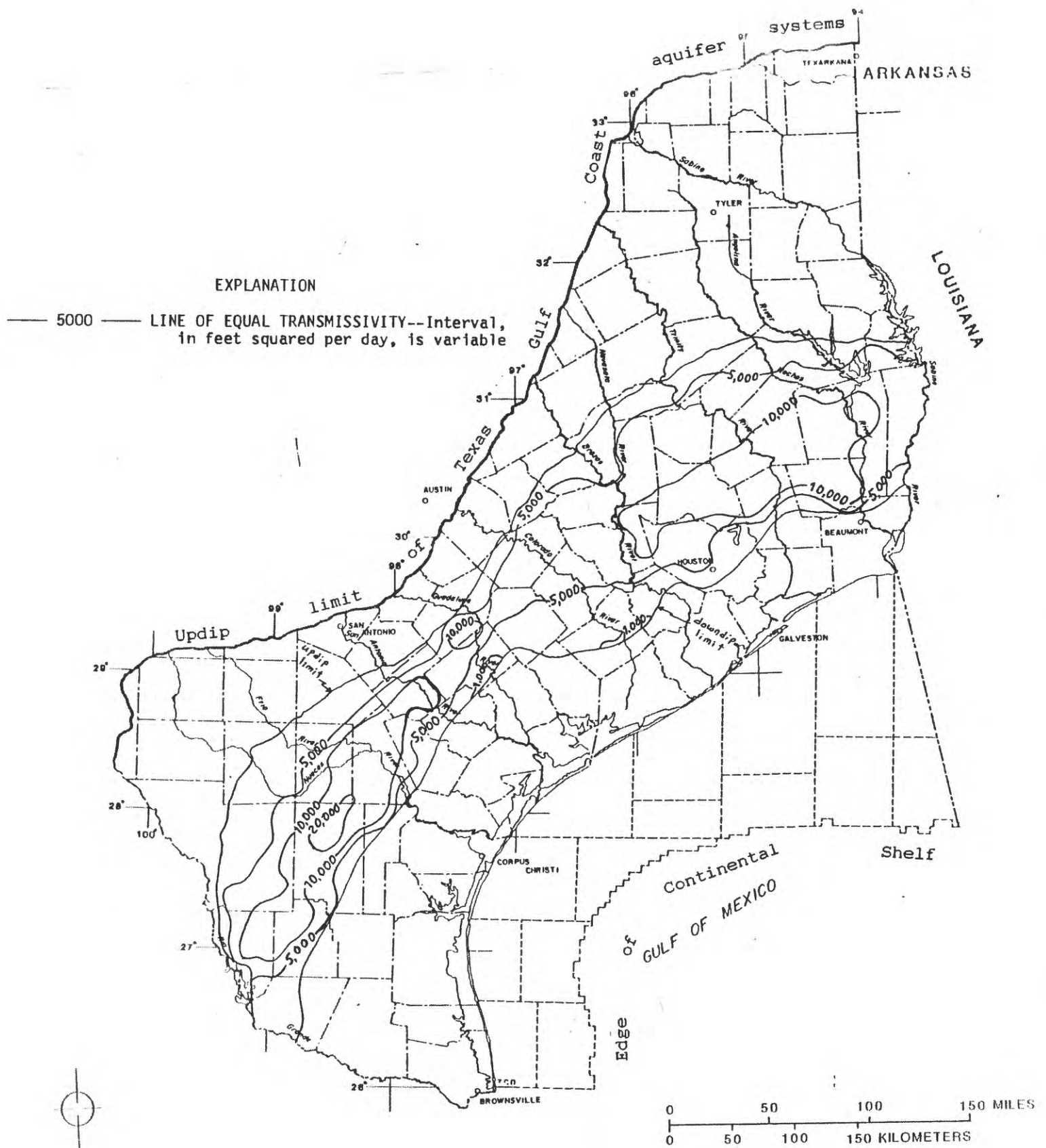


Figure 13.--Simulated transmissivity of the upper Claiborne aquifer.

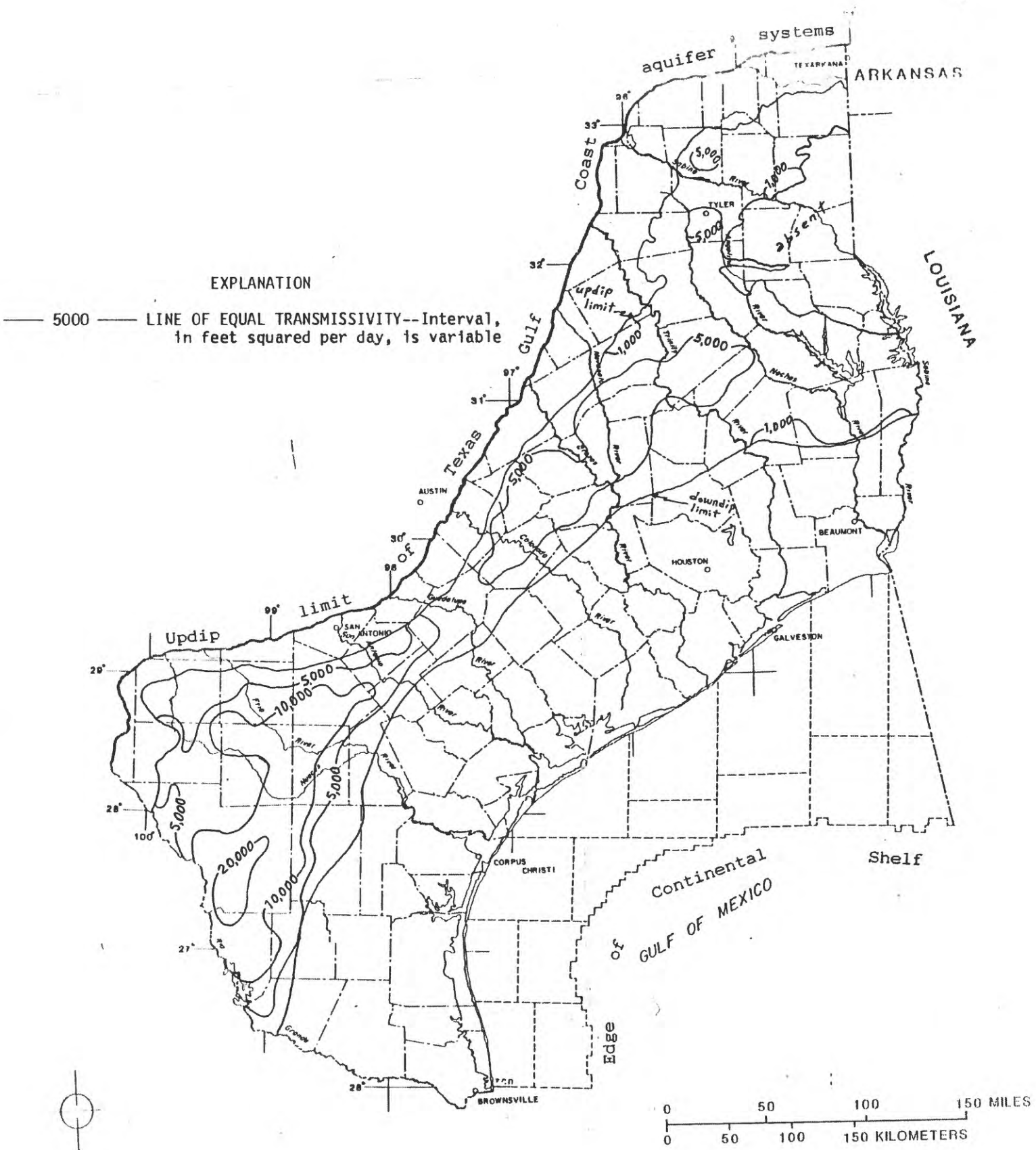


Figure 14.—Simulated transmissivity of the middle Claiborne aquifer.

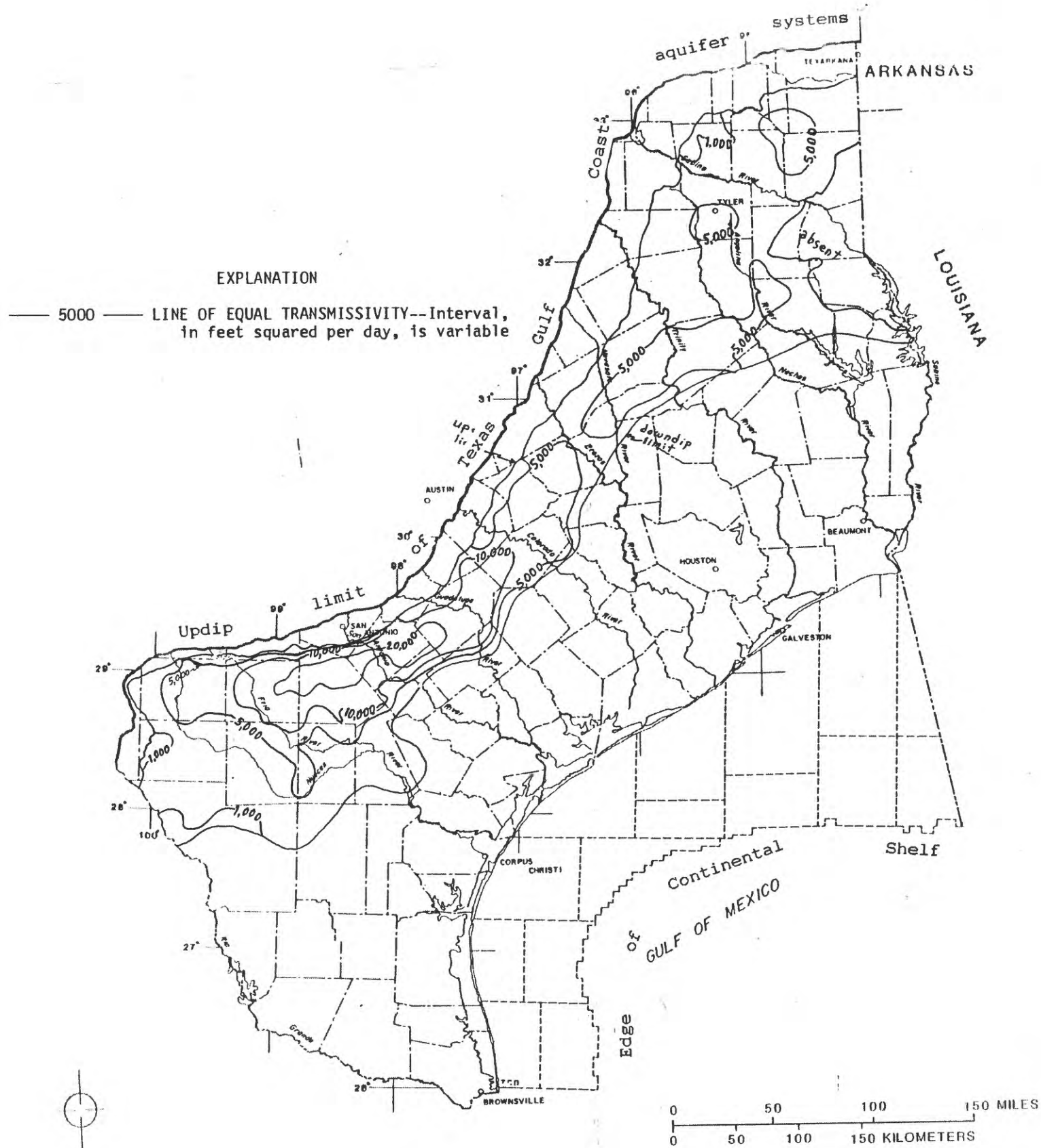


Figure 15.--Simulated transmissivity of the lower Claiborne-upper Wilcox aquifer.

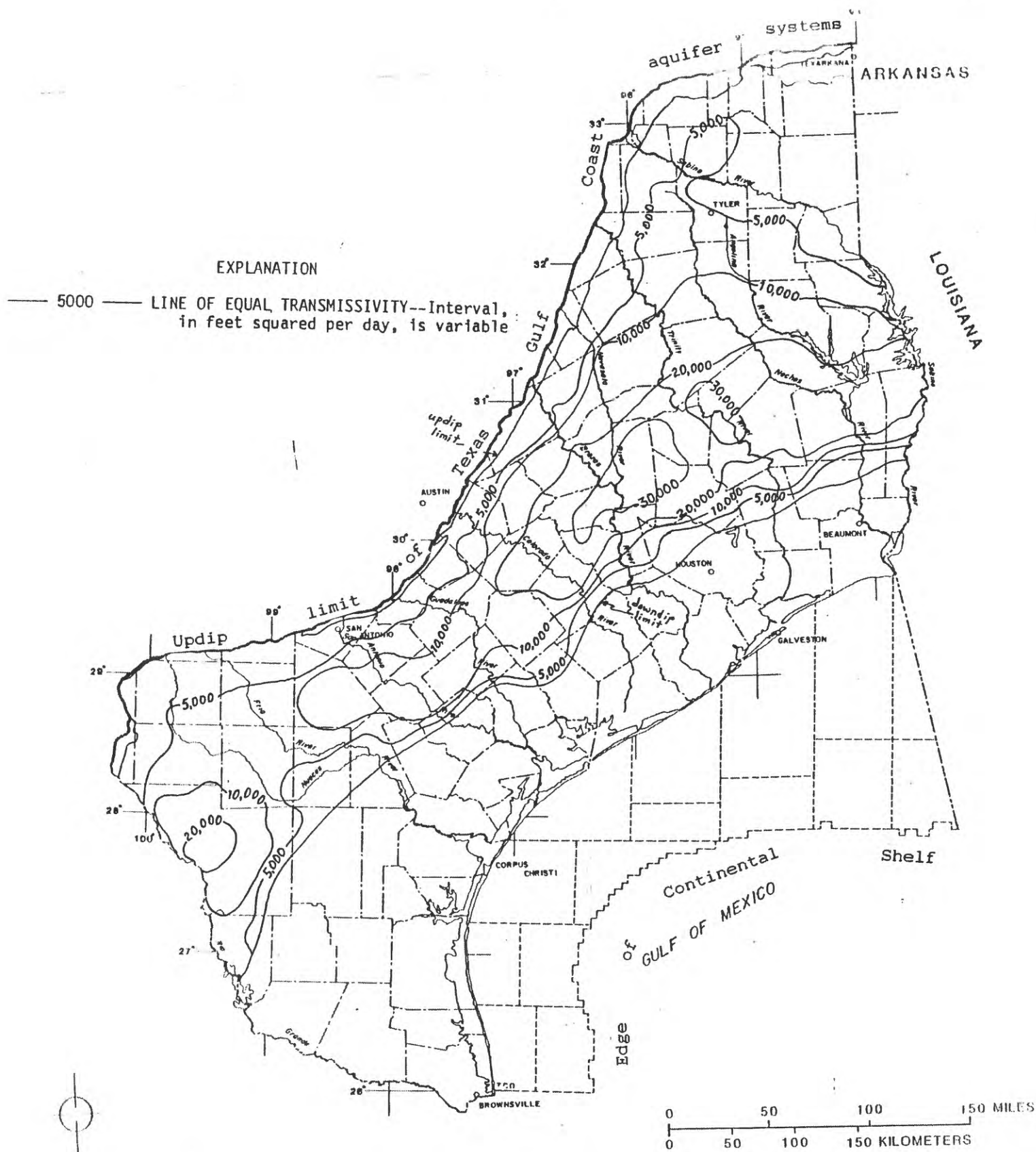


Figure 16.--Simulated transmissivity of the middle Wilcox aquifer.

EXPLANATION



Dissolved-solids concentration less than 2,000 milligrams per liter

— 500 — LINE OF EQUAL DISSOLVED-SOLIDS CONCENTRATION OF WATER IN PERMEABLE ZONE A, 1987--
Dissolved-solids concentration estimated from chemical analyses and depth-averaged geophysical well-log data. Interval, in milligrams per liter, is variable

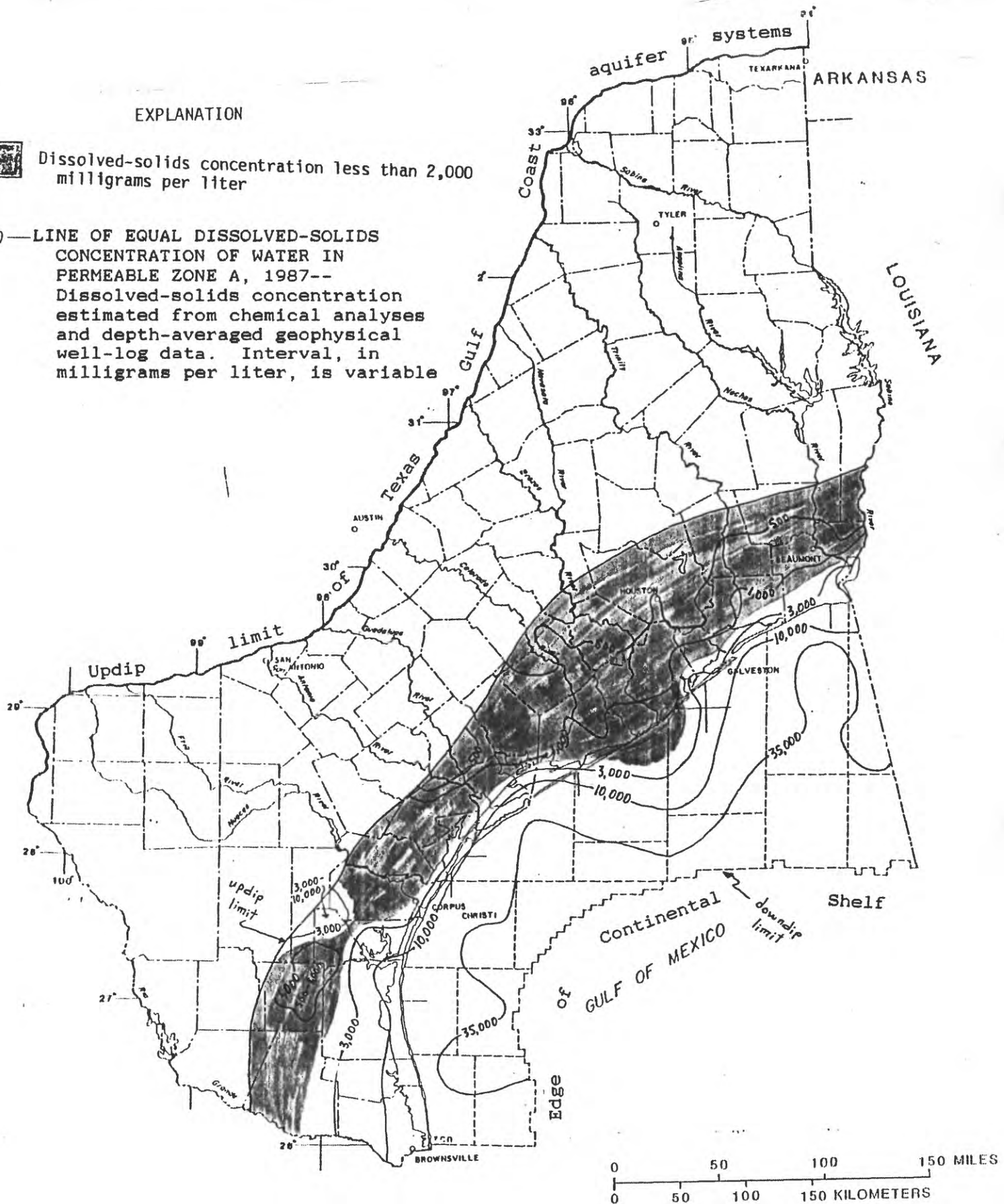


Figure 17.--Estimated dissolved-solids concentration in water from permeable zone A. (Modified from Pettijohn and others, 1988.)

EXPLANATION



Dissolved-solids concentration less than 2,000 milligrams per liter

500— LINE OF EQUAL DISSOLVED-SOLIDS CONCENTRATION OF WATER IN PERMEABLE ZONE B, 1987--
Dissolved-solids concentration estimated from chemical analyses and depth-averaged geophysical well-log data. Interval, in milligrams per liter, is variable

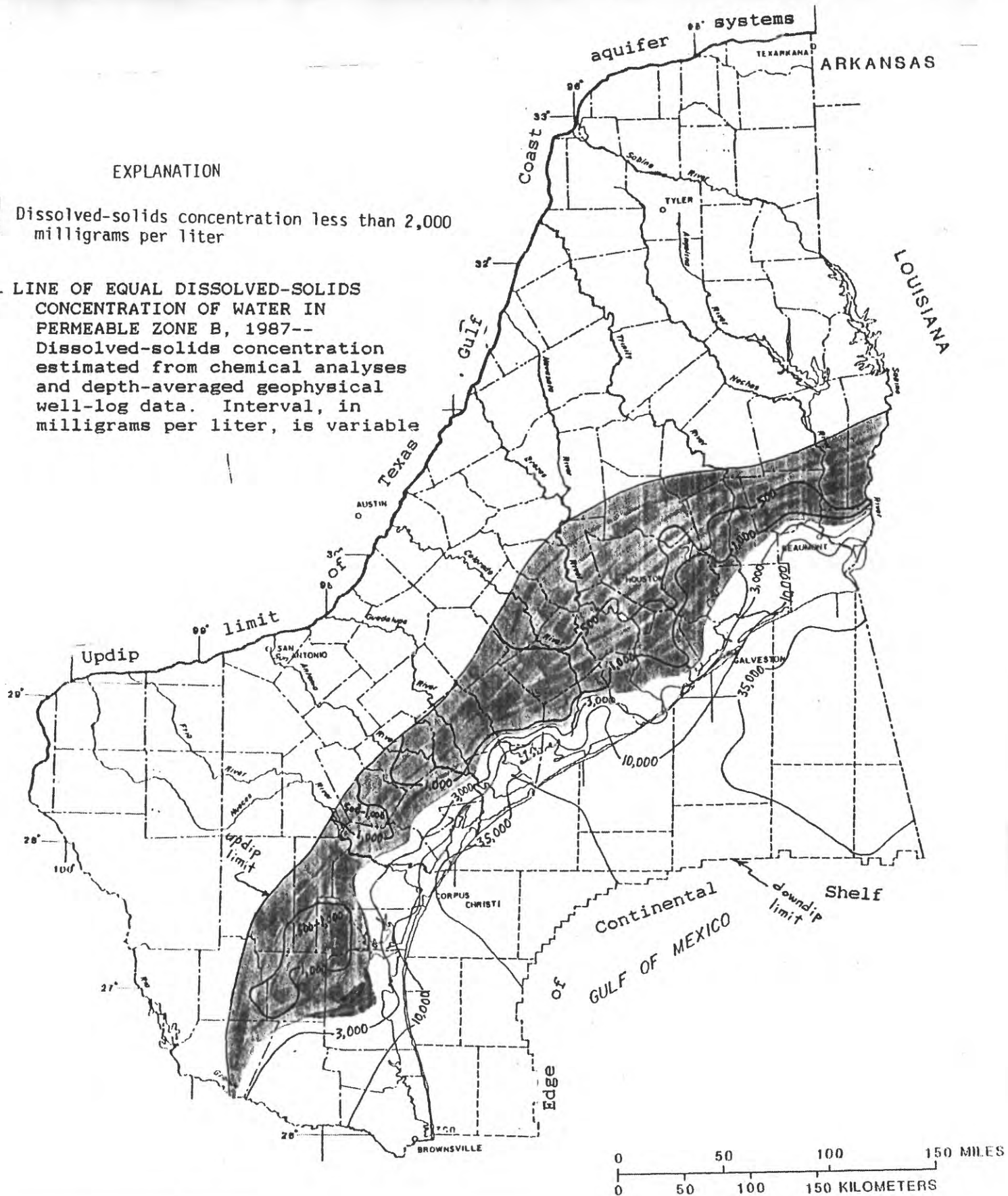


Figure 18.--Estimated dissolved-solids concentration in water from permeable zone B. (Modified from Pettijohn and others, 1988.)

EXPLANATION



Dissolved-solids concentration less than 2,000 milligrams per liter

500—LINE OF EQUAL DISSOLVED-SOLIDS CONCENTRATION OF WATER IN PERMEABLE ZONE C, 1987--
Dissolved-solids concentration estimated from chemical analyses and depth-averaged geophysical well-log data. Interval, in milligrams per liter, is variable

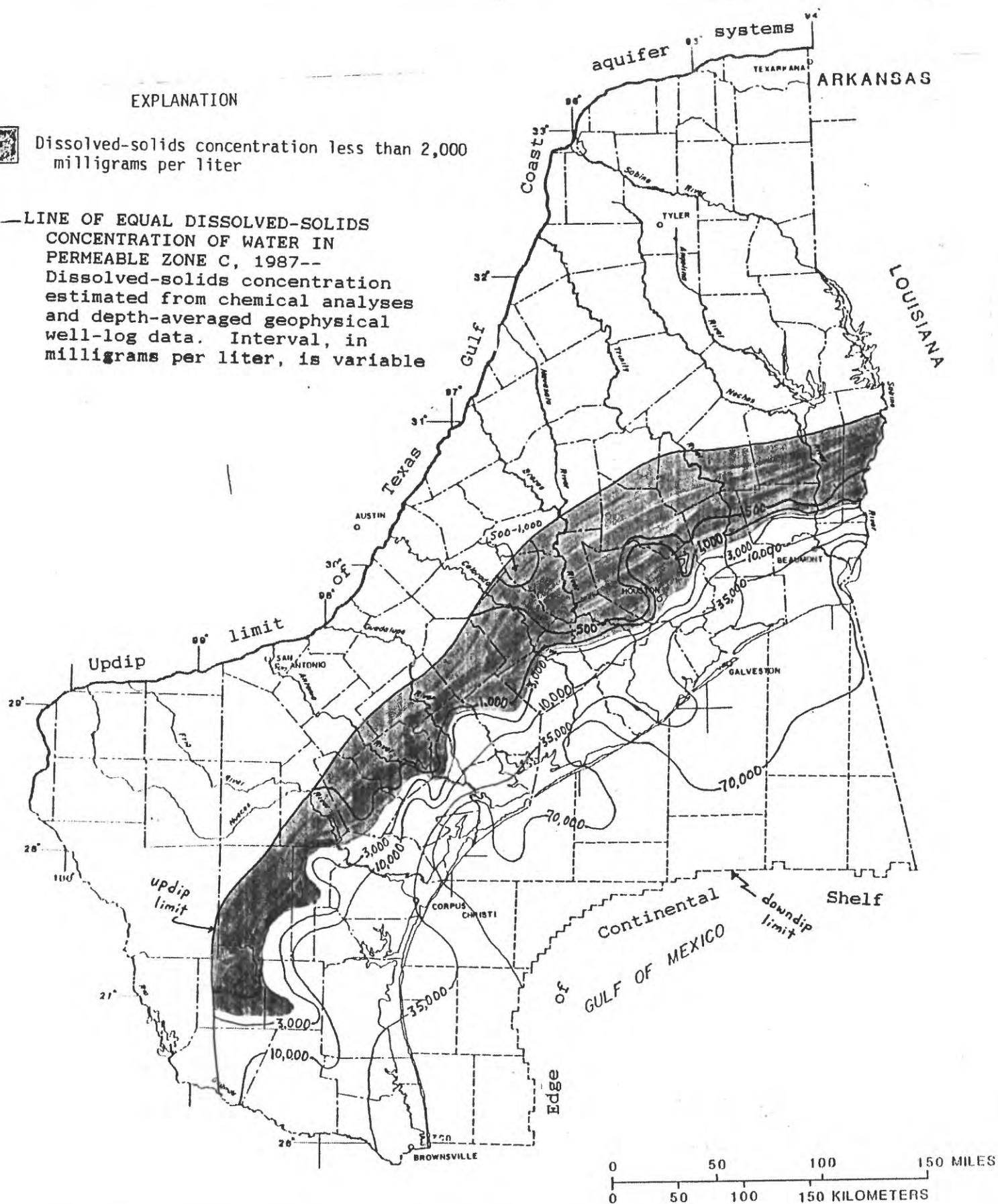


Figure 19.--Estimated dissolved-solids concentration in water from permeable zone C. (Modified from Pettijohn and others, 1988.)

EXPLANATION



Dissolved-solids concentration less than 2,000 milligrams per liter

— 500 — LINE OF EQUAL DISSOLVED-SOLIDS CONCENTRATION OF WATER IN PERMEABLE ZONE D, 1987--
Dissolved-solids concentration estimated from chemical analyses and depth-averaged geophysical well-log data. Interval, in milligrams per liter, is variable

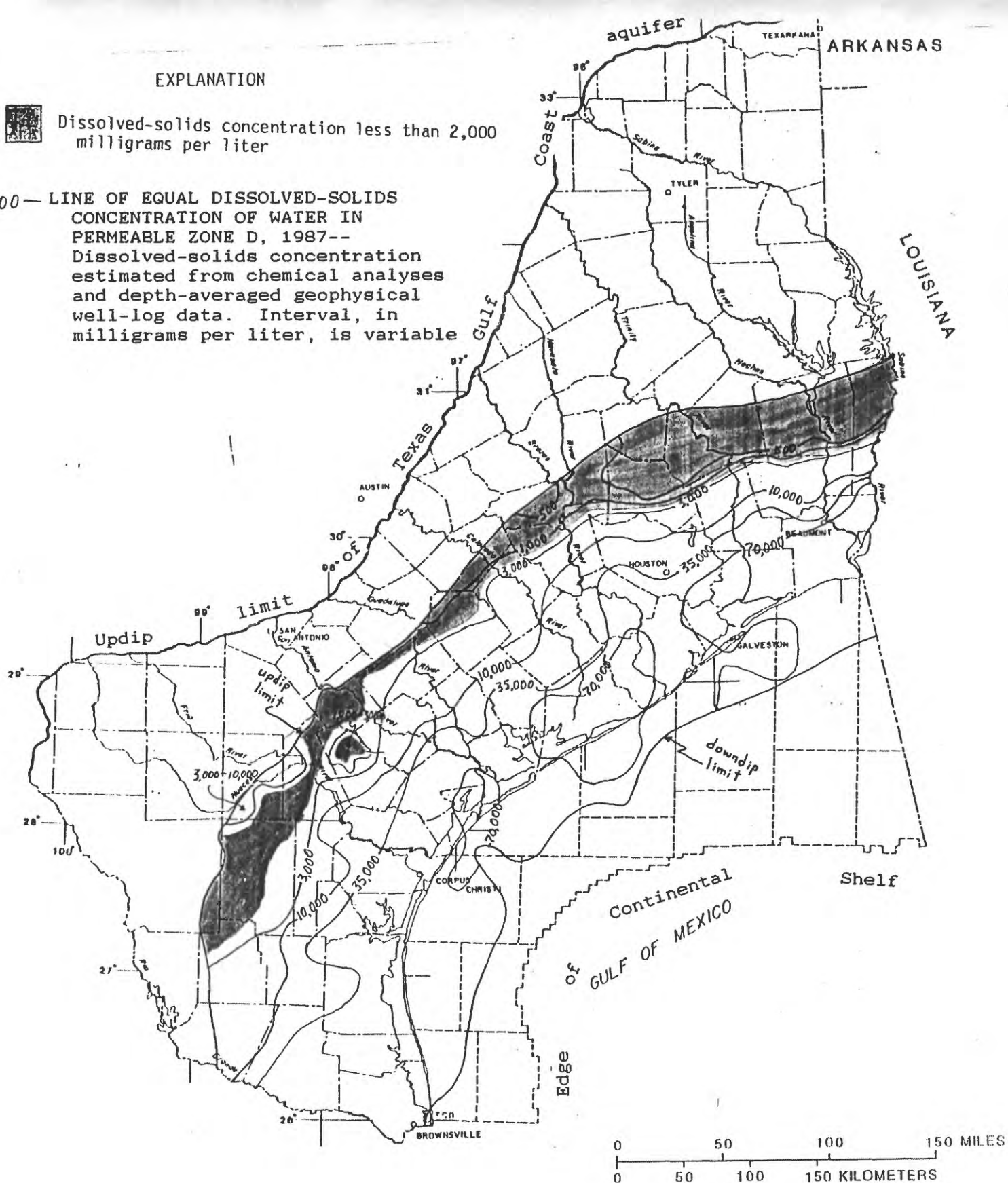


Figure 20.--Estimated dissolved-solids concentration in water from permeable zone D. (Modified from Pettijohn and others, 1988.)

EXPLANATION



Dissolved-solids concentration less than 2,000 milligrams per liter

500 — LINE OF EQUAL DISSOLVED-SOLIDS CONCENTRATION OF WATER IN PERMEABLE ZONE E, 1987--
Dissolved-solids concentration estimated from chemical analyses and depth-averaged geophysical well-log data. Interval, in milligrams per liter, is variable

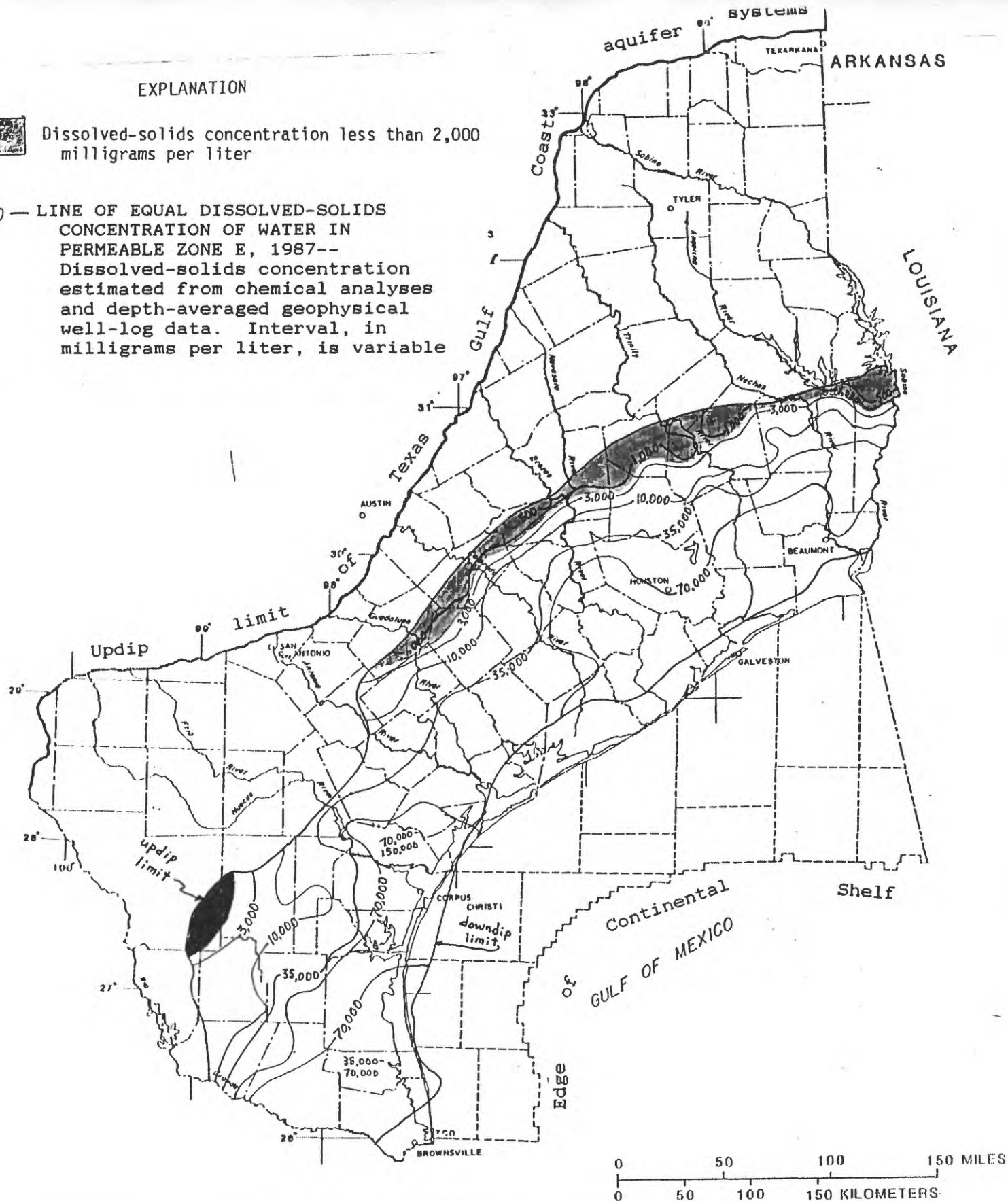


Figure 21. --Estimated dissolved-solids concentration in water from permeable zone E. (Modified from Pettijohn and others, 1988.)

EXPLANATION



Dissolved-solids concentration less than 2,000 milligrams per liter

500—LINE OF EQUAL DISSOLVED-SOLIDS CONCENTRATION OF WATER IN THE UPPER CLAIBORNE AQUIFER, 1987-- Dissolved-solids concentration estimated from chemical analyses and depth-averaged geophysical well-log data. Interval, in milligrams per liter, is variable

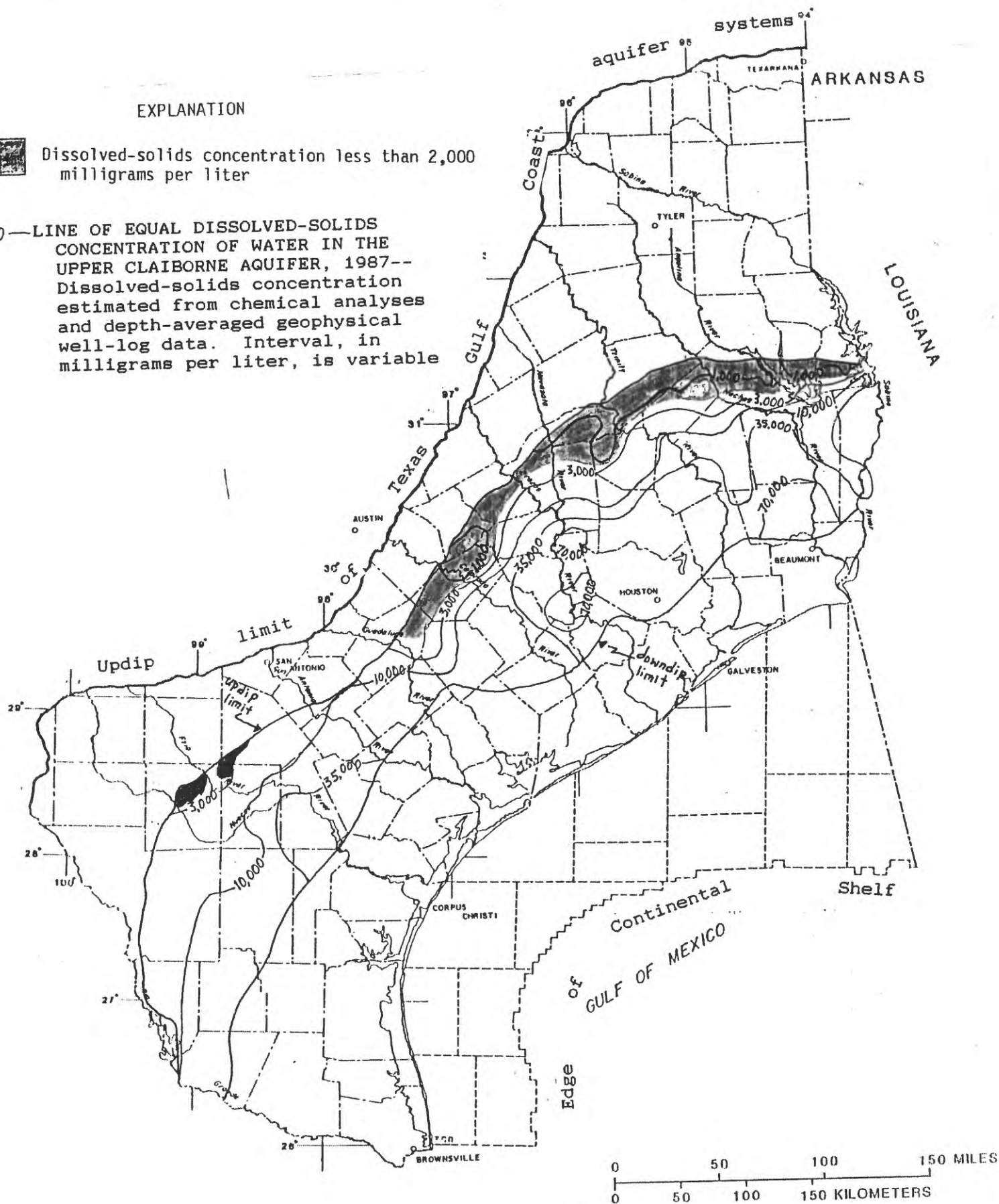


Figure 22.--Estimated dissolved-solids concentration in water from the upper Claiborne aquifer. (Modified from Pettijohn and others, 1988.)

EXPLANATION



Dissolved-solids concentration less than 2,000 milligrams per liter

— 500 — LINE OF EQUAL DISSOLVED-SOLIDS CONCENTRATION OF WATER IN THE MIDDLE CLAIBORNE AQUIFER, 1987-- Dissolved-solids concentration estimated from chemical analyses and depth-averaged geophysical well-log data. Interval, in milligrams per liter, is variable

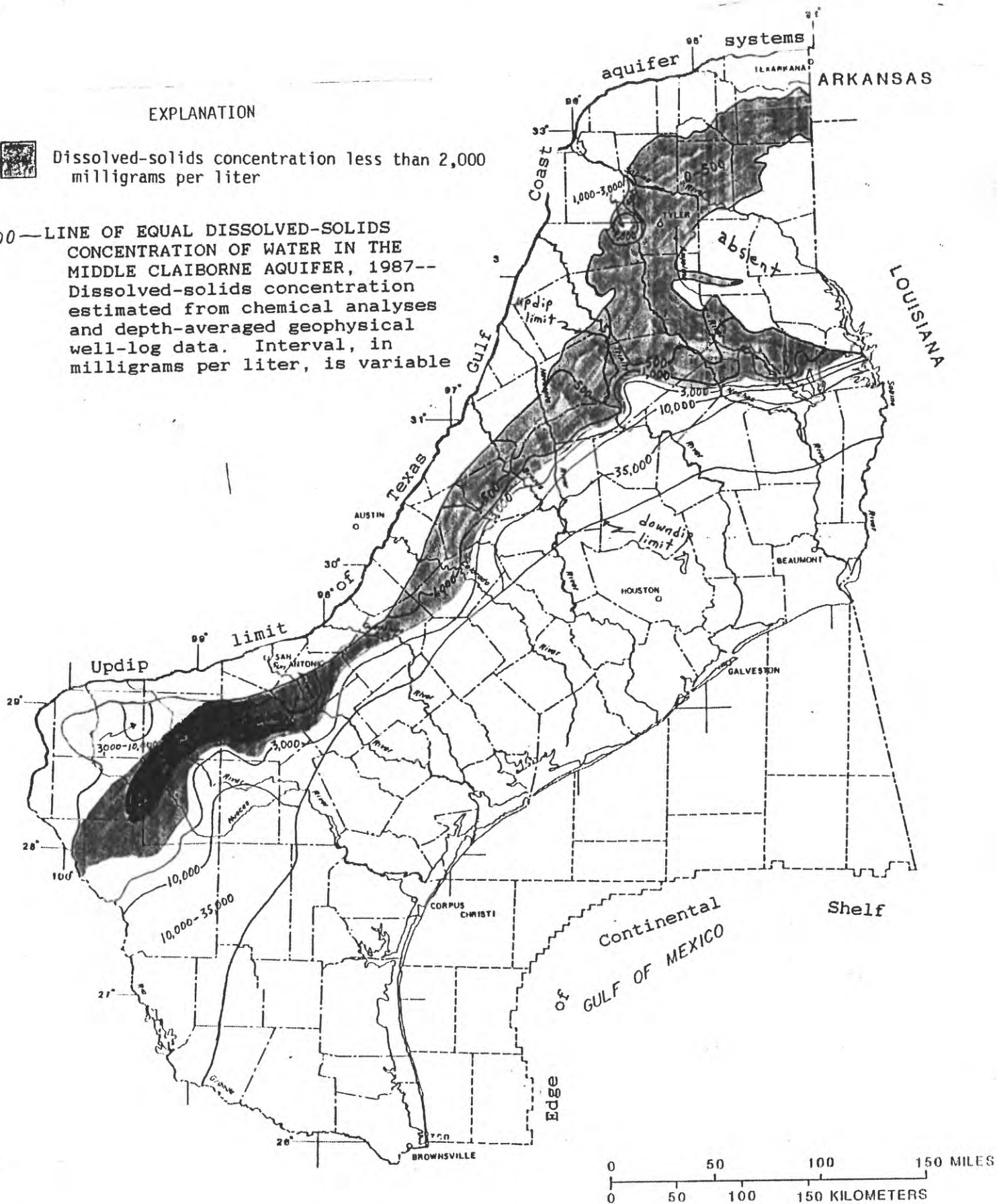


Figure 23.--Estimated dissolved-solids concentration in water from the middle Claiborne aquifer. (Modified from Pettijohn and others, 1988.)

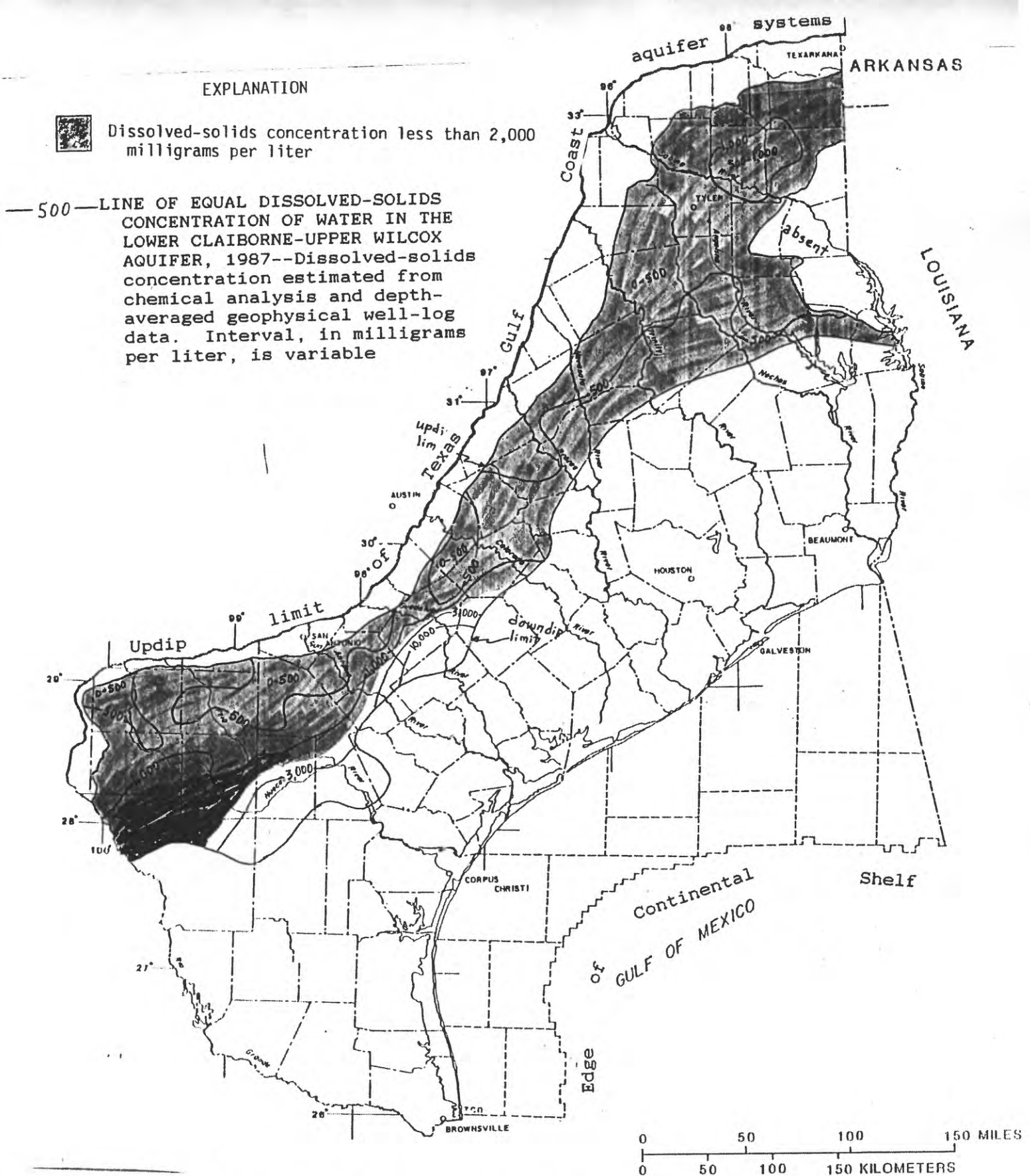


Figure 24.--Estimated dissolved-solids concentration in water from the lower Claiborne-Upper Wilcox aquifer. (Modified from Pettijohn and others, 1988.)

EXPLANATION



Dissolved-solids concentration less than 2,000 milligrams per liter

— 500 — LINE OF EQUAL DISSOLVED-SOLIDS CONCENTRATION OF WATER IN THE MIDDLE WILCOX AQUIFER, 1987-- Dissolved-solids concentration estimated from chemical analyses and depth-averaged geophysical well-log data. Interval, in milligrams per liter, is variable

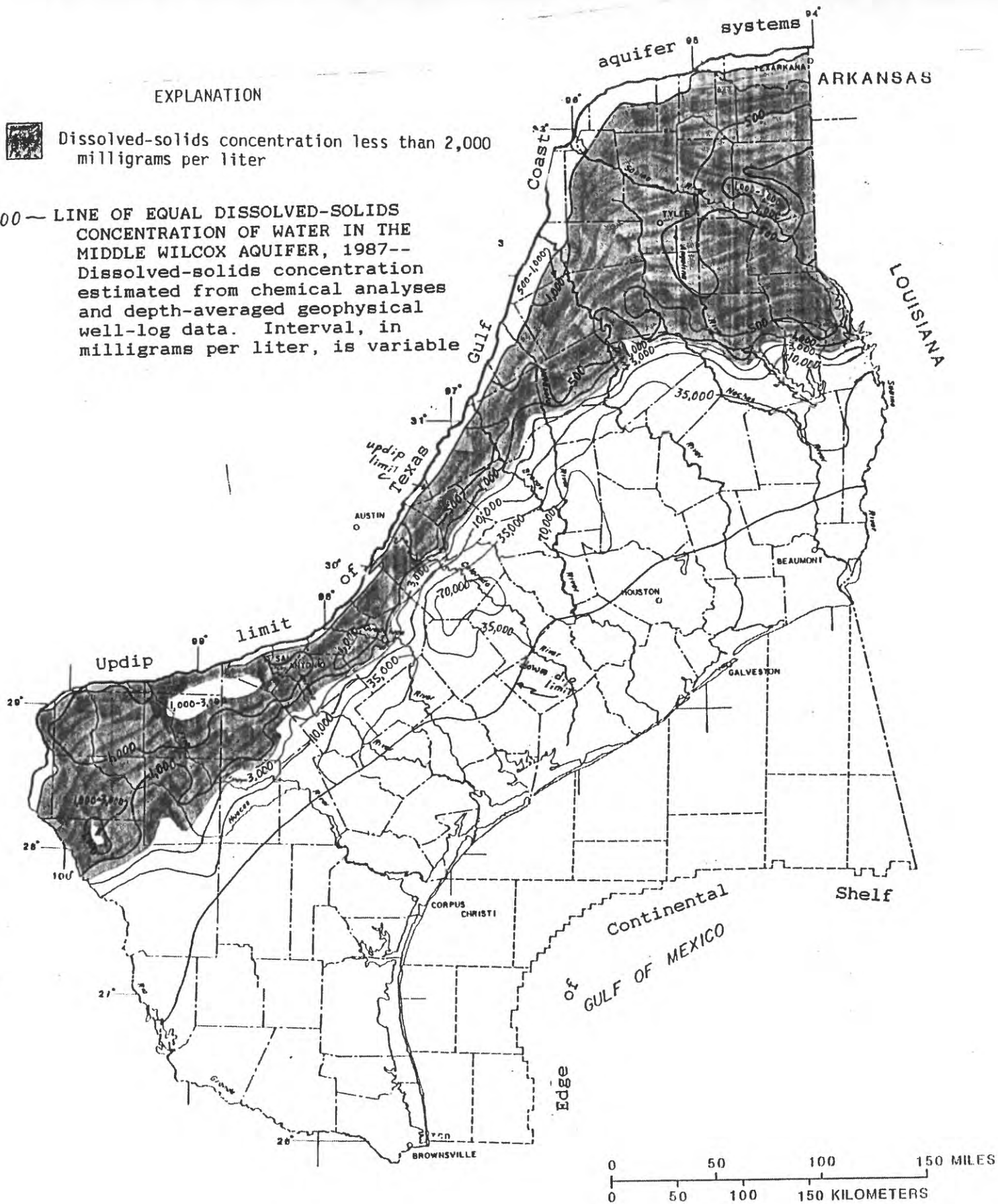


Figure 25.--Estimated dissolved-solids concentration in water from the middle Wilcox aquifer. (Modified from Pettijohn and others, 1988.)

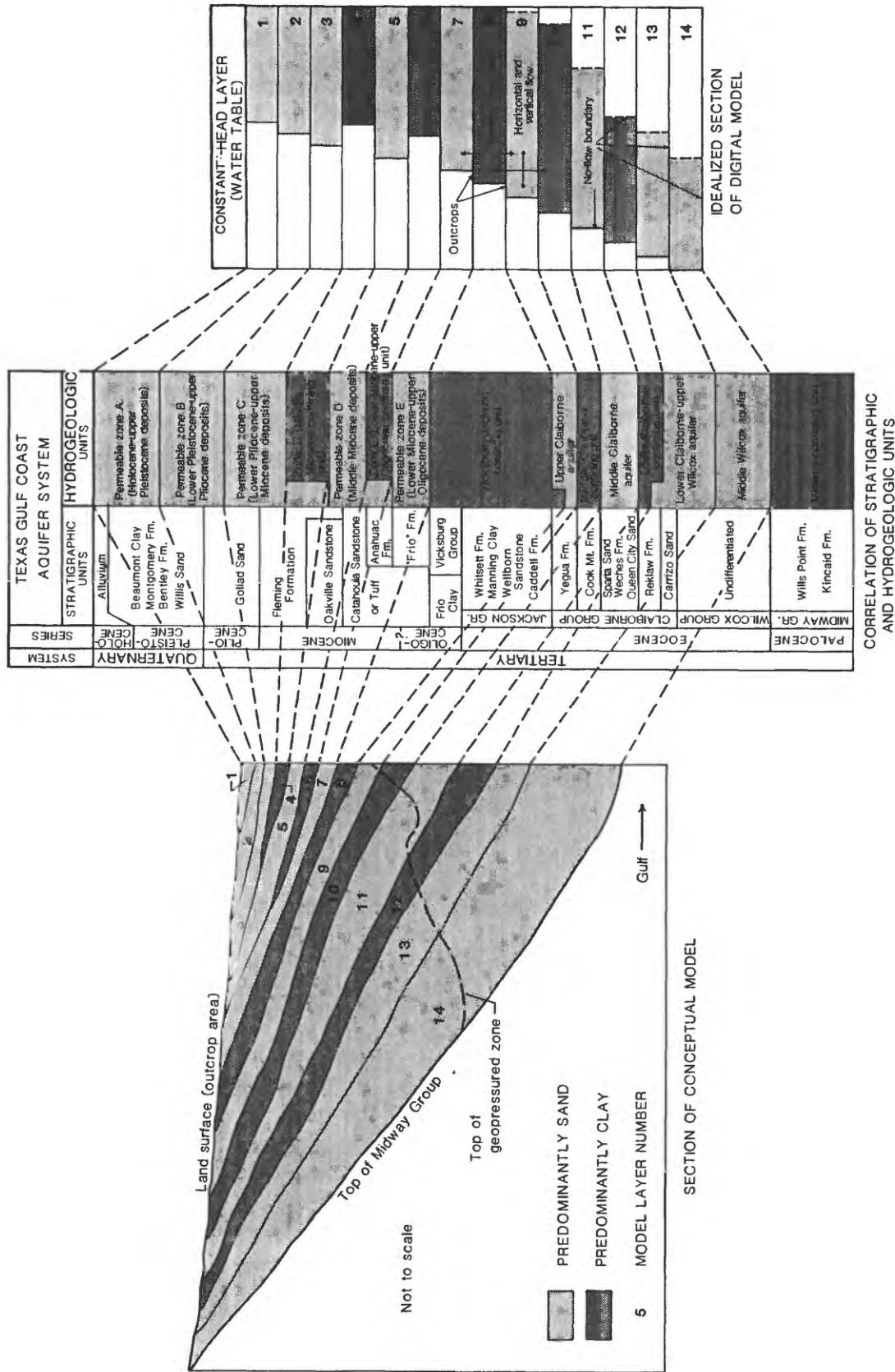


Figure 2.6.--Conceptual model of aquifer systems and generalized representation in the digital model

EXPLANATION

SIMULATED RECHARGE AND
DISCHARGE, IN INCHES PER YEAR

1	2 to 3	} RECHARGE
2	1 to 2	
3	0 to 1	} DISCHARGE
4	0 to 1	
5	1 to 2	

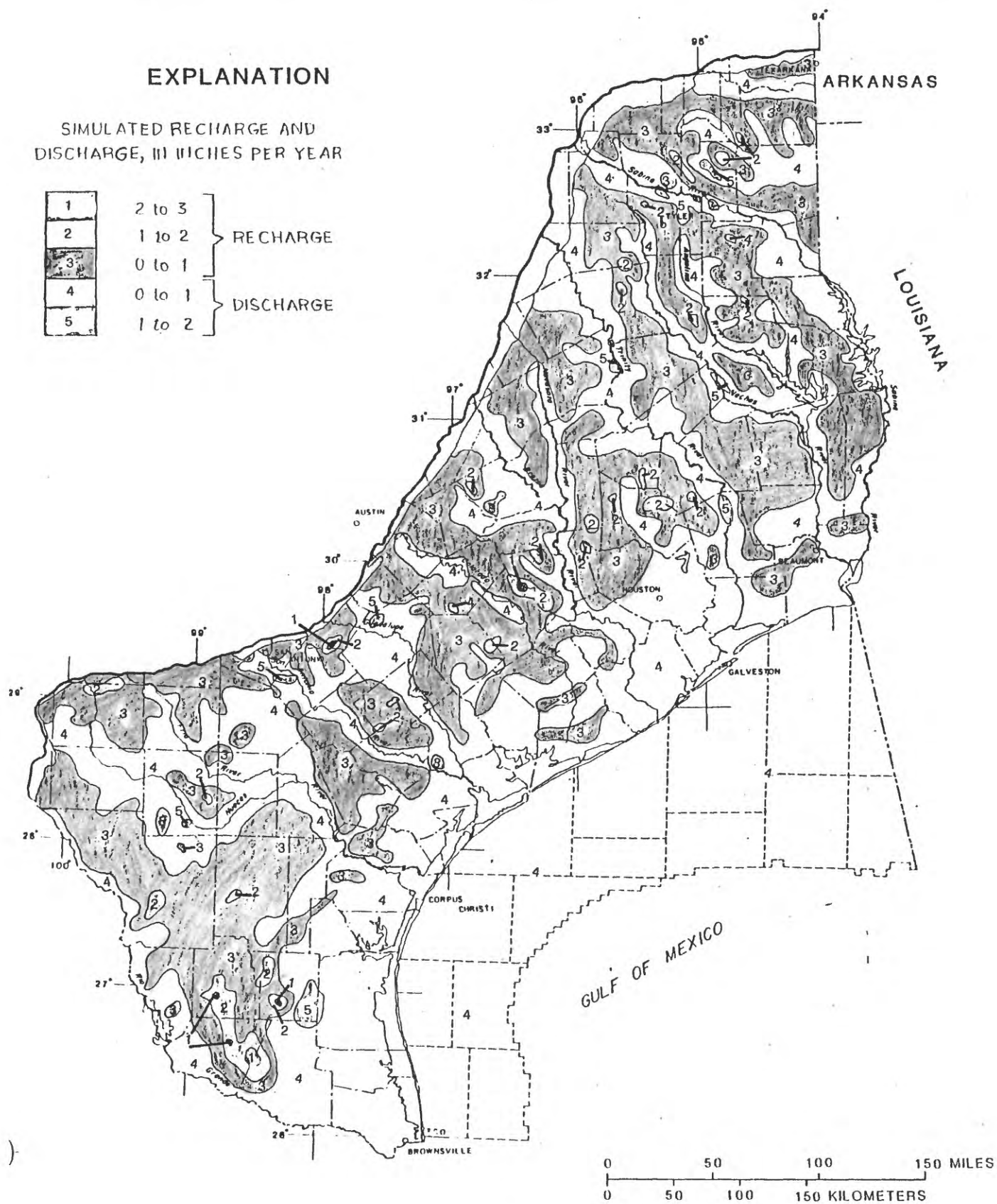


Figure 27.--Simulated predevelopment recharge and discharge in the outcrop areas of aquifers, permeable zones, and confining units.

EXPLANATION

AQUIFER OR PERMEABLE ZONE AND IDENTIFIER

- ① Permeable zone A
- ② Permeable zone B
- ③ Permeable zone C
- ⑤ Permeable zone D
- ⑦ Permeable zone E
- ⑨ Upper Claiborne aquifer
- ⑪ Middle Claiborne aquifer
- ⑬ Lower Claiborne-upper Wilcox aquifer
- ⑭ Middle Wilcox aquifer

CONFINING UNIT

TOTAL RECHARGE OR DISCHARGE IN OUTCROP AREA--Includes flow through superjacent confining unit where the confining unit is exposed at the surface. Number is flow rate, in million cubic feet per day

↓ 15
↑ 15
Recharge
Discharge

NET RECHARGE OR DISCHARGE IN OUTCROP AREA--Includes flow through superjacent confining unit where the confining unit is exposed at the surface. Number is flow rate, in million cubic feet per day

↓ (4)
↑ (3)
Recharge
Discharge

TOTAL LEAKAGE THROUGH BOTTOM OF AQUIFER--

Number is flow rate, in million cubic feet per day

↑ 16
↓ 2
Upward
Downward

NET LEAKAGE THROUGH BOTTOM OF AQUIFER--

Number is flow rate, in million cubic feet per day

↑ (5)
↓ (5)
Upward
Downward

NET LATERAL FLOW IN (+) OR OUT (-) OF STUDY AREA
 $L = -2$

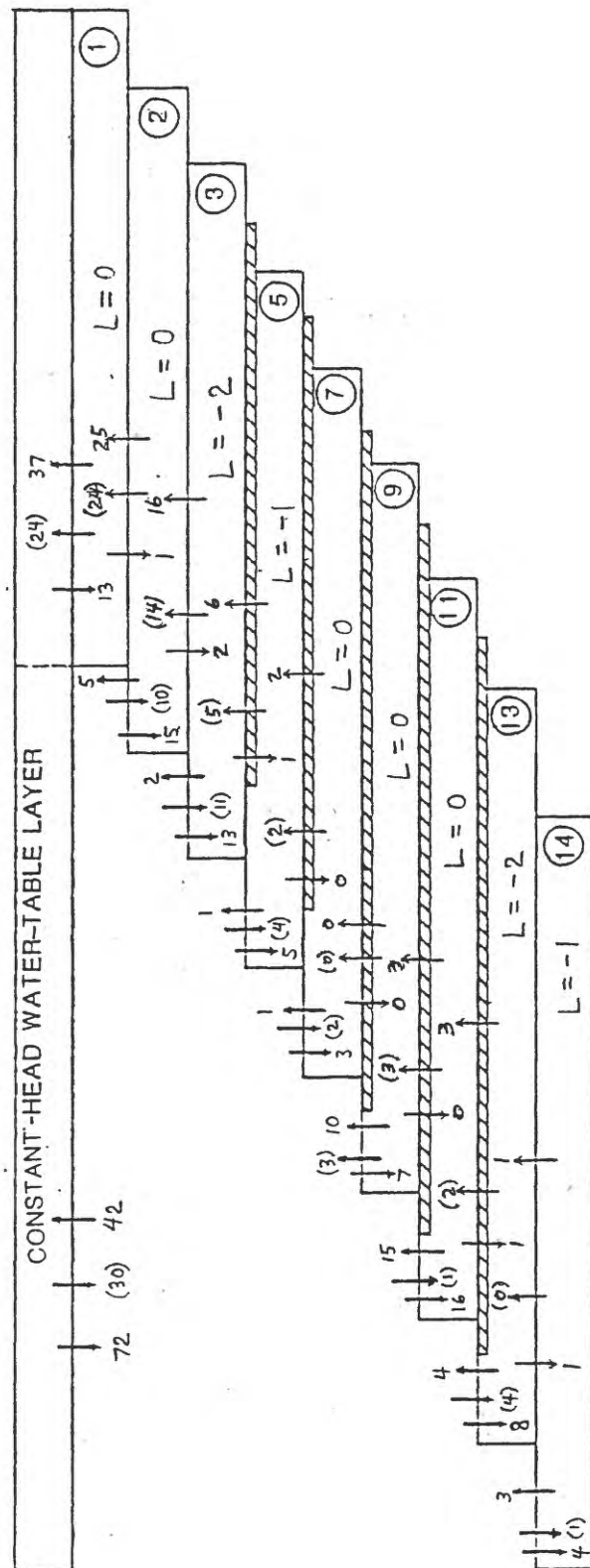
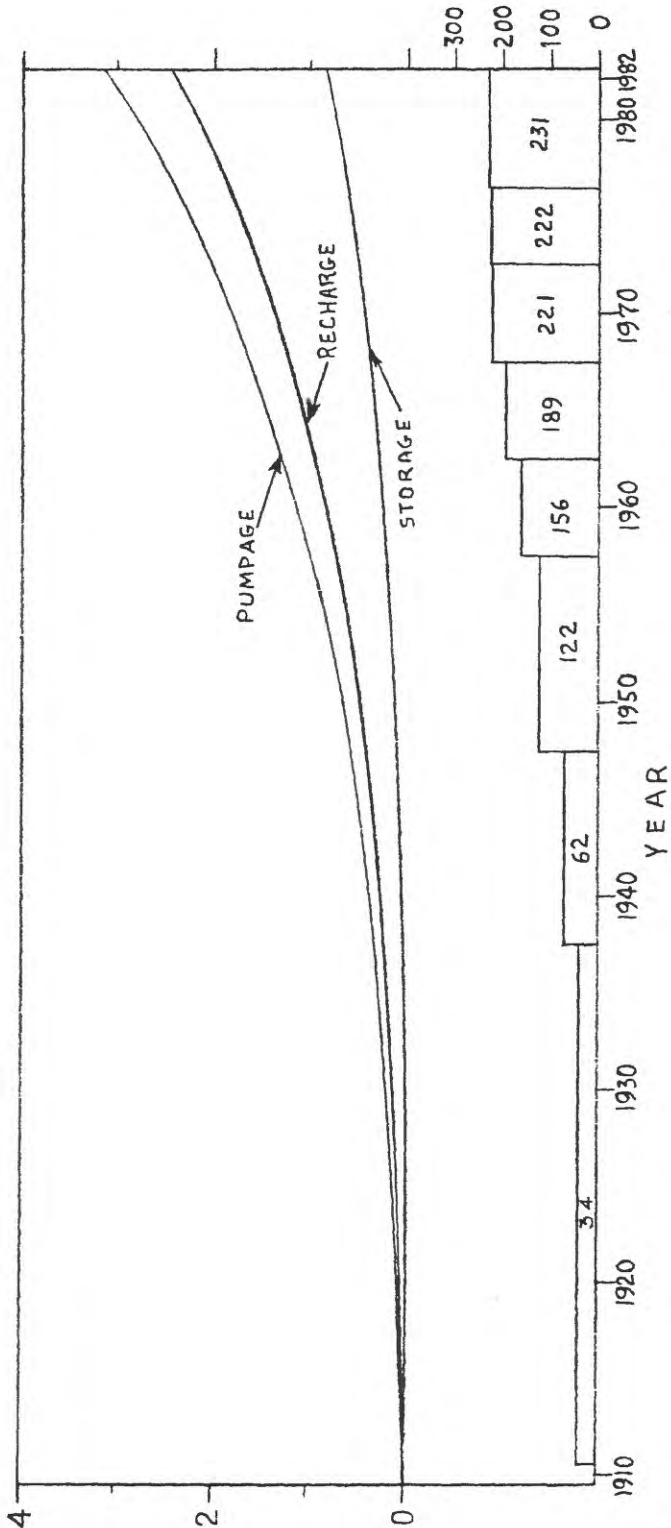


Figure 28.--Simulated predevelopment vertical flow rates across hydrogeologic units in study area.

CUMULATIVE VOLUME OF WATER,
IN CUBIC FEET X 10¹²



PUMPING RATE, IN MILLION
CUBIC FEET PER DAY

Figure 28a .--Simulated pumpage, recharge, and depletion of storage in the Texas Gulf Coast aquifer systems, 1910-82.

EXPLANATION

Ground-water pumpage, in million gallons per day (Mgal/d) for blocks with 0.5 Mgal/d or more pumpage

○	0.5 - 0.9
□	1.0 - 4.9
◆	5.0 - 9.9
▣	10.0 - 24.9

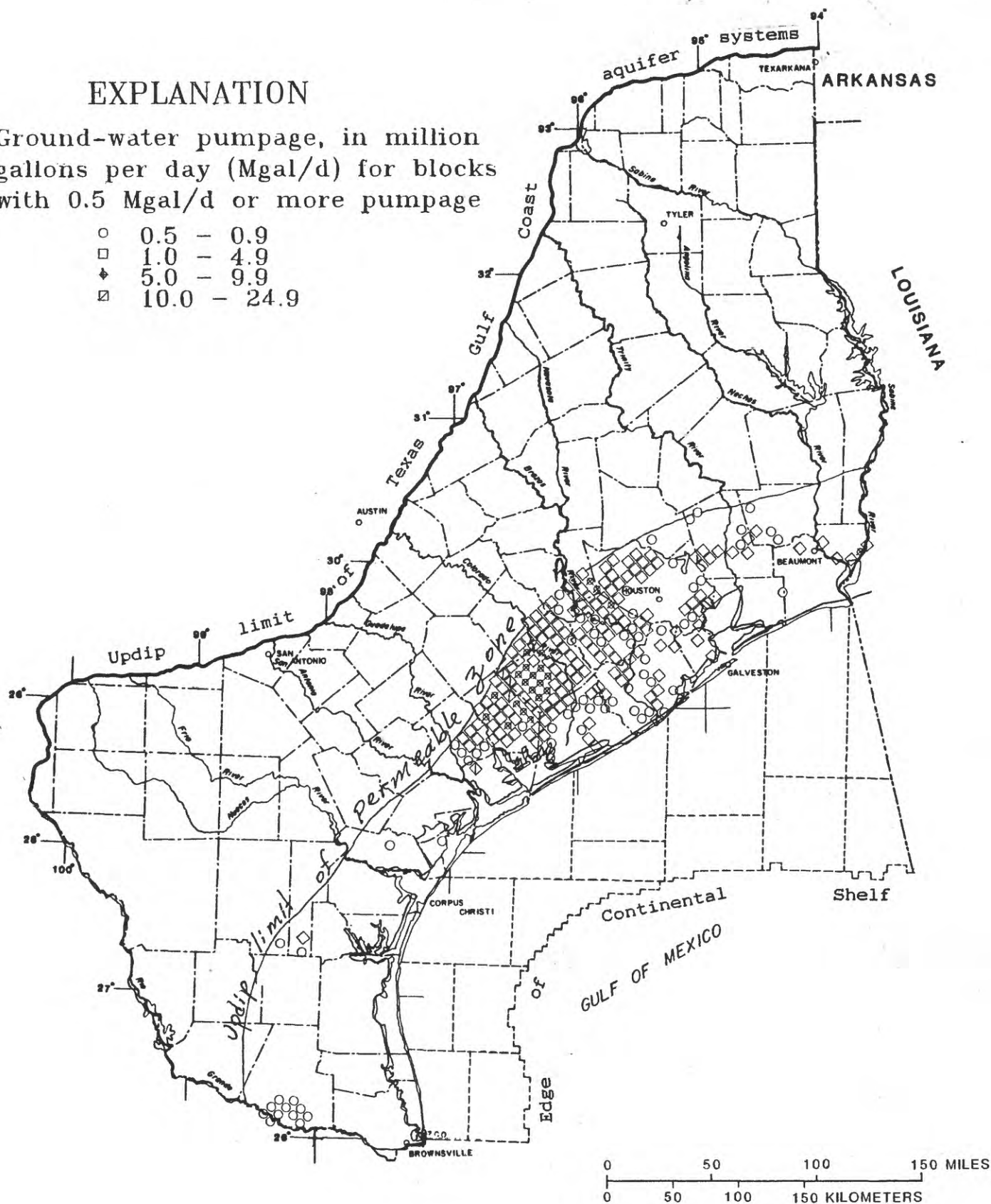


Figure 29.--Estimated pumpage in 1980, by 25-square-mile grid block, for permeable zone A.

EXPLANATION

Ground-water pumpage, in million gallons per day (Mgal/d) for blocks with 0.5 Mgal/d or more pumpage

○	0.5	—	0.9
□	1.0	—	4.9
◆	5.0	—	9.9
▣	10.0	—	24.9

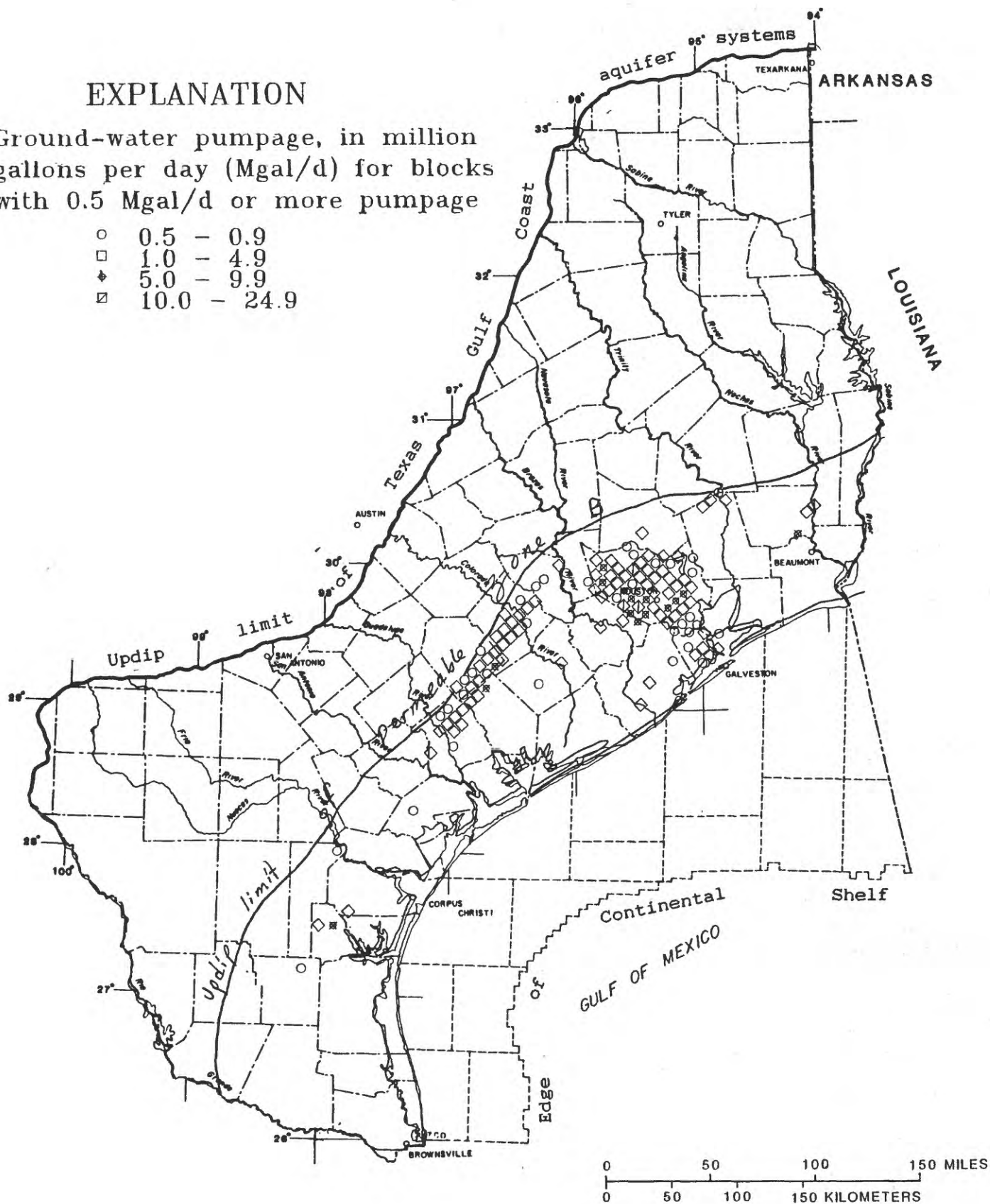


Figure 30.--Estimated pumpage in 1980, by 25-square-mile grid block, for permeable zone B.

EXPLANATION

Ground-water pumpage, in million gallons per day (Mgal/d) for blocks with 0.5 Mgal/d or more pumpage

○	0.5	—	0.9
□	1.0	—	4.9
◆	5.0	—	9.9
▣	10.0	—	24.9

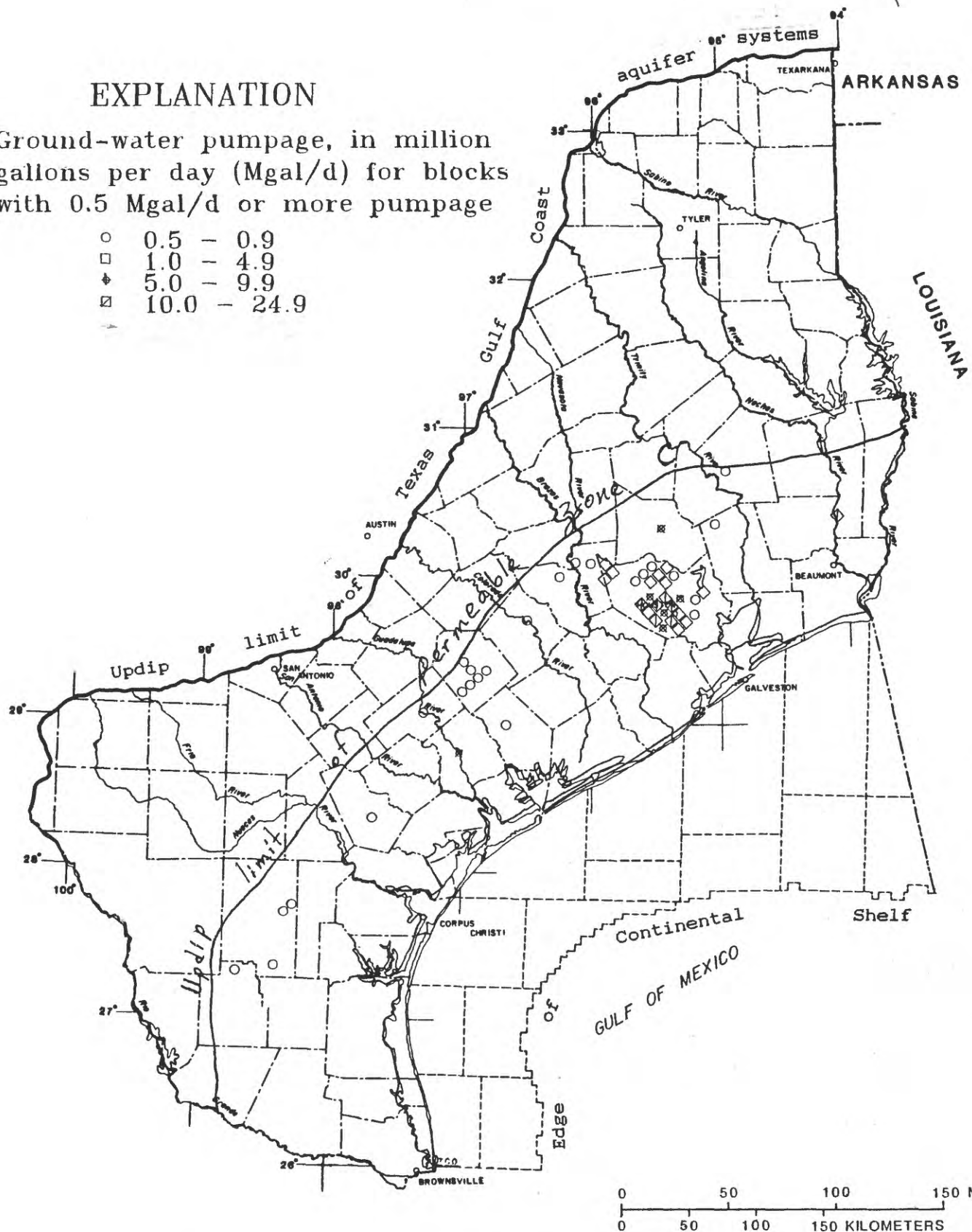


Figure 31.--Estimated pumpage in 1980, by 25-square-mile grid block, for permeable zone C.

EXPLANATION

Ground-water pumpage, in million gallons per day (Mgal/d) for blocks with 0.5 Mgal/d or more pumpage

- 0.5 - 0.9
- 1.0 - 4.9

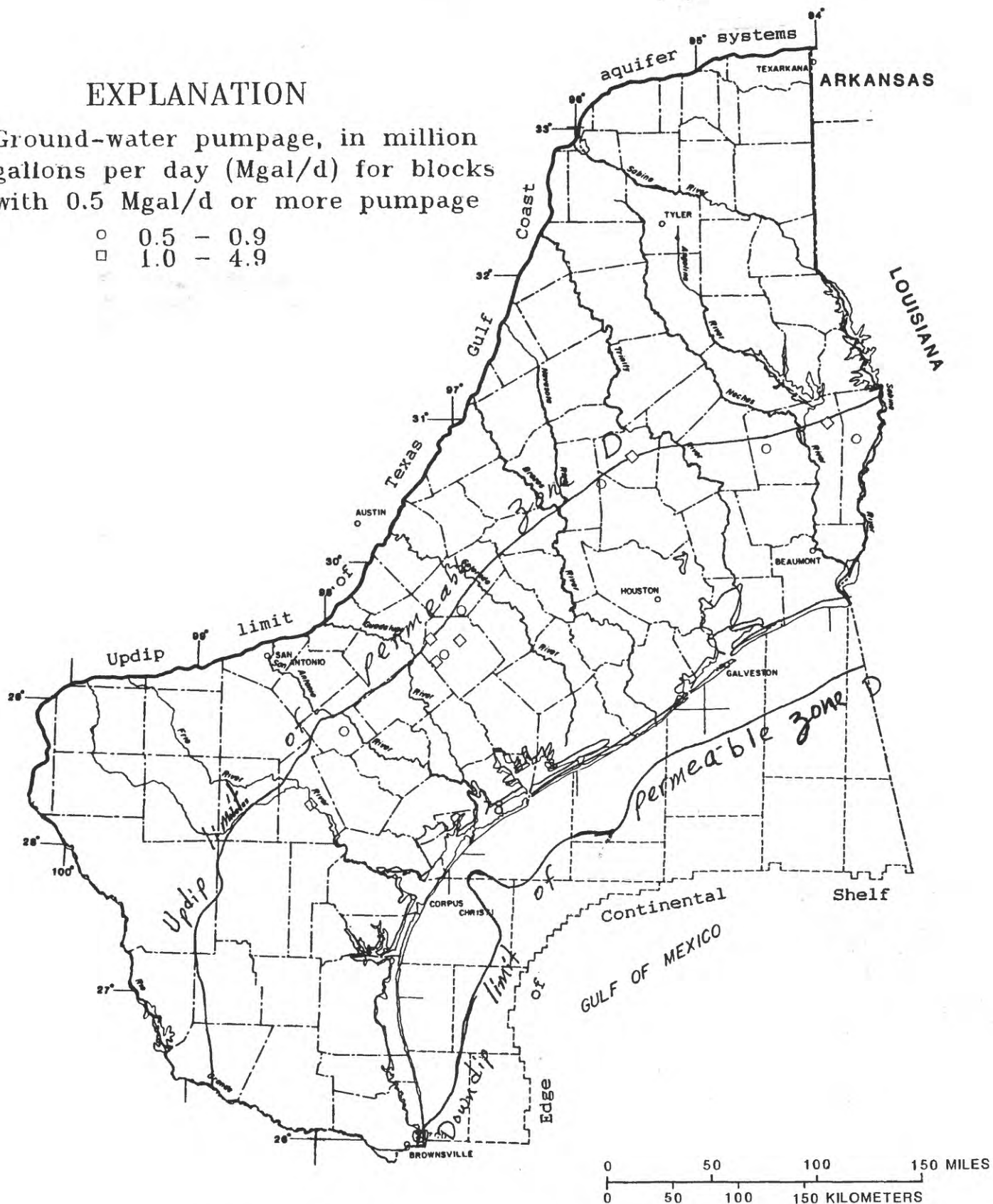


Figure 32.--Estimated pumpage in 1980, by 25-square-mile grid block, for permeable zone D.

EXPLANATION

Ground-water pumpage, in million gallons per day (Mgal/d) for blocks with 0.5 Mgal/d or more pumpage

- 0.5 - 0.9
- 1.0 - 4.9

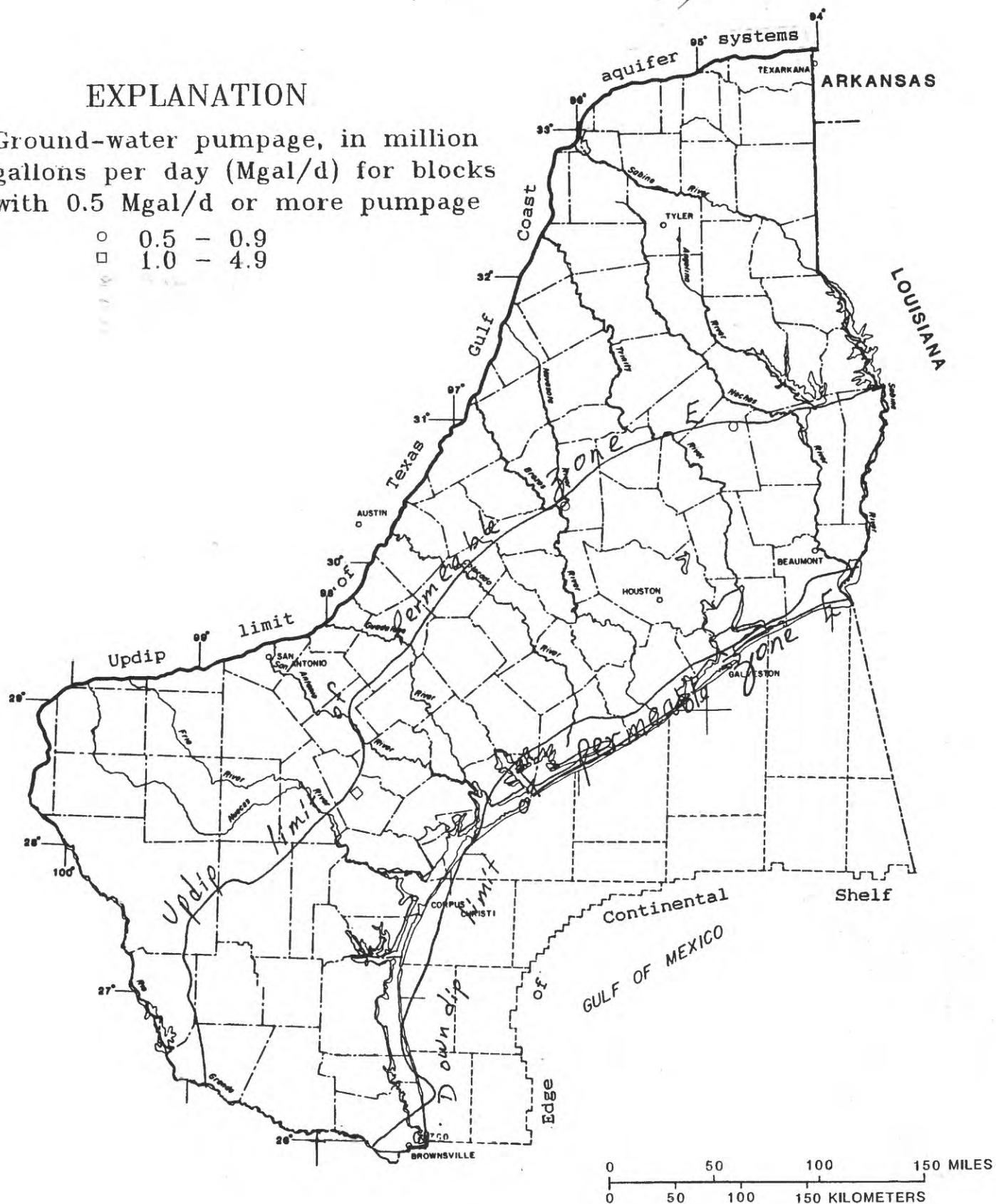


Figure 33.--Estimated pumpage in 1980, by 25-square-mile grid block, for permeable zone E.

EXPLANATION

Ground-water pumpage, in million gallons per day (Mgal/d) for blocks with 0.5 Mgal/d or more pumpage

- 0.5 - 0.9
- 1.0 - 4.9

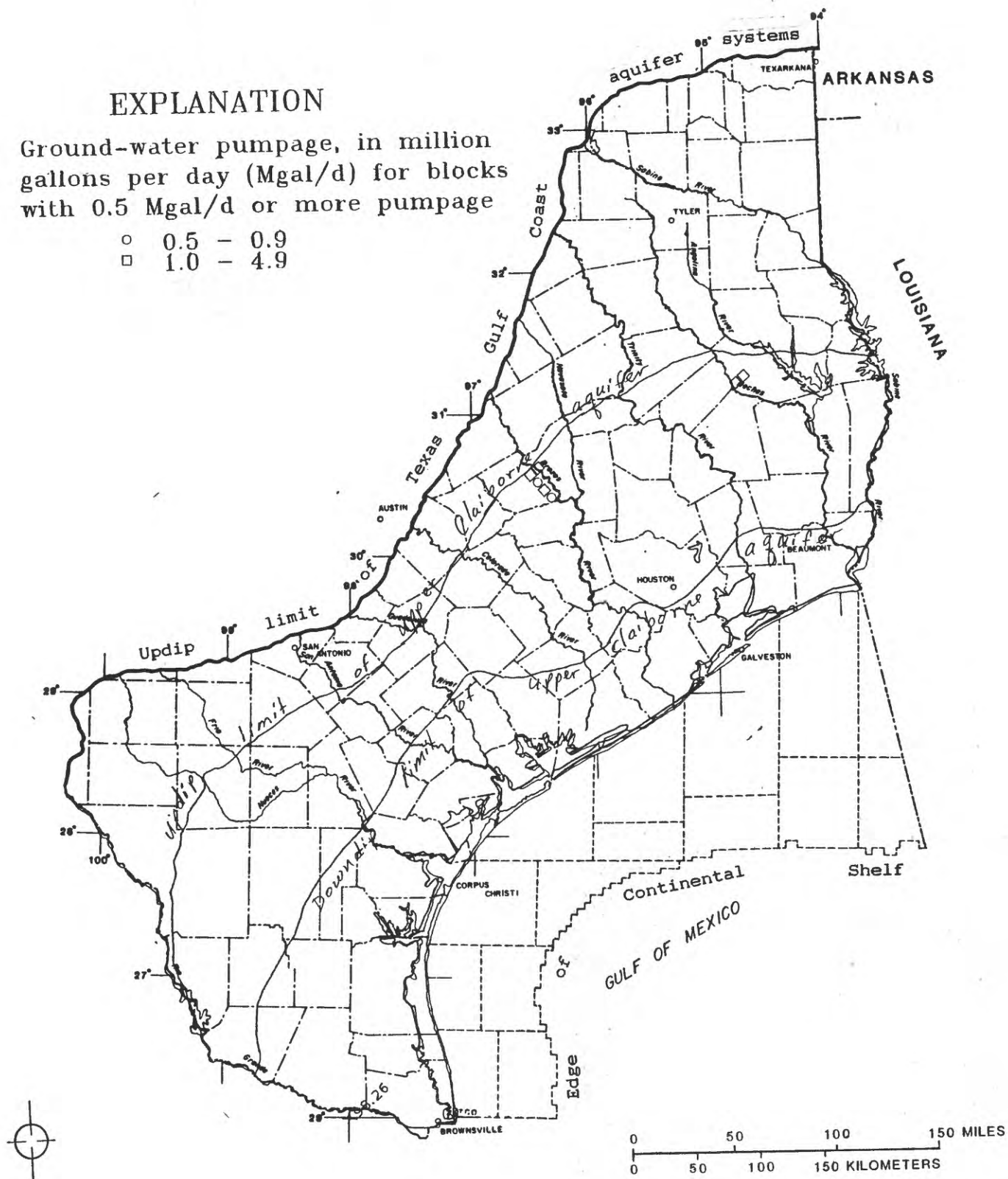


Figure 34.--Estimated pumpage in 1980, by 25-square-mile grid block, for the upper Claiborne aquifer.

EXPLANATION

Ground-water pumpage, in million gallons per day (Mgal/d) for blocks with 0.5 Mgal/d or more pumpage

○	0.5 - 0.9
□	1.0 - 4.9
◆	5.0 - 9.9

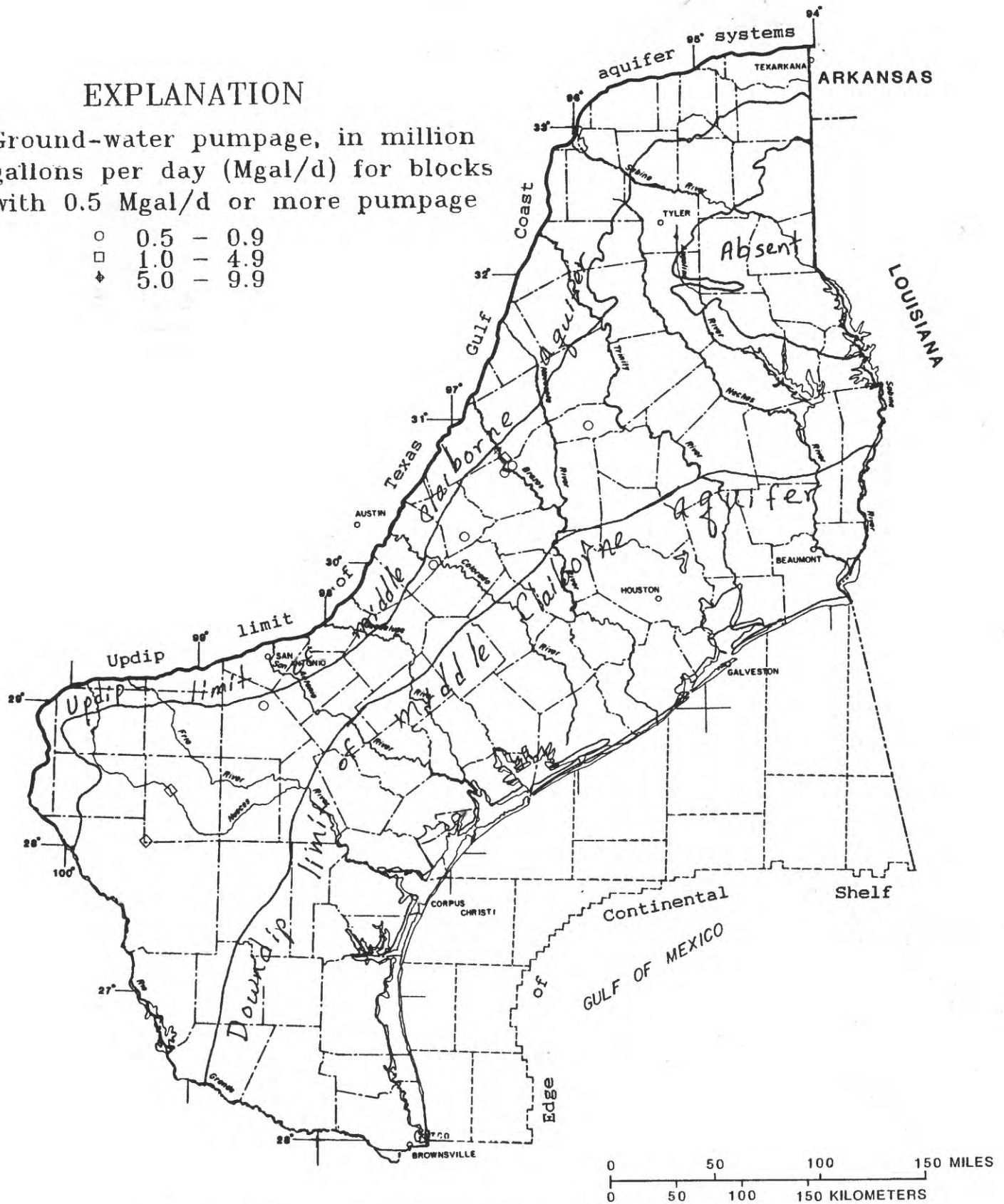


Figure 35.--Estimated pumpage in 1980, by 25-square-mile grid block, for the middle Claiborne aquifer.

EXPLANATION

Ground-water pumpage, in million gallons per day (Mgal/d) for blocks with 0.5 Mgal/d or more pumpage

○	0.5	—	0.9
□	1.0	—	4.9
◆	5.0	—	9.9
▣	10.0	—	24.9

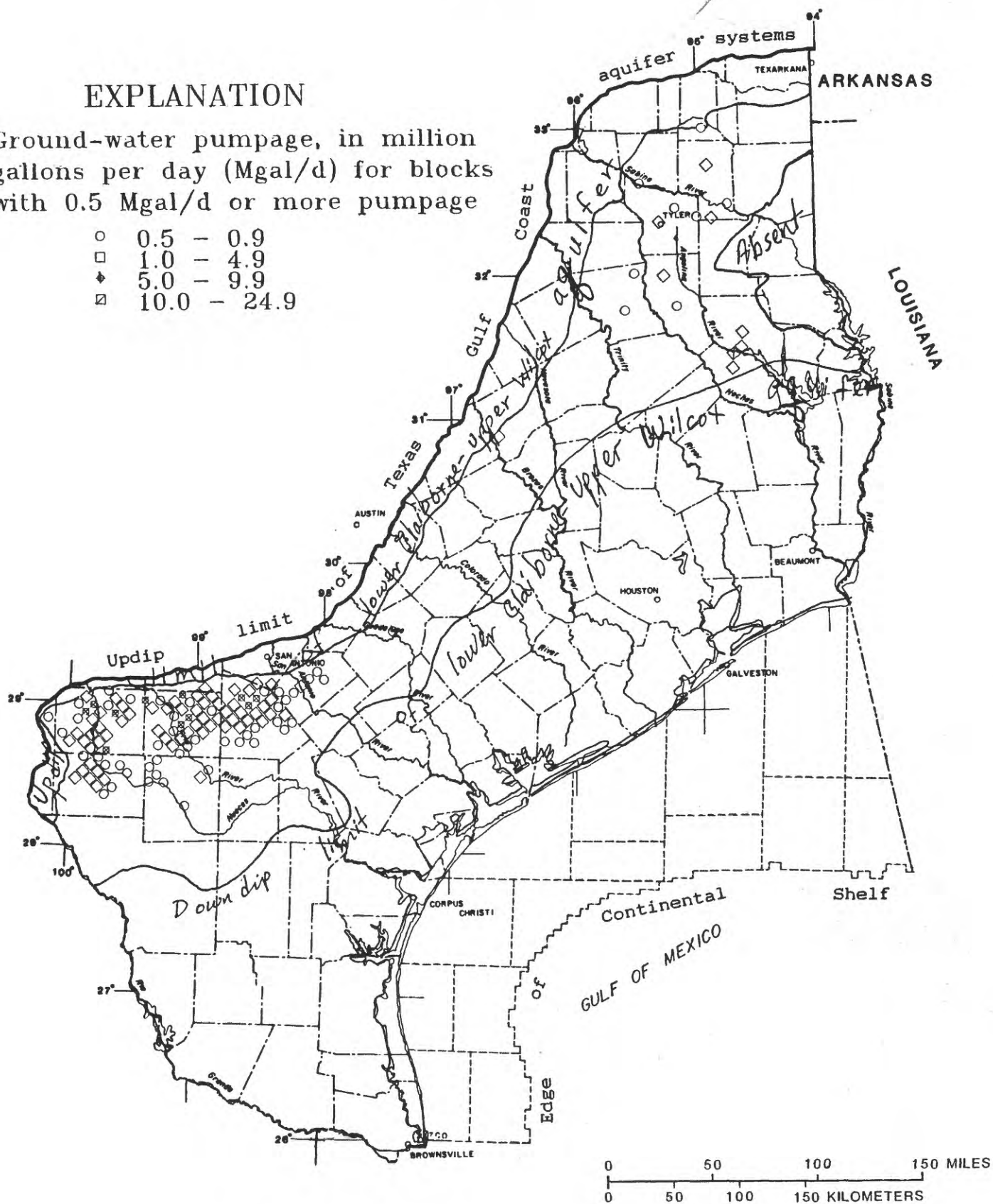


Figure 36.--Estimated pumpage in 1980, by 25-square-mile grid block, for the lower Claiborne-upper Wilcox aquifer.

EXPLANATION

Ground-water pumpage, in million gallons per day (Mgal/d) for blocks with 0.5 Mgal/d or more pumpage

○	0.5	—	0.9
□	1.0	—	4.9
◆	5.0	—	9.9

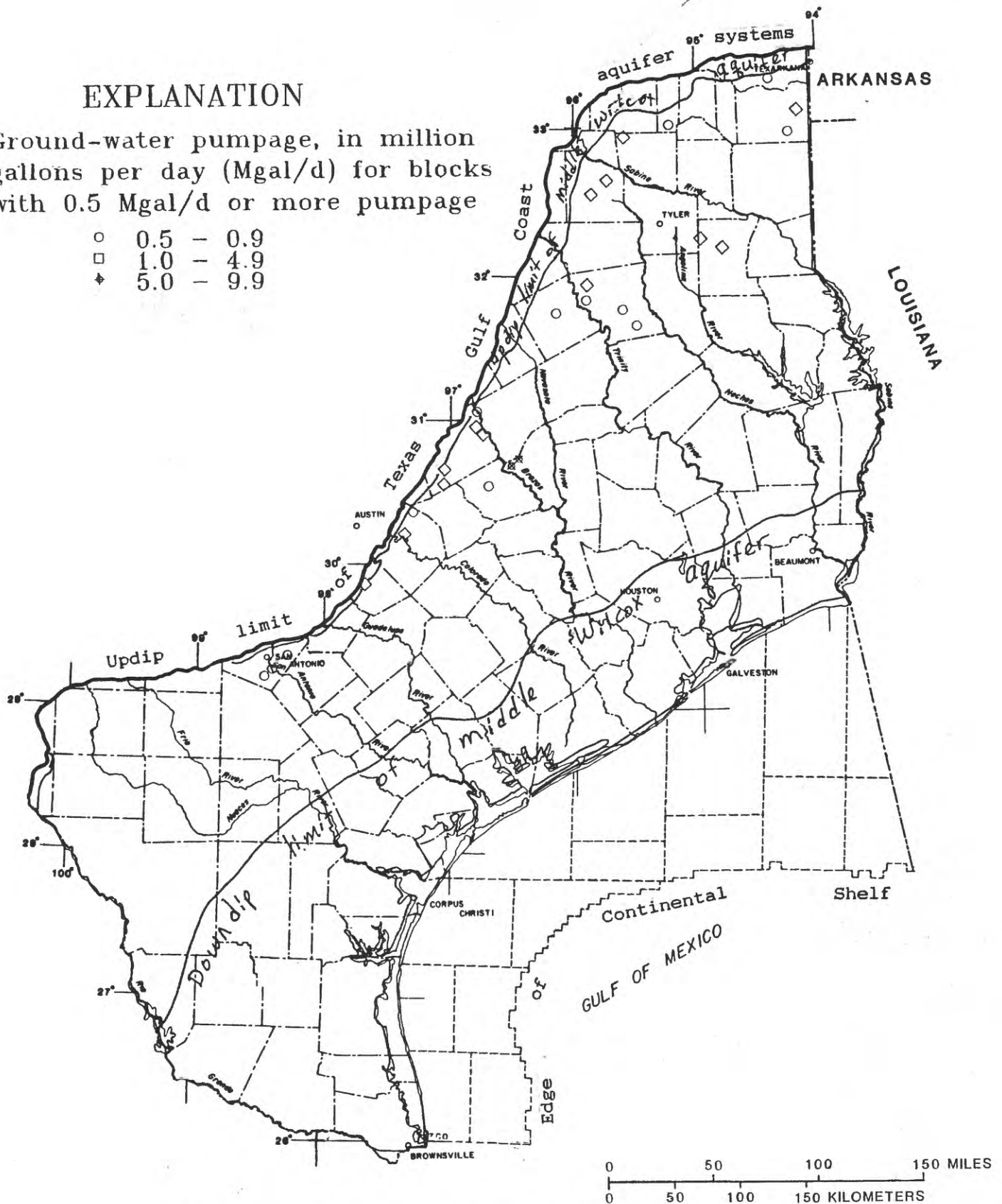


Figure 37.--Estimated pumpage in 1980, by 25-square-mile grid block, for the middle Wilcox aquifer.

EXPLANATION

SIMULATED RECHARGE AND
DISCHARGE, IN INCHES PER YEAR

1	5 to 6	} RECHARGE
2	4 to 5	
3	3 to 4	
4	2 to 3	
5	1 to 2	
6	0 to 1	} DISCHARGE
7	0 to 1	
8	1 to 2	

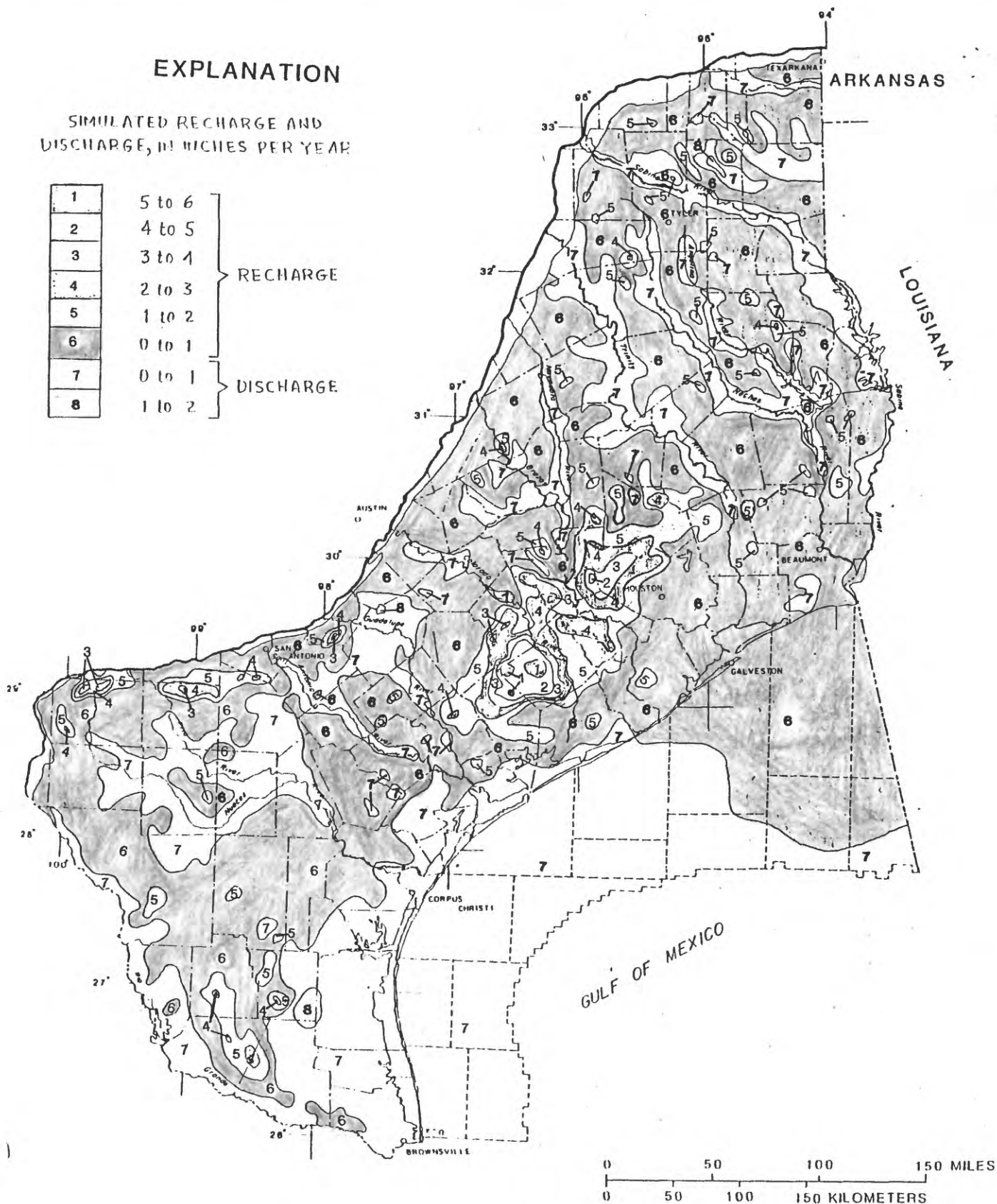


Figure 38.--Simulated recharge and discharge in the outcrop areas of aquifers, permeable zones, and confining units for 1982.

EXPLANATION

SIMULATED INCREASE IN RECHARGE OR
DECREASE IN DISCHARGE, IN INCHES PER YEAR

1	LESS THAN 0.5
2	0.5 to 1
3	1 to 2
4	2 to 3
5	3 to 4
6	4 to 5
7	5 to 6

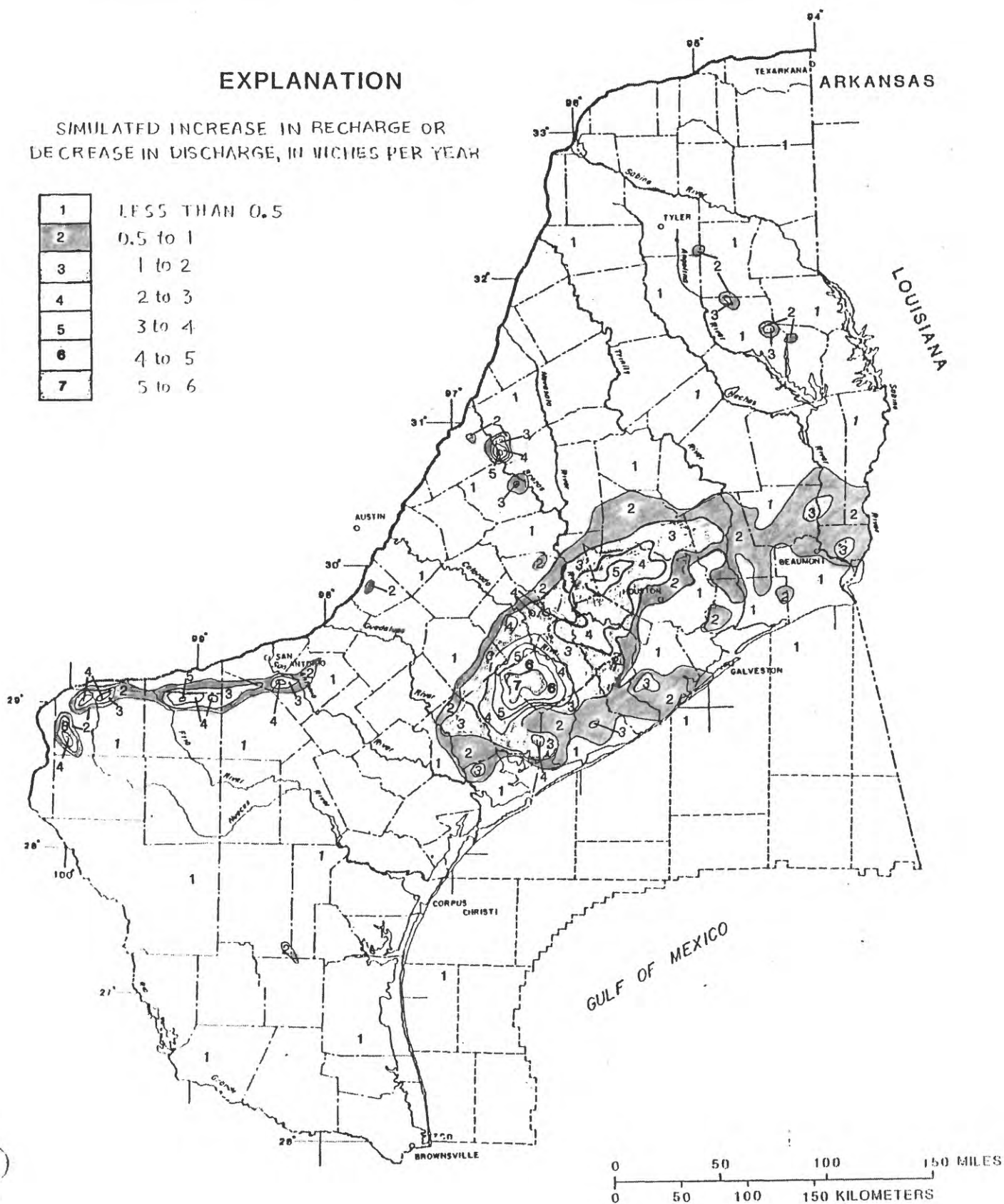


Figure 39.--Change in simulated recharge and discharge in the outcrop areas of aquifers, permeable zones, and confining units, predevelopment to 1982.

EXPLANATION

AQUIFER OR PERMEABLE ZONE AND IDENTIFIER

- ① Permeable zone A
- ② Permeable zone B
- ③ Permeable zone C
- ⑤ Permeable zone D
- ⑦ Permeable zone E
- ⑨ Upper Claiborne aquifer
- ⑪ Middle Claiborne aquifer
- ⑬ Lower Claiborne-upper Wilcox aquifer
- ⑭ Middle Wilcox aquifer

CONFINING UNIT

TOTAL RECHARGE OR DISCHARGE IN OUTCROP AREA--Includes flow through superjacent confining unit where the confining unit is exposed at the surface. Number is flow rate, in million cubic feet per day

- ↓ Recharge
- ↑ Discharge

NET RECHARGE OR DISCHARGE IN OUTCROP AREA--

Includes flow through superjacent confining unit where the confining unit is exposed at the surface. Number is flow rate, in million cubic feet per day

- ↓ Recharge
- ↑ Discharge

TOTAL LEAKAGE THROUGH BOTTOM OF AQUIFER--

Number is flow rate, in million cubic feet per day

- ↑ Upward
- ↓ Downward

NET LEAKAGE THROUGH BOTTOM OF AQUIFER--

Number is flow rate, in million cubic feet per day

- ↑ Upward
- ↓ Downward

NET LATERAL FLOW IN (+) OR OUT (-) OF STUDY AREA

L = -2

TOTAL WATER BALANCE--Numbers are million cubic feet per day. Million gallons per day in parenthesis

Total pumpage (P) = -231 (1,728)
 Net lateral flow (L) = -5 (37)
 Total release of water from storage (S) = 57 (426)
 Net recharge from constant heads = 179 (1,339)

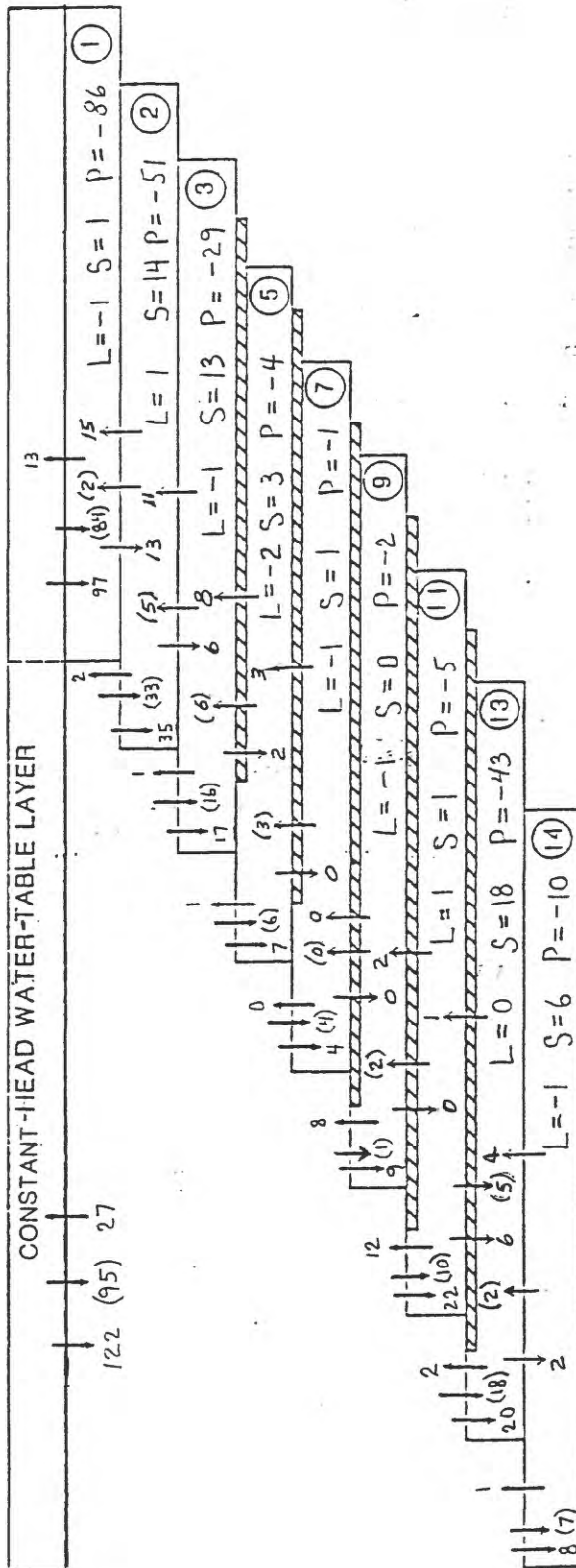


Figure 40.--Simulated 1982 vertical flow rates across hydrogeologic units in study area.

[Sum of flow rates may not exactly balance due to independent rounding.]

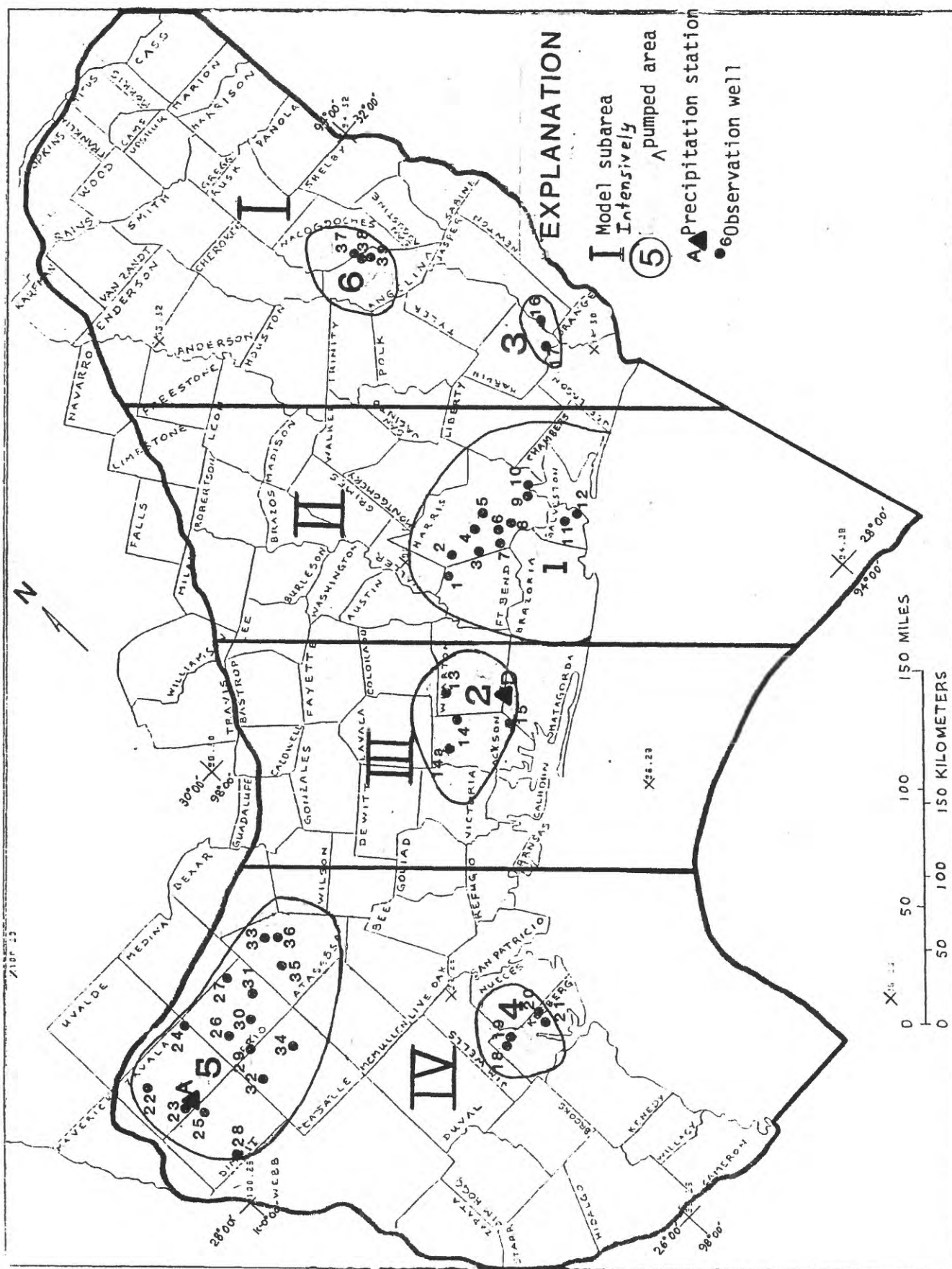


Figure 4 | --Locations of observation wells and precipitation stations in selected intensively pumped areas, and model subareas.

EXPLANATION

Pumpage scale, in million gallons per day
(Scale may vary according to county)

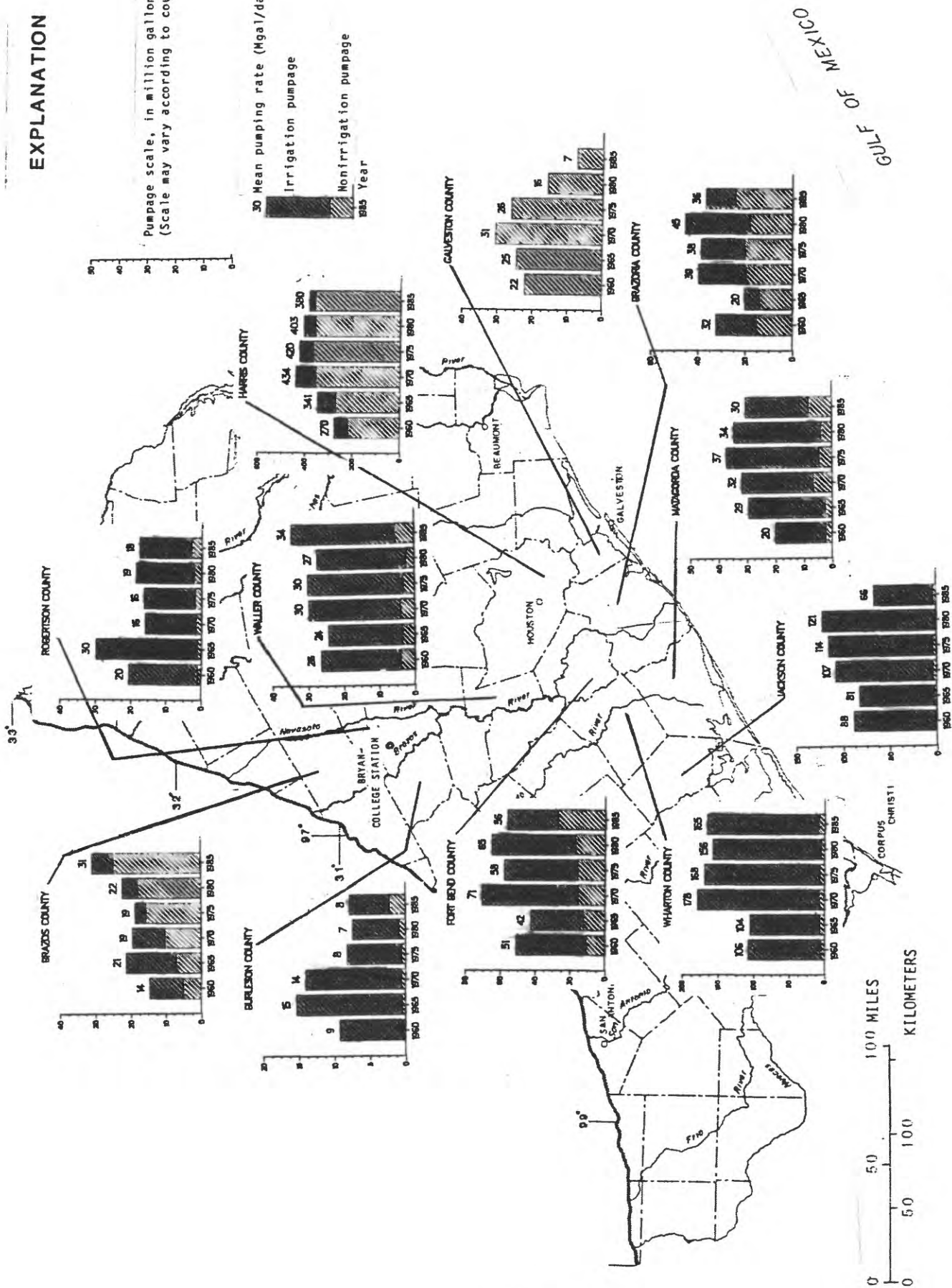
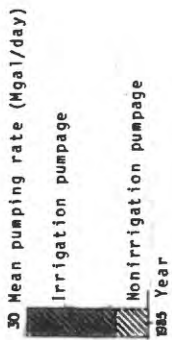


Figure 42. --Ground-water pumpage in selected counties in central part of study area, 1960-85.

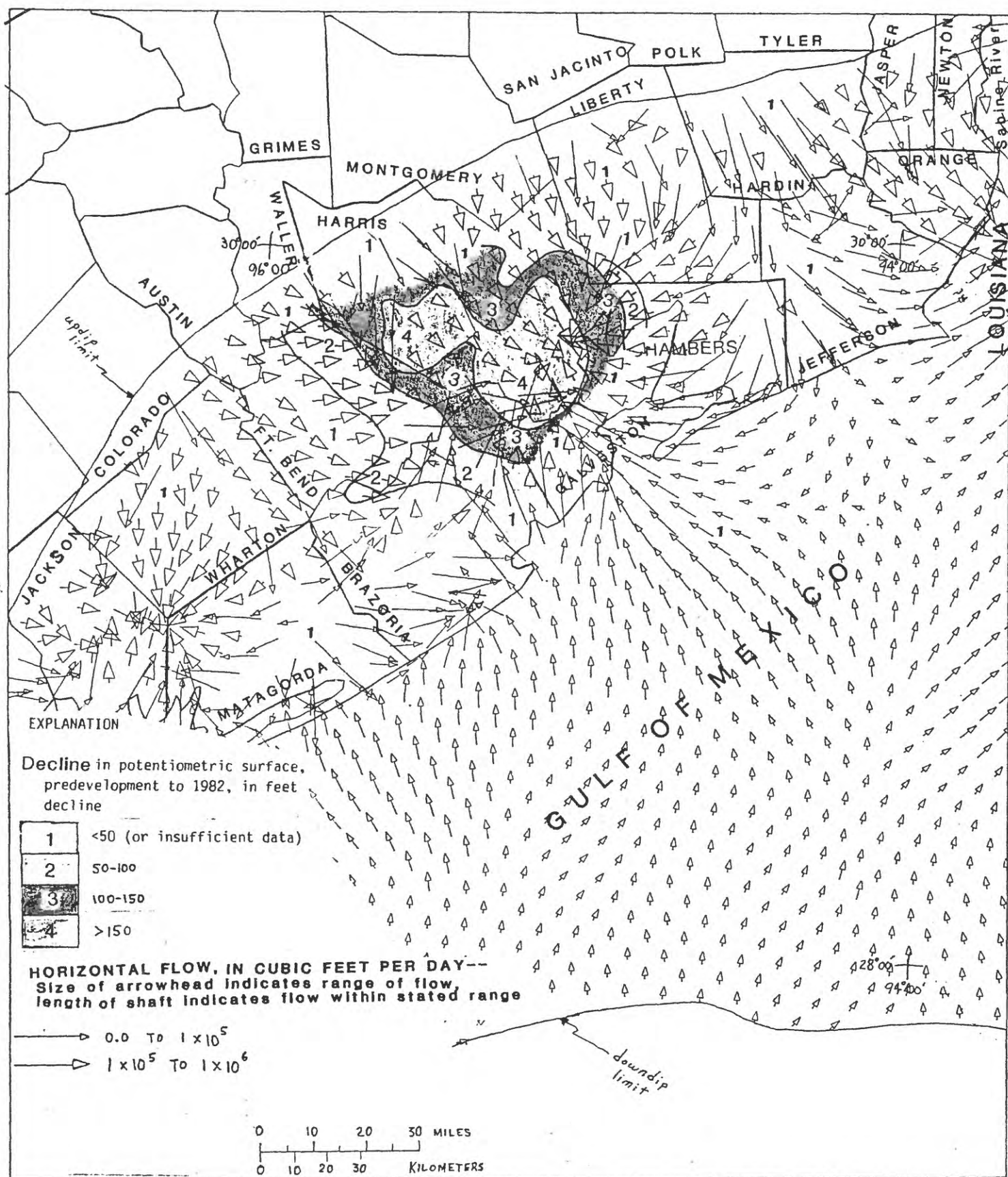


Figure 44.--Decline of potentiometric surface of permeable zone A, predevelopment to 1982, and simulated 1982 horizontal flow vectors, Houston-Galveston area.

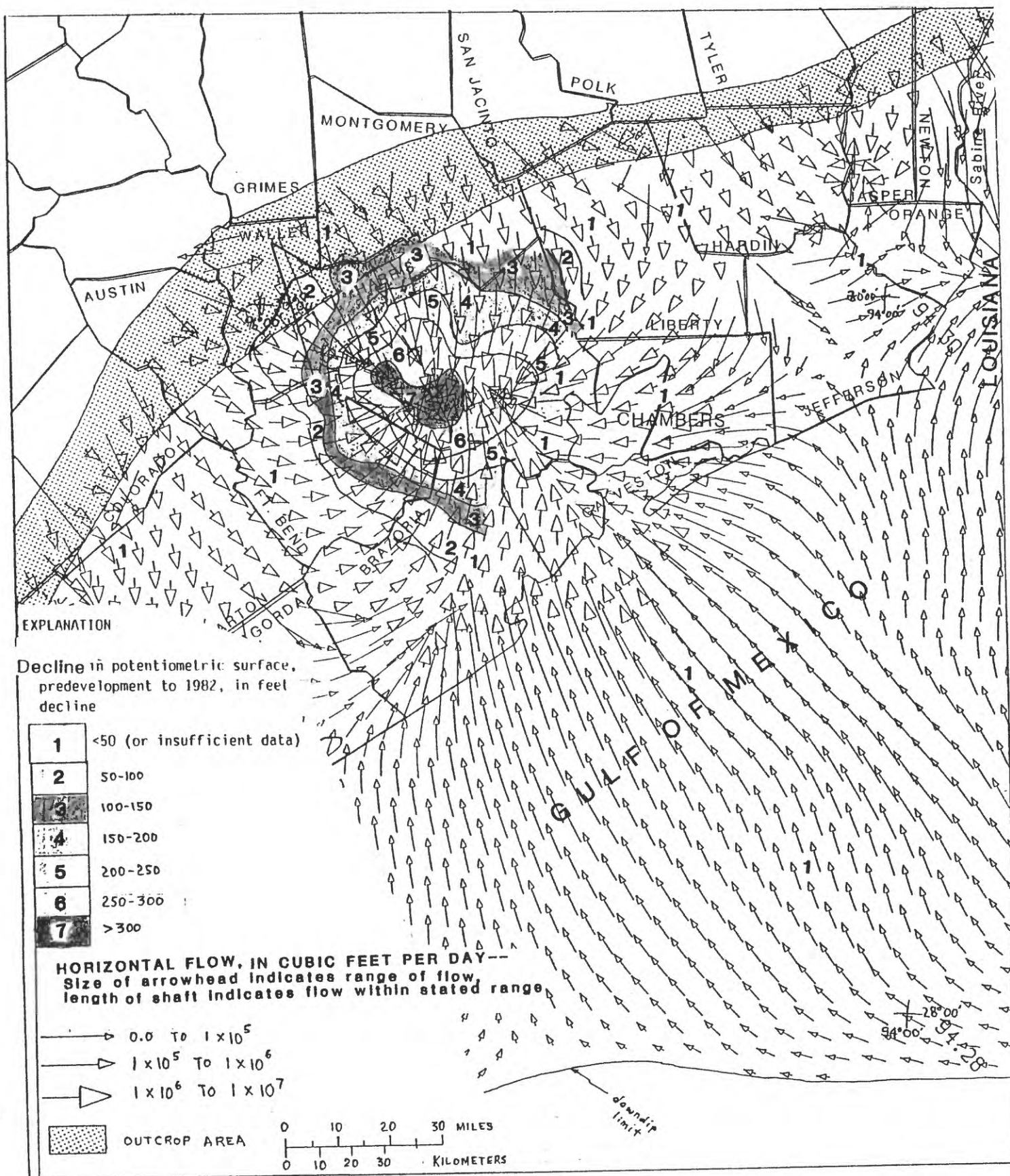


Figure 45.- Decline of potentiometric surface of permeable zone B, predevelopment to 1982, and simulated 1982 horizontal flow direction and relative magnitude, Houston-Galveston area.

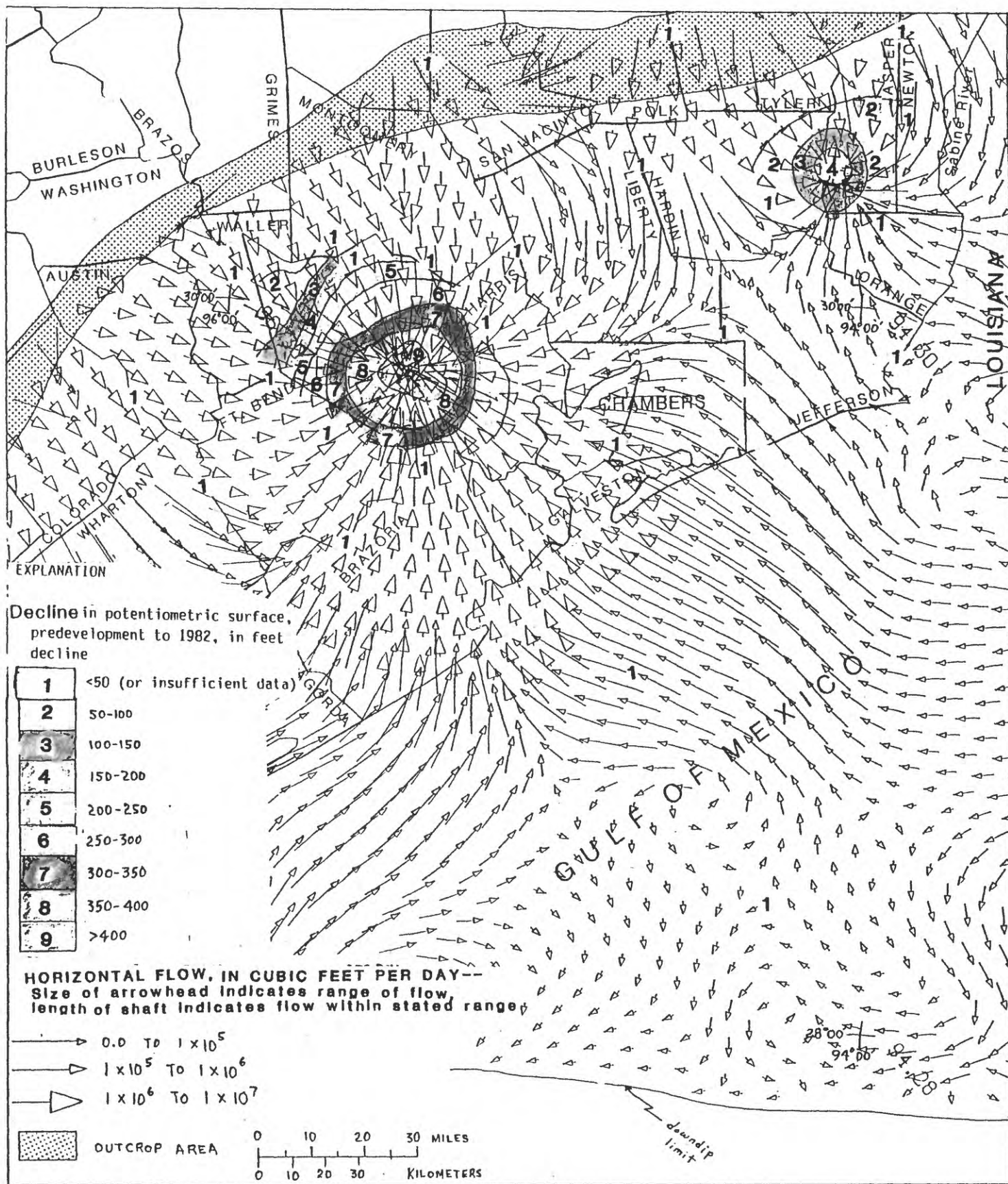


Figure 46.--Decline of potentiometric surface of permeable zone C, predevelopment to 1982, and simulated 1982 horizontal flow direction and relative magnitude, Houston-Galveston area, and Evadale-Beaumont area.

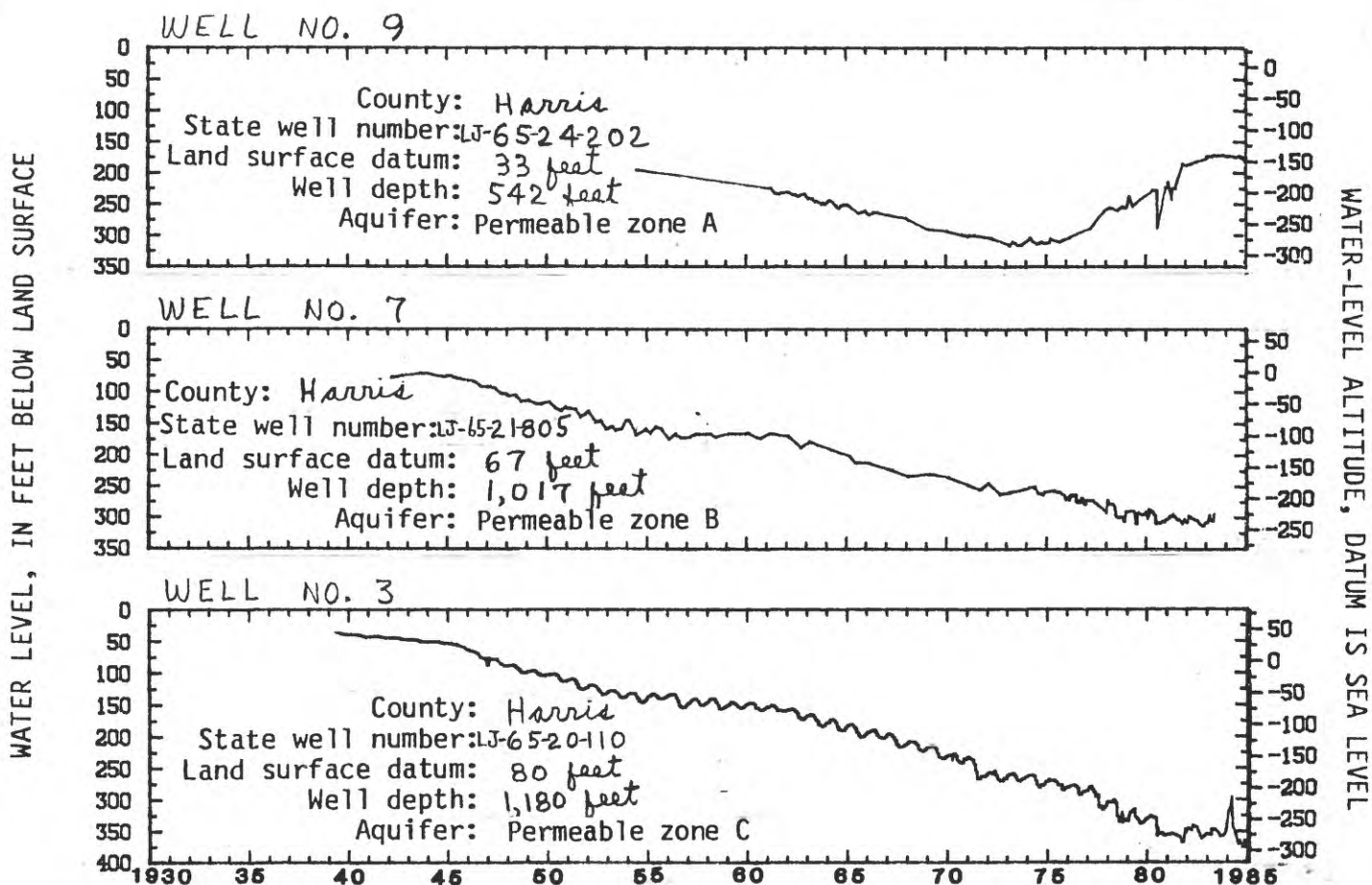


Figure 47.--Ground-water levels in Harris County. (See fig. 41 for location.)

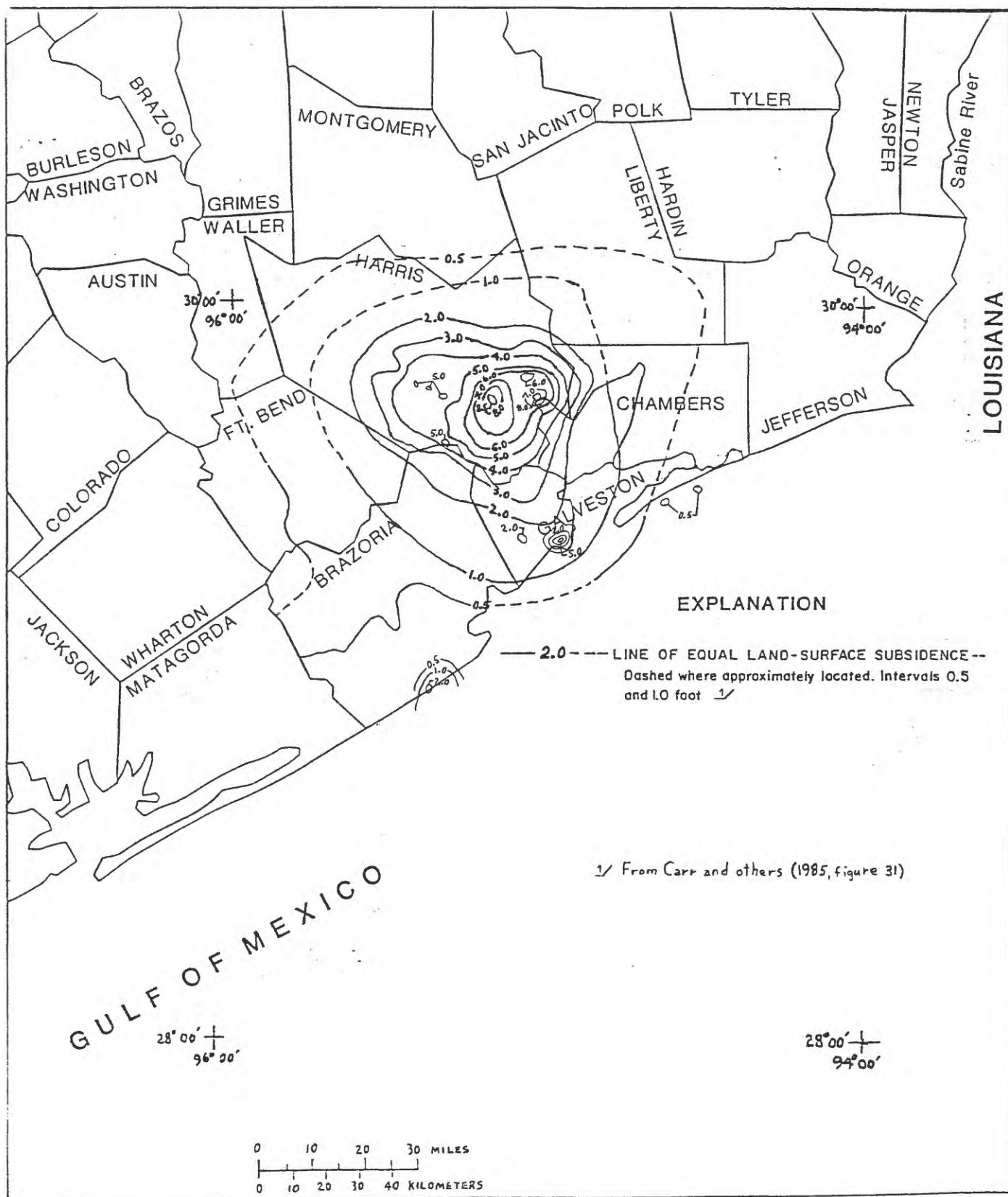


Figure 48.--Land-surface subsidence in the Houston-Galveston area, predevelopment to 1973.

EXPLANATION

AQUIFER OR PERMEABLE ZONE AND IDENTIFIER

- ① Permeable zone A
- ② Permeable zone B
- ③ Permeable zone C
- ⑤ Permeable zone D
- ⑦ Permeable zone E
- ⑨ Upper Claiborne aquifer
- ⑪ Middle Claiborne aquifer
- ⑬ Lower Claiborne-upper Wilcox aquifer
- ⑭ Middle Wilcox aquifer

CONFINING UNIT

TOTAL RECHARGE OR DISCHARGE IN OUTCROP AREA--Includes flow through superjacent confining unit where the confining unit is exposed at the surface. Number is flow rate, in million cubic feet per day

- ↓ Recharge
- ↑ Discharge

NET RECHARGE OR DISCHARGE IN OUTCROP AREA--

Includes flow through superjacent confining unit where the confining unit is exposed at the surface. Number is flow rate, in million cubic feet per day

- ↓ Recharge
- ↑ Discharge

TOTAL LEAKAGE THROUGH BOTTOM OF AQUIFER--

Number is flow rate, in million cubic feet per day

- ↑ Upward
- ↓ Downward

NET LEAKAGE THROUGH BOTTOM OF AQUIFER--

Number is flow rate, in million cubic feet per day

- ↑ Upward
- ↓ Downward

NET LATERAL FLOW IN (+) OR OUT (-) OF STUDY AREA

L = -2

TOTAL WATER BALANCE--Numbers are million cubic feet per day. Million gallons per day in parenthesis

Total pumpage (P) = -102 (763)
 Net lateral flow (L) = 4 (30)
 Total release of water from storage (S) = 29 (217)
 Net recharge from constant heads = 69 (516)

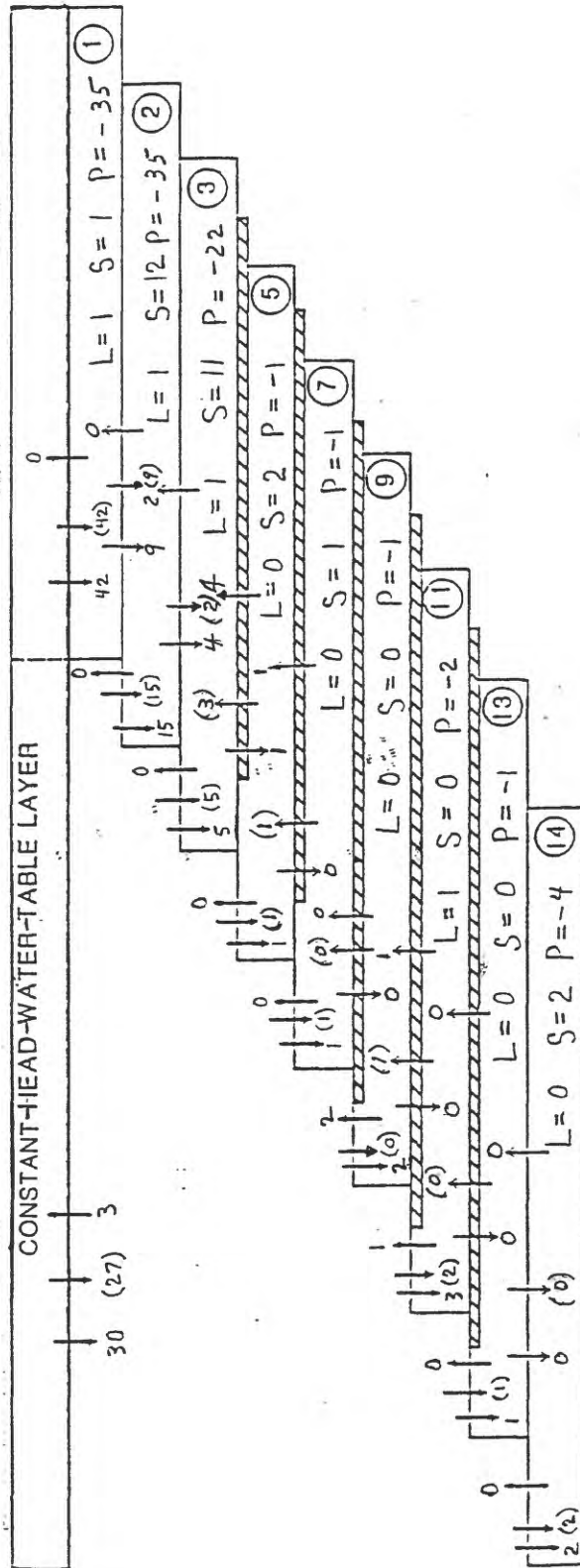


Figure 49.--Simulated 1982 vertical flow rates across hydrogeologic units in model subarea III (fig. 41). [Sum of flow rates may not exactly balance due to independent rounding.]

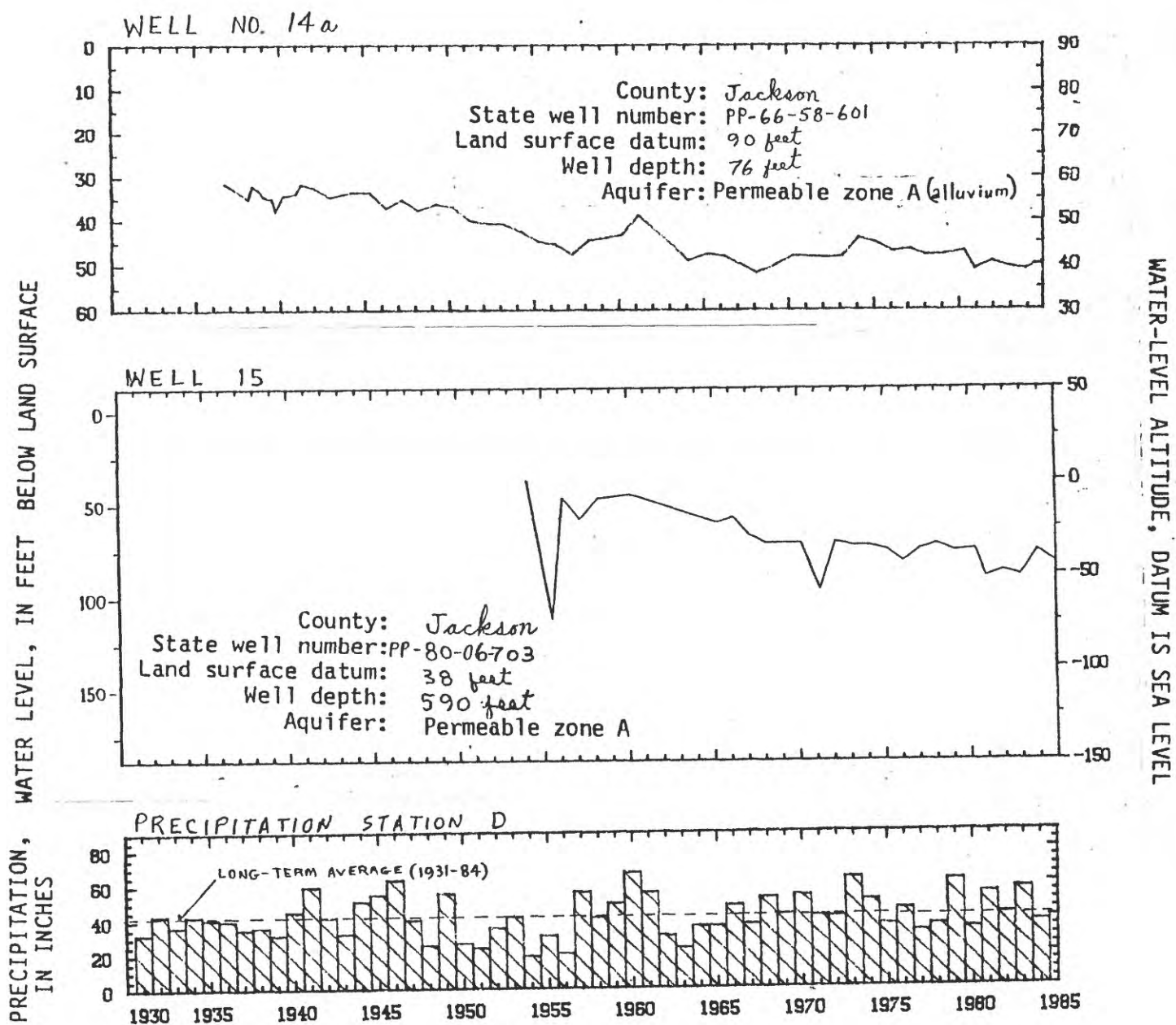


Figure 50.--Ground-water levels ^{in Jackson County} and precipitation data in
 (See figure 41 for locations.)

Wharton County

EXPLANATION

AQUIFER OR PERMEABLE ZONE AND IDENTIFIER

- ① Permeable zone A
- ② Permeable zone B
- ③ Permeable zone C
- ⑤ Permeable zone D
- ⑦ Permeable zone E
- ⑨ Upper Claiborne aquifer
- ⑪ Middle Claiborne aquifer
- ⑬ Lower Claiborne-upper Wilcox aquifer
- ⑭ Middle Wilcox aquifer

CONFINING UNIT

TOTAL RECHARGE OR DISCHARGE IN OUTCROP AREA--Includes flow through superjacent confining unit where the confining unit is exposed at the surface. Number is flow rate, in million cubic feet per day

- ↓ 15 Recharge
- ↑ 15 Discharge

NET RECHARGE OR DISCHARGE IN OUTCROP AREA--

Includes flow through superjacent confining unit where the confining unit is exposed at the surface. Number is flow rate, in million cubic feet per day

- ↓ (4) Recharge
- ↑ (3) Discharge

TOTAL LEAKAGE THROUGH BOTTOM OF AQUIFER--

Number is flow rate, in million cubic feet per day

- ↑ 16 Upward
- ↓ 2 Downward

NET LEAKAGE THROUGH BOTTOM OF AQUIFER--

Number is flow rate, in million cubic feet per day

- ↑ (5) Upward
- ↓ (5) Downward

NET LATERAL FLOW IN (+) OR OUT (-) OF STUDY AREA

- ↓ L = -2

TOTAL WATER BALANCE--Numbers are million cubic feet per day.
Million gallons per day in parenthesis

Total pumpage (P) = -58 (434)
Net lateral flow (L) = -3 (22)
Total release of water from storage (S) = 4 (30)
Net recharge from constant heads = 57 (426)

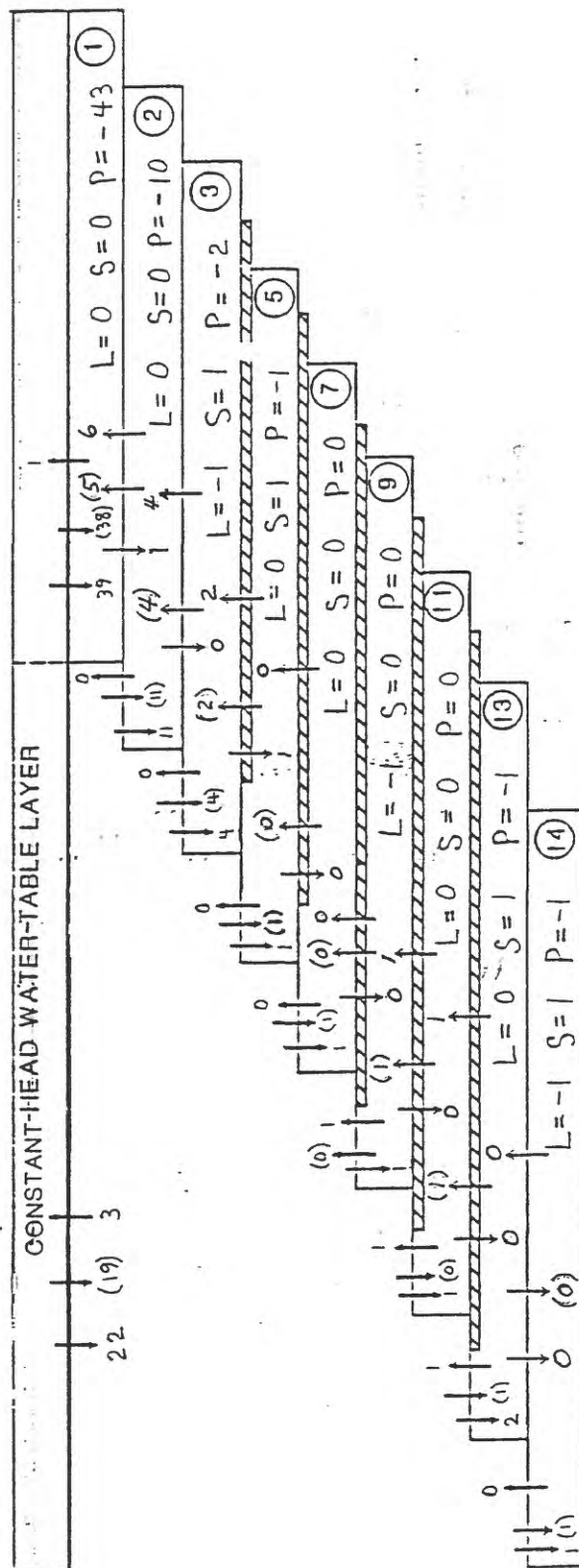


Figure 51 --Simulated 1982 vertical flow rates across hydrogeologic units in model subarea III (fig. 44). [Sum of flow rates may not exactly balance due to independent rounding.]

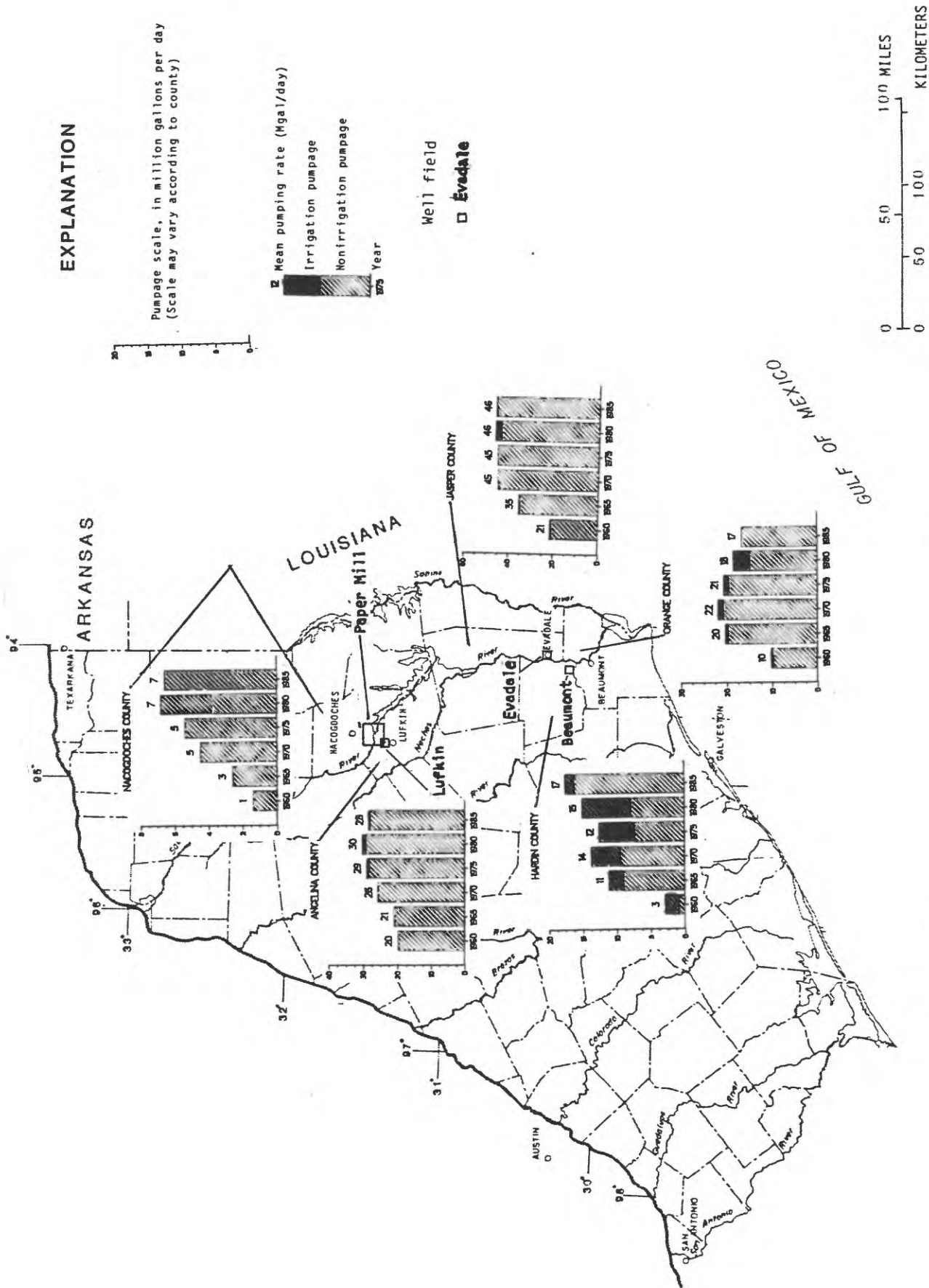
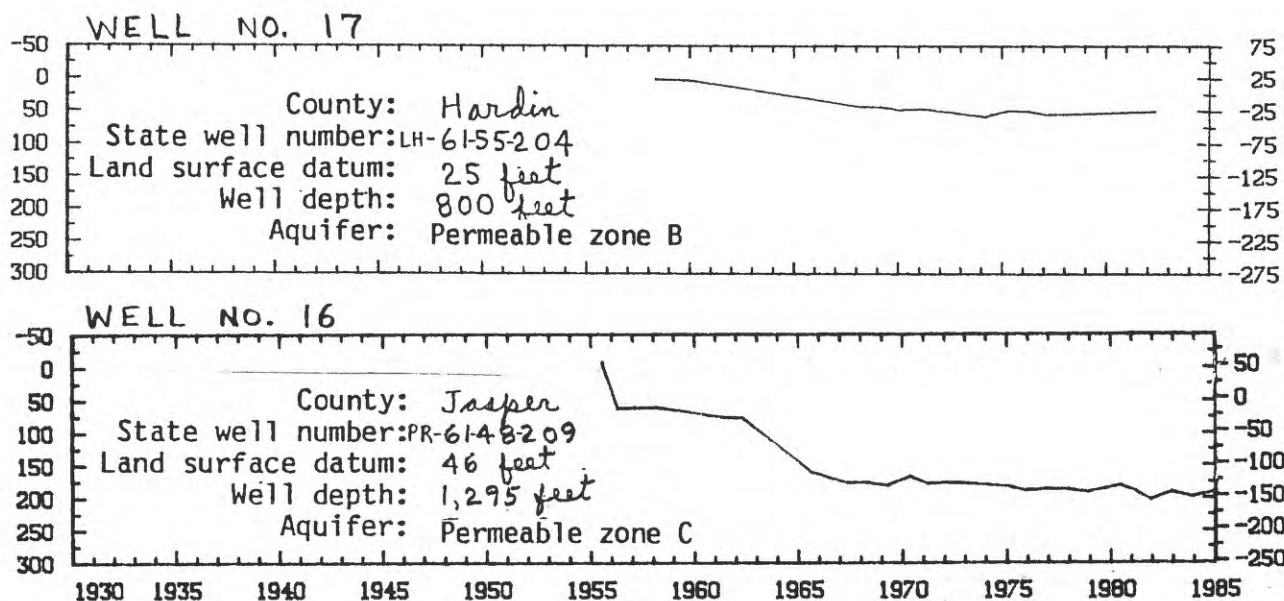


Figure 52.--Ground-water pumpage in selected counties in eastern part of study area, 1960-85.

WATER LEVEL, IN FEET BELOW LAND SURFACE



WATER-LEVEL ALTITUDE, DATUM IS SEA LEVEL

Figure 53.--Ground-water levels in Jasper and Hardin Counties. (See fig. 41 for locations.)

EXPLANATION

AQUIFER OR PERMEABLE ZONE AND IDENTIFIER

- ① Permeable zone A
- ② Permeable zone B
- ③ Permeable zone C
- ⑤ Permeable zone D
- ⑦ Permeable zone E
- ⑨ Upper Claiborne aquifer
- ⑪ Middle Claiborne aquifer
- ⑬ Lower Claiborne-upper Wilcox aquifer
- ⑭ Middle Wilcox aquifer

CONFINING UNIT

TOTAL RECHARGE OR DISCHARGE IN OUTCROP AREA--Includes flow through superjacent confining unit where the confining unit is exposed at the surface. Number is flow rate, in million cubic feet per day

- ↓ Recharge
- ↑ Discharge

NET RECHARGE OR DISCHARGE IN OUTCROP AREA--Includes flow through superjacent confining unit where the confining unit is exposed at the surface. Number is flow rate, in million cubic feet per day

- ↓ Recharge
- ↑ Discharge

TOTAL LEAKAGE THROUGH BOTTOM OF AQUIFER--Number is flow rate, in million cubic feet per day

- ↑ Upward
- ↓ Downward

NET LEAKAGE THROUGH BOTTOM OF AQUIFER--Number is flow rate, in million cubic feet per day

- ↑ Upward
- ↓ Downward

NET LATERAL FLOW IN (+) OR OUT (-) OF STUDY AREA

TOTAL WATER BALANCE--Numbers are million cubic feet per day. Million gallons per day in parenthesis

Total pumping (P) = -29 (217)
 Net lateral flow (L) = -3 (22)
 Total release of water from storage (S) = 5 (37)
 Net recharge from constant heads = 27 (202)

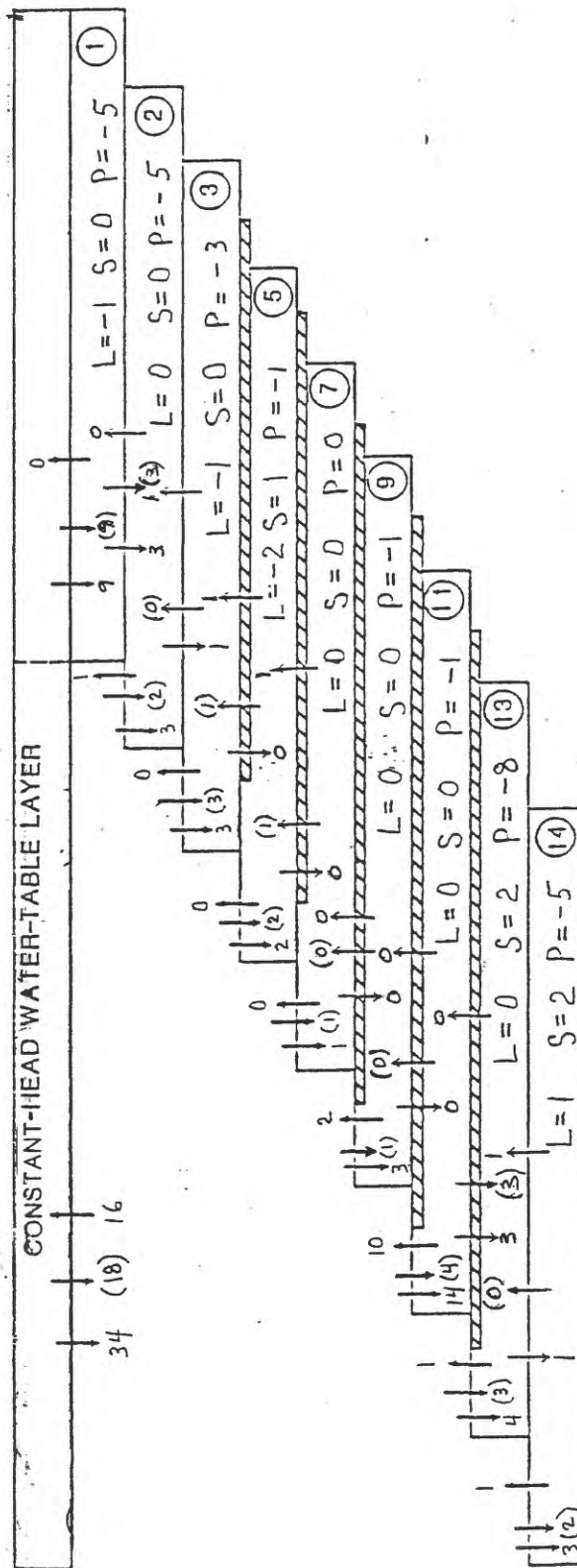


Figure 54.--Simulated 1982 vertical flow rates across hydrogeologic units in model subarea I (fig. 41). [Sum of flow rates may not exactly balance due to independent rounding.]

EXPLANATION

Pumpage scale, in million gallons per day
(Scale may vary according to county)

Mean pumping rate (Mgal/day)
Irrigation pumpage
Nonirrigation pumpage
1965 Year
1965 and 1970 pumpage modified from
Klemm and others (1976, fig. 7)

Well field

Kingsville

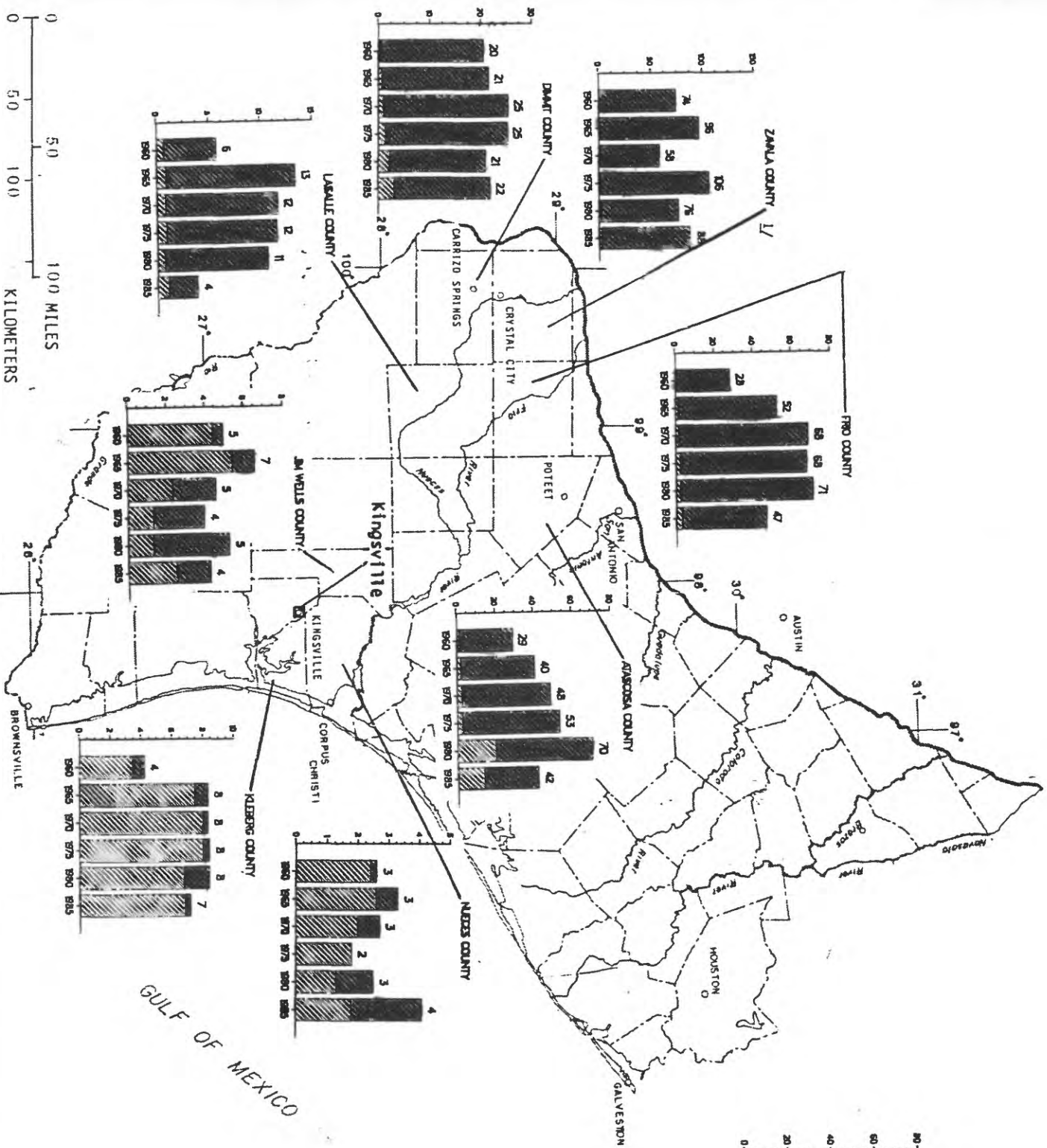


Figure 55.--Ground-water pumpage in selected counties in western part of study area, 1960-85.

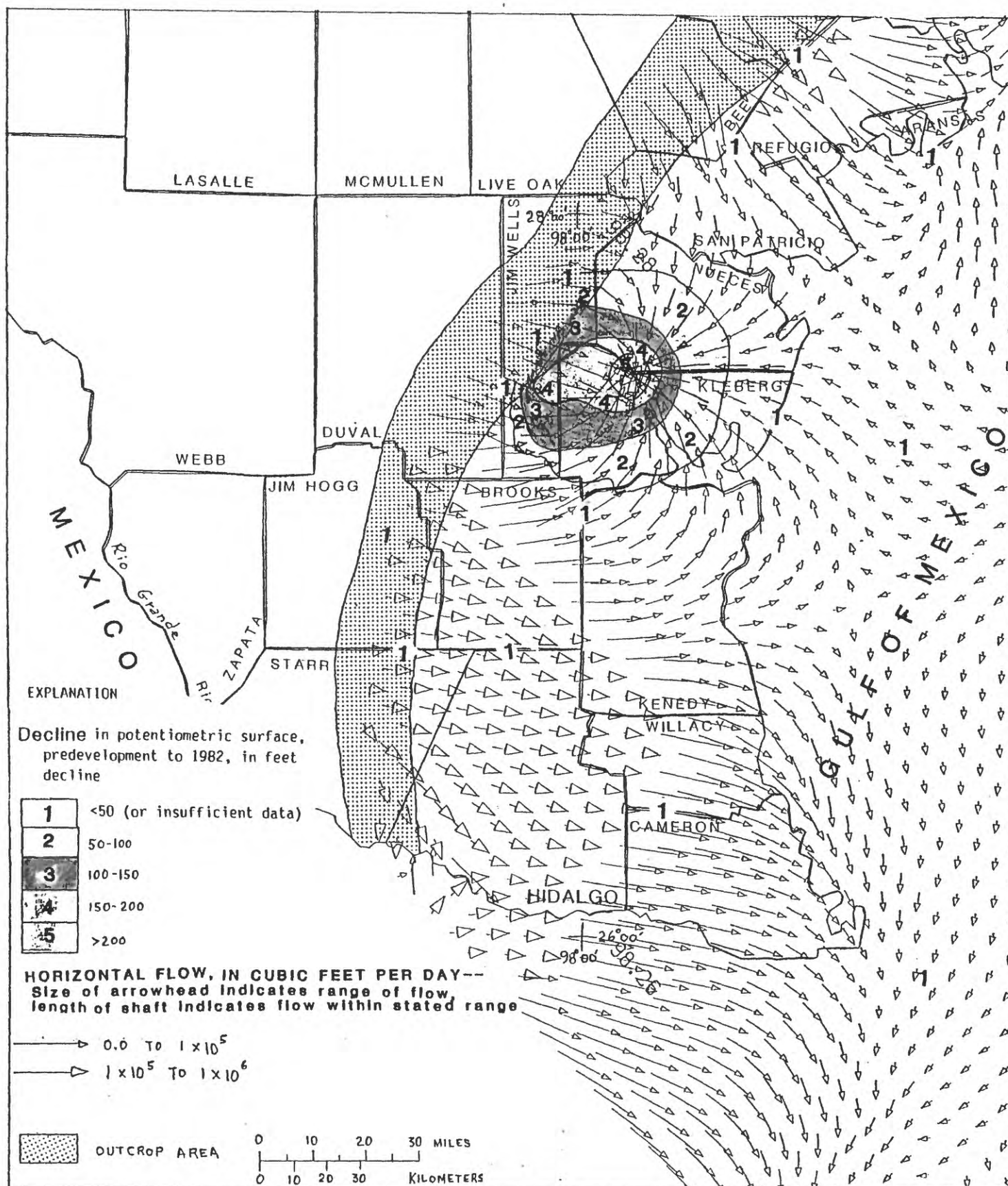


Figure 56.--Decline of potentiometric surface of permeable zone B, predevelopment to 1982, and simulated 1982 horizontal flow direction and relative magnitude, Kingsville area.

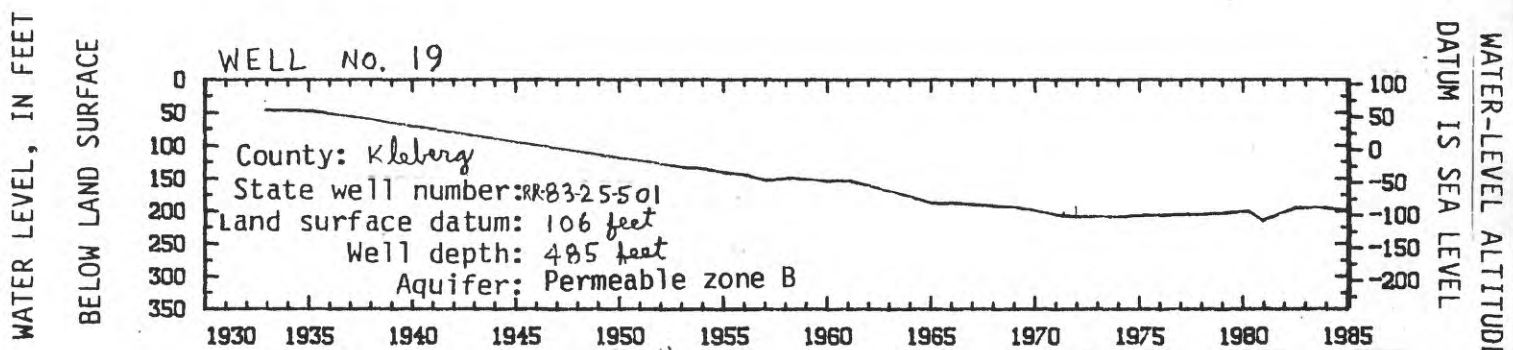


Figure 57.--Ground-water levels in Kleberg County. (See fig. 41 for location.)

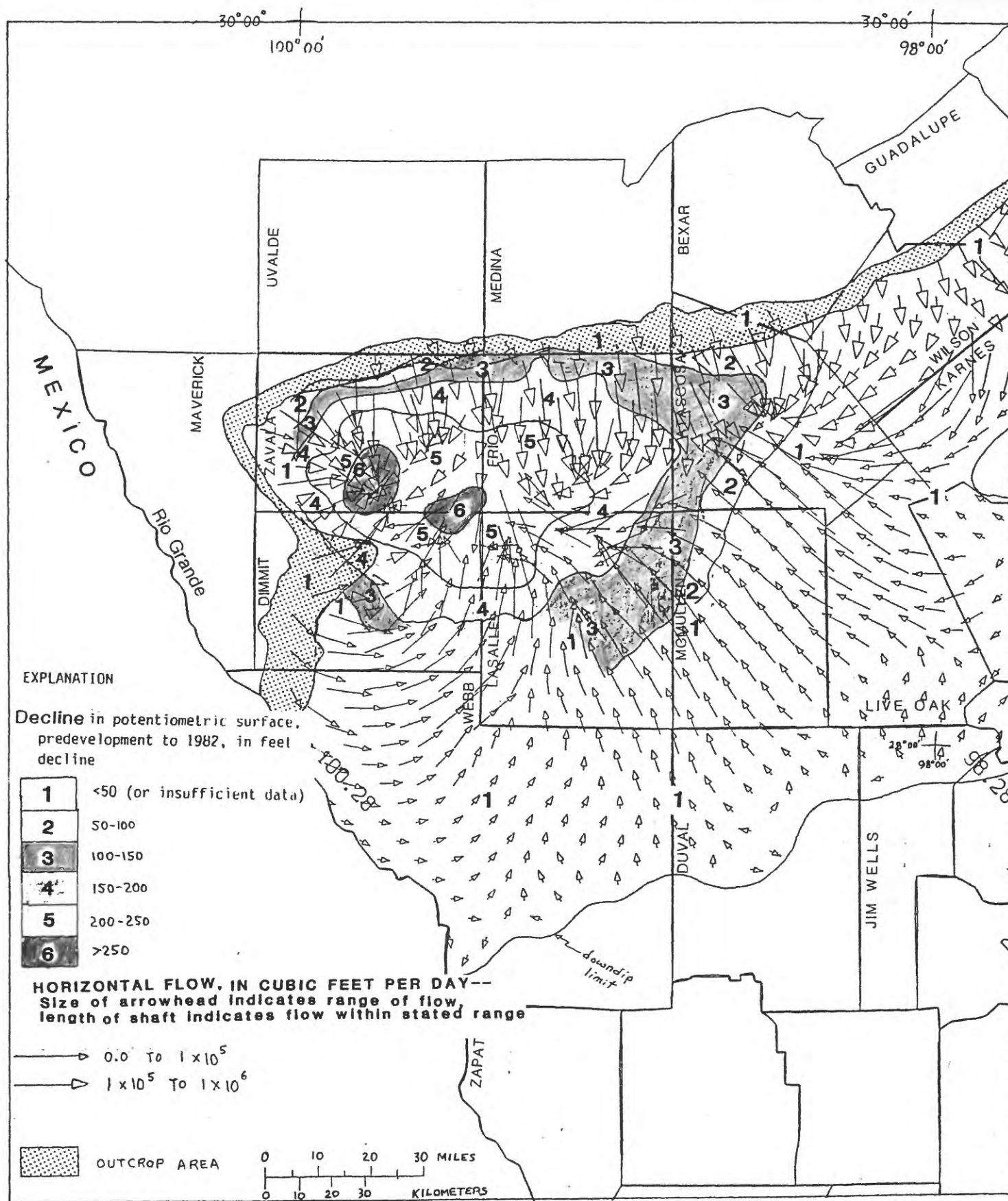


Figure 59.--Decline of potentiometric surface of the lower Claiborne-upper Wilcox aquifer, predevelopment to 1982, and simulated 1982 horizontal flow direction and relative magnitude, Winter Garden area.

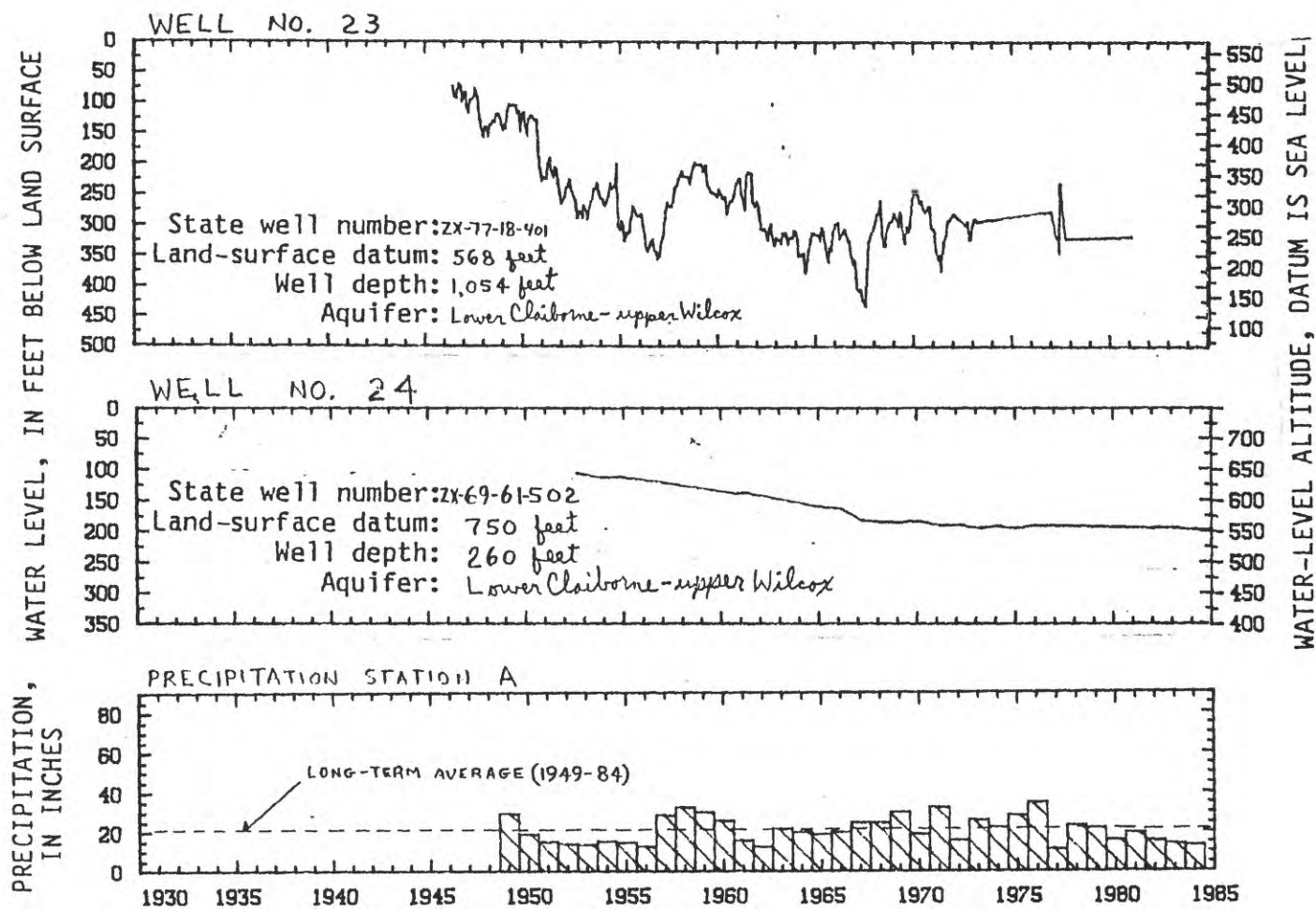


Figure 60.--Ground-water levels and precipitation data in Zavala County.
 (See figure 41 for locations.)

EXPLANATION

AQUIFER OR PERMEABLE ZONE AND IDENTIFIER

- ① Permeable zone A
- ② Permeable zone B
- ③ Permeable zone C
- ④ Permeable zone D
- ⑤ Permeable zone E
- ⑥ Upper Claiborne aquifer
- ⑦ Middle Claiborne aquifer
- ⑧ Lower Claiborne-upper Wilcox aquifer
- ⑨ Middle Wilcox aquifer

CONFINING UNIT

TOTAL RECHARGE OR DISCHARGE IN OUTCROP AREA--Includes flow through superjacent confining unit where the confining unit is exposed at the surface. Number is flow rate, in million cubic feet per day

- ↓ Recharge
- ↑ Discharge

NET RECHARGE OR DISCHARGE IN OUTCROP AREA--

Includes flow through superjacent confining unit where the confining unit is exposed at the surface. Number is flow rate, in million cubic feet per day

- ↓ Recharge
- ↑ Discharge

TOTAL LEAKAGE THROUGH BOTTOM OF AQUIFER--

Number is flow rate, in million cubic feet per day

- ↑ Upward
- ↓ Downward

NET LEAKAGE THROUGH BOTTOM OF AQUIFER--

Number is flow rate, in million cubic feet per day

- ↑ Upward
- ↓ Downward

NET LATERAL FLOW IN (+) OR OUT (-) OF STUDY AREA

L = -2

TOTAL WATER BALANCE--Numbers are million cubic feet per day; Million gallons per day in parenthesis

Total pumping (P) = -41 (307)
 Net lateral flow (L) = -3 (22)
 Total release of water from storage (S) = 18 (135)
 Net recharge from constant heads = 26 (194)

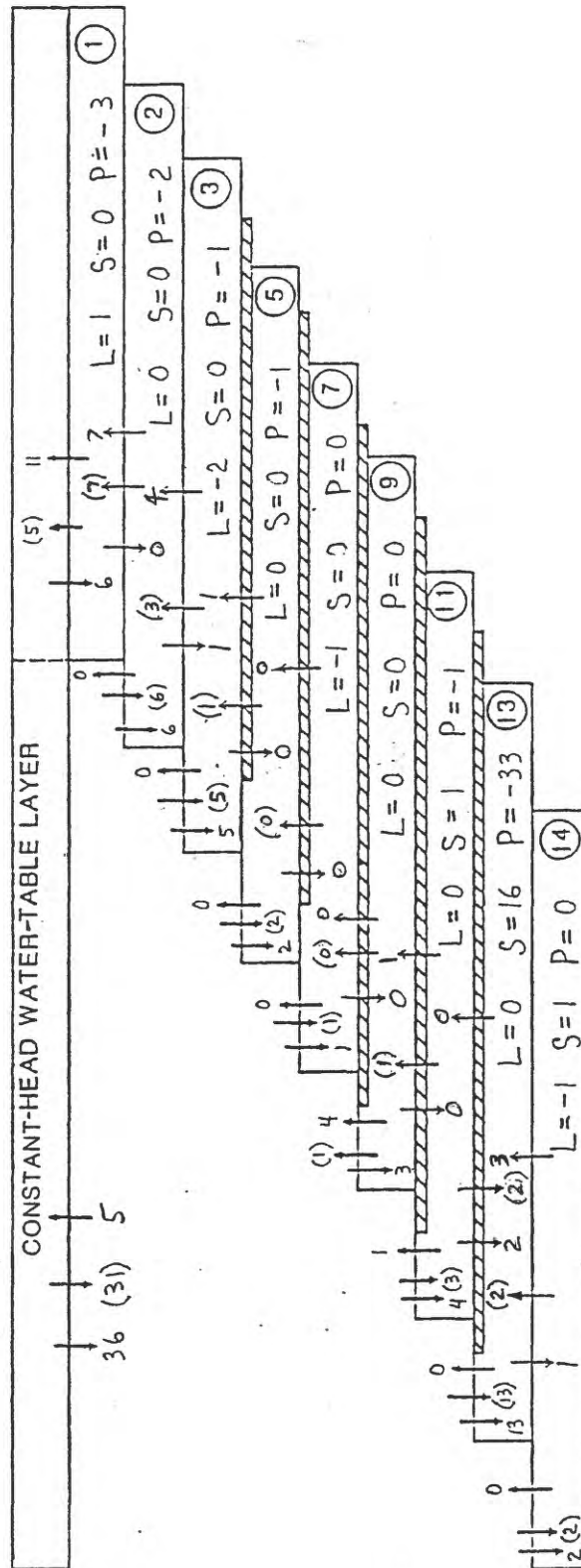


Figure 58.--Simulated 1982 vertical flow rates across hydrogeologic units in model subarea IV (fig. 4-1). [Sum of flow rates may not exactly balance due to independent rounding.]

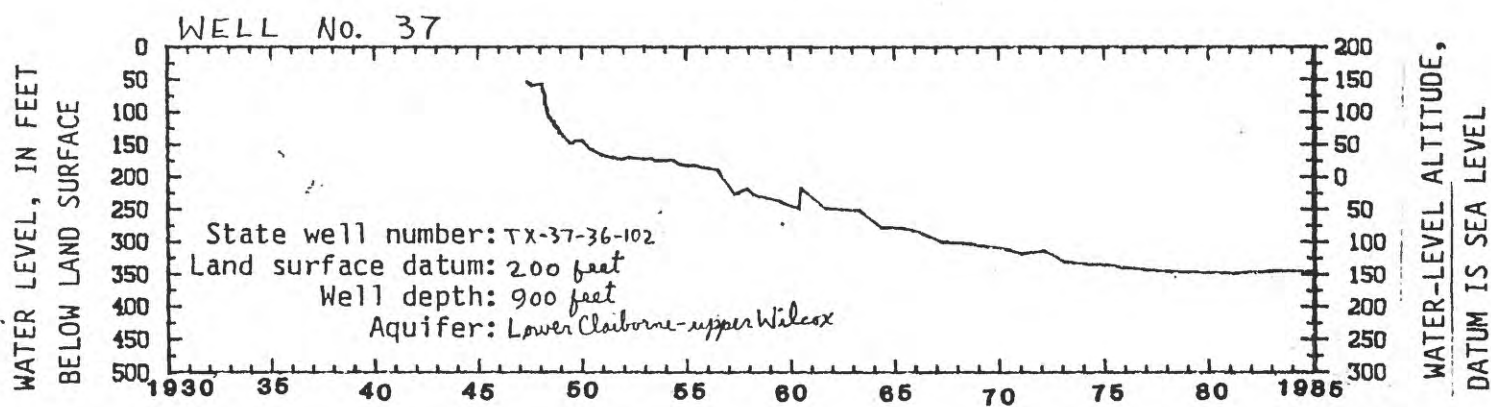


Figure 61.--Ground-water levels in Nacogdoches County. (See fig. 41 for location.)

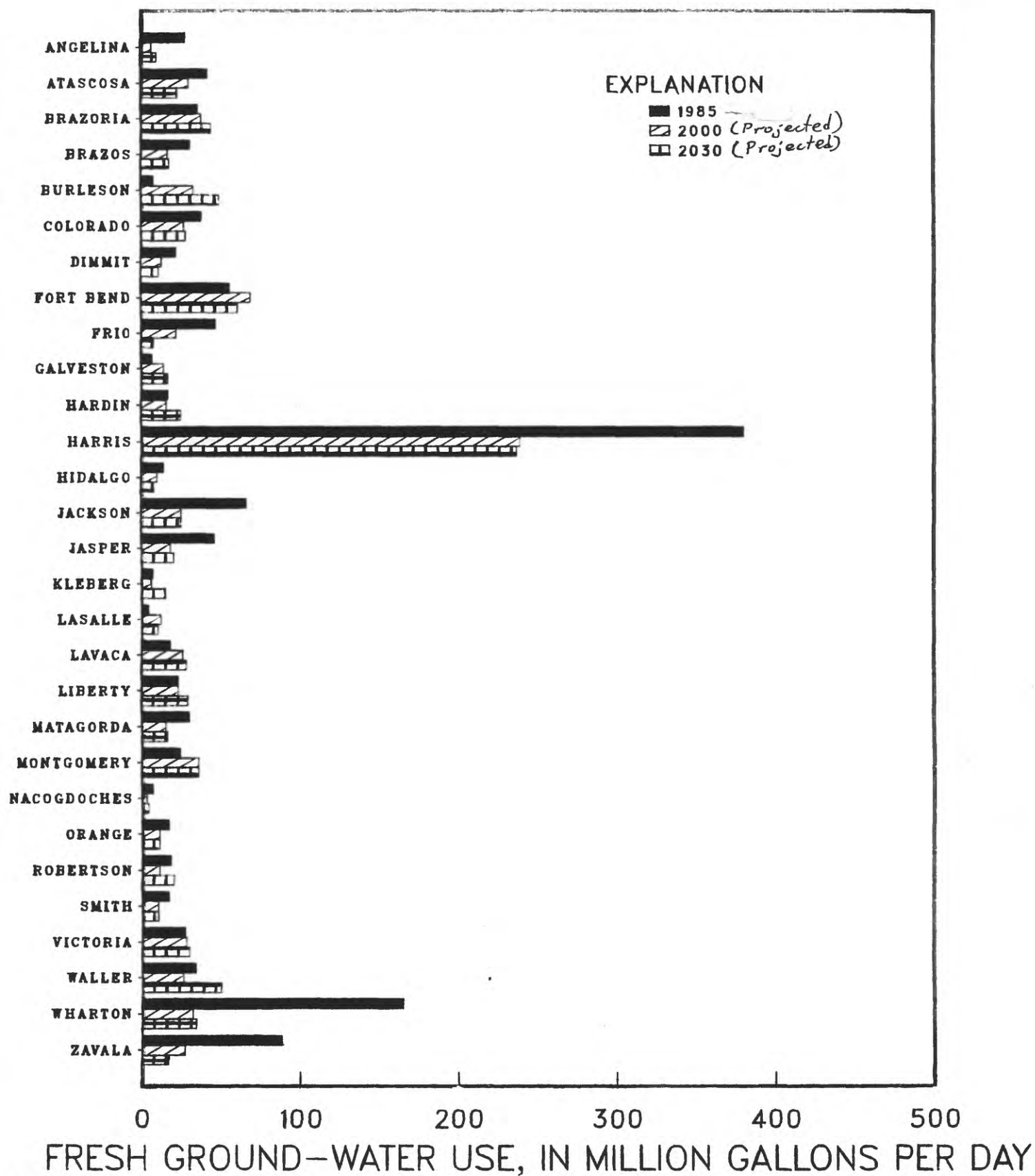
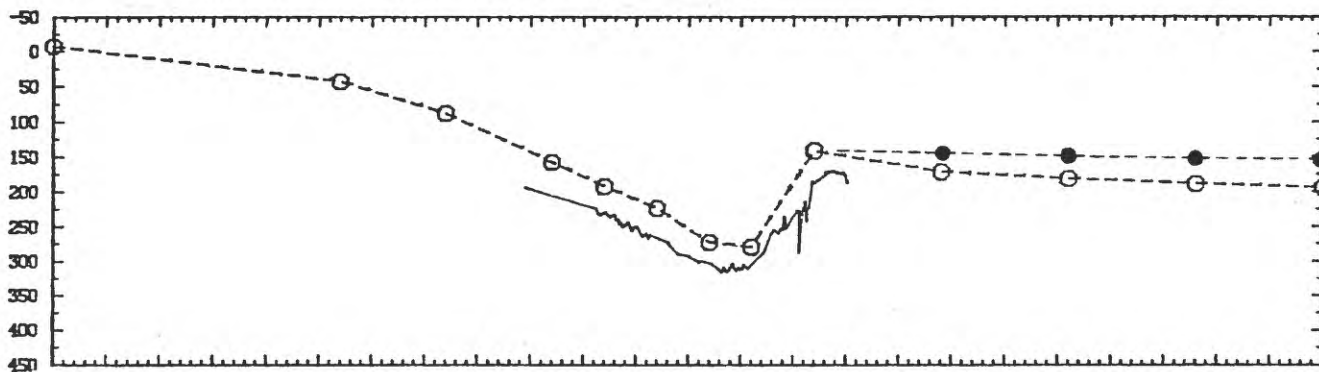


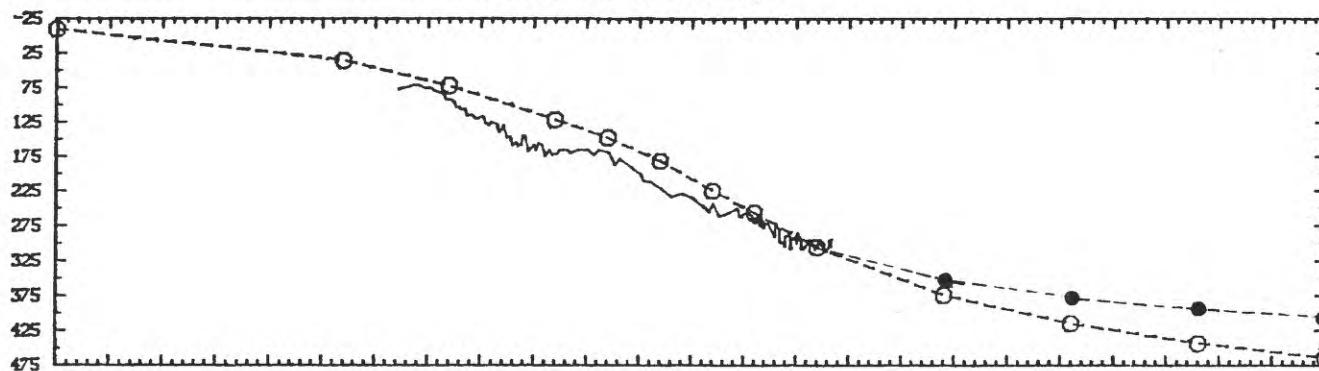
Figure 62 .--Projected fresh ground-water use for selected counties, 1985 - 2030. (Data from Texas Water Development Board.)

WATER LEVEL, IN FEET BELOW LAND SURFACE

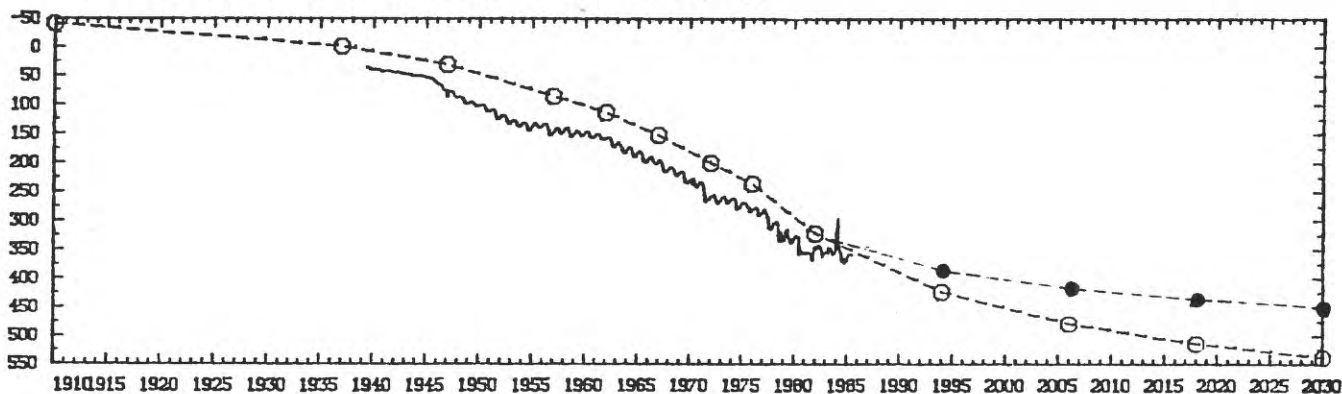
A. Permeable zone A. Well No. 9. Harris County.



B. Permeable zone B. Well No. 7. Harris County.



C. Permeable zone C. Well No. 3. Harris County.



EXPLANATION

- MEASURED WATER LEVEL
- — ○ SIMULATED WATER LEVEL (WITH INCREASED PUMPAGE FOR 1983-2030)
- — ● SIMULATED WATER LEVEL (WITH 1980 PUMPAGE FOR 1983-2030)

Figure 63. --Measured and simulated water levels in the Houston-Galveston area, projected to year 2030. (See fig. 41 for locations.)

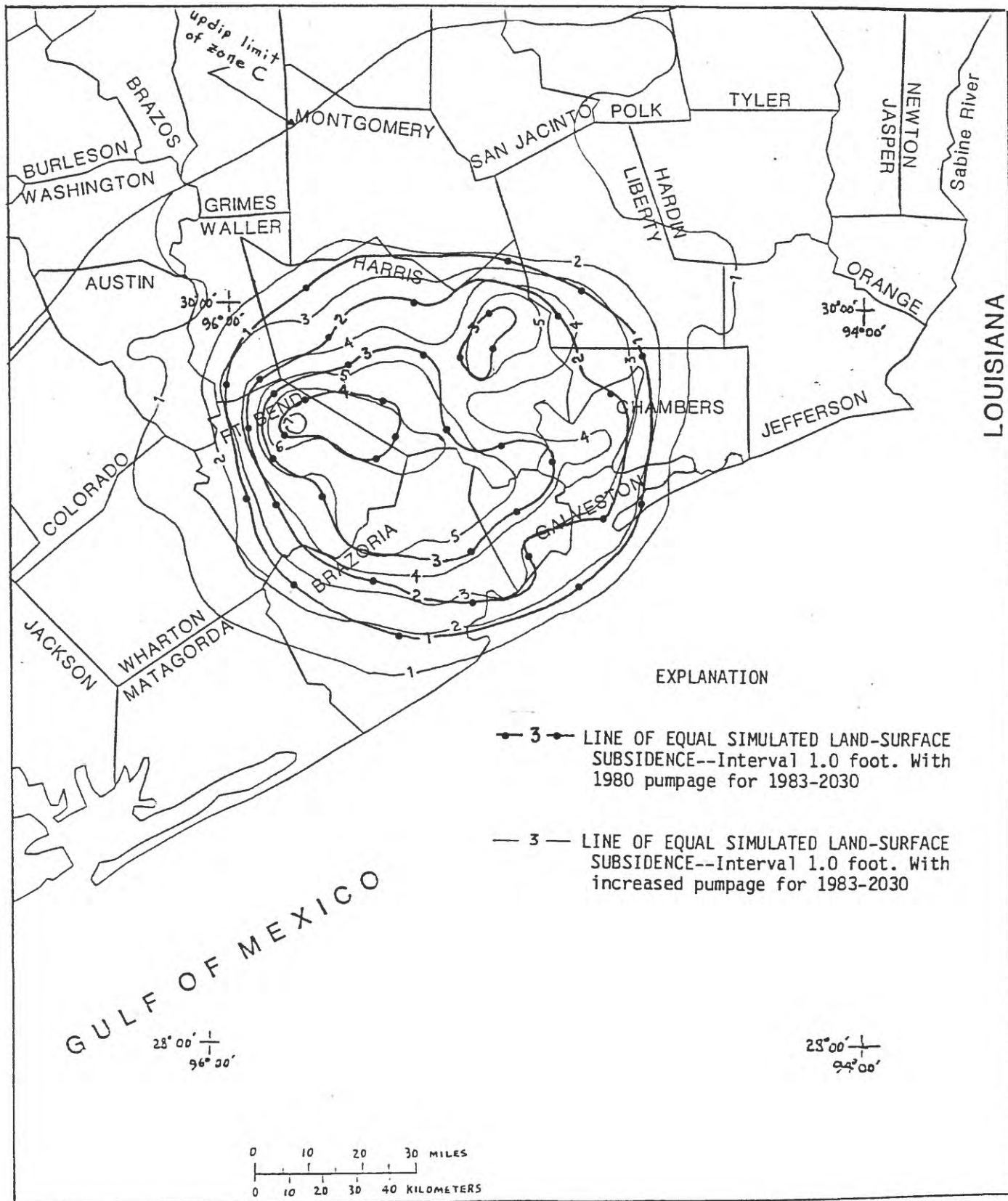
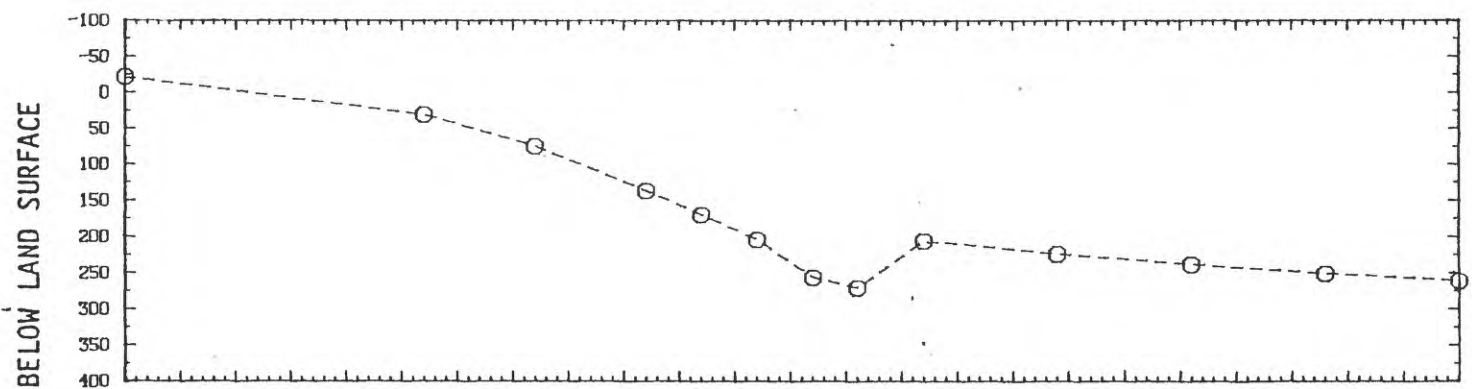


Figure 64.--Projected land-surface subsidence in the Houston-Galveston area, 1973 to 2030.

A. Permeable zone B. In vicinity of well no. 9, Harris County



B. Permeable zone C. In vicinity of well no. 9, Harris County

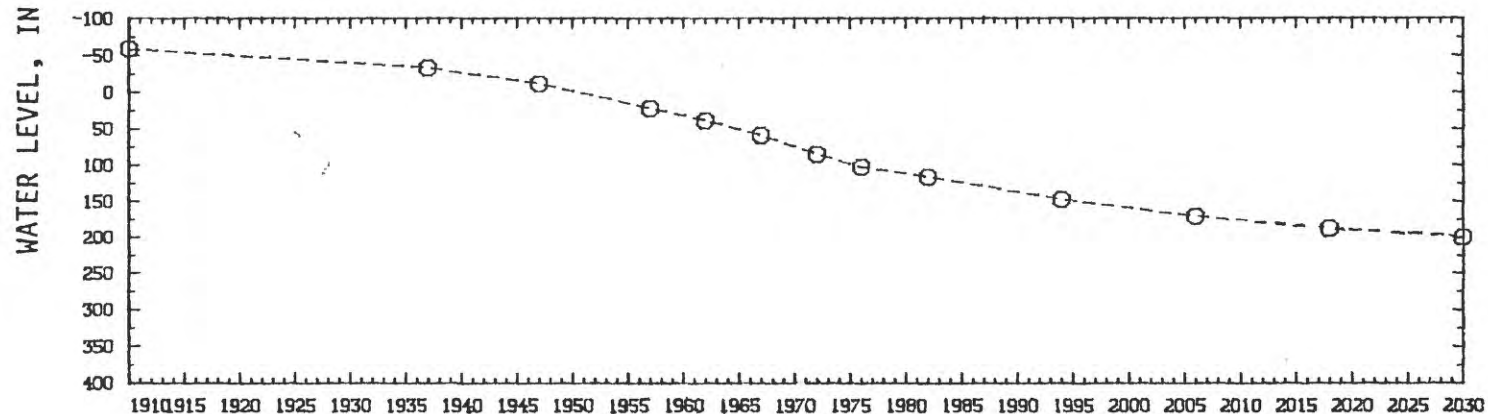


Figure 65.--Simulated water levels in southeastern Harris County, projected to 2030 with 1980 pumpage.

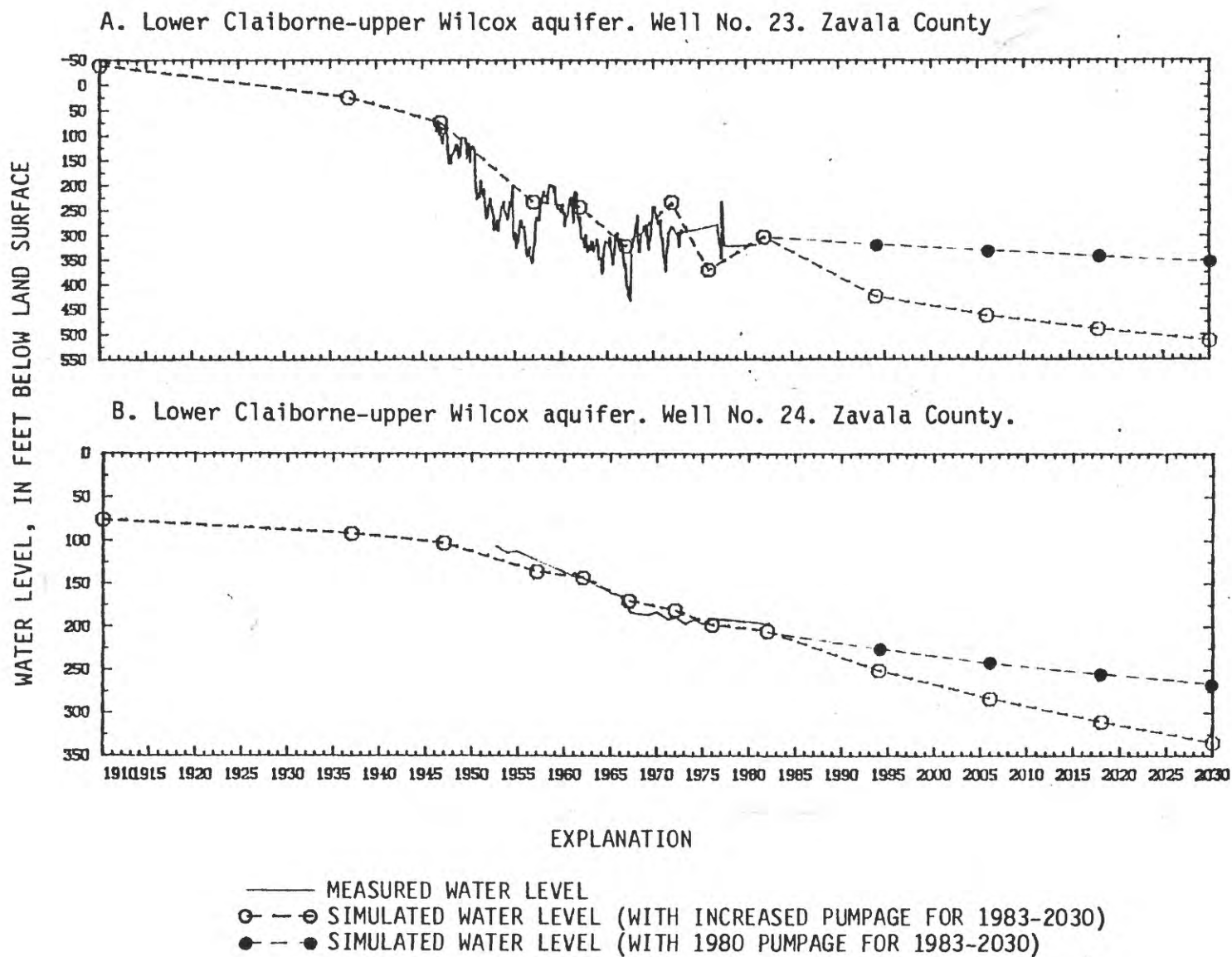


Figure 66.--Measured and simulated water levels in the Winter Garden area, projected to 2030. (See fig. 41 for locations.)

EXPLANATION

AQUIFER OR PERMEABLE ZONE AND IDENTIFIER

- ① Permeable zone A
- ② Permeable zone B
- ③ Permeable zone C
- ⑤ Permeable zone D
- ⑦ Permeable zone E
- ⑨ Upper Claiborne aquifer
- ⑪ Middle Claiborne aquifer
- ⑬ Lower Claiborne-upper Wilcox aquifer
- ⑭ Middle Wilcox aquifer

CONTAINING UNIT

TOTAL RECHARGE OR DISCHARGE IN OUTCROP AREA--Includes flow through superjacent confining unit where the confining unit is exposed at the surface. Number is flow rate, in million cubic feet per day

- Recharge
- Discharge

NET RECHARGE OR DISCHARGE IN OUTCROP AREA--

Includes flow through superjacent confining unit where the confining unit is exposed at the surface. Number is flow rate, in million cubic feet per day

- Recharge
- Discharge

TOTAL LEAKAGE THROUGH BOTTOM OF AQUIFER--

Number is flow rate, in million cubic feet per day

- Upward
- Downward

NET LEAKAGE THROUGH BOTTOM OF AQUIFER--

Number is flow rate, in million cubic feet per day

- Upward
- Downward

NET LATERAL FLOW IN (+) OR OUT (-) OF STUDY AREA

TOTAL WATER BALANCE--Numbers are million cubic feet per day. Million gallons per day in parenthesis

Total pumpage (P) = -548 (4,099)
 Net lateral flow (L) = 13 (97)
 Total release of water from storage (S) = 86 (643)
 Net recharge from constant heads = 449 (3,359)

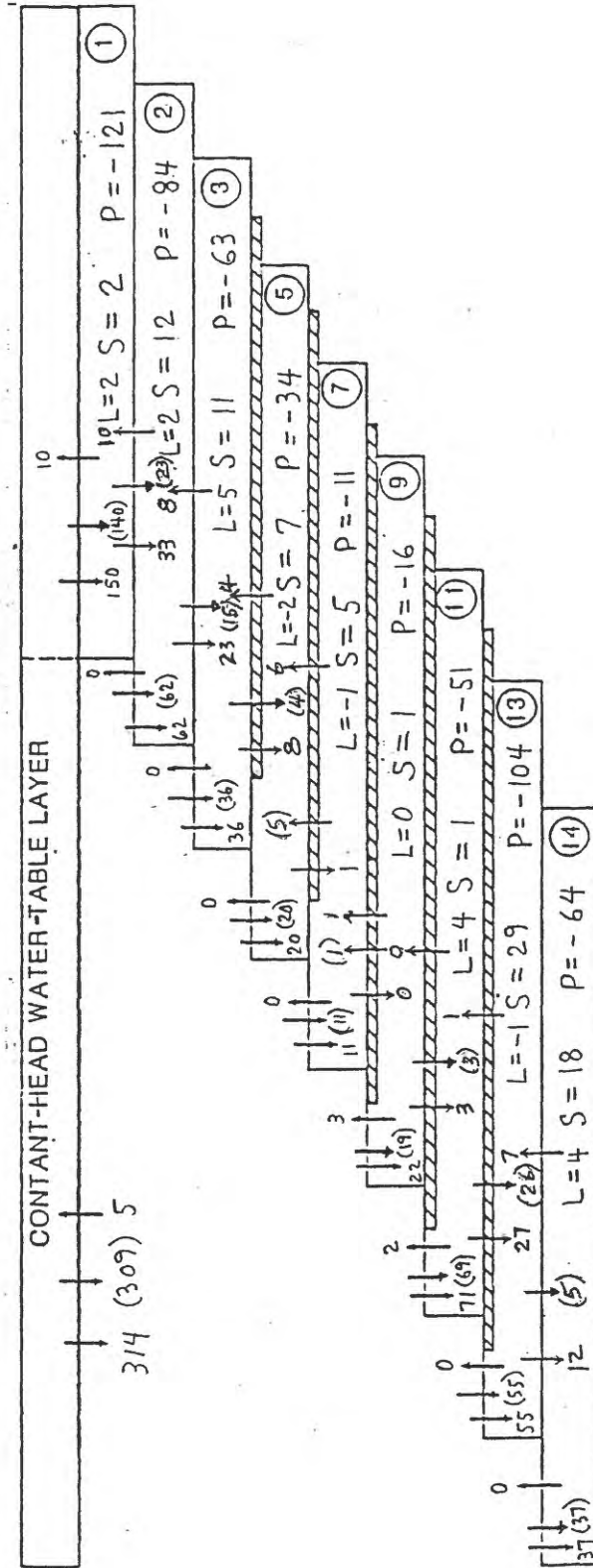


Figure 67.--Simulated 2030 vertical flow rates across hydrogeologic units in study area.

[Sum of flow rates may not exactly balance due to independent rounding.]

EXPLANATION

POTENTIAL FOR ADDITIONAL GROUND-WATER DEVELOPMENT

- 0** Additional development possible
- 1** Some additional development possible. Development may be limited by water-level declines, aquifer thickness, or lack of potential recharge
- 2** Limited potential for development because dissolved-solids concentration in water is greater than 2,000 milligrams per liter

— 50 — LINE OF EQUAL DIFFERENCE IN 2030 POTENTIOMETRIC SURFACE—
Shows amount of difference between simulations with 1980 withdrawals and with 1980 plus additional withdrawals.
Interval 25 feet

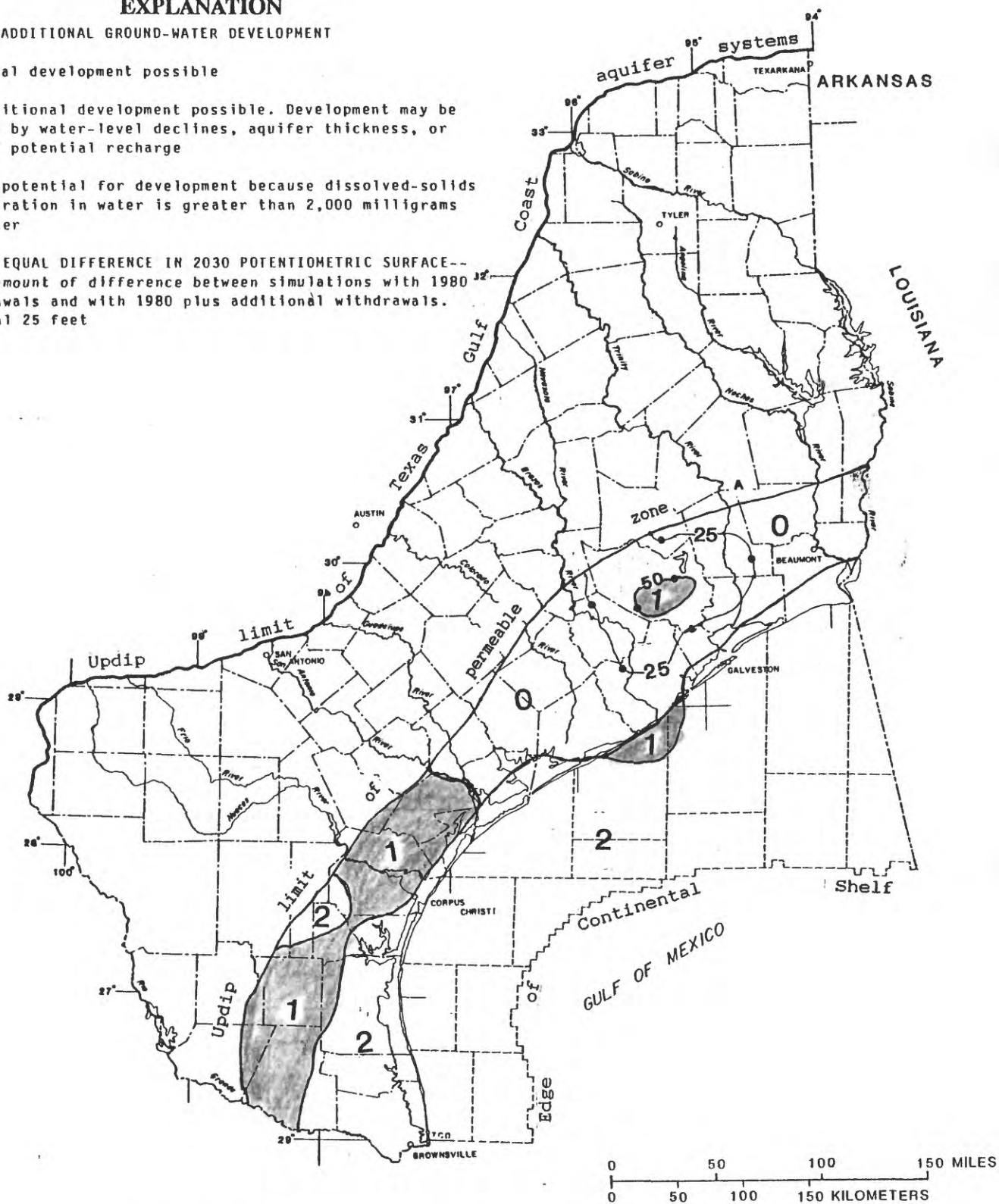


Figure 68.--Potential areas for development of large ground-water supplies from permeable zone A.

EXPLANATION

POTENTIAL FOR ADDITIONAL GROUND-WATER DEVELOPMENT

- 0** Additional development possible
- 1** Some additional development possible. Development may be limited by water-level declines, aquifer thickness, or lack of potential recharge
- 2** Limited potential for development because dissolved-solids concentration in water is greater than 2,000 milligrams per liter
- 3** Limited potential for development because of water-level declines, saturated thickness of aquifer less than 25 feet, or lack of potential recharge

—●— 50 — LINE OF EQUAL DIFFERENCE IN 2030 POTENTIOMETRIC SURFACE-- Shows amount of difference between simulations with 1980 withdrawals and with 1980 plus additional withdrawals. Interval 50 and 100 feet

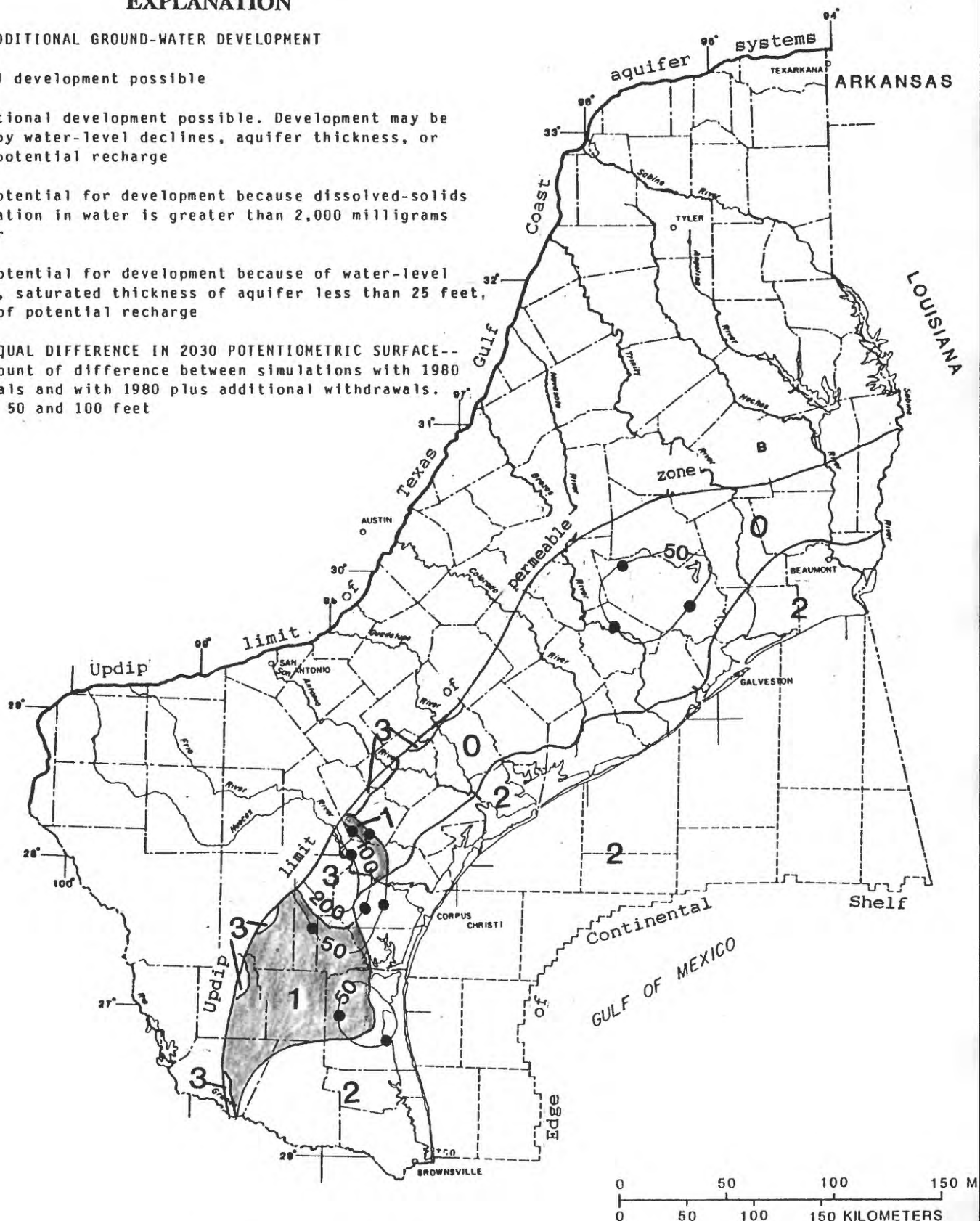


Figure 69.---Potential areas for development of large ground-water supplies from permeable zone B.

EXPLANATION

POTENTIAL FOR ADDITIONAL GROUND-WATER DEVELOPMENT

- 0** Additional development possible
- 1** Some additional development possible. Development may be limited by water-level declines, aquifer thickness, or lack of potential recharge
- 2** Limited potential for development because dissolved-solids concentration in water is greater than 2,000 milligrams per liter
- 3** Limited potential for development because of water-level declines, saturated thickness of aquifer less than 25 feet, or lack of potential recharge

— 50 — LINE OF EQUAL DIFFERENCE IN 2030 POTENTIOMETRIC SURFACE —
Shows amount of difference between simulations with 1980 withdrawals and with 1980 plus additional withdrawals.
Interval 50 and 100 feet

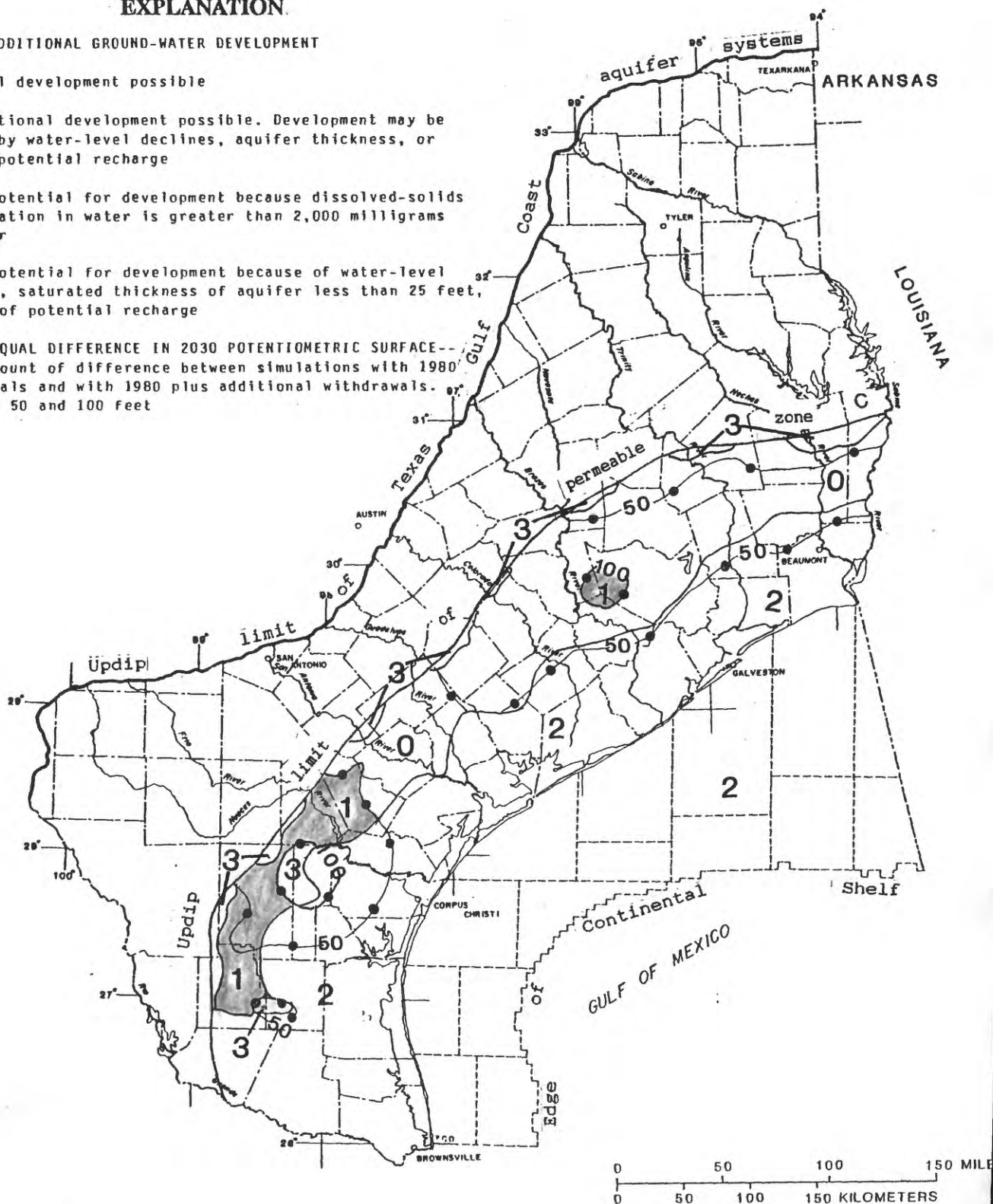


Figure 70. ---Potential areas for development of large ground-water supplies from permeable zone C.

EXPLANATION

POTENTIAL FOR ADDITIONAL GROUND-WATER DEVELOPMENT

- 0** Additional development possible
- 1** Some additional development possible. Development may be limited by water-level declines, aquifer thickness, or lack of potential recharge
- 2** Limited potential for development because dissolved-solids concentration in water is greater than 2,000 milligrams per liter
- 3** Limited potential for development because of water-level declines, saturated thickness of aquifer less than 25 feet, or lack of potential recharge

100—LINE OF EQUAL DIFFERENCE IN 2030 POTENTIOMETRIC SURFACE—
Shows amount of difference between simulations with 1980 withdrawals and with 1980 plus additional withdrawals
Interval 50 feet

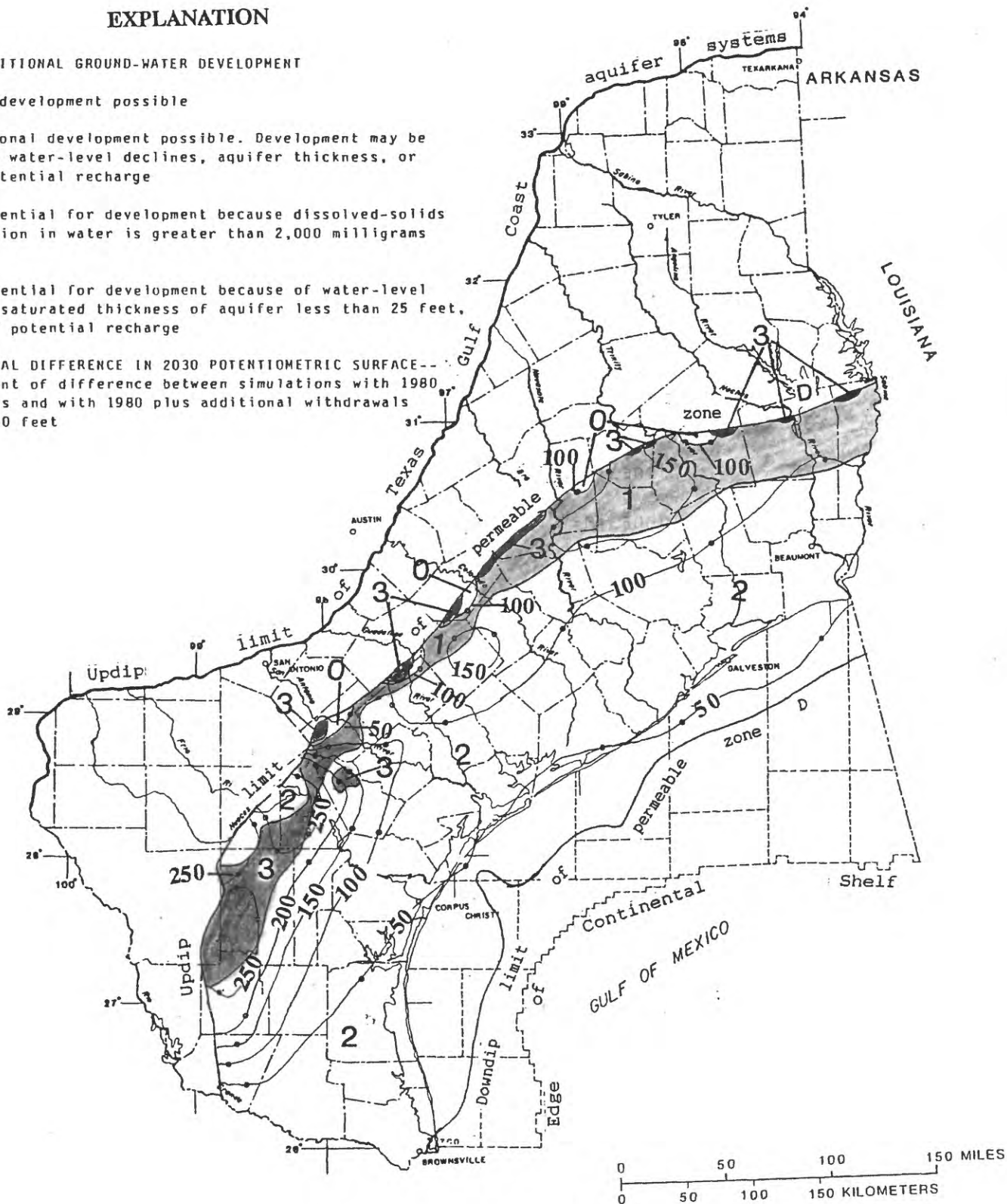


Figure 71.--Potential areas for development of large ground-water supplies from permeable zone D.

EXPLANATION

POTENTIAL FOR ADDITIONAL GROUND-WATER DEVELOPMENT

- 0** Additional development possible
- 1** Some additional development possible. Development may be limited by water-level declines, aquifer thickness, or lack of potential recharge
- 2** Limited potential for development because dissolved-solids concentration in water is greater than 2,000 milligrams per liter
- 3** Limited potential for development because of water-level declines, saturated thickness of aquifer less than 25 feet, or lack of potential recharge

—100— LINE OF EQUAL DIFFERENCE IN 2030 POTENTIOMETRIC SURFACE--
Shows amount of difference between simulations with 1980 withdrawals and with 1980 plus additional withdrawals
Interval 50 feet

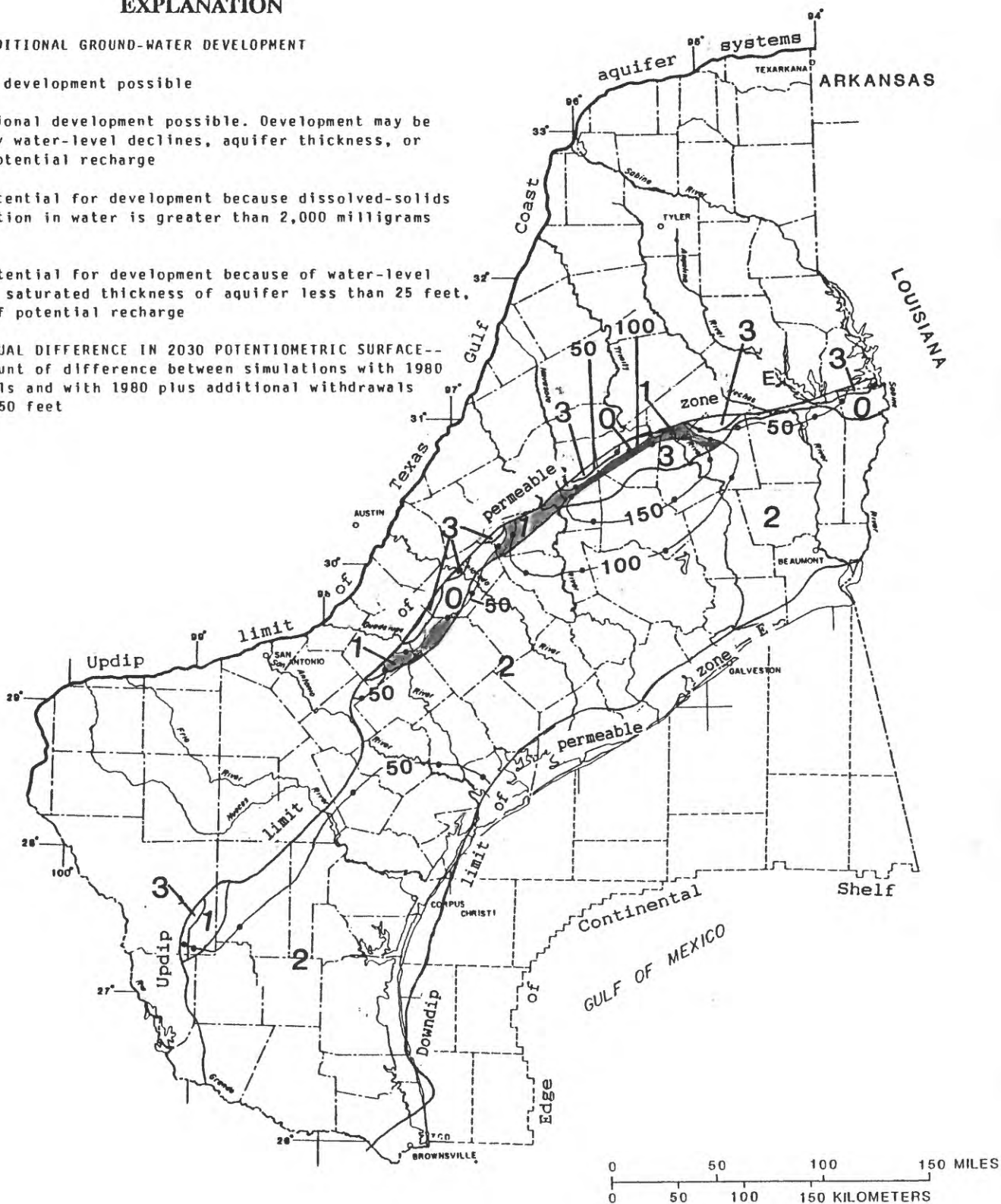


Figure 72.--Potential areas for development of large ground-water supplies from permeable zone E.

EXPLANATION

POTENTIAL FOR ADDITIONAL GROUND-WATER DEVELOPMENT

- 0** Additional development possible
- 1** Some additional development possible. Development may be limited by water-level declines, aquifer thickness, or lack of potential recharge
- 2** Limited potential for development because dissolved-solids concentration in water is greater than 2,000 milligrams per liter
- 3** Limited potential for development because of water-level declines, saturated thickness of aquifer less than 25 feet, or lack of potential recharge

— 50 — LINE OF EQUAL DIFFERENCE IN 2030 POTENTIOMETRIC SURFACE--
Shows amount of difference between simulations with 1980 withdrawals and with 1980 plus additional withdrawals. Interval 50 and 100 feet

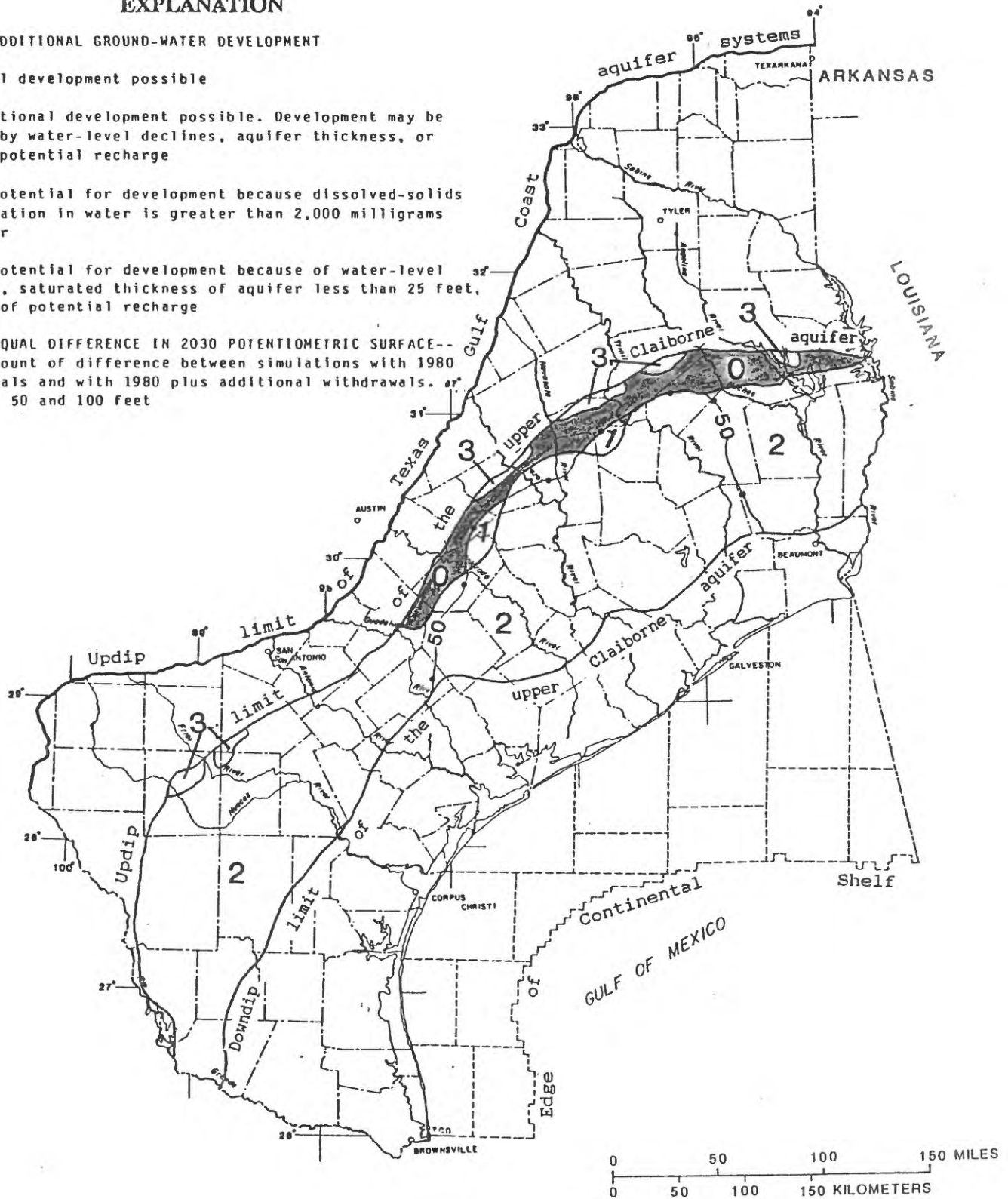


Figure 73.--Potential areas for development of large ground-water supplies from the upper Claiborne aquifer.

EXPLANATION

POTENTIAL FOR ADDITIONAL GROUND-WATER DEVELOPMENT

- 0** Additional development possible
- 1** Some additional development possible. Development may be limited by water-level declines, aquifer thickness, or lack of potential recharge
- 2** Limited potential for development because dissolved-solids concentration in water is greater than 2,000 milligrams per liter
- 3** Limited potential for development because of water-level declines, saturated thickness of aquifer less than 25 feet, or lack of potential recharge

100—LINE OF EQUAL DIFFERENCE IN 2030 POTENTIOMETRIC SURFACE-- Shows amount of difference between simulations with 1980 withdrawals and with 1980 plus additional withdrawals
Interval 50 feet

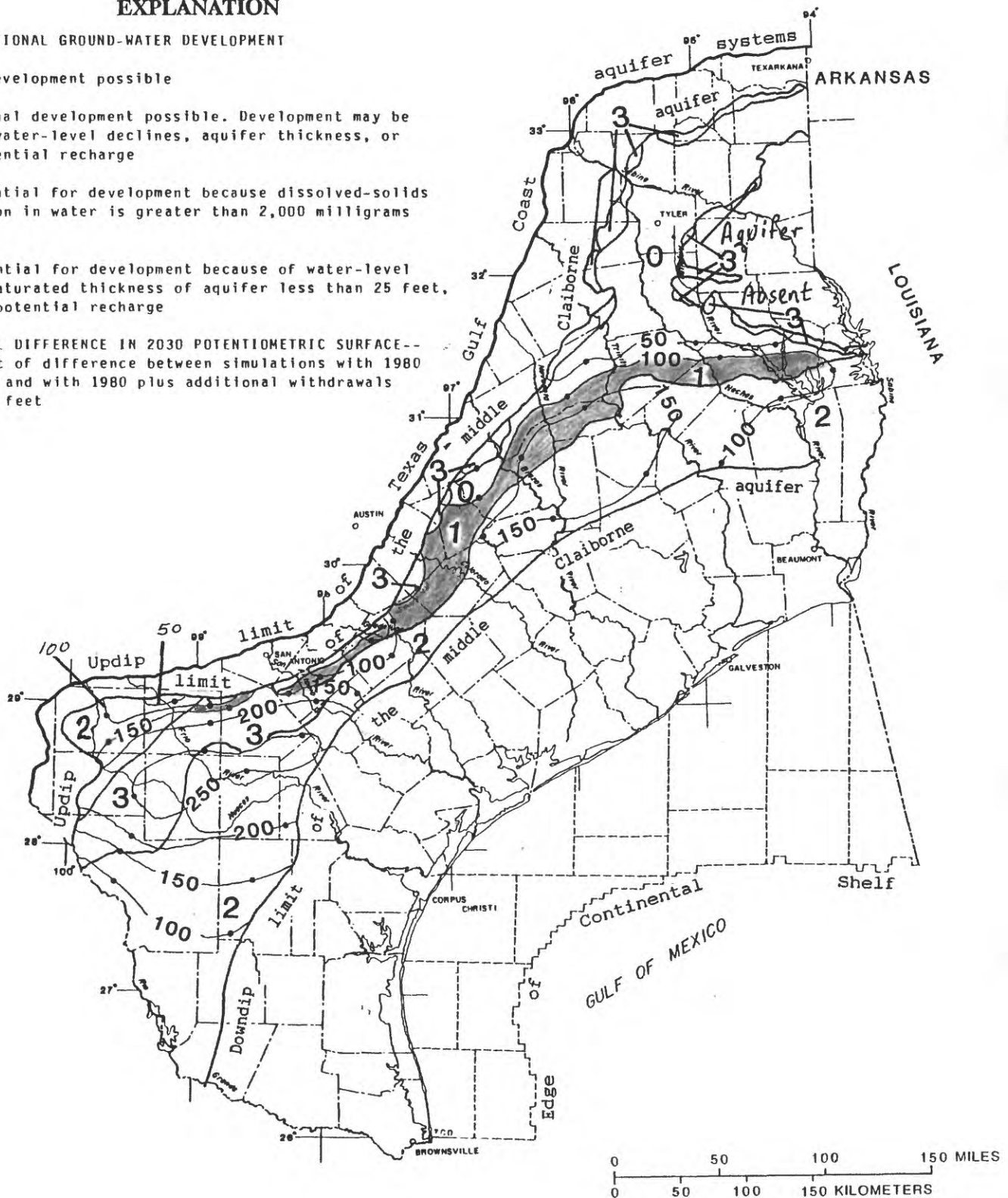


Figure 74.--Potential areas for development of large ground-water supplies from the middle Claiborne aquifer.

EXPLANATION

POTENTIAL FOR ADDITIONAL GROUND-WATER DEVELOPMENT

- 0** Additional development possible
- 1** Some additional development possible. Development may be limited by water-level declines, aquifer thickness, or lack of potential recharge
- 2** Limited potential for development because dissolved-solids concentration in water is greater than 2,000 milligrams per liter
- 3** Limited potential for development because of water-level declines, saturated thickness of aquifer less than 25 feet, or lack of potential recharge

—200— LINE OF EQUAL DIFFERENCE IN 2030 POTENTIOMETRIC SURFACE--
Shows amount of difference between simulations with 1980 withdrawals and with 1980 plus additional withdrawals. Interval, in feet, is variable

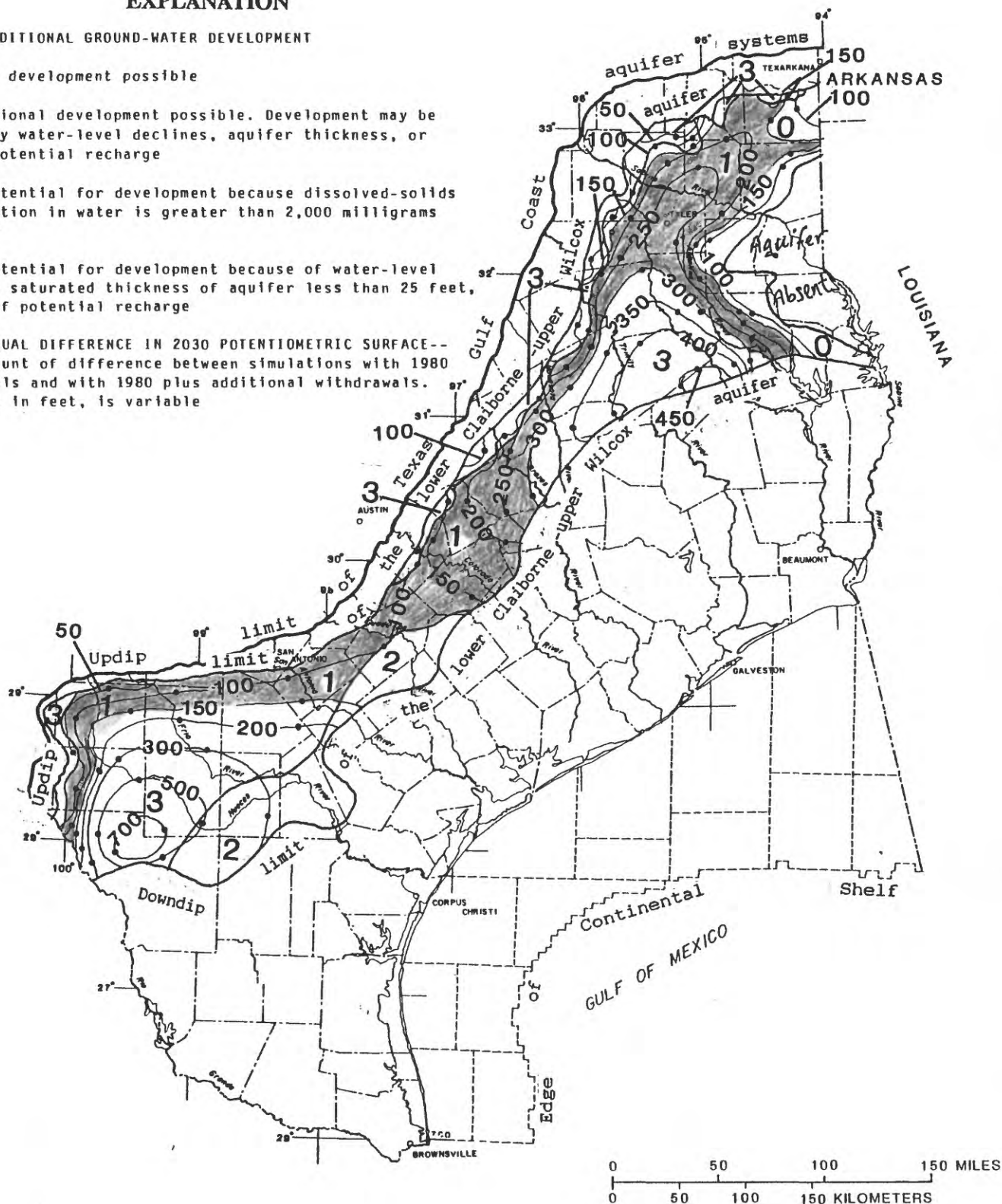


Figure 75.--Potential areas for development of large ground-water supplies from the lower Claiborne-upper Wilcox aquifer.

EXPLANATION

POTENTIAL FOR ADDITIONAL GROUND-WATER DEVELOPMENT

- 0** Additional development possible
- 1** Some additional development possible. Development may be limited by water-level declines, aquifer thickness, or lack of potential recharge
- 2** Limited potential for development because dissolved-solids concentration in water is greater than 2,000 milligrams per liter
- 3** Limited potential for development because of water-level declines, saturated thickness of aquifer less than 25 feet or lack of potential recharge
- Results unreliable because of lateral boundary effects

200 LINE OF EQUAL DIFFERENCE IN 2030 POTENTIOMETRIC SURFACE--
Shows amount of difference between simulations with 1980 withdrawals and with 1980 plus additional withdrawals
Interval, in feet, is variable

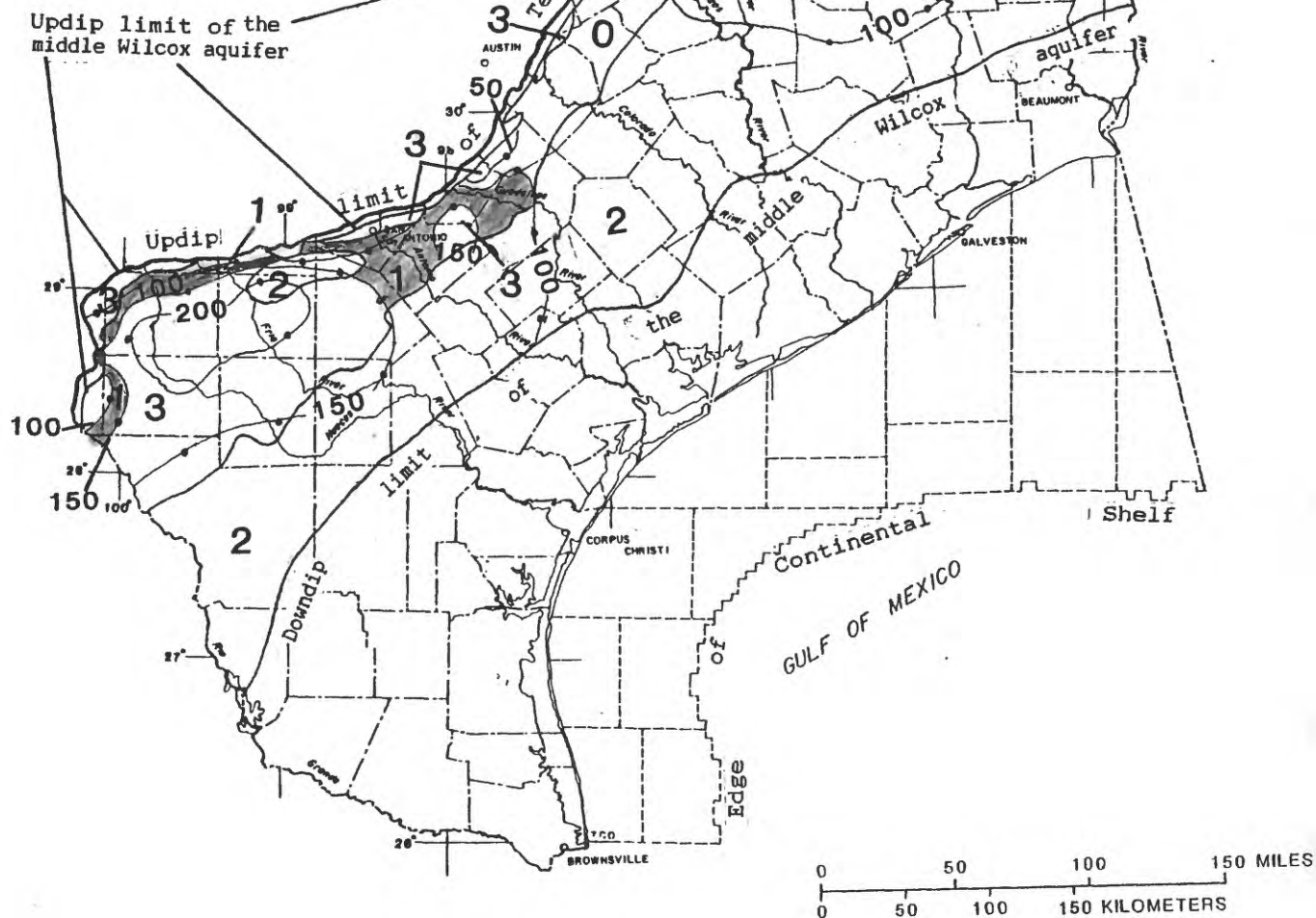


Figure 76.--Potential areas for development of large ground-water supplies from the middle Wilcox aquifer.

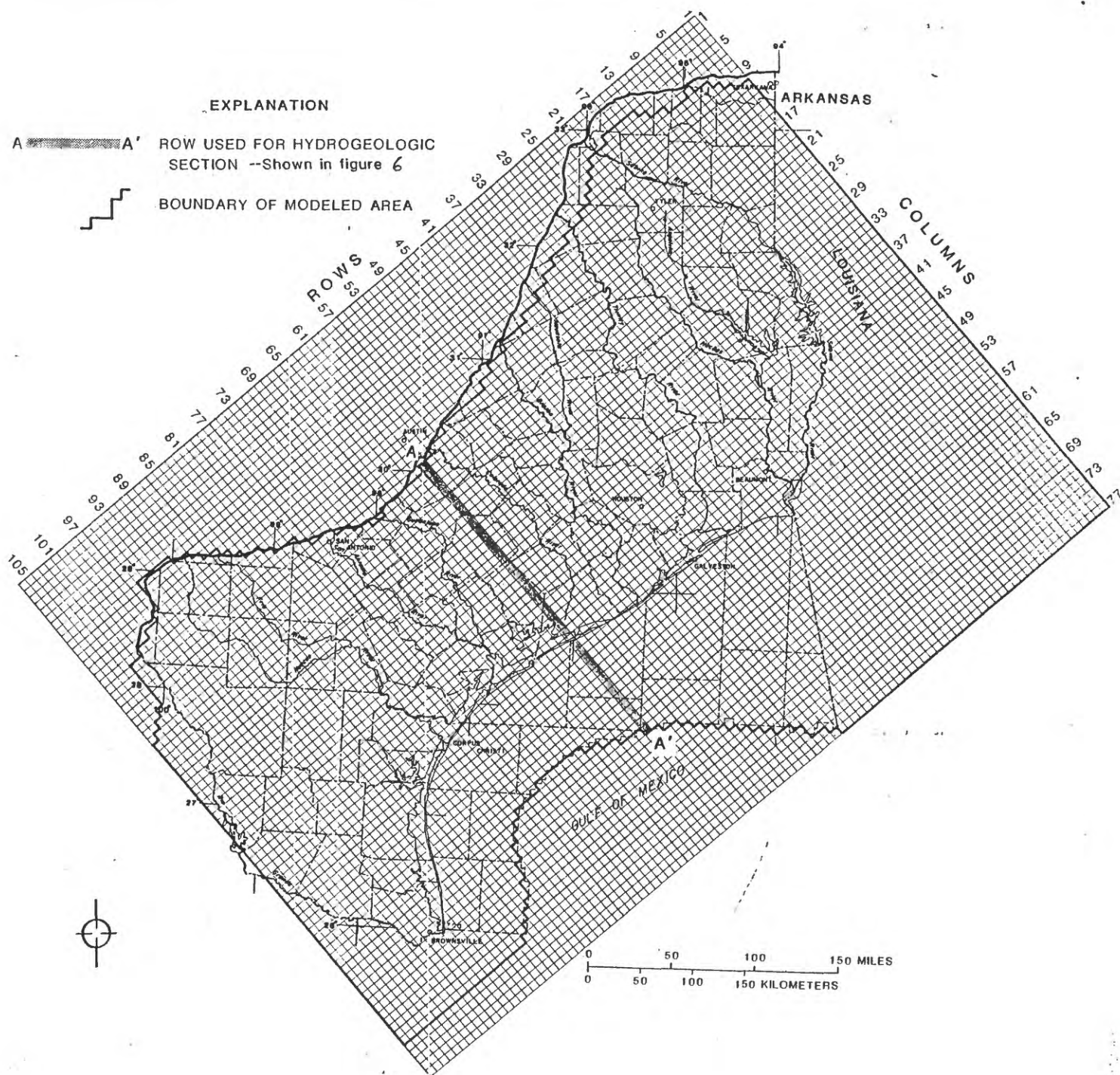


Figure 7.--Finite-difference grid superimposed on modeled area and study area.

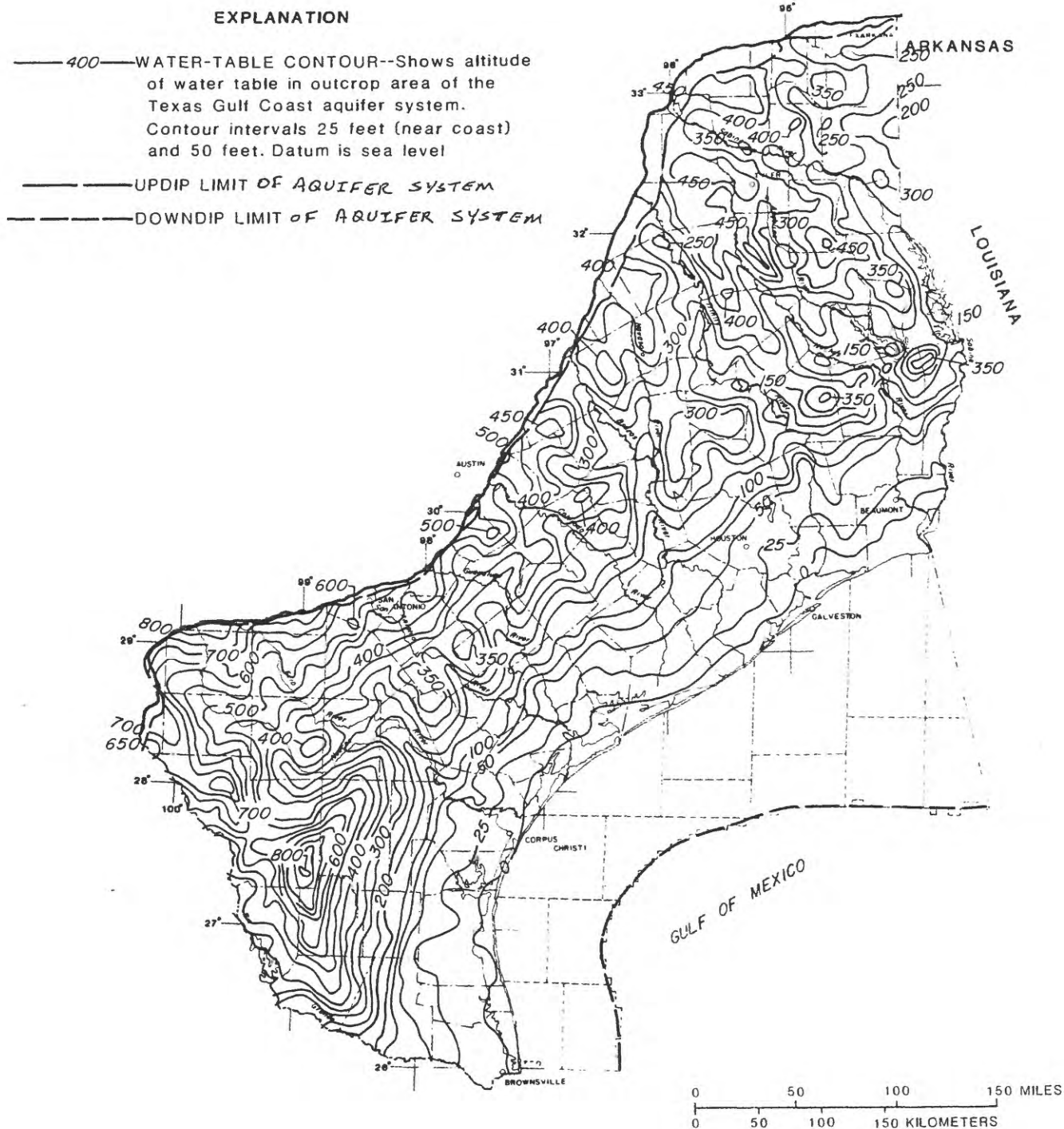


Figure 78--Estimated altitude of the water table for the model constant-head boundary.

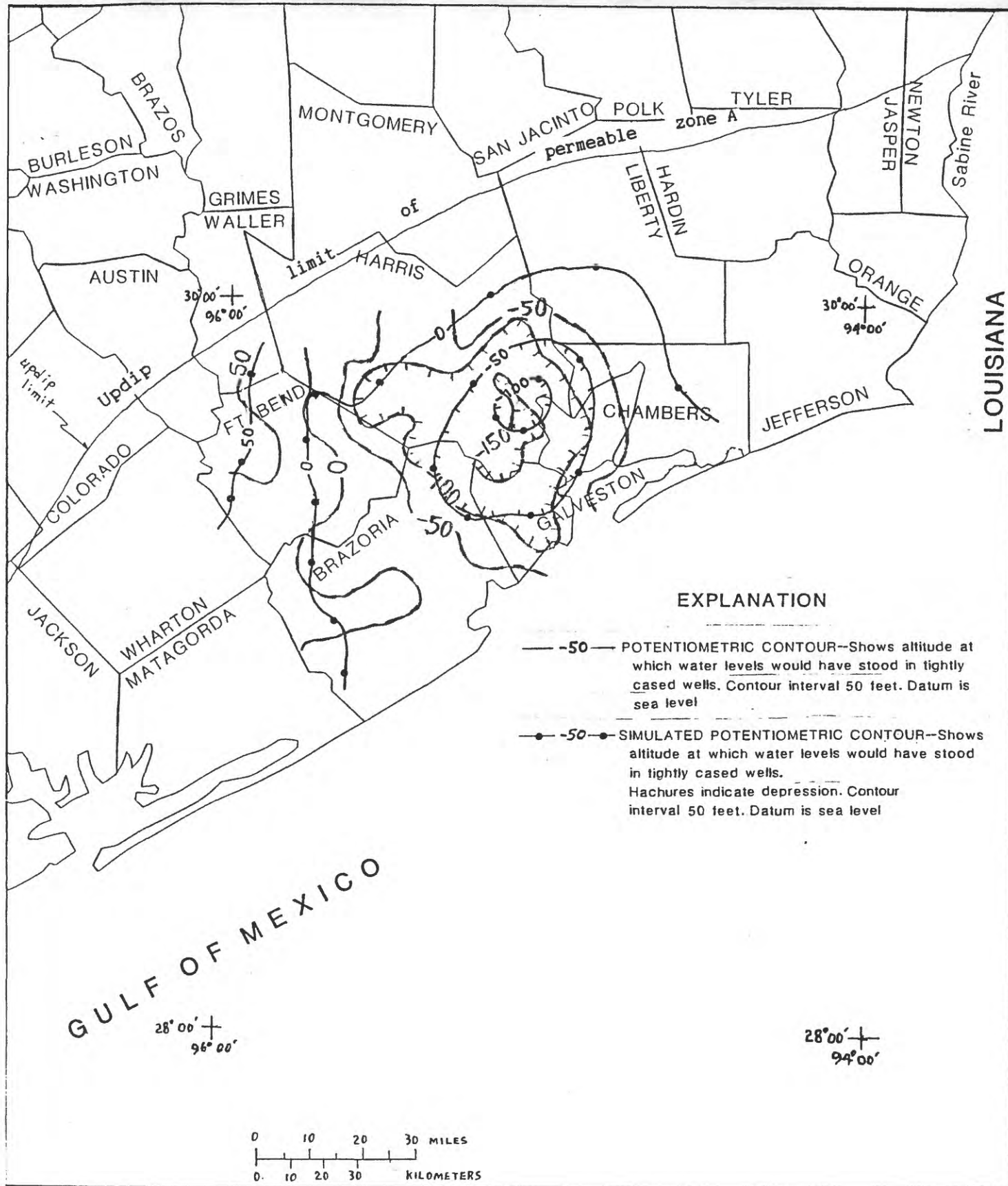


Figure 79.--Measured and simulated altitude of the potentiometric surface of permeable zone A in the Houston-Galveston area, 1982.

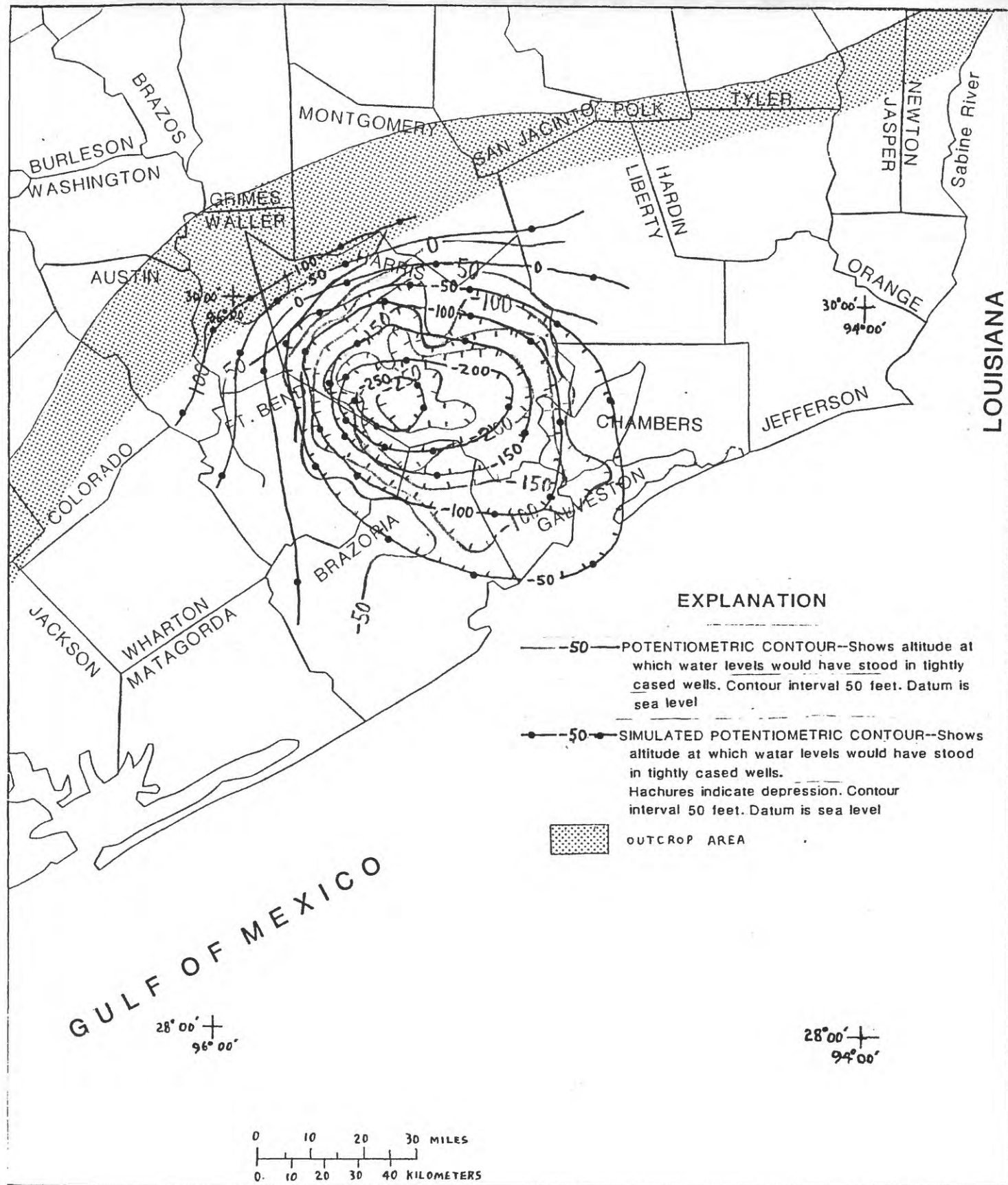


Figure 80.--Measured and simulated altitude of the potentiometric surface of permeable zone B in the Houston-Galveston area, 1982.

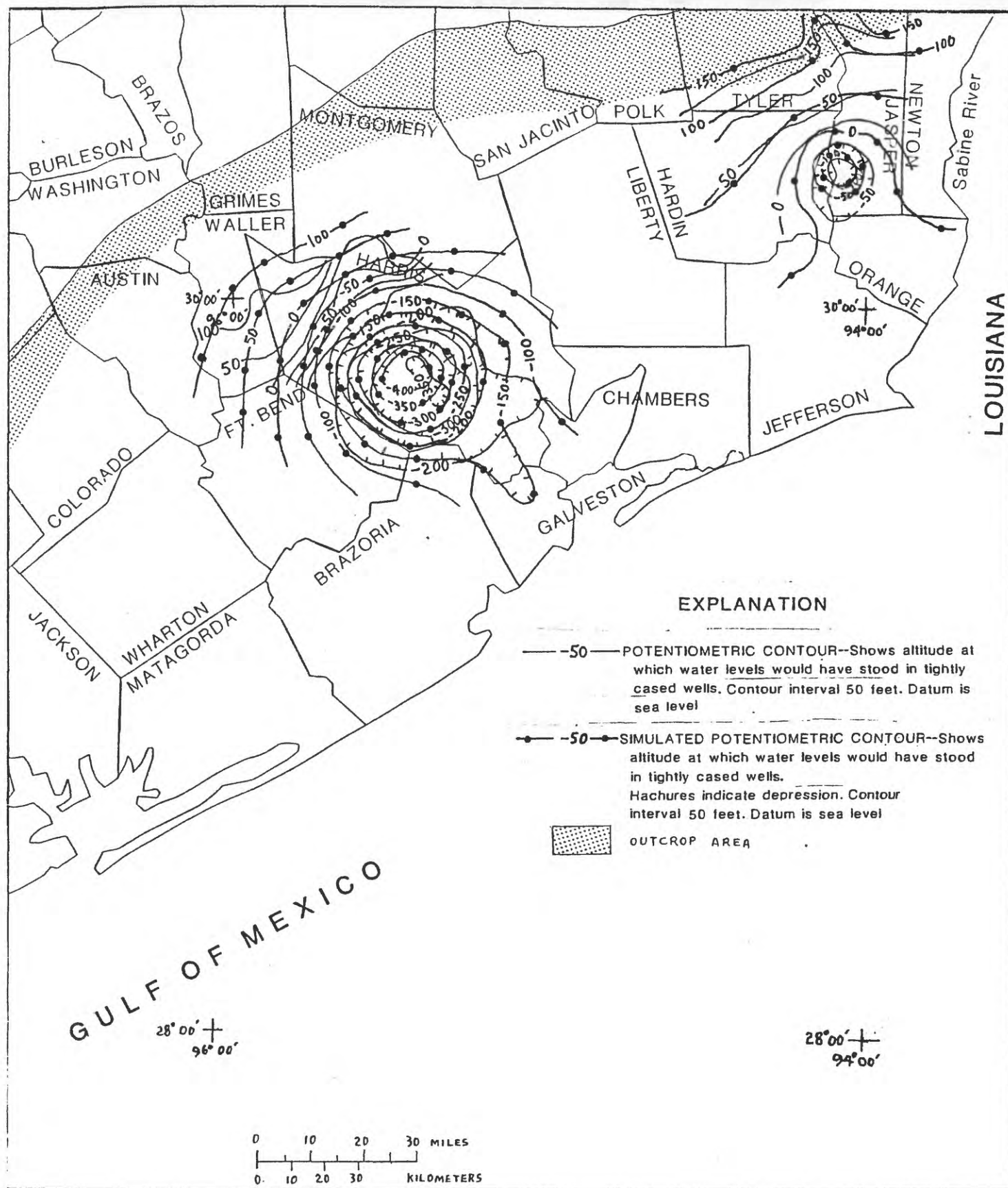


Figure 81.--Measured and simulated altitude of the potentiometric surface of permeable zone C in the Houston-Galveston and Evadale areas, 1982.

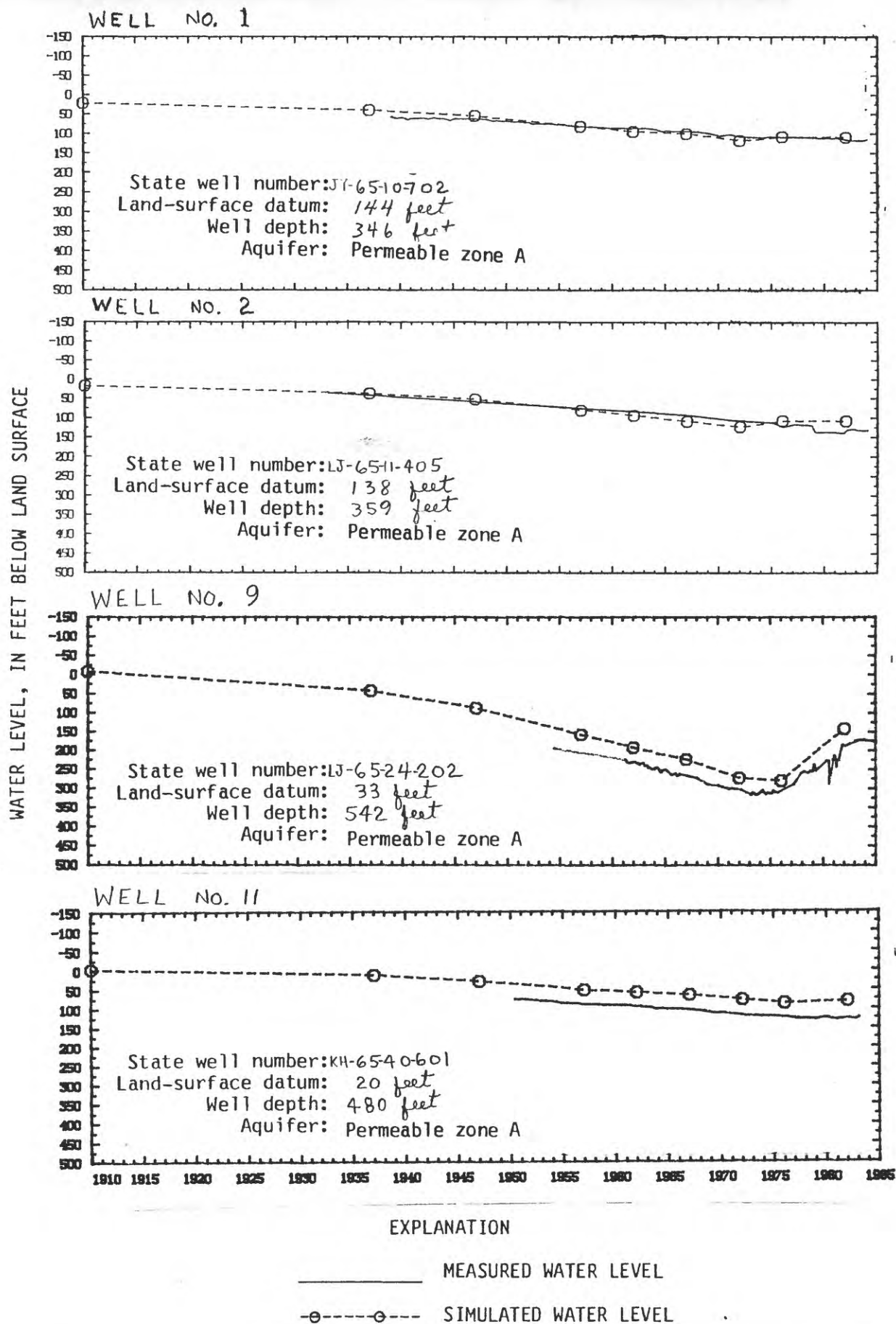


Figure 82.—Measured and simulated water levels in wells 1, 2, 9, and 11 in the Houston-Balveston area.

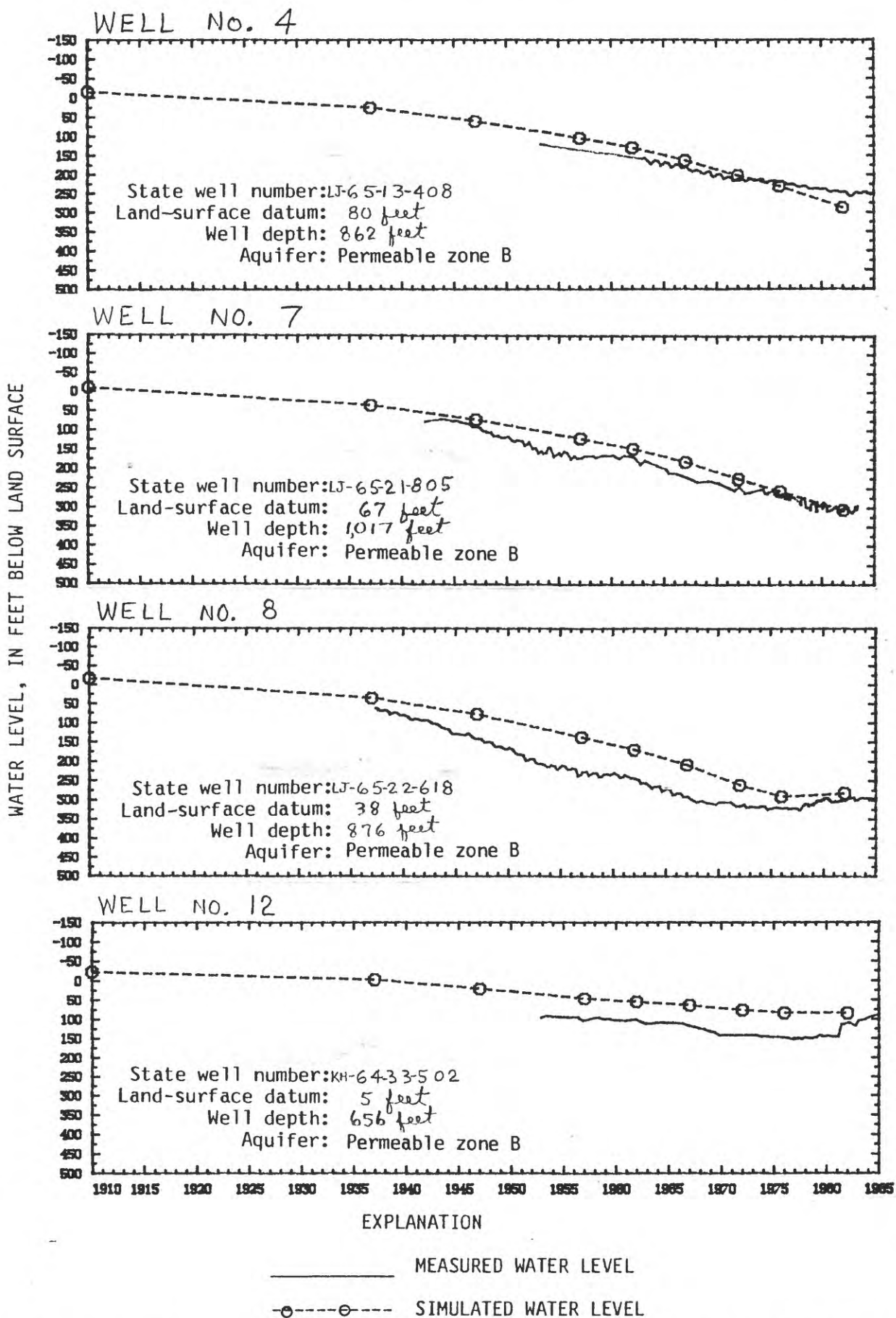


Figure 83.—Measured and simulated water levels in wells 4, 7, 8, and 12 in the Houston-Galveston area.

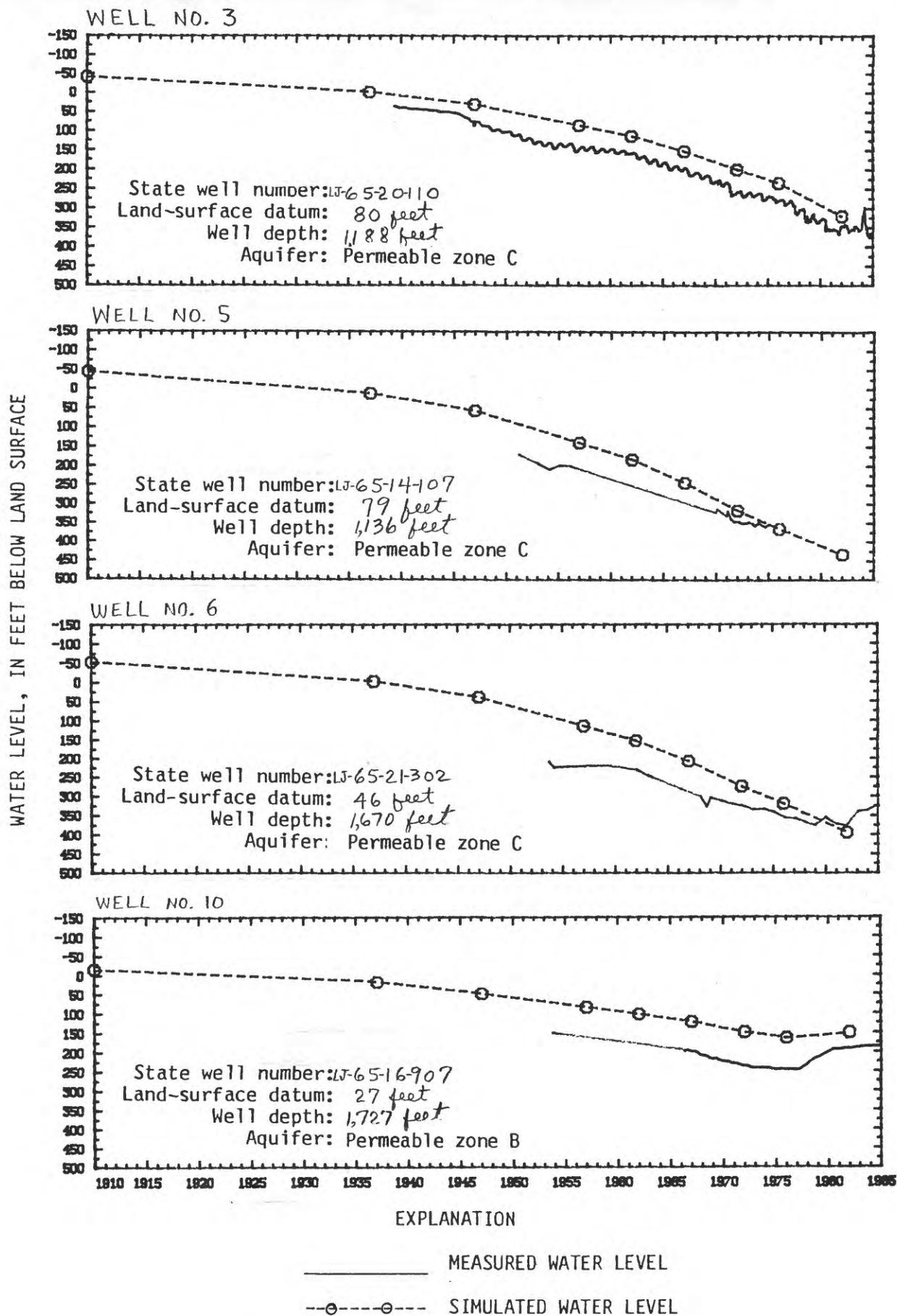


Figure 84.—Measured and simulated water levels in wells 3, 5, 6, and 10 in the Houston-Galveston area.

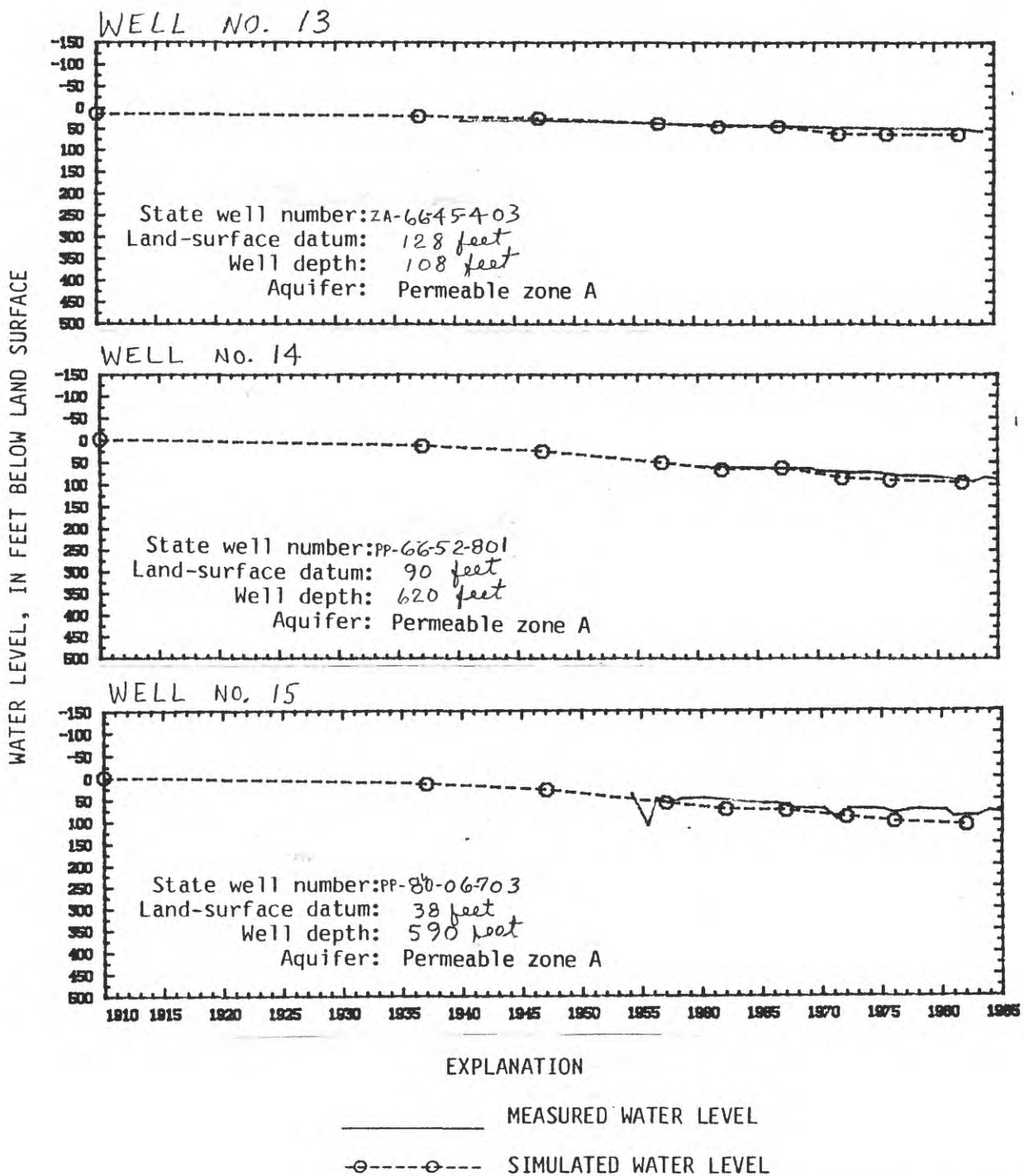


Figure 85.—Measured and simulated water levels in wells 13, 14, and 15 in Jackson and Harton Counties.

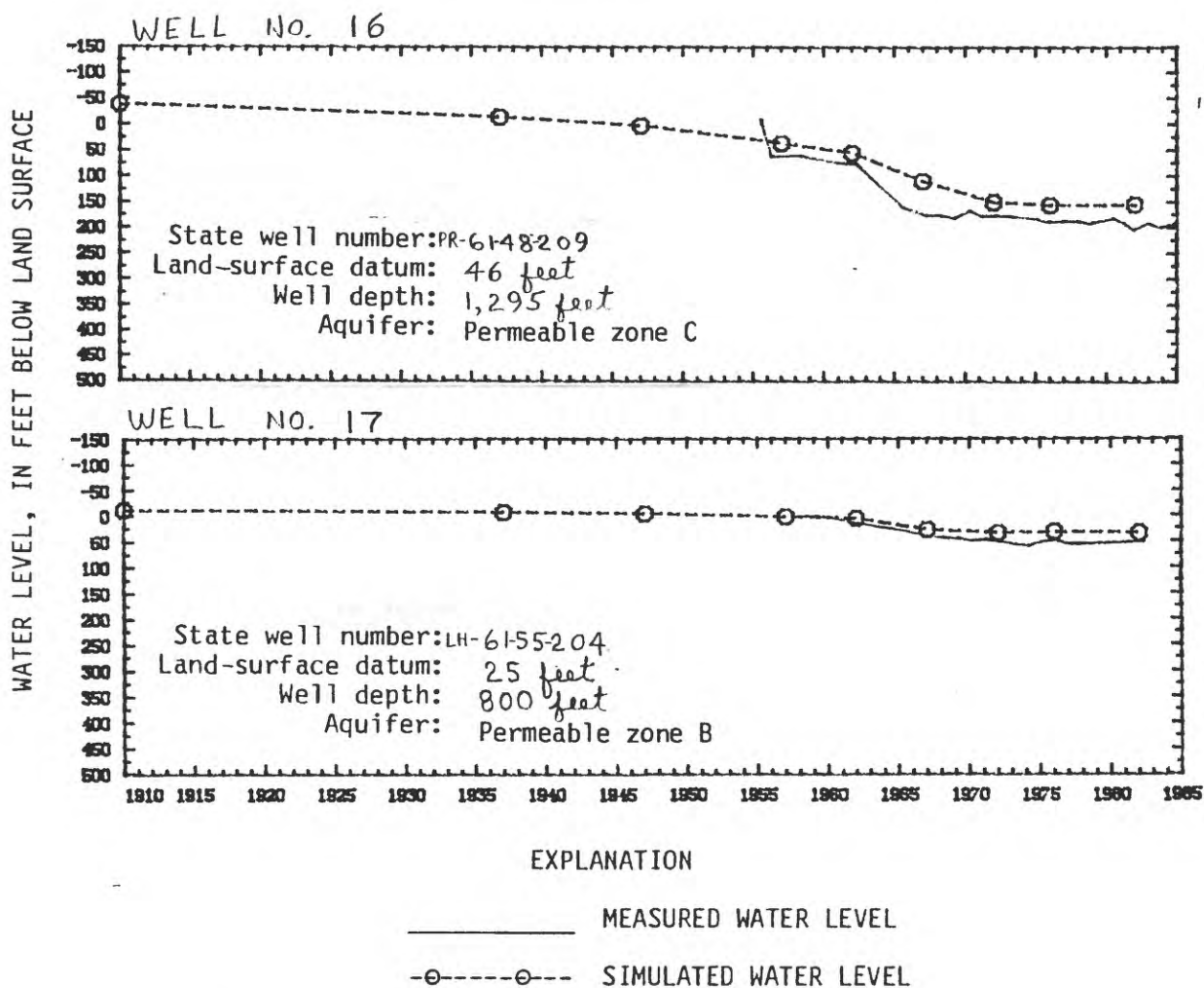


Figure 86.—Measured and simulated water levels in wells 16 and 17 in the Evadale-Beaumont area.

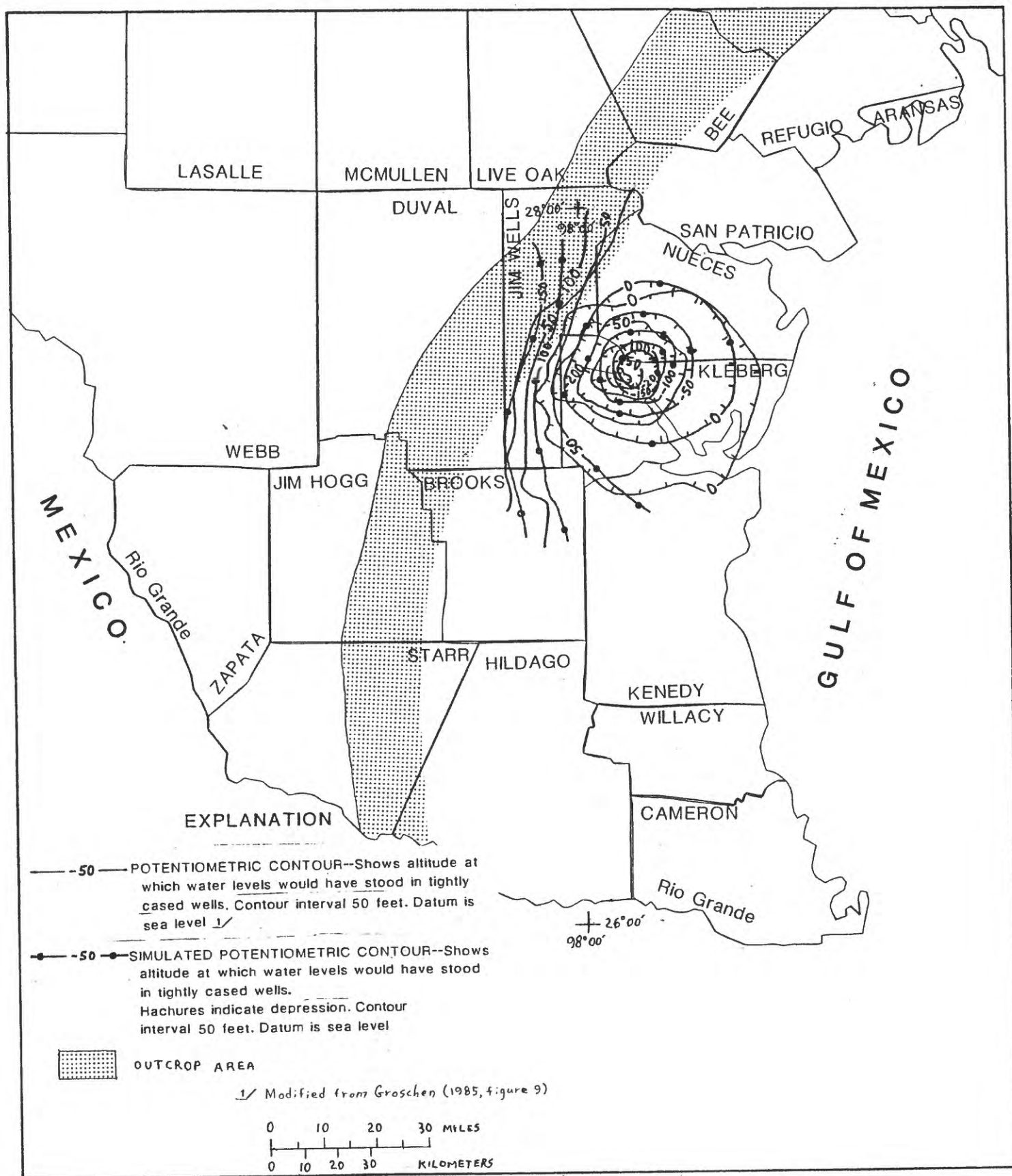
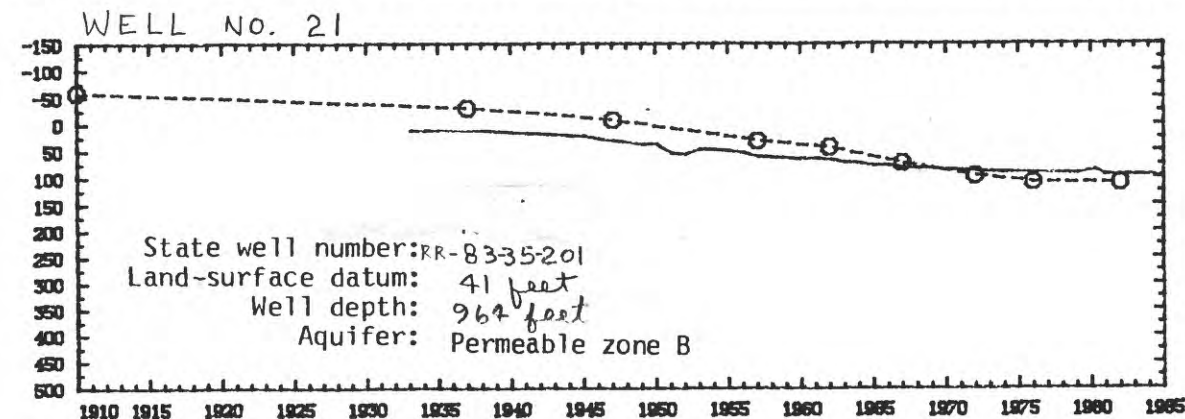
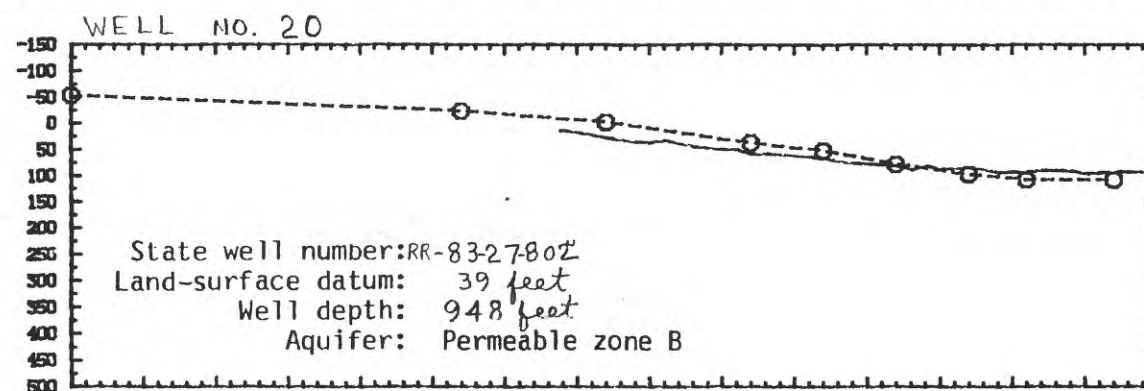
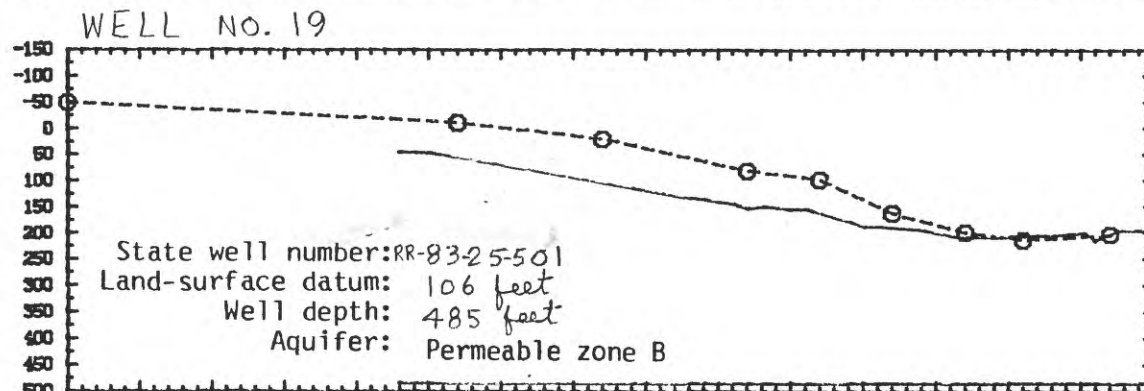
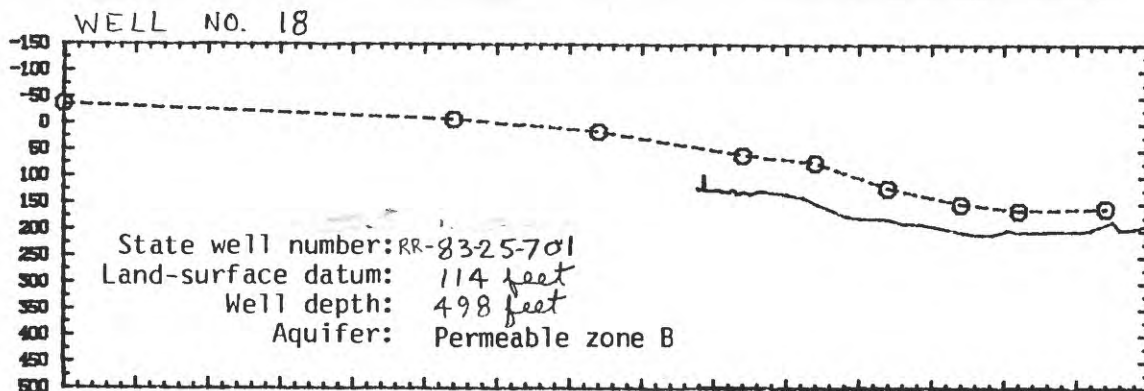


Figure 87.--Measured and simulated altitude of the potentiometric surface of permeable zone B in the Kingsville area, 1982.

WATER LEVEL, IN FEET BELOW LAND SURFACE



EXPLANATION

————— MEASURED WATER LEVEL
 -○- -○- - SIMULATED WATER LEVEL

Figure 88.—Measured and simulated water levels in wells 18, 19, 20, and 21 in the Kingsville area.

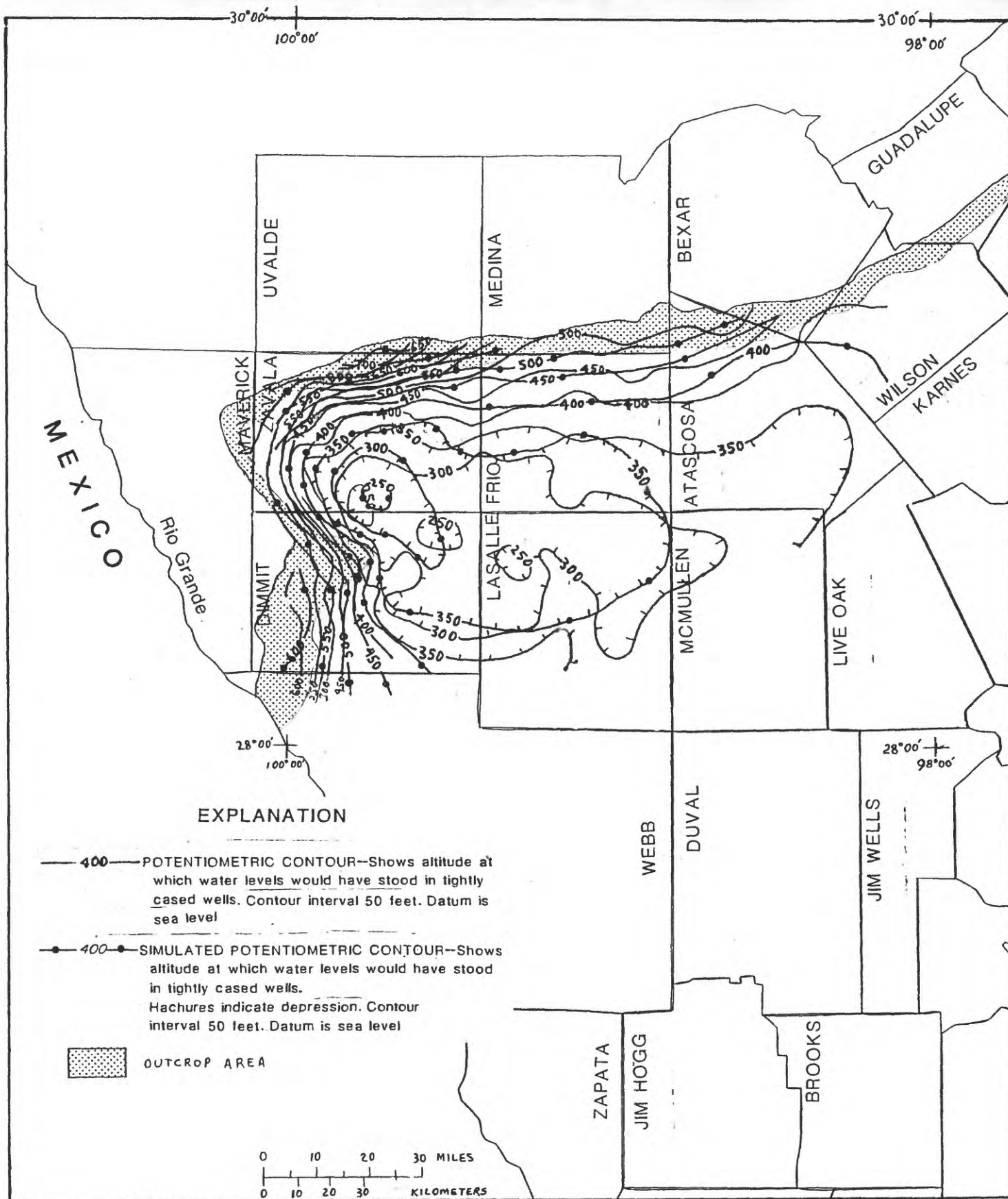


Figure 89.--Measured and simulated altitude of the potentiometric surface of the lower Claiborne-upper Wilcox aquifer in the Winter Garden area, 1982.

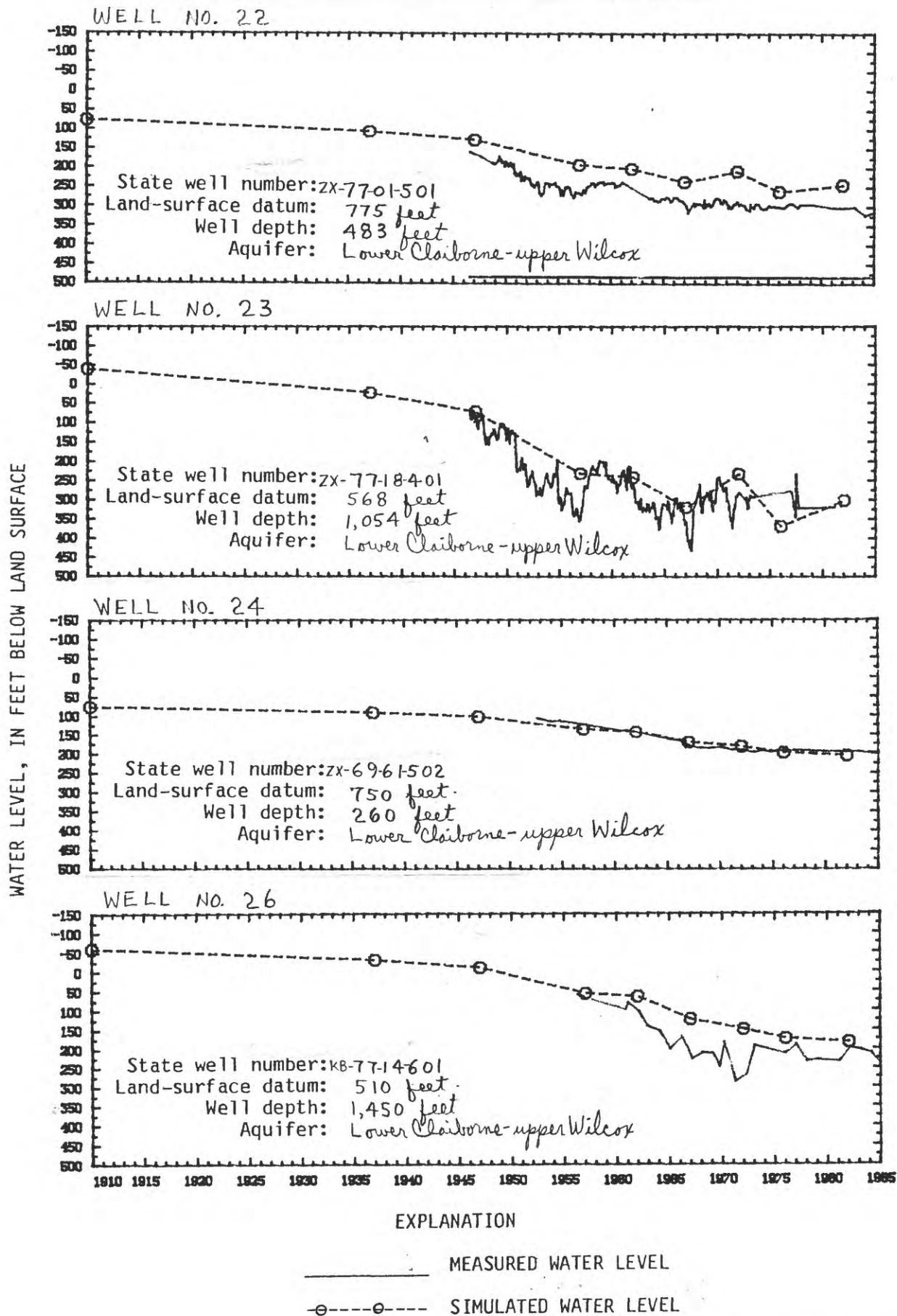


Figure 90.—Measured and simulated water levels in wells 22, 23, 24, and 26 in the Winter Garden area.

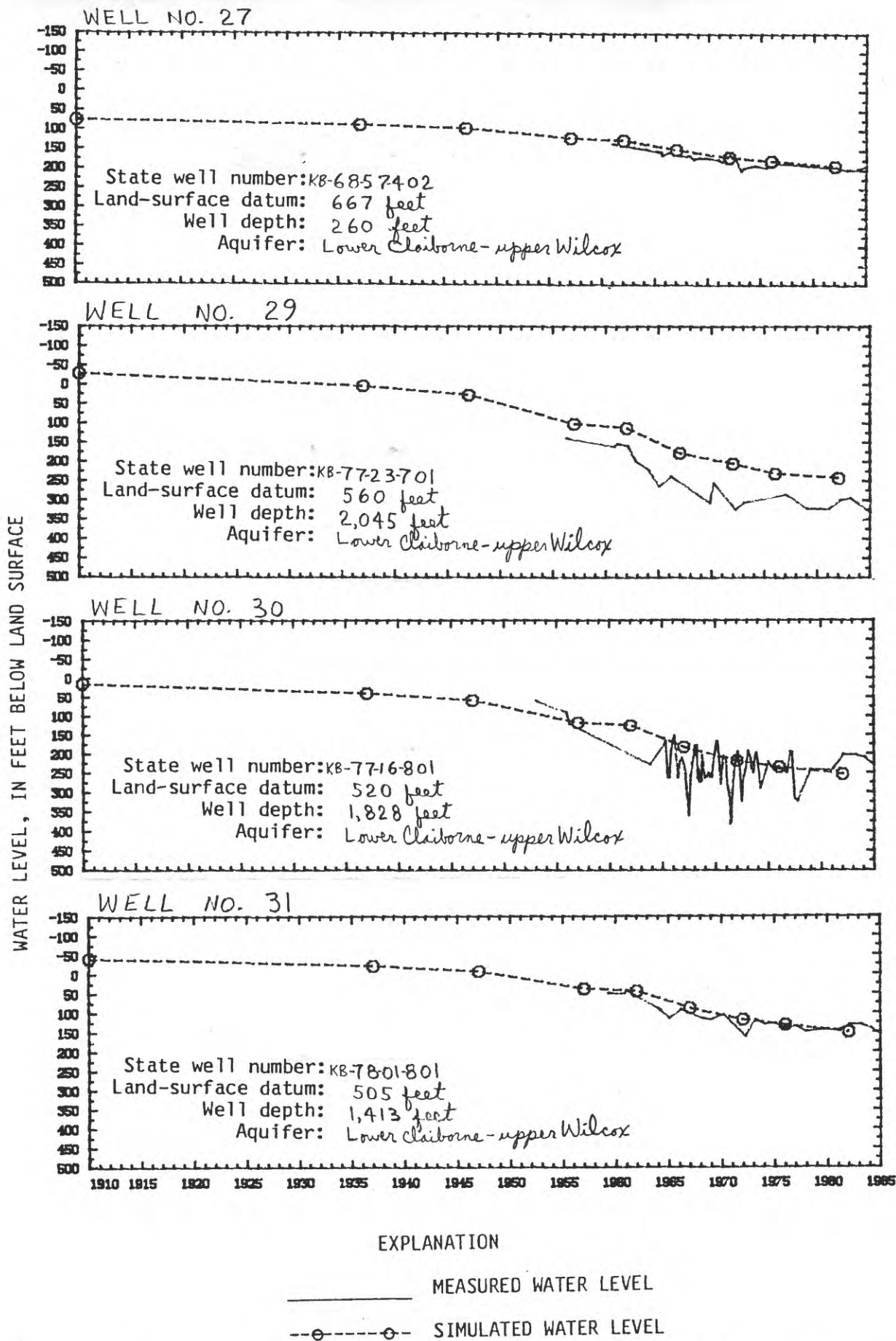
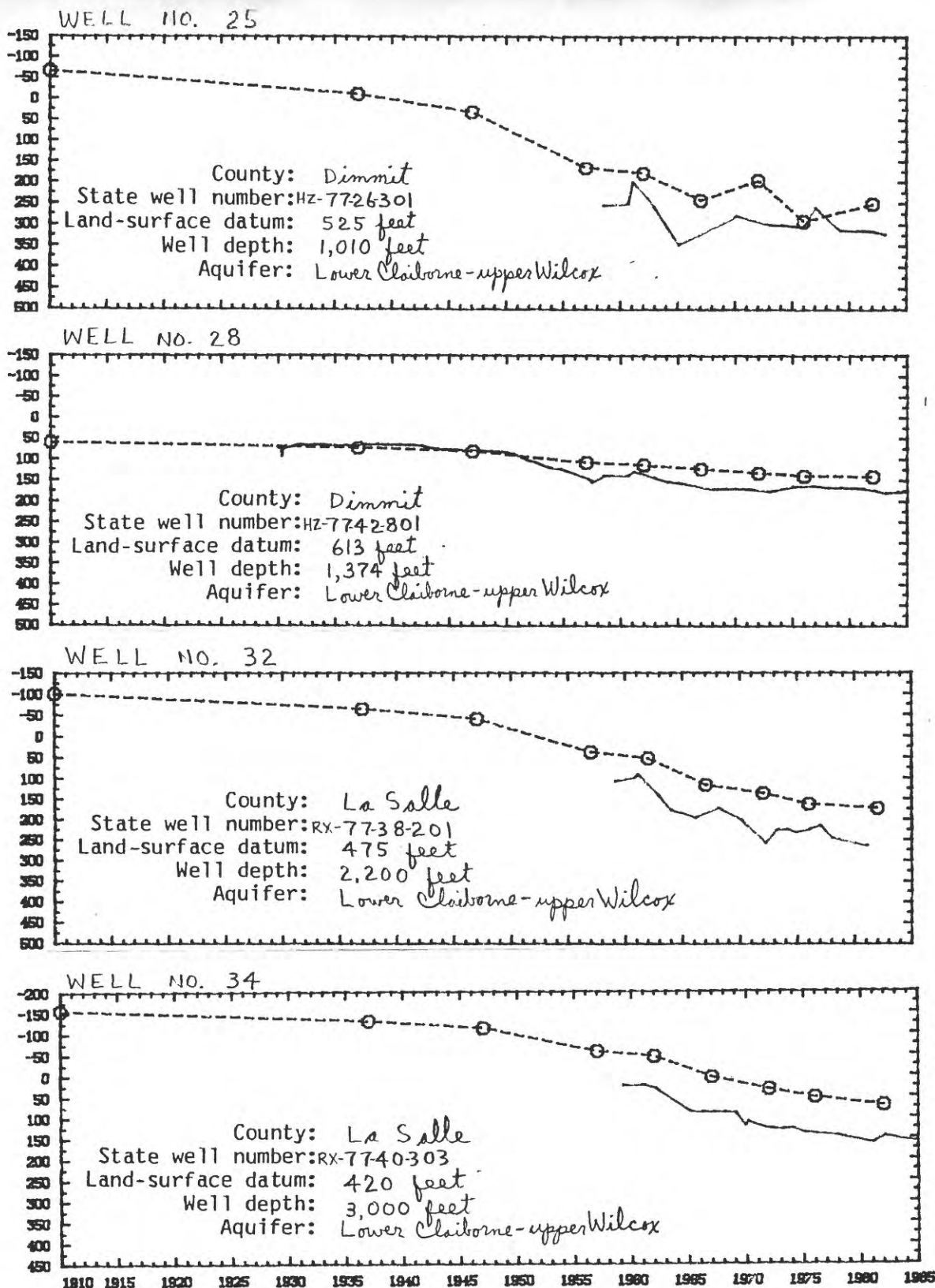


Figure 91. —Measured and simulated water levels in wells 27, 29, 30, 31, and 32 in the Winter Garden area.

WATER LEVEL, IN FEET BELOW LAND SURFACE



EXPLANATION

————— MEASURED WATER LEVEL
 --○-- SIMULATED WATER LEVEL

Figure 92.—Measured and simulated water levels in wells 25, 28, 32, and 34 in the Winter Garden area.

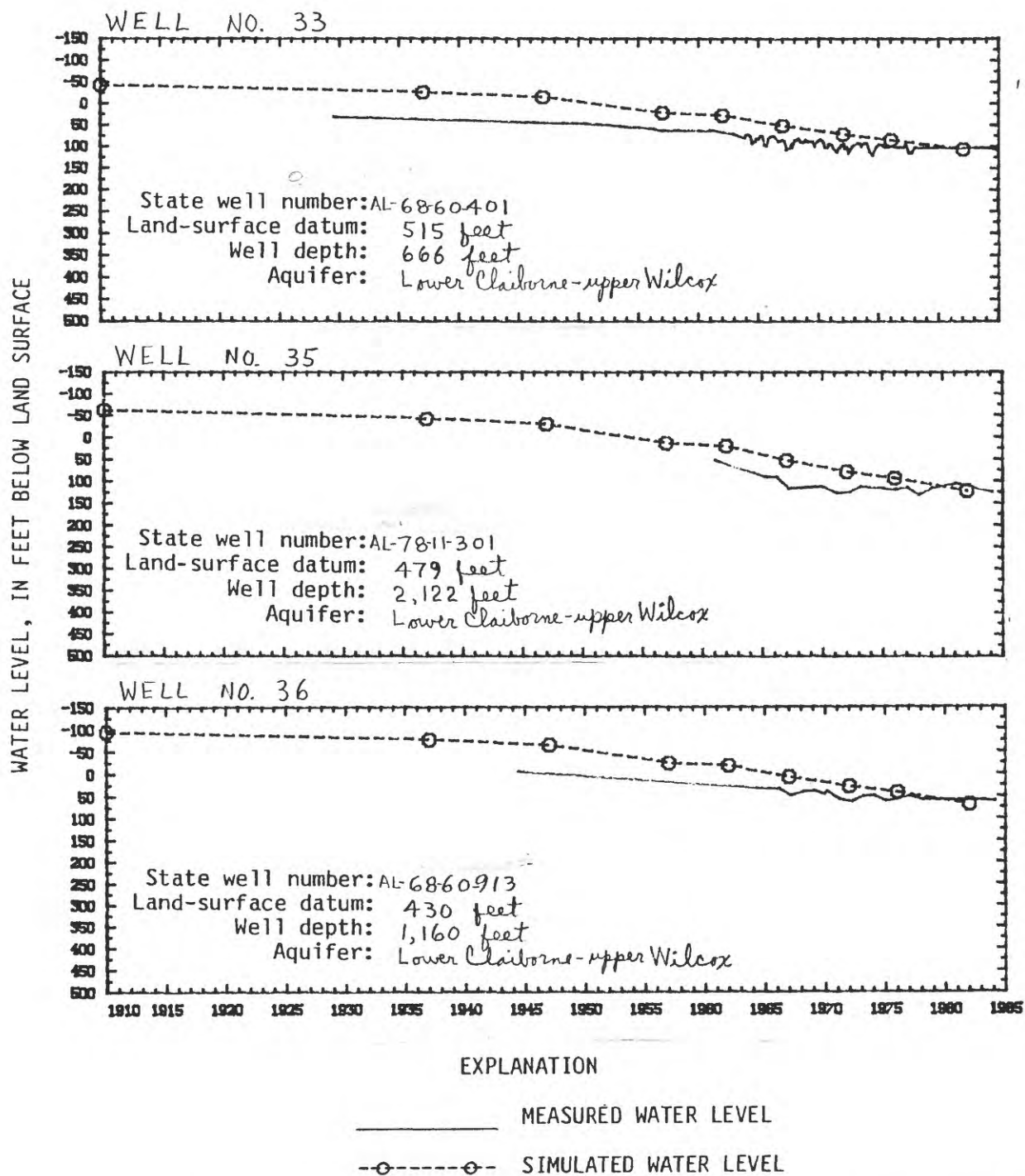
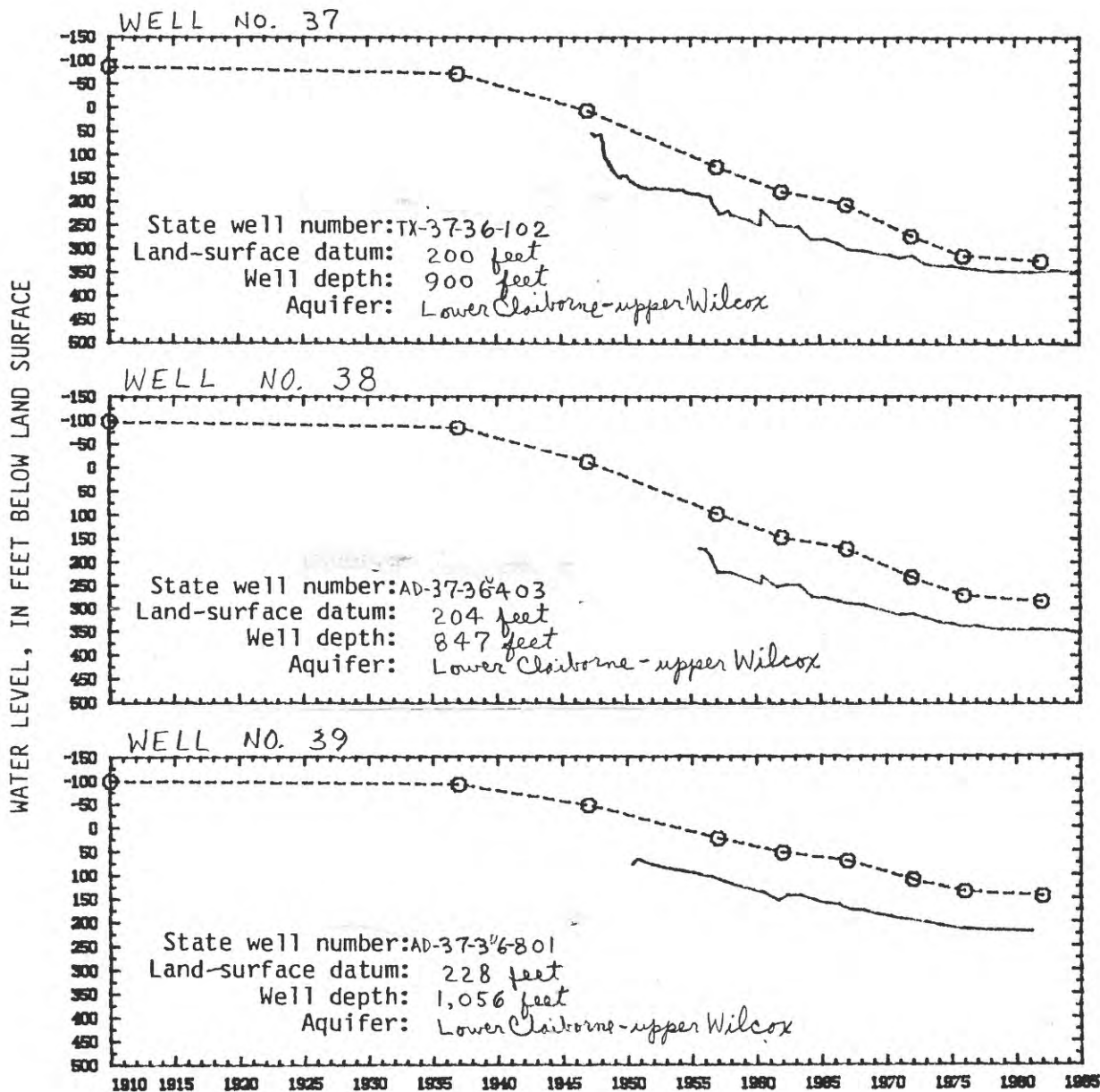


Figure 93.—Measured and simulated water levels in wells 33, 35, and 36 in the Winter Garden area.



EXPLANATION

- MEASURED WATER LEVEL
- SIMULATED WATER LEVEL

Figure 94.—Measured and simulated water levels in wells 37, 38, and 39 in the Lufkin ^{-Nacogdoches} area.

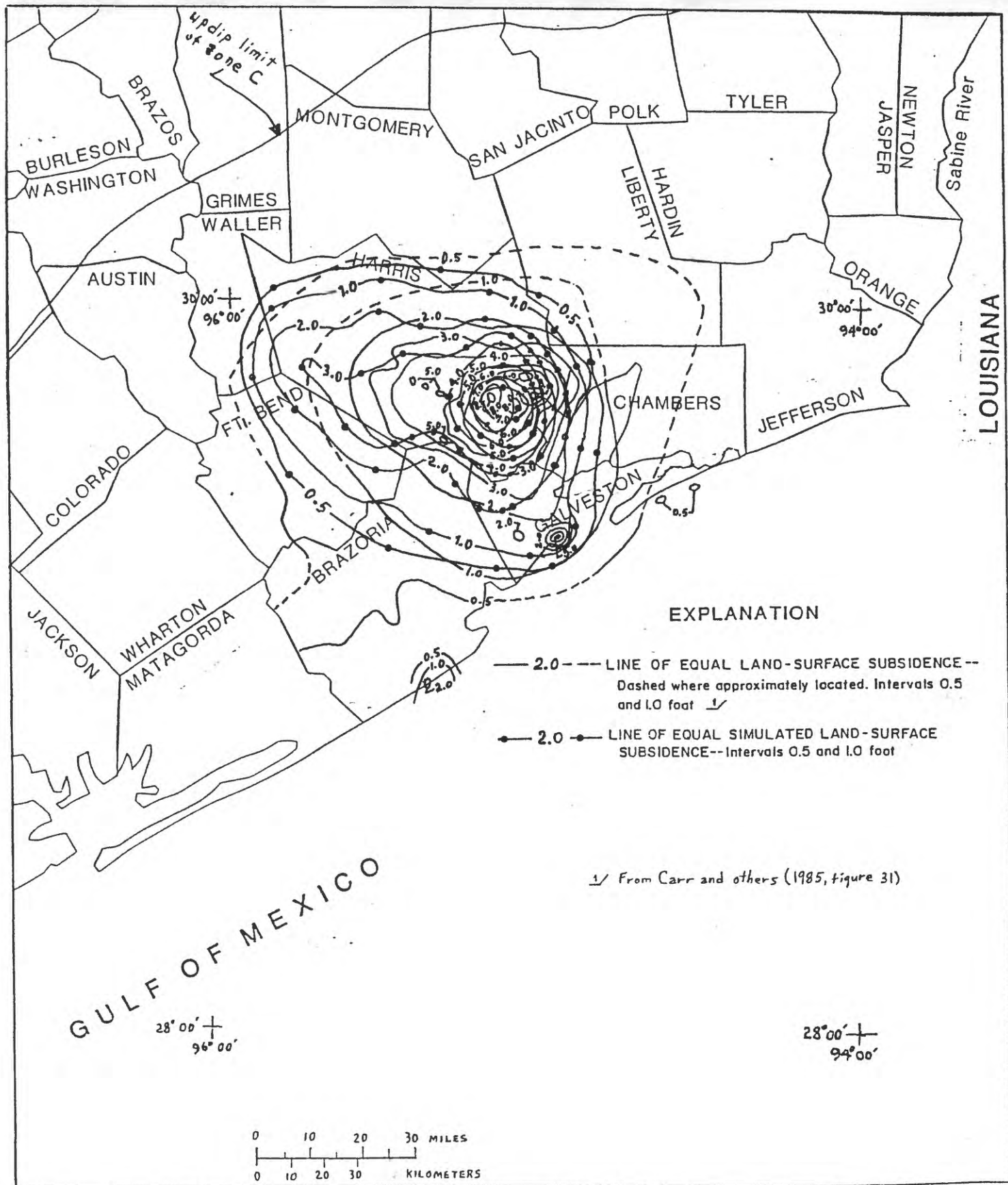
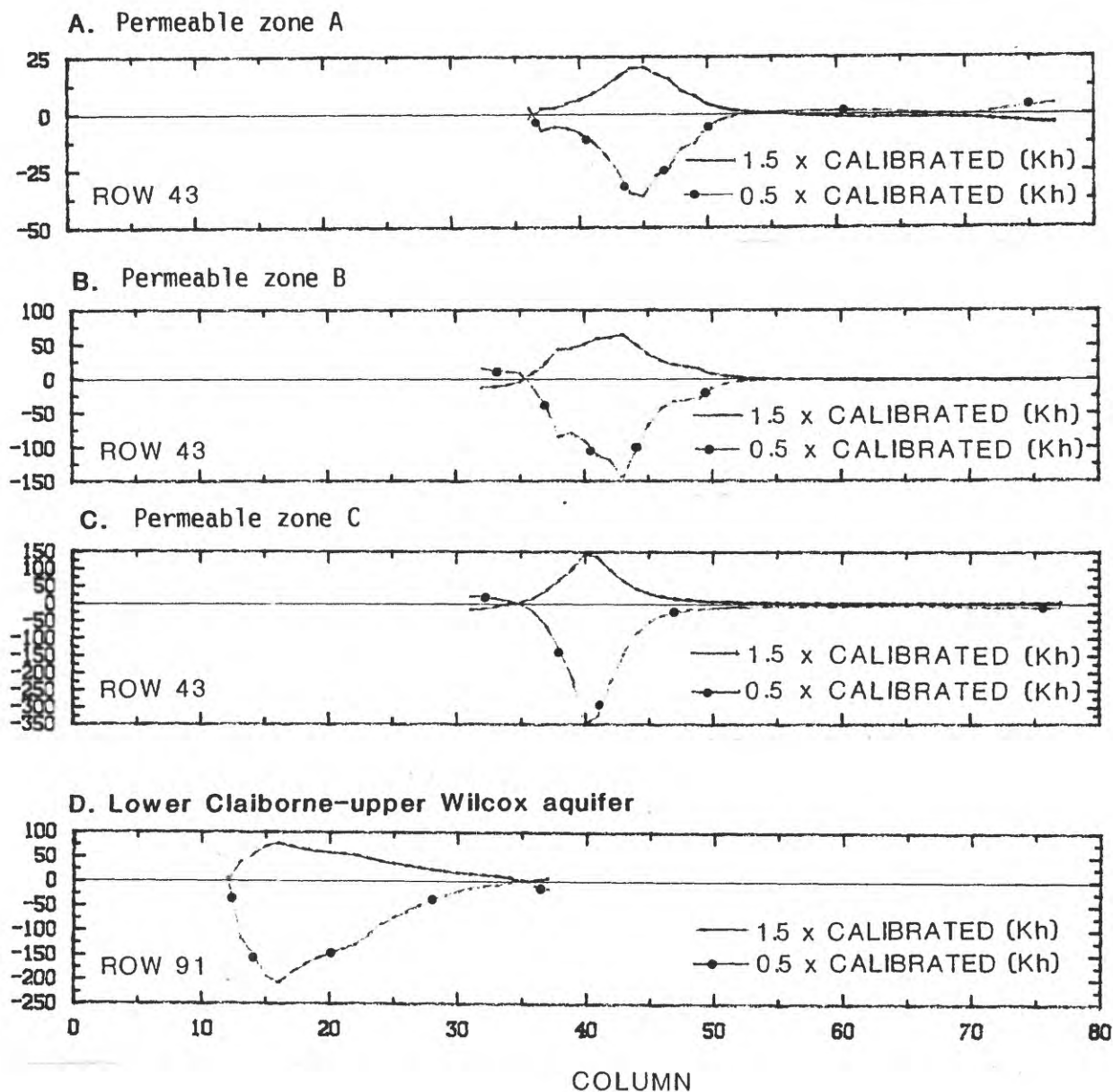


Figure 95.--Measured and simulated land-surface subsidence in the Houston-Galveston area, predevelopment to 1973.

DEPARTURE OF REVISED HEAD FROM CALIBRATED HEAD, IN FEET



1982
Figure 96.--Sensitivity of simulated heads to change in horizontal hydraulic conductivity (Kh).

DEPARTURE OF REVISED HEAD FROM CALIBRATED HEAD, IN FEET

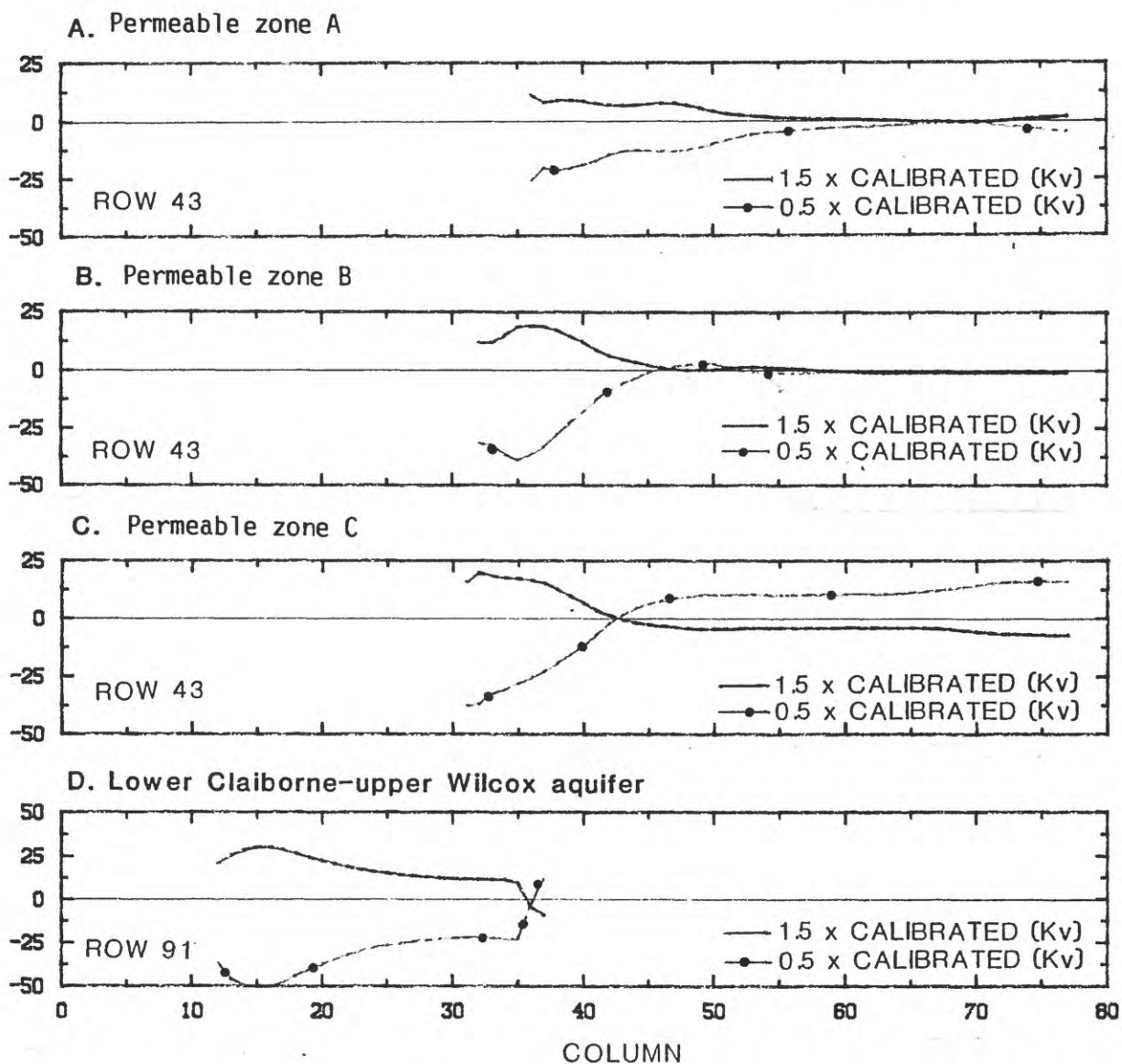


Figure 7. -- Sensitivity of simulated ¹⁹⁸²heads to change in vertical hydraulic conductivity (Kv).

DEPARTURE OF REVISED HEAD FROM CALIBRATED HEAD, IN FEET

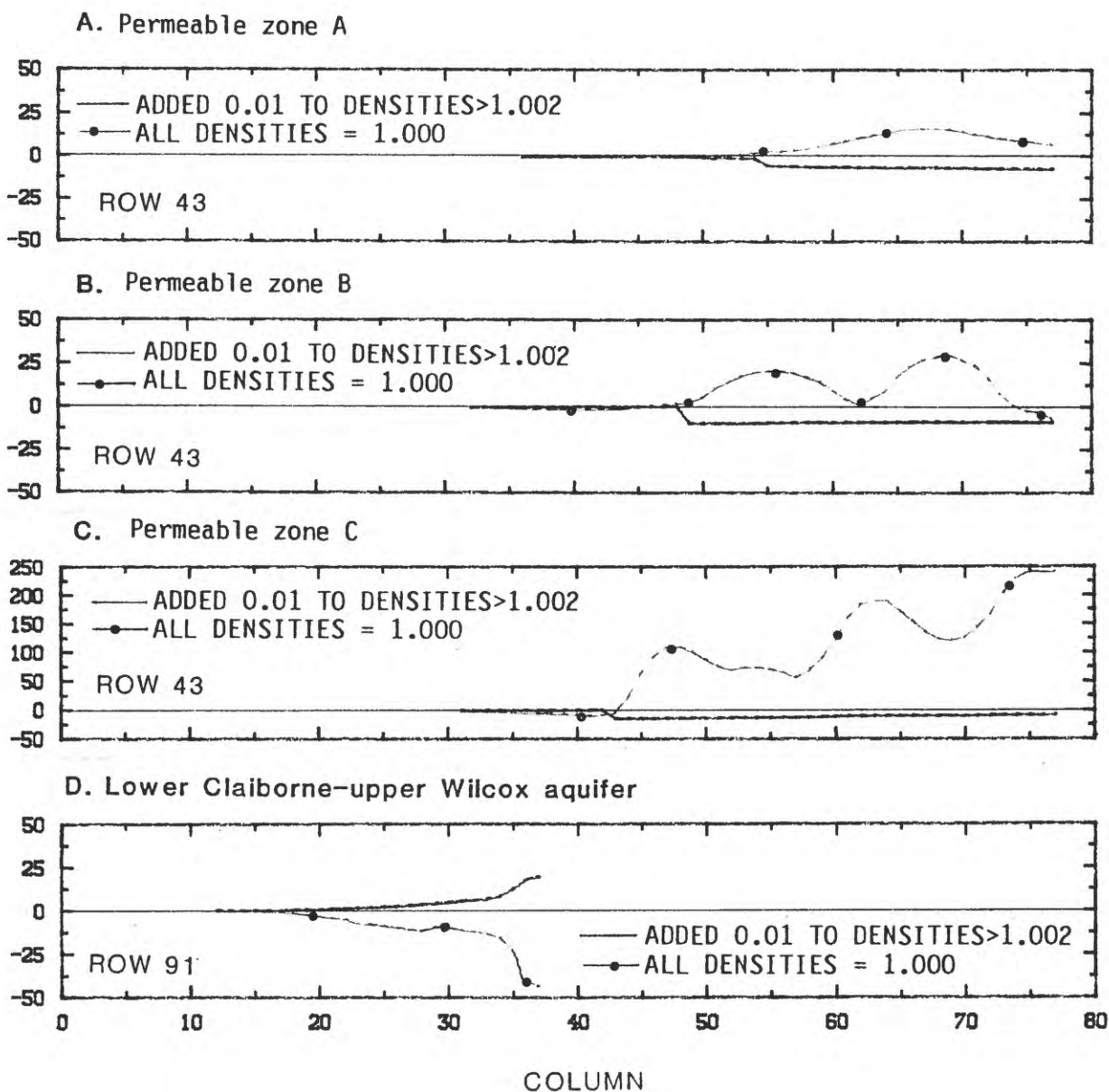


Figure 98. --Sensitivity of simulated 1982 heads to changes in water density.

DEPARTURE OF REVISED HEAD FROM CALIBRATED HEAD, IN FEET

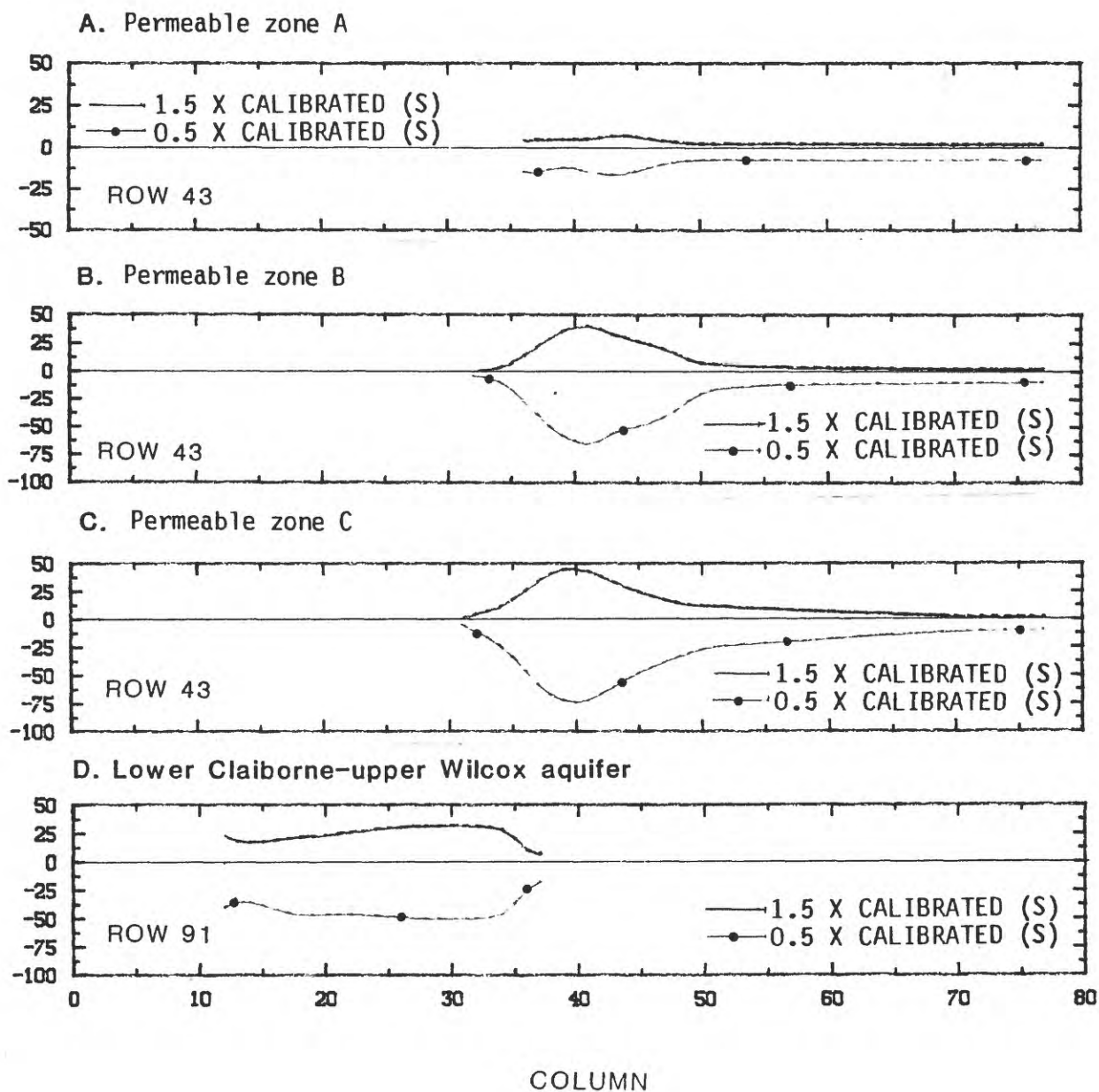


Figure 99. --Sensitivity of simulated 1982 heads to changes in aquifer storage coefficient (S).

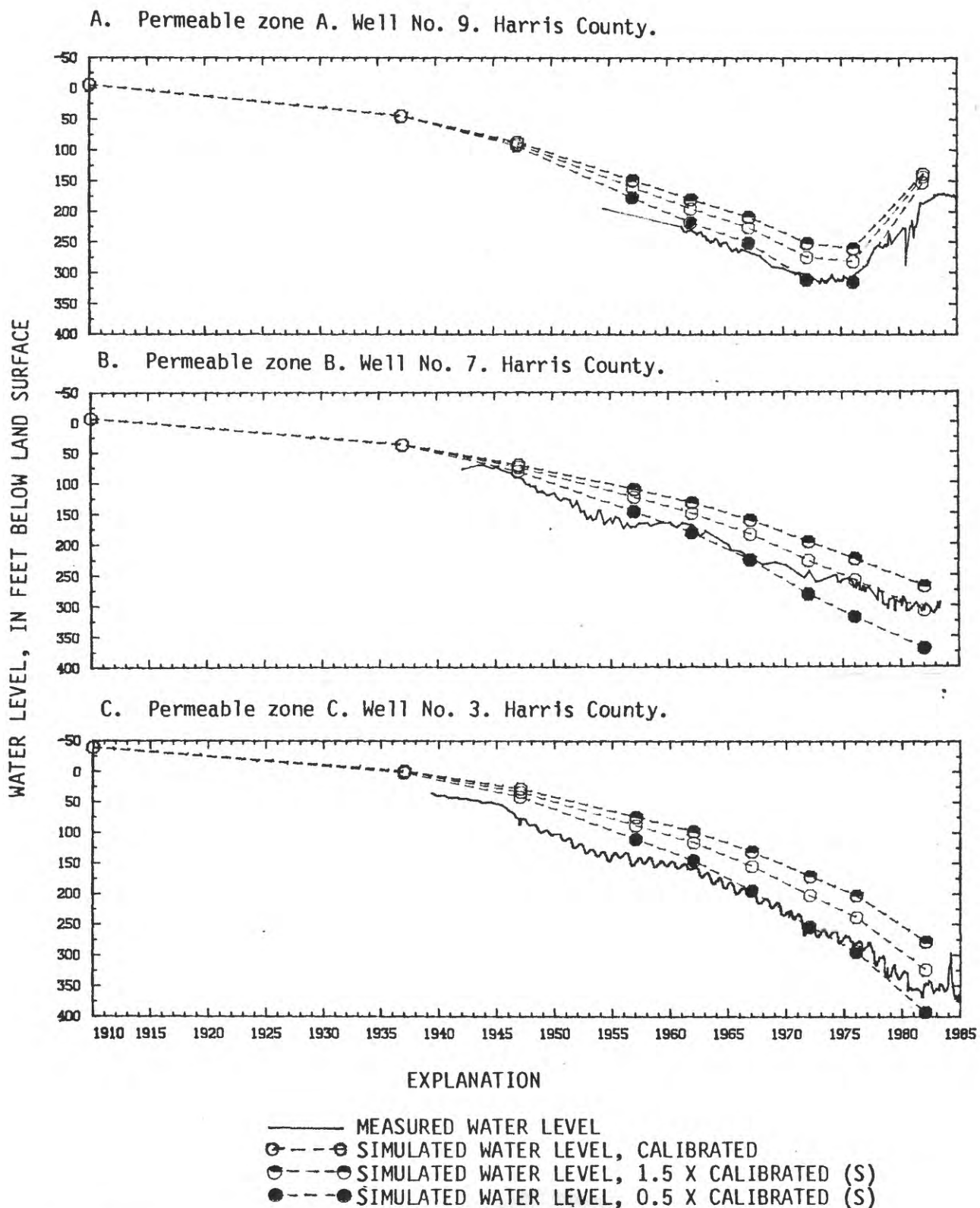
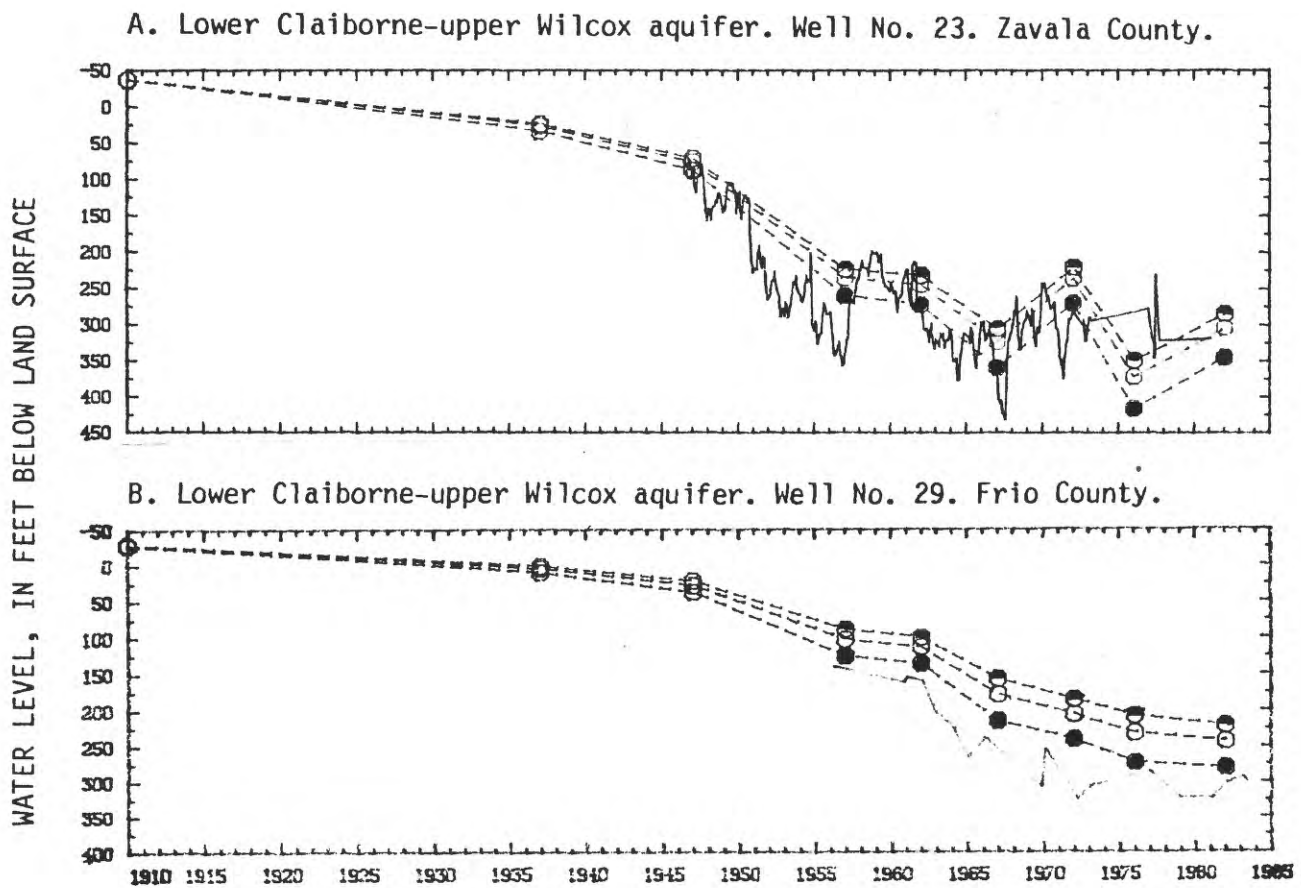


Figure 100. --- Sensitivity of simulated ^{water levels}, 1910-82, to changes in aquifer storage coefficient (S).



EXPLANATION

- MEASURED WATER LEVEL
- SIMULATED WATER LEVEL, CALIBRATED
- SIMULATED WATER LEVEL, 1.5 X CALIBRATED (S)
- SIMULATED WATER LEVEL, 0.5 X CALIBRATED (S)

Figure 10. ---Sensitivity of simulated ^{water levels}, 1910-82, to changes in aquifer storage coefficient (S).